

Metrology and Molecular Diagnosis of Infection

Eloise Joanne Busby

UCL

PhD Infection & Immunity

2020

I, Eloise Joanne Busby, confirm that the work presented in this thesis is my own. Where information has been derived from other sources, I confirm that this has been indicated in the thesis.

Acknowledgements

I would like to express my sincere gratitude to my supervisors Professor Timothy McHugh and Dr Jim Huggett for their guidance, support and encouragement throughout this process. I would also like to thank Dr Emmanuel Wey and Dr Jeremy Garson as members of my thesis committee for their expertise and advice.

I am very grateful to my employer, LGC, for supporting me throughout my studies. I would like to thank my colleagues in the Molecular and Cell biology team and beyond, both past and present, for providing a supportive and nurturing environment in which to grow and develop as a scientist, and for providing moral support throughout.

Having such an incredibly supportive family and network of friends has been instrumental in completing my PhD – thank you to my parents Claire and Jon, my sister Jo, the netball girls, ‘home-crew’ and too many others to name for always supporting my dreams and ideas and motivating me to achieve them.

I would like to give special thanks to Tom for being there through the highs and the lows and for bringing me tea, snacks and 5pm wine.

I would like to dedicate this thesis to the memory of my Grandad, Kenneth Busby.

Author contributions

Data included in this thesis were generated as part of several collaborative projects, funded by The Department for Business, Energy and Industrial Strategy (BEIS) and The European Metrology Programme for Innovation and Research (EMPIR). Numerous other colleagues are to be acknowledged for their contributions. Affiliations are correct for the period in which the work was performed.

Chapter 3. Investigating differences between reverse transcription (RT) digital PCR methods for quantification of HIV-1 genomic RNA

Culture of 8E5 (ATCC® CRL-8993™) and Jurkat (ATCC® TIB-152™) cell lines was performed by Dr Gary Morley (LGC). I acknowledge Dr Ben Ayer (LGC BioSearch Technologies) for custom BHQnova™ probe design which was provided in kind. I acknowledge Dr Samreen Falak at Physikalisch-Technische Bundesanstalt (PTB) who performed initial assay optimisations for the HIV-1 RNA EQA material analysis. Extracted RNA from cultured viral stocks was provided by Dr Clare Morris at the National Institute of Biological Standards and Control (NIBSC). dPCR data included for the Virus Genome Detection HIV-1 (RNA) Program 1 (360) and Virus Genome Detection-HIV-1 (RNA) additional Training Program 2 (382) (Figure 3.10) were obtained at LGC, with input from the following colleagues: I performed the experimental work with statistical input from Drs Jim Huggett, Denise O'Sullivan, Alison Devonshire and Simon Cowen, LGC. Data were also provided by PTB, National Institute of Biology (NIB) and other study participants. Analysis of the EQA scheme was provided in consultation with colleagues from INSTAND e.V., Institut fuer Qualitaetssicherung in der Virusdiagnostik (IQVD) and Gesellschaft für Biotechnologische Diagnostik mbH (GBD). Part of the work described in this chapter is included in a manuscript submitted for peer review (Appendix 11, Section 10.11.3).

Chapter 4. Calibrating quantitative measurements of HIV-1 DNA using digital PCR

Culture of the 8E5 (ATCC® CRL-8993™) cell line was performed by Dr Gary Morley (LGC). Dr Bridget Ferns (UCLH) performed the qPCR analyses of patient samples, and Dr Sarah Watters (UCL) designed the HIV-1 LTR-*gag* and PDH qPCR assays. Additional sources of 8E5 DNA were provided in kind by Dr Paul Grant (UCLH) and Dr Simon Carne (PHE). Much of the work presented

in this chapter is adapted from a peer-reviewed publication (Busby *et al.*, 2017) (Appendix 11, Section 10.11.2).

Chapter 5. Quantification of methicillin resistance in *Staphylococcus spp* using digital PCR

Dr Rebecca Sanders (LGC) performed the DNA extraction kit comparison and fluorometric quantification of genomic DNA controls. I acknowledge Dr Beniam Ghebremedhin (Helios University Clinic Wuppertal) and Tracey Noblett (LGC Microbiology Proficiency Testing) for preparation and provision of bacterial materials. I acknowledge Dr Kathryn Harris (GOSH) for provision of the residual clinical DNA extracts along with associated qPCR data. I acknowledge NIB and PTB for provision of data included in the interlaboratory comparison, and Dr Denise O'Sullivan (LGC) for performing statistical analyses.

Chapter 6. Characterising sources of experimental variability in MALDI-TOF MS strain typing and evaluating applicability of the technique to resolving nosocomial outbreaks

I acknowledge staff at Health Services Laboratories (HSL) and the Royal Free London NHS Foundation trust (RFL) for provision of pre-analysed clinical bacterial isolates, and for provision of associated epidemiological data. I acknowledge Giuseppina (Jo) Maniscalco (UCL) for assistance with collection, culturing and cataloguing of isolates. I acknowledge Gema Mendez-Cervantes (Clover BioSoft) for performing bioinformatic analysis of MALDI-TOF MS spectra using custom software. I acknowledge Dr Jane Turton (PHE) for provision of reference typing data for the isolates. I acknowledge Dr Ronan Doyle (GOSH) for performing whole genome sequencing (WGS) and phylogenetic analysis of the *Acinetobacter baumannii* isolates. Part of the work described in this chapter is included in a manuscript being prepared for peer review (Appendix 11, Section 10.11.4).

Associated manuscripts

Copies of manuscripts can be found in Appendix 11.

10.11.1: Jones, G. M., Busby, E., Garson, J. A., Grant, P. R., Nastouli, E., Devonshire, A. S. & Whale, A. S. 2016. Digital PCR Dynamic Range is Approaching that of Real-Time Quantitative PCR. *Biomolecular Detection And Quantification*, 10, 31–33.

10.11.2: Busby, E., Whale, A. S., Ferns, R. B., Grant, P. R., Morley, G., Campbell, J., Foy, C. A., Nastouli, E., Huggett, J. F. & Garson, J. A. 2017. Instability of 8E5 Calibration Standard Revealed by Digital PCR Risks Inaccurate Quantification of HIV DNA in Clinical Samples by qPCR. *Scientific Reports*, 7, 1209.

10.11.3: Falak, S., Macdonald, R., Busby, E., O'Sullivan, D., Milavec, M., Plauth, A., Kammel, M., Zeichhardt, H., Grunert, H., Huggett, J. & Kummrow, A. An Assessment of the Reproducibility of Reverse Transcription Digital PCR Quantification of HIV-1 Viral RNA Genome. *In preparation*.

10.11.4: Busby, E., Doyle, R., Solanki, P., Leboireiro Babe, C., Pang, V., Méndez-Cervantes, G., Harris, K., O'Sullivan, D., Huggett, J., McHugh, T. & Wey, E. Evaluation of MALDI-TOF MS and other emerging methods for molecular typing of *Acinetobacter baumannii*. *In preparation*.

Abstract

Metrology, the study of measurement, is an emerging concept within molecular diagnosis of infection. Metrology promotes high-quality, reproducible data to be used in clinical management of infection, through characterisation of technical error and measurement harmonisation. This influences measurement accuracy, which has implications for setting thresholds between healthy and disease states, monitoring disease progression, and establishing cures. This thesis examines the placing of metrology in molecular diagnosis of infectious diseases. Sources of experimental error in advanced methodologies – dPCR and MALDI-TOF MS – that can influence measurement accuracy for RNA, DNA and protein biomarkers were investigated for HIV-1, methicillin-resistant *Staphylococcus* spp and organisms associated with hospital transmission. Measurement error introduced at different stages of a method can directly impact upon clinical results. A 30% bias was introduced between dPCR and qPCR quantification of HIV-1 DNA in clinical samples, owing to instability in the qPCR calibration material. In addition, experimental variability was found to influence classification of protein profiles which can limit the resolution of MALDI-TOF MS for strain typing bacteria. This thesis also addresses the prospective role of these advanced methods in supporting accurate clinical measurements. dPCR offers precise measurements of RNA and DNA targets and could be used to support qPCR, or for value assignment of reference materials to harmonise inter-laboratory results. MALDI-TOF MS demonstrated potential for strain typing *Acinetobacter baumannii*; results correlated with epidemiological data and WGS, although were not consistent with reference typing. Further work should examine the extent to which MALDI-TOF MS can support or replace contemporary strain typing methods for identifying nosocomial outbreaks. Molecular approaches possess a crucial role in the detection, quantification and characterisation of pathogens, and are invaluable tools for managing emerging diseases. Supporting accuracy and reproducibility in molecular measurements could help to strengthen diagnostic efforts, streamline clinical pathways and provide overall benefit to patient care.

Impact statement

The role of metrology in ensuring measurement accuracy, reproducibility and reliability in molecular diagnosis of infection offers demonstrable impact within academia, industry, clinical practice, policy making and beyond. The data presented in this thesis were obtained during several measurement research projects for infectious diseases, under the work of the National Measurement Laboratory (NML) at LGC, Teddington. Much of the data contributes to inter-laboratory collaboration with clinical partners, an international network of National Measurement Institutes (NMIs), international External Quality Assessment (EQA) providers, and reference material producers and distributors. This reveals a diverse network promoting metrology within molecular diagnosis of infection, illustrating the further reaching impact of the work beyond this thesis. Appreciable impact of the work presented here includes peer-reviewed publication in internationally renowned journals. Much of Chapter 4 was included in a peer review publication (Busby *et al.*, 2017), which has since been cited both in the academic literature and also on the NIH AIDS reagent website for the 8E5 cell line (https://www.aidsreagent.org/reagentdetail.cfm?t=cell_lines&id=75, accessed 14th August 2020). The website details the findings of Chapter 4, highlighting that instability has been observed in the cell line and informing prospective researchers. This represents a further-reaching impact of the work not just within the measurement community, but for academics and other groups working in the field of HIV research. Other manuscripts based on this thesis are currently in draft, with a view to imminent submission for peer-review (Appendix 11).

The role of metrology within molecular biology is evolving. This is demonstrated by the recent update to the 2013 digital MIQE guidelines to reflect developments in dPCR technologies, and increased uptake of the method by laboratories for making advanced measurements of nucleic acid (The dMIQE Group and Huggett, 2020). The importance of ensuring data reliability and transparency is relevant to academia, industry and clinical laboratories (among others). This thesis may contribute to the wider understanding of metrological principles for molecular diagnosis of infection. This is through demonstrating the importance of standardising methods, harmonisation of results and the role of emerging technologies for supporting measurement accuracy using current methods. In addition, dPCR value assignment of candidate reference materials in this work could represent a commercial benefit for producers and distributors, especially if metrological traceability of their products can be assured.

Contents

Acknowledgements	2
Author contributions	3
Associated manuscripts	5
Abstract	6
Impact statement	7
Contents	8
List of figures	16
List of tables	21
Non-standard abbreviations	23
1. Introduction	25
1.1. Introduction to metrology	25
1.1.1. What is metrology?	25
1.1.1.1. A brief history of measurement.....	25
1.1.1.2. Analytical accuracy in measurement	27
1.1.1.2.1. Reference materials and traceability	27
1.1.1.2.2. Measurement error: precision and bias.....	28
1.1.2. Metrology in the biological sciences	30
1.1.2.1. The concept of 'bio-metrology'	30
1.2. Molecular measurements and infectious diseases.....	31
1.2.1. Diagnosis of infectious diseases.....	31
1.2.2. Molecular methods for detection, quantification and advanced analysis of pathogens ³²	
1.2.3. Nucleic acid-based methods.....	35
1.2.3.1. Introduction to polymerase chain reaction (PCR).....	35
1.2.3.2. Real-time PCR (qPCR)	37
1.2.3.3. Digital PCR (dPCR)	38
1.2.3.4. Isothermal nucleic acid amplification approaches	40
1.2.3.5. Next generation sequencing (NGS).....	41
1.2.4. Proteomic analysis of pathogens.....	42
1.2.4.1. Matrix assisted laser desorption/ionisation time of flight mass spectrometry (MALDI-TOF MS)	42

1.3.	Improving measurement accuracy in molecular diagnosis of infectious diseases	45
1.3.1.	Harmonising molecular measurements	45
1.3.1.1.	Establishing metrological frameworks	45
1.3.1.2.	Inter-laboratory collaboration and comparison of clinical measurements	46
1.3.1.3.	Transparency in data reporting	48
1.3.2.	Development and characterisation of reference materials and methods	49
1.3.2.1.	International reference standards	49
1.3.2.2.	SI traceability in infectious disease diagnostics	50
1.3.2.3.	Biological complexity of reference materials	52
1.3.3.	Characterising sources of experimental variability contributing to measurement error	54
1.4.	Contribution to the field	55
1.5.	Thesis aims	56
1.6.	Hypotheses	57
2.	General methods and preparation of reagents	60
2.1.	Nucleic acid analysis	60
2.1.1.	Plastic-ware for nucleic acid analysis	60
2.1.2.	Oligonucleotide design	60
2.1.3.	Preparation of oligonucleotides for PCR	60
2.1.4.	Calculating molecular weight (MW) and copy number of synthetic constructs	61
2.1.5.	General dPCR protocol for the Bio-Rad QX200 system	61
2.2.	Protein analysis	62
2.2.1.	Plastic-ware for proteomic analysis	62
2.2.2.	Preparation of 70% formic acid solution	62
2.2.3.	Preparation of Bruker Bacterial Test Standard (BTS)	62
2.2.4.	Preparation of Bruker α -Cyano-4-hydroxycinnamic acid (HCCA) matrix	62
3.	Investigating differences between reverse transcription (RT) digital PCR methods for quantification of HIV-1 genomic RNA	63
3.1.	Introduction	63
3.1.1.	Human immunodeficiency virus type 1 (HIV-1)	63
3.1.2.	Clinical quantification of HIV-1 RNA viral load	63
3.1.3.	Variability associated with reverse transcription and the potential impact on RNA quantification	64

3.1.4.	The role of digital PCR for quantification of viral RNA.....	65
3.2.	Materials and methods	67
3.2.1.	Study materials	67
3.2.1.1.	Culture of cell lines.....	67
3.2.1.2.	Extraction of RNA	67
3.2.1.3.	Synthetic construct for comparison of reverse transcriptase enzymes	67
3.2.1.4.	In vitro transcription of synthetic RNA.....	68
3.2.1.5.	Total HIV-1 genomic RNA reference material	68
3.2.1.6.	Whole viral External Quality Assessment (EQA) materials	69
3.2.2.	Assays for quantification of HIV-1 RNA.....	69
3.2.2.1.	Oligonucleotide sequences.....	69
3.2.2.2.	Assay verification	72
3.2.3.	Evaluation of reverse transcriptase kits for absolute quantification of RNA by dPCR	72
3.2.3.1.	FIREScript RT cDNA synthesis kit.....	73
3.2.3.2.	Maxima First Strand cDNA Synthesis Kit for RT-qPCR	73
3.2.3.3.	SuperScript™ III Reverse Transcriptase	73
3.2.3.4.	One-Step RT-ddPCR Advanced Kit for Probes	74
3.2.4.	General protocol for RNA quantification by dPCR.....	74
3.2.5.	Evaluating the sensitivity of different reverse transcriptase enzymes by RT-dPCR	74
3.2.6.	Data analysis	75
3.3.	Results and discussion.....	76
3.3.1.	Design and in vitro transcription of a synthetic HIV-1 RNA molecule for characterisation of reverse transcription (RT) dPCR.....	76
3.3.2.	Verification of dPCR assays for comparing RT kits.....	78
3.3.3.	Comparison of different kits for performing reverse transcription using dPCR	79
3.3.3.1.	Assessing the analytical sensitivity of RT dPCR	82
3.3.3.2.	Considerations for selecting reverse transcriptase kits for HIV RNA quantification	85
3.3.4.	Application of RT-dPCR to EQA materials for HIV-1 RNA quantification.....	86
3.3.4.1.	Characterisation of assays and materials.....	86
3.3.4.2.	Analysis of test EQA materials	89

3.3.4.3.	Intra-laboratory analysis of EQA materials for HIV RNA quantification	90
3.3.4.4.	Inter-laboratory analysis of EQA materials for HIV RNA quantification	92
3.3.5.	RT-dPCR analysis of clinical samples from HIV-1 positive individuals.....	94
3.4.	Conclusions.....	94
4.	Calibrating quantitative measurements of HIV-1 DNA using digital PCR	96
4.1.	Introduction	96
4.1.1.	The proviral reservoir: a barrier to curing HIV-1	96
4.1.2.	Quantification of HIV-1 DNA	96
4.1.3.	A role for dPCR in HIV-1 DNA quantification	97
4.2.	Materials and methods.....	99
4.2.1.	Study materials.....	99
4.2.1.1.	Patient samples.....	99
4.2.1.2.	Cell lines	99
4.2.2.	Culture of 8E5 'Standard 3' cells.....	99
4.2.3.	DNA extraction	100
4.2.4.	PCR assays.....	100
4.2.5.	qPCR analysis of clinical samples	102
4.2.6.	Digital PCR basic protocol	102
4.2.6.1.	Digital PCR analysis of clinical samples	103
4.2.6.2.	Digital PCR characterisation of 8E5 cells.....	103
4.2.6.3.	Effect of different 8E5 calibrator sources on qPCR analysis of clinical samples	104
4.2.7.	Data Analysis	104
4.3.	Results and Discussion.....	105
4.3.1.	Measurement of HIV-1 DNA in patient samples by dPCR and qPCR	105
4.3.2.	Investigating discrepancies between the two dPCR systems.....	107
4.3.3.	Investigating the discrepancies between dPCR and qPCR quantification of HIV DNA	109
4.3.3.1.	Digital PCR characterisation of the 8E5 cell line.....	109
4.3.3.2.	Evaluating the impact of the 8E5 calibrator on qPCR quantification HIV DNA	113
4.3.3.3.	Application of cell lines for calibration of qPCR quantification of HIV-1 DNA	114

4.3.3.4.	General use of cell lines for qPCR calibration	117
4.3.4.	Comparison of qPCR and dPCR for HIV DNA quantification	117
4.3.5.	Sensitive estimations of the size of the HIV proviral reservoir normalised to one million cells.....	121
4.4.	Conclusions	122
5.	Quantification of methicillin resistance in <i>Staphylococcus spp</i> using digital PCR	124
5.1.	Introduction	124
5.1.1.	Methicillin resistant <i>Staphylococcus aureus</i> (MRSA)	124
5.1.2.	Colonisation and infection with MRSA.....	124
5.1.3.	Molecular diagnosis of MRSA and the clinical relevance of coagulase-negative staphylococci (CoNS)	125
5.1.4.	A role for DNA quantification in managing MRSA infections	126
5.1.5.	A role for digital PCR in quantifying MRSA DNA.....	127
5.2.	Materials and methods	128
5.2.1.	Study materials	128
5.2.1.1.	ATCC genomic DNA controls	128
5.2.1.2.	Whole bacterial cell materials	128
5.2.1.3.	Residual clinical DNA extracts	128
5.2.2.	Optimisation of a protocol for DNA extraction from bacteria	129
5.2.3.	Oligonucleotides	130
5.2.3.1.	Staphylococcus epidermidis femA assay design.....	131
5.2.4.	Quantification by digital PCR	131
5.2.4.1.	Dynamic range of assays	131
5.2.4.2.	dPCR quantification of methicillin resistance in genomic DNA admixtures	132
5.2.4.3.	General protocol for the Naica System™ for Crystal Digital™ PCR	132
5.2.5.	Inter-laboratory analysis of whole bacterial cell materials	133
5.2.6.	dPCR analysis of clinical isolates	134
5.2.7.	Data analysis	134
5.3.	Results and discussion.....	135
5.3.1.	Method development	135
5.3.1.1.	Assay specificity.....	135

5.3.1.2.	Dynamic range	136
5.3.1.3.	Application of assays to genomic DNA admixtures	139
5.3.1.4.	Optimisation of DNA extraction	142
5.3.2.	Intra-laboratory analysis of whole bacterial cell materials.....	144
5.3.3.	Inter-laboratory study of method reproducibility	146
5.3.4.	Analysis of clinical isolates	149
5.3.4.1.	Comparison of dPCR and qPCR results	152
5.3.4.2.	Co-colonisation of <i>S. aureus</i> with CoNS	154
5.4.	Conclusions.....	155
6.	Characterising sources of experimental variability in MALDI-TOF MS strain typing and evaluating applicability of the technique to resolving nosocomial outbreaks	156
6.1.	Introduction	156
6.1.1.	Nosocomial transmission of bacterial infections	156
6.1.2.	Molecular strain typing of bacteria	157
6.1.3.	Matrix Assisted Laser Desorption/Ionisation-Time of Flight Mass Spectrometry (MALDI-TOF MS) as a method for strain typing	158
6.2.	Materials and methods.....	160
6.2.1.	Study materials.....	160
6.2.1.1.	Clinical isolates.....	160
6.2.1.2.	Commercial reference strains	160
6.2.2.	Bacterial culture.....	160
6.2.3.	Reference laboratory strain typing of isolates.....	161
6.2.4.	General protocol for formic acid extraction of proteins from bacterial cells ..	161
6.2.5.	Spectral acquisition for strain typing using MALDI-TOF MS.....	161
6.2.6.	Characterising sources of variability in sample preparation for MALDI-TOF MS typing	162
6.2.6.1.	Variability from culture-subculture cycle.....	162
6.2.6.2.	Variability from formic acid protein extraction	163
6.2.6.2.1.	Preparation of a 0.5 McFarland standard	163
6.2.6.2.2.	Comparison between two biomass collection and delivery methods ..	163
6.2.6.2.3.	Varying volumes of extraction reagents.....	163
6.2.6.3.	Assessing day-to-day stability of the bacterial test standard (BTS).....	163
6.2.7.	Assessing peak intensity at different stages of the typing protocol	164

6.2.8.	Data handling and analysis of typing spectra	164
6.2.8.1.	Bruker FlexAnalysis method	164
6.2.8.2.	Bioinformatics software.....	165
6.2.9.	Whole genome sequencing and phylogenetic analysis.....	165
6.3.	Results and Discussion	167
6.3.1.	Part 1: Evaluating sources of variability in the MALDI-TOF MS strain typing protocol	167
6.3.1.1.	Variability in spectra attributed to sample preparation	167
6.3.1.1.1.	Culture-subculture cycle and phase of bacterial growth	167
6.3.1.1.2.	Formic acid extraction of proteins	170
6.3.1.2.	Peak intensity as a metric for evaluating robustness of replicate spectra.....	172
6.3.1.2.1.	Evaluating inter-experimental variability in peak intensity for a standardised protein solution.....	172
6.3.1.2.2.	Variability in peak intensity for clinical isolates	173
6.3.1.3.	Choice of data analysis method for MALDI-TOF MS strain typing.....	176
6.3.1.3.1.	Bruker FlexAnalysis method	176
6.3.1.3.2.	Bioinformatics approaches.....	178
6.3.1.4.	Practical implications of variability in the MALDI-TOF MS strain typing workflow	180
6.3.2.	Part 2: Can MALDI-TOF MS be used to strain type bacteria?	182
6.3.2.1.	MALDI-TOF MS strain typing of <i>Acinetobacter baumannii</i>	182
6.3.2.1.1.	Peak intensity as a metric for discrimination of peak classes using MALDI-TOF MS typing	185
6.3.2.1.2.	Potential identification of a nosocomial transmission event.....	187
6.3.2.2.	MALDI-TOF MS strain typing of <i>Staphylococcus aureus</i>	189
6.3.2.3.	The potential for integration of MALDI-TOF MS typing into routine clinical diagnostics.....	192
6.4.	Conclusions	194
7.	Final discussion.....	195
7.1.	Experimental variability impacts upon accuracy of molecular measurements of pathogen biomarkers.....	195
7.1.1.	Sample preparation and extraction of nucleic acids and proteins.....	195
7.1.2.	Efficiency of enzymatic processes for molecular biology	197
7.1.3.	Variability in analysis and interpretation of molecular data	199

7.2.	Development of reference methods and materials holds a key role in promoting measurement accuracy	200
7.3.	Advanced molecular approaches can support measurement accuracy for current diagnostic methods, and may hold a future role for direct analysis of clinical samples.....	202
8.	Concluding remarks and future work	205
9.	References	207
10.	Appendices	244
10.1.	Appendix 1	244
10.2.	Appendix 2	245
10.3.	Appendix 3	248
10.4.	Appendix 4	249
10.5.	Appendix 5	250
10.6.	Appendix 6	251
10.7.	Appendix 7	252
10.8.	Appendix 8	253
10.9.	Appendix 9	254
10.10.	Appendix 10	258
10.11.	Appendix 11	263

List of figures

Figure 1.1: A set of Harappan weights displayed in Mumbai, India	26
Figure 1.2: Calibration traceability chain for a clinical measurement (Gantzer and Miller, 2012)	28
Figure 1.3: Schematic representation of random and systematic error in a set of measurements that can result in reduced accuracy.....	29
Figure 1.4: Development of methods for detection of (a) viral diseases (Rasmussen, 2015) and (b) antimicrobial resistant bacteria (Shanmugakani et al., 2020) over the past century.	34
Figure 1.5: Sample partitioning, thermal cycling and detection of fluorescence that takes place during digital PCR. A total reaction volume containing template (A) is split into multiple partitions under pressure (B). Each partition hosts an individual PCR reaction (C), and the resulting fluorescent signal is detected. Partitions are categorised as positive or negative (D) (Dongngam et al., 2015).....	39
Figure 1.6: Principles of MALDI-TOF MS. A: the co-crystallised sample-matrix is ionised by a laser beam, accelerated through the linear flight tube and detected based on time-of-flight. B: an example mass spectrum with peaks of varying m/z values (Wieser et al., 2012).	43
Figure 1.7: Calibration traceability chain for quantitative molecular measurements, demonstrating the positioning of dPCR as a reference measurement procedure (RMP). Figure adapted from Gantzer (2012).....	52
Figure 1.8: Varying complexity of microbiological standards and reference materials (Devonshire et al., 2015). A material that closely resembles a complete organism within a clinical sample matrix (A) may be used to assess the full analytical workflow including extraction. In some cases, pre-extracted material such as genomic nucleic acid (B) or synthetic constructs (C) may be more appropriate options.	53
Figure 3.1: Bioanalyzer 2100 gel-like images depicting (A) linearised plasmid DNA expected at 8,125 bp visualised using a DNA7500 kit (B) in vitro transcribed RNA visualised using a RNA6000 nano kit. The three lanes represent neat [1], 10-fold [2] and 100-fold [3] dilutions of the RNA (C) heat denaturation of the neat RNA [lanes 1 & 2] and a 10-fold dilution [lanes 3 & 4] at 70 [1 & 3] and 95°C [2 & 4]. L indicates the molecular weight ladder for each kit.	77
Figure 3.2: Digital PCR verification of single and double-quenched HIV LTR- <i>gag</i> and <i>pol</i> assays using plasmid DNA. Error bars represent standard deviation. The dashed line represents equivalence.....	79

Figure 3.3: Comparison of RT kits for total RNA and synthetic RNA. HIV-1 cDNA copy number was found to be dependent on assay target as well as RT kit. Δ HIV-1 *pol* assay \square HIV-1 LTR-*gag* assay. Each data point represents a single RT-dPCR replicate..... 80

Figure 3.4: Comparison of copy numbers per μL for the four reverse transcriptase kits compared with orthogonal methods: NanoDrop (black), Qubit (dark grey) and Bioanalyser (light grey) for the LTR-*gag* (red) and *pol* (pink) assays. Error bars represent standard deviation. 81

Figure 3.5: Log_{10} transformed observed versus expected cDNA copies per μL for the HIV *pol* assay using (a) Maxima two-step and (b) Bio-Rad one-step kits. The dashed line represents equivalence. 83

Figure 3.6: The HIV *gag* (Bosman) and HIV *gag* (Kondo)/*pol-vif* assay duplex was applied to (a) the HXB2 synthetic RNA transcript and the viral RNA extract. A comparison was performed between (b) the HXB2 RNA transcript and the corresponding DNA plasmid. 87

Figure 3.7: QX200 dot plots showing the HIV *gag* (Bosman) assay applied to (a) the HXB2 RNA molecule and (b) the viral RNA extract and the HIV *gag* (Kondo)/*pol-vif* duplex applied to (c) the synthetic HXB2 RNA molecule and (d) the viral RNA extract. Blue dots represent partitions containing HIV *gag* target, green dots represent HIV *pol-vif*. 88

Figure 3.8: Copies per μL for the *gag* and *pol-vif* assays and the expected values from the 2017 EQA scheme. Upper and lower expected values are based on 95% confidence intervals given by the scheme providers. 90

Figure 3.9: HIV RNA EQA intra-laboratory results. (a) Copies of HIV *gag* per μL for 8 EQA samples across two extraction batches represented on a logarithmic scale. (b) Mean copies *gag* per μL are plotted against %CV indicative of an inverse relationship between the two. 91

Figure 3.10: dPCR results obtained by two NMIs for the EQA samples. Bars show the acceptance range based on the consensus value from all quantitative results for the respective sample for the whole INSTAND EQA scheme, including calibration using the 4th WHO International Standard. Blue symbols represent PTB dPCR results, black symbols represent NML dPCR results. Figure based on data provided by NML, PTB and participants of Virus Genome Detection HIV-1 (RNA) Program 1 (360) and the Virus Genome Detection-HIV-1 (RNA) additional Training Program 2 (382) (INSTAND) of the 2019 EQA scheme (Section 10.11.3; Appendix 11). 93

Figure 4.1: Comparison between qPCR and dPCR measurements of HIV DNA copies per million cells for 18 PBMC samples. Red markers are where qPCR results were calculated assuming one HIV DNA copy per $8\text{E}5$ cell. Blue markers are where qPCR results were calculated assuming 0.6 HIV DNA copy per $8\text{E}5$ cell. Samples in which HIV DNA was not detected are not plotted. The dashed line represents equivalence. 111

Figure 4.2: HIV DNA copies per cell determined by dPCR for three different 8E5 cell line sources. (a) Comparison of 8E5 Standards 1, 2 and 3 on the RainDrop® and QX200 platforms. (b) Effect of serial culture on HIV DNA content per cell for 8E5 Standard 3 measured using the RainDrop® dPCR platform (c) Effect of serial culture on HIV DNA content per cell for 8E5 Standard 3 measured using the QX200™ dPCR platform. Mean values with standard deviations are plotted (Busby et al., 2017)..... 112

Figure 4.3: Median HIV DNA copies per million cells of seven clinical samples assayed by qPCR and calibrated using 8E5 Standards 1, 2 and 3 (boxplots shown with interquartile and range). (a) Calculated assuming one HIV DNA copy per 8E5 cell for all three Standards. (b) Calculated using the dPCR-determined number of HIV DNA copies per cell for each of the three different sources of 8E5 (Busby et al., 2017). 114

Figure 5.1: Digital PCR dot-plots showing detection of (a) *mecA* & *coA* and (b) *mecA* & *femA* using MRSA and MRSE ATCC genomic DNA controls, respectively; (c) and (d) represent MSSA ATCC genomic DNA and MSSE extract, respectively. Blue dots represent presence of FAM-labelled target (*mecA*), green dots represent HEX-labelled targets (*coA* & *femA*), orange dots represent both targets present in a droplet, grey dots represent no amplification. 136

Figure 5.2: Dynamic range for MRSA and MRSE expressed as *mecA* versus species-specific gene (*coA* for MRSA, *femA* for MRSE). The dashed line represents equivalence. 138

Figure 5.3: Mean ratio of *mecA* copies per µL relative to the species-specific gene targets (*coA* and *femA* for MRSA and MRSE, respectively) measured using the QX200™ (blue markers) and Naica™ (red markers) dPCR platforms. For samples d1, d2 and d3, copy numbers for *mecA* were compared to the summed copy numbers for *coA* and *femA*. For the MRSA and MRSE only controls, *mecA* copy numbers were compared directly to *coA* or *femA*, respectively. The expected ratio in all cases is 1.0. 139

Figure 5.4: dPCR quantification of *mecA* where MRSA is present alongside (a) MSSA and (b) MSSE. *mecA* copies per µL correlates with % MRSA relative to a constant copy number concentration (200 copies per µL) of methicillin sensitive population. 140

Figure 5.5: DNA extraction was performed on lyophilised MSSA organisms using three commercial kits. DNA yields expressed as *coA* copy number per µL were compared using dPCR and Qubit. Plotted results are based on triplicate technical measurements performed on three extraction replicates, obtained across triplicate experiments (3 extracts per day). The dashed line represents the expected copies per µL based on CFU estimates performed during material preparation (1 genomic copy = 1 CFU) (EURAMET, 2019). 143

Figure 5.6: dPCR quantification of methicillin resistance (*mecA*), *S. aureus* (*coA*) and *S. epidermidis* (*femA*) in the four test materials. The materials were identified as a high (Material 1) and a low (Material 2) concentration MRSA, MRSE in a background of MSSA (Material 3), and MRSA in MSSA (Material 4) by comparing the copy number ratios for each gene target. Materials

3 and 4 represent more challenging mixtures that could be representative of clinical scenarios involving co-colonisation of organisms.	145
Figure 5.7: Ratio of <i>mecA</i> to species-specific (host) gene targets for the four materials for each of the laboratories	148
Figure 5.8: Log ₁₀ transformed copy number concentrations for the 22 clinical isolates analysed using the Bio-Rad QX200 and Stilla Naica dPCR platforms. Note that <i>mecA</i> (a) and <i>mecA</i> (b) refer to the value returned for <i>mecA</i> when measured in duplex with <i>coA</i> and <i>femA</i> , respectively, using the QX200. The assay targets were analysed in triplex using the Naica platform, so a single value is plotted for <i>mecA</i>	149
Figure 5.9: Ratios between <i>mecA</i> and <i>coA/femA</i> for samples identified as MRSA and MRSE. QX200 (blue markers), Naica (red markers). Filled markers represent MRSA, unfilled represent MRSE. Expected ratio of <i>mecA</i> to host genomic targets is 1.0.	151
Figure 6.1: (a) Comparison of spectra between six individual Cryobank™ beads; condition i (Section 6.2.6.1). (b) Comparison of spectra obtained for three fresh cultures from a single Cryobank™ bead with fresh sub-culture every 24 hours; condition ii (Section 6.2.6.1). (c) Example of changes to mass spectra plots for condition iii (Section 6.2.6.1). Spectra in red represent organisms at 24 hours; green and blue spectra represent organisms at 48 and 72 hours, respectively. Common peaks were observed at approximately 6150 (*) and 6300 (**) m/z Note the presence of an additional peak at 6100 m/z (indicated by the arrow) after 48 and 72 hours that is absent at 24 hours, and absent in (a) and (b).	168
Figure 6.2: Inter-experimental variability in the number of peaks called for different concentrations of bacterial cell preparations. Key: □ 1 µL loop + volume of extraction reagent (µL) ♦ 0.5 McFarland standard + volume of extraction reagent (µL).	171
Figure 6.3: Evaluating variability in peak intensity and the stability of the bacterial test standard (BTS) across three days. Mean peak intensity is plotted for the summed 15 replicate spectra per day.....	173
Figure 6.4: Evaluating variability in peak height at (a) different stages of MALDI-TOF MS typing of <i>A. baumannii</i> isolates and (b) repeated after one year in storage at -80°C. Each coloured marker represents an isolate of <i>A. baumannii</i> . Keys contain lists of the m/z peaks chosen for the comparison.....	175
Figure 6.5: Workflow for spectral acquisition from bacteria using MALDI-TOF MS. The central arrow represents the overall experimental process from bacterial isolate to characteristic mass spectrum for that organism. Peripheral branches represent various stages of the experimental process that have the potential to introduce variability. Aspects addressed in this chapter are highlighted in green.....	181

Figure 6.6: Hierarchical clustering of *A. baumannii* isolates calculated in (a) BioNumerics and (b) Clover MS data analysis software using UPGMA based on MALDI-TOF MS spectra. The isolates clustered into two main groups: Group I and Group II. The coloured key represents the 8 MALDI Biotypes listed in Table 6.4 (Groups A-H). Note: For (a) cophenetic correlation is indicated at base of each node (Section 10.11.4; Appendix 11). 184

Figure 6.7: Variability in peak height at different stages of the MALDI-TOF MS typing protocol. The 'Group II/MALDI Biotypes B' isolates are represented by the following coloured spots: Red – MBT16-005, Yellow – MBT16-011, Grey – MBT16-039. Unfilled spots represent the other 15 isolates. *m/z* 5178 and 5751 represent peak classes common to all isolates; *m/z* 3723 represents a peak only observed for the Group II/MALDI Biotypes B isolates following analysis in BioNumerics (Section 10.11.4; Appendix 11). 186

Figure 6.8: WGS SNV analysis compared with MALDI Biotypes (Section 10.11.4; Appendix 11). 188

Figure 6.9: Hierarchical clustering of *S. aureus* isolates calculated in BioNumerics using UPGMA based on MALDI-TOF MS spectra. The key represents the 5 MALDI Biotypes listed in Table 6.6 (Groups A-E). Cophenetic correlation is indicated at base of each node. 191

List of tables

Table 3.1: Primer and probe sequences for HIV-1 detection.....	70
Table 3.2: Primers and probes used in interlaboratory analysis of HIV-1 RNA materials	71
Table 3.3: Reverse transcriptase enzymes and kits used in the study.....	73
Table 4.1: Primer and probe sequences for detection of human reference genes.....	101
Table 4.2: Number of HIV DNA copies measured in single replicates of 18 clinical samples using qPCR and the two dPCR platforms. (a) Raw HIV DNA copies measured by qPCR, RainDrop® dPCR and QX200™ dPCR. (b) HIV DNA copies normalised to million cells for the three methods. Approximate input volumes for dPCR refer to the volume loaded into the cartridge prior to droplet generation.	106
Table 4.3: Samples flagged as discrepant following the qPCR-dPCR-dPCR comparison. (a) Raw QX200™ dPCR data for HIV and PDH targets for all 18 samples. Saturation of partitions is indicated by a PDH lambda (λ) greater than or equal to 4.0 (highlighted red). λ values were calculated by subtracting the natural logarithm (LN) of the number of partitions containing no target (w) from LN of the total number of partitions accepted by QuantaSoft for that sample (i.e. positive plus negative partitions in this instance, n). (b) Raw HIV DNA copies per reaction for the 'saturated' samples for each of the three techniques. QX200™ dPCR results are given before and after template dilution.....	107
Table 4.4: Variety of materials used to calibrate quantification of HIV-1 DNA in the literature.	116
Table 4.5: Attributes and limitations of the techniques evaluated in this study for HIV DNA quantification. 'qPCR' and 'dPCR' refer to the specific protocols described in this chapter, although other protocols and platforms exist for these techniques.....	118
Table 4.6: Approximate reaction and sample volumes analysed and lost depends on the number of accepted partitions per reaction well using the QX200™ dPCR platform. The maximum number of partitions (23,981) is based on the assumption that all 20 μ L reaction volume is converted into droplets, and assuming a partition size of 0.834 nL (Corbisier et al., 2015). The values given for 'accepted number of partitions per reaction' are examples based on typical experiments performed in this study.....	120
Table 5.1: Primer and probe sequences for detection of <i>Staphylococcus</i> spp.....	130
Table 5.2: Copies per μ L for each of the assays analysed in duplex using genomic DNA as template.....	135
Table 5.3: Dynamic range of assays for analysis of (a) MRSA and (b) MRSE ATCC genomic DNA. Results are expressed as copies per μ L in the neat extract.	137

Table 5.4: Mean copies per μL for each dilution point depicted in Figure 5.4. The observed % abundances based on the copy number ratios for each of the assays correlate strongly with the expected values.....	141
Table 5.5: Copies per μL reported from three laboratories obtained for four different materials. Each value represents the concentration obtained from the extraction of three different units of each material across three different days and triplicate reactions analysed using dPCR. Relative standard uncertainties are shown expressed as a percentage. N/A: not applicable, LOQ: limit of quantification, n.d.: not detected (EURAMET, 2019).	147
Table 5.6: Analysis of clinical isolates on the Naica and QX200 dPCR platforms. Assays were applied in triplex (all three assays in one reaction) and duplex (two in one reaction) on the respective platforms.....	150
Table 5.7: Comparison of qPCR and dPCR interpretations following analysis of 22 residual DNA extracts from clinical samples. qPCR data were obtained as part of the routine diagnostic service provided by the Department of Microbiology at Great Ormond Street Hospital for Children NHS Foundation Trust. NQ – not quantified, which was defined when copy number was $< 2 \text{ cp}/\mu\text{L}$. ND – not done.....	153
Table 6.1: Bacterial cell concentration was shown to impact upon the number of peaks that were identified in MALDI-TOF MS spectra. Note that lower volumes were added to the 0.5 McFarland pellets, which were smaller than with the 1 μL loop pellets owing to lower initial input CFU per mL.	170
Table 6.2: MALDI-TOF MS peak classes identified as potential biomarkers for strain typing isolates of <i>A. baumannii</i> using the Bruker FlexAnalysis method. Shaded boxes indicate the presence of a peak, blank boxes represent absence.	177
Table 6.3: UniProtKB/Swiss-Prot search results for <i>A. baumannii</i> (Tax ID: 470) performed using TagIdent tool (https://web.expasy.org/tagident/) compared with the full range of peaks for the 18 isolates classified using each method. MW range for the search was 2 to 9 kDa. Presumed matched ribosomal proteins (Da) and corresponding m/z peaks ($\pm 20 \text{ Da}$) detected using each approach are highlighted in green.	179
Table 6.4: Bruker MALDI Biotyper groups assigned to each of the 18 <i>A. baumannii</i> isolates based on presence or absence of visually chosen mass to charge (m/z) peak classes.....	183
Table 6.5: Biomarker peak classes for strain typing <i>Staphylococcus aureus</i> isolates identified using the Bruker FlexAnalysis Biotyper approach. Shaded boxes represent the presence of a peak, blank represents absence.....	190
Table 6.6: Bruker MALDI Biotyper groups assigned to each of the 11 <i>S. aureus</i> isolates based on presence or absence of visually chosen peak classes.....	191

Non-standard abbreviations

ART – Antiretroviral Treatment

BHQ-1 – Black Hole Quencher-1

CFU – Colony forming units

CLED – Cystine lactose electrolyte deficient agar

Cq – Quantification cycle

Cy5 – Cyanine-5

ESBL – Extended Spectrum β -lactamase

EQ – Eclipse quencher

FAM (6-FAM) – 6-Carboxyfluorescein

GES-5 – Guiana extended spectrum (beta lactamase)-5

HCCA – α -Cyano-4-hydroxycinnamic acid

HEX - 6-carboxy-2 ,4,4 ,5 ,7,7 -hexachlorofluorescein succinimidyl ester

HIV – Human Immunodeficiency Virus

IABkFQ – Iowa Black® Dark Quencher

LTR – Long terminal repeat

MALDI-TOF MS – Matrix Assisted Laser Desorption/Ionization Time-of-Flight Mass

Spectrometry

MDR – Multidrug resistant

MGB – Minor groove binder

MRSA – Methicillin Resistant *Staphylococcus aureus*

MRSE – Methicillin Resistant *Staphylococcus epidermidis*

NDM – New Delhi Metallo-beta-lactamase

NFQ – Non-fluorescent quencher

PCR – Polymerase Chain Reaction

dPCR – Digital Polymerase Chain Reaction

qPCR – Quantitative Polymerase Chain Reaction

PDH – Pyruvate dehydrogenase

VIM – Verona integron-encoded metallo- β -lactamase

VRE – Vancomycin-resistant Enterococci

1. Introduction

1.1. Introduction to metrology

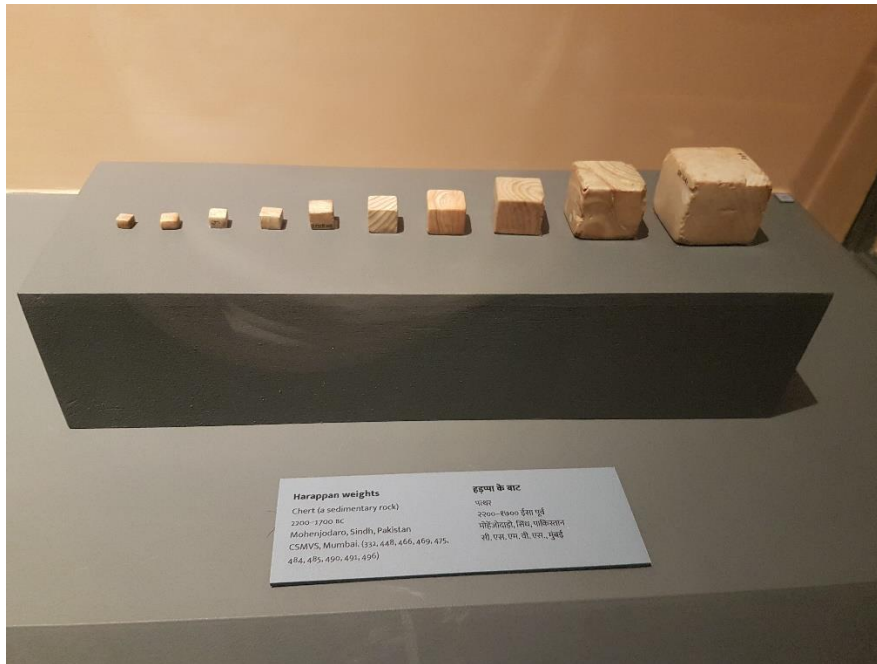
1.1.1. *What is metrology?*

Metrology, defined as the scientific study of measurement, is well established within manufacturing, engineering and physical sciences (Lindqvist *et al.*, 2016, Ameta *et al.*, 2011, Stuart *et al.*, 2016, Richard, 2014, Teague, 1989). Metrology supports quality consistency in production, reliability of infrastructures and consumer safety by ensuring that measurements are accurate. Accurate measurements help to ensure that pharmaceutical compounds present in medicines are of high purity and within the therapeutic dose ranges, and ensure that ingredients in food products are included at correct quantities and are of sufficient quality to maintain labelling accuracy, nutritional value and appeal to the senses. Accuracy in measurement enables precise determination of the quantity of fuel filling a car's tank and the monetary cost associated with it, and determine the distance subsequently driven in the car (Felton, 2013, Amato and Galvez, 2015, Losada-Urzáiz *et al.*, 2015, Rychlik *et al.*, 2018). Promoting the underpinning principles of metrology in analytical science can assist in the development of new methodologies to produce high-quality, reproducible data. This holds relevance for global health, particularly through clinical diagnostics, where accuracy in measurements has implications for setting thresholds between healthy and disease states, monitoring disease progression, and establishing cures.

1.1.1.1. *A brief history of measurement*

Measurement can be defined as the process of experimentally obtaining one or more values that can be attributed to quantity by comparison with another entity (Joint Committee for Guides in Metrology, 2012). Early records of measurement systems date back to the 3rd or 4th millennium BC, developed by ancient civilisations for the purposes of agriculture, trade and construction. Details of the cubit, used to measure length of an object compared to the length of the forearm from the elbow to the tip of the middle finger, have been found in Egyptian and Babylonian records dating back to 2nd millennium BC (Stone, 2014). Archaeological findings from Harappa, Pakistan, serve as evidence of precise stone weighing apparatus from approximately the same era (Petrucci, 1981) (Figure 1.1).

Figure 1.1: A set of Harappan weights displayed in Mumbai, India



As civilisations expanded, so did industry and technology and with them the requirement for more sophisticated and standardised measurement systems. Preliminary calculations for the meter and kilogram were defined in the 18th century during the French Revolution, serving as precursors to the metric system of measurement units which were enforced in France in 1795 (Hallerberg, 1973, Moreau, 1953). The metric system of measurement became widely adopted as a unified, global measurement system in science and commerce. This was reinforced by the signing of The Metre Convention in Paris in 1875 by representatives of 17 nations, along with the foundation of the International Bureau of Weights and Measures (BIPM), establishing a standardised organisational framework to coordinate the international system of measurement.

The Convention was modified to expand scope within the discipline of physics in 1921, and in 1960 following the 11th General Conference on Weights and Measures (CGPM), the International System of Units (SI) was formally introduced. Many of the SI base units were initially defined by physical objects, such as the kilogram (kg), which was defined by a mass of platinum-iridium alloy kept under a specific set of conditions. However, the evolution and progression of the sciences during the 20th century necessitated a system that is independent of physical entities (Stock *et al.*, 2019). The most recently revised SI base units, as of 20th May 2019, are defined in terms of constants that describe the natural world including the speed of light in a vacuum c , the Planck constant h and the Avogadro constant N_A (BIPM., 2019). The SI serves as the international standard for measurements, enabling traceability and standardisation of values for time, length,

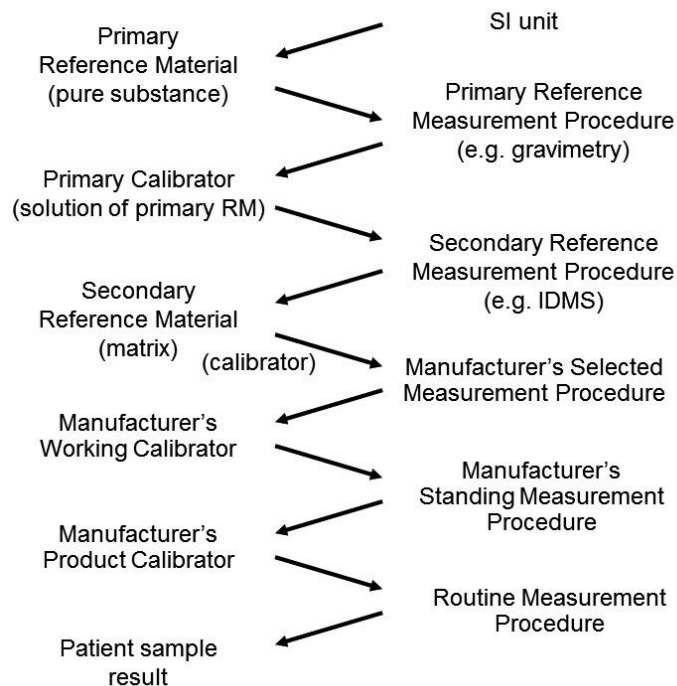
mass, electric current, thermodynamic temperature, amount of substance and luminous intensity. These units are widely implemented across various scientific fields, particularly within the physical and chemical disciplines.

1.1.1.2. Analytical accuracy in measurement

1.1.1.2.1. Reference materials and traceability

The most accurate measurements are those that best represent a true value, defined by a known value or a standard (Joint Committee for Guides in Metrology, 2012) (further definitions of metrological terms can be found in Appendix 1). Accuracy can be facilitated using reference standards or materials against which measurements can be made. A reference material is defined as a “material, sufficiently homogeneous and stable with respect to one or more specified properties, which has been established to be fit for its intended use in a measurement process” (Wise, 2018). Calibration of equipment and standardisation of analytical procedures using reference materials can help to ensure measurement traceability (Akdogan, 2018), defined as unbroken chain of calibrations relating back to a reference. Ensuring traceability enables 1) the reproducibility of a measurement to be demonstrated by ensuring that it is traceable to a pre-defined unit or process that can be repeated in future and 2) to establish the ‘trueness’ of a measured value. Discussion of true metrological traceability often centres around the SI, where a measurement can be traceable back to the defining constant of the SI unit (De Bièvre, 2010). Idealistically, a traceability chain can be followed from a clinical analyte back to the SI via end-user standard operating procedures (SOPs), secondary calibrators, reference measurement procedures and primary reference materials as detailed in Figure 1.2.

Figure 1.2: Calibration traceability chain for a clinical measurement (Gantzer and Miller, 2012)



A primary reference material relates to a pure substance that is directly traceable to the SI. This material may be a single compound, such as cholesterol, which can be used to initiate traceability for measuring cholesterol in serum and plasma (Thomas *et al.*, 2012). Primary reference materials are an important aspect of demonstrating traceability since they form the metrological foundation for the value assignment of secondary reference materials (Bunk, 2007). Secondary, or matrix-based reference materials, are used by manufacturers of commercial diagnostic platforms to evaluate the accuracy and trueness of their own calibrators. Using the cholesterol example above, a secondary reference material might be a pool of plasma from healthy donors spiked with known quantities of the pure cholesterol standard.

1.1.1.2.2. Measurement error: precision and bias

To best represent a true value, the most accurate analytical measurements will be unbiased and fall within the expected measurement range. In addition, an accurate measurement will be precise with minimal variability between repeats. These factors are encompassed by the term 'measurement error', which contributes to the uncertainty surrounding a measurement.

Measurement uncertainty is a statistical parameter representing a range within which the true value lies (Meyer, 2007). In general, measurement error is classified as 'random' or 'systematic'. Random error is inherent to and expected of an experiment; it may occur due to changes in the environment (e.g. laboratory temperature), instrument limitations and day effects (e.g. natural variability in how an analyst would pipette between experiments), and how the data are analysed (e.g. rounding up or down of values). This can be attributed to measurement precision between replicates, within and between experiments, analysts or centres. Systematic error will impact upon measurements to the same effect and is often the result of a controllable variable. For example, systematic error may occur when instrumentation is calibrated incorrectly, such as a pipette or balance, which can introduce bias and impact upon the trueness of downstream measurements. Bias can also be introduced by measurement against an inaccurate or incorrect reference standard, highlighting how each of these aspects function as a dynamic system to enable the most accurate measurements (Hutcheon *et al.*, 2010).

Figure 1.3: Schematic representation of random and systematic error in a set of measurements that can result in reduced accuracy.

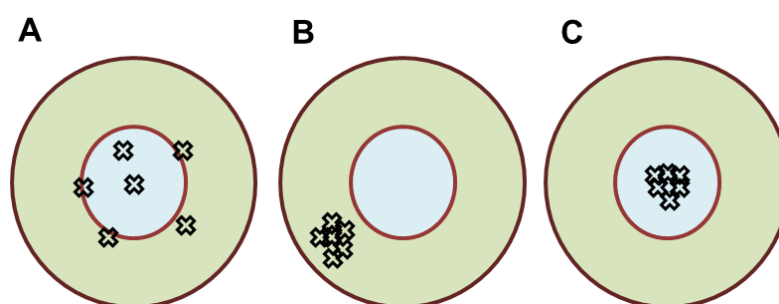


Figure 1.3 depicts a schematic representation of random and systematic error in a set of measurements that can contribute to measurement uncertainty and result in reduced accuracy. The blue central circle represents the expected range for a value, and the shaded green area represents values outside of this range. The crosses represent six replicate measurements in an analytical process. In scenario A the replicate measurements fall within the expected range, suggesting that systematic bias is small and could indicate that the procedure has been calibrated correctly. However, the replicate measurements appear to be highly variable indicating reduced precision. This could represent measurements made using a technique that is sensitive to subtle changes in the laboratory environment. In this scenario, attempts to keep error to a minimum could include keeping the instrumentation in a temperature-controlled laboratory. This may serve

to improve precision and increase measurement accuracy. In contrast, scenario B represents a set of precise measurements. However, they appear to be biased away from the expected range which may have been introduced by inaccurate calibration. This situation could be controlled for by ensuring that the reference material used to calibrate the instrument is within specification and appropriate, and that the calibration procedure was followed correctly. In scenario C the set of measurements appear to be unbiased and precise, suggesting that they are more accurate.

1.1.2. Metrology in the biological sciences

1.1.2.1. The concept of 'bio-metrology'

Metrological concepts are relatively new within biological fields compared to the physical and chemical sciences. Biological entities are complex and prone to variability, which can lead to greater uncertainty in associated analytical measurements (Coxon *et al.*, 2019). An example of this is the measurement of bone density in humans using dual-energy X-ray absorption. The method itself obeys physical parameters for density, volume, and weight. However, measurement is complicated by inherent variations in physiological parameters such as bioavailability and adsorption of nutrients into the bone, which can vary within and between subjects. This could present difficulties for establishing 'normal' ranges and thresholds for healthy versus disease states, where measurements may be influenced by significant variability even for an individual patient (Iyengar, 2007). This illustrates the necessity for systematic evaluation of method variability to assign appropriate measurement uncertainties and set standard values, against which other measurements can be compared. This could improve accuracy of measurements for bone density and ensure that reproducible data are obtained.

Bio-metrology should be regarded and promoted as a critically important area of modern metrology (Park *et al.*, 2012). The field holds a key role in clinical care to ensure that erroneous measurements do not, ultimately, jeopardise patient safety and public health (Squara *et al.*, 2015). This maintains relevance for techniques that utilise molecular biology, which are widespread within clinical diagnostics. The introduction of molecular techniques to clinical diagnostics has revolutionised how diseases are detected, treated and monitored (Tang *et al.*, 1997, Speers, 2006). Biological macromolecules can be utilised as biomarkers, where determination of their structure, sequence and number can assist with diagnosis of disease, and monitoring responses

to treatment. A plethora of commercial molecular platforms are available to clinical and research laboratories, alongside in-house protocols (Adams, 2015). To support such widespread adoption and utilisation of these methods it is critical that measurements of molecular biomarkers are accurate, reproducible and reliable. Implementation of sound metrological principles within molecular diagnostics can facilitate accuracy in measurement and continue to support the field within clinical diagnostics.

1.2. Molecular measurements and infectious diseases

1.2.1. Diagnosis of infectious diseases

Humans and diseases such as malaria, cholera, tuberculosis (TB) and leprosy have had long-standing relationships with one another, with cases still being reported in the 21st century (Karlsson *et al.*, 2014). The introduction of antimicrobial drugs and vaccines to modern medicine, along with improved hygiene practices, has reduced the impact of infections on humans and contributed to a general increase in global life expectancy (Brachman, 2003). The development of microscopy methods, staining protocols and culture-based techniques historically aided the detection and diagnosis of micro-organisms responsible for disease. In addition, rapid and specific diagnoses have been facilitated by the incorporation of molecular technologies into clinical microbiology laboratories. Molecular approaches can provide alternatives to culture based methods that rely on phenotypic characteristics of microorganisms (Pavsic *et al.*, 2015, Honeyborne *et al.*, 2014, Benagli *et al.*, 2011, Kothari *et al.*, 2014). Suitable diagnostic methods are necessary to continue to detect infections with long-established pathogens, which prevail alongside newly emerging threats linked to increased human migration and travel.

Numerous viral diseases have emerged over the past century leading to national and international epidemics, and pandemics, including the 1918 H1N1 'Spanish flu', HIV/AIDS, Ebola, Zika, severe acute respiratory syndrome (SARS), Middle East Respiratory Syndrome (MERS) and coronavirus disease 2019 (COVID-19). Occasional smaller scale outbreaks of bacterial diseases including plague and cholera are also reported in endemic regions such as Madagascar and Yemen, respectively (Bloom and Cadarette, 2019). The mounting threat of antiviral and antimicrobial resistance contributes to a weakened ability to control outbreaks, which could result in increased mortality particularly within immunocompromised groups. The growing number of modern

outbreaks has led to countries devising plans to cope with future epidemics or pandemics. In particular, the 2003 SARS pandemic and 2014 Ebola outbreak in West Africa exposed gaps in preparedness in terms of disease detection, contact tracing and quarantine procedures, among other aspects. These shortcomings are particularly evident in resource-limited settings and highlight the necessary role of diagnostic infrastructures for diseases that may present with generalised indicators, such as respiratory symptoms or fever (Madhav *et al.*, 2017).

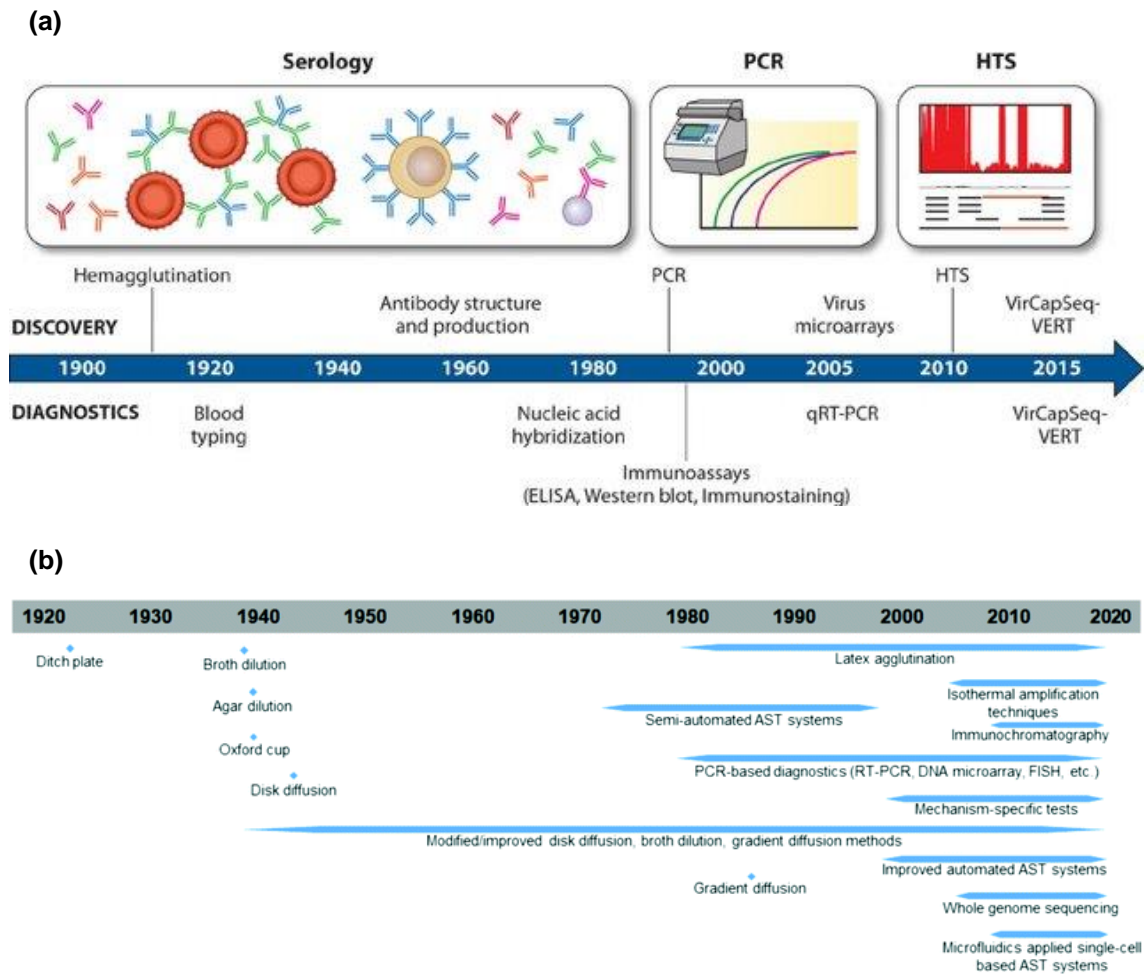
Diagnostics are a fundamental part of outbreak containment, with each pathogen presenting unique challenges (Kelly-Cirino *et al.*, 2019). Molecular methods in particular have become an essential tool in the detection and diagnosis of many emerging infectious diseases (Dong *et al.*, 2008, Dwivedi *et al.*, 2017). The COVID-19 global pandemic, which emerged early in 2020 and is caused by the pathogen SARS-CoV-2, has so far resulted in the infection of over 40 million people with the novel coronavirus (World Health Organisation, 2020b); 08th November 2020. Detection of the virus to track the spread of disease, and control the outbreak in lieu of cure or vaccination, has largely been facilitated by rapid development of molecular approaches. These approaches can be developed at short notice to detect the viral genome, even in the absence of comprehensive sequence information. The pathogen shares similarities to SARS-CoV (Xu *et al.*, 2020), which served as a basis for development of assays whilst sequence data for the novel virus were being obtained (Corman *et al.*, 2020). Prompt design and publication of such approaches enabled widespread adoption of assays for in-house testing, diagnostic use and emergency release of commercial products. However, the rapidly evolving nature of the pandemic and haste for new diagnostic methods presents a key opportunity to highlight the importance of standardisation and analytical accuracy in measurement within molecular diagnostics; a consideration for emerging infectious diseases both present and future (Huggett *et al.*, 2020a, Huggett *et al.*, 2020b).

1.2.2. Molecular methods for detection, quantification and advanced analysis of pathogens

Technological advances within molecular biology over the past 50 years have continued to expand and improve upon diagnostic capabilities for infection. A growing repertoire of methodologies is available for sensitive, specific and comprehensive analyses of molecular biomarkers for viral, bacterial, fungal and parasitic diseases. Development of methods for

detecting pathogen nucleic acids, including polymerase chain reaction (PCR) and high throughput sequencing (HTS), has enabled rapid analysis of pathogen genetic sequences for numerous diseases. Figure 1.4 shows a timeline illustrating how diagnostic methods for infectious diseases, namely viruses and antimicrobial resistant bacteria, have developed over the past century. Methods for detection of nucleic acids are prevalent in the latter portion of each timeline, following the discovery of PCR. Nucleic acid amplification techniques (NAATs) feature heavily in the modern armoury of molecular tests for infectious diseases (Caliendo *et al.*, 2013), and have significantly influenced the landscape of diagnostic testing. Nucleic acid-based approaches offer advantages over conventional culture-based methods for detecting fastidious organisms such as *Bartonella* spp and *Yersinia pestis* (Fenollar and Raoult, 2004), or for pathogens that carry infection risks during culture such as SARS-CoV and MERS-CoV (Ginocchio, 2016). In addition, technologies such as matrix-assisted laser desorption/ionisation time-of-flight mass spectrometry (MALDI-TOF MS), which are capable of measuring proteins and other molecules, enable rapid detection and identification of organisms responsible for symptomatic infections and sepsis. Molecular methods can facilitate pathogen detection where organisms are present in low numbers and are able to differentiate between strains where this would otherwise be unachievable, based on phenotypic methods.

Figure 1.4: Development of methods for detection of (a) viral diseases (Rasmussen, 2015) and (b) antimicrobial resistant bacteria (Shanmugakani et al., 2020) over the past century.



Molecular methods are also used to quantify pathogens in a range of clinical sample types, which can be of great benefit to infectious disease diagnostics (Turano and Pirali, 1988). Quantifying changes in pathogen load over time can assist with monitoring response to therapy. In addition, quantitative information may be correlated with disease severity, and may help to set thresholds for pathogen carriage versus invasive disease. Virology possesses some of the furthest advancements in quantitative molecular diagnostics for infection (Gullett and Nolte, 2015). Commercially available assays and reference standards for quantifying nucleic acids are employed for monitoring human immunodeficiency virus 1 (HIV-1), hepatitis B and C (HBV & HCV) and human cytomegalovirus (HCMV) viral load (Watzinger *et al.*, 2004), to assist in patient management. Absolute quantification and measurement of log decline of HCV viral load has directly been applied clinically as a marker for shortening antiviral strategies in treatment naive, non-cirrhotic patients (Terrault *et al.*, 2005). Quantitative viral load measurements for less common filoviral diseases including Ebola and Marburg are also of interest to clinicians as they

can be predictive of disease severity, survival and infectivity, and for establishing detection limits for diagnostic assays (Cnops *et al.*, 2016). The role of quantification in clinical microbiology is relatively new compared to virology, and current applications tend to be research-led. However, bacterial load quantification has been described for numerous pathogens and sample types including TB in sputum (Honeyborne *et al.*, 2011), total bacterial load in stool samples (Brukner *et al.*, 2015), airway microbiota in cystic fibrosis patients (Zemanick *et al.*, 2010) and for determining disease severity in meningococcal disease (Darton *et al.*, 2009).

In addition to quantification, the role of advanced molecular analyses of microbes continues to develop for understanding disease dynamics and surveillance of infections. This specifically relates to emerging approaches in infectious diseases including next generation sequencing, mass spectrometry methods such as MALDI-TOF MS, and Fourier-transform infra-red (FTIR) spectroscopy. These methods are capable of processing large datasets for entire proteomes, genomes and 'moleculomes' (i.e. analysis of unique, combined lipid, carbohydrate, protein, nucleic acid, etc fingerprints by FTIR (Vogt *et al.*, 2019)), respectively. Characterisation of these complex biochemical repertoires can help to create unique profiles for pathogens, and to infer relationships between organisms of the same species for the purposes of surveillance and outbreak control.

1.2.3. Nucleic acid-based methods

1.2.3.1. Introduction to polymerase chain reaction (PCR)

Early approaches utilising DNA probe hybridisation technologies, such as colony hybridisation by Southern blotting, were used for detecting nucleic acids from bacterial pathogens, including enterotoxigenic *Escherichia coli*, *Mycobacterium tuberculosis* complex and *Neisseria gonorrhoeae* (Moseley *et al.*, 1980, Musial *et al.*, 1988, Lewis *et al.*, 1993). These approaches enabled rapid, specific detection of microbial gene targets, circumvented the need for culture and were able to demonstrate relatedness between bacterial strains (Tang *et al.*, 1997). Many of these approaches were superseded by polymerase chain reaction (PCR), which has been at the forefront of the molecular revolution since its inception in 1983 (Mullis and Faloona, 1987). PCR is an enzyme-driven method of amplifying a single DNA molecule through thermal cycling. A segment of the target sequence referred to as the amplicon is amplified exponentially generating,

in theory, billions of copies of DNA (Yang and Rothman, 2004). Following conventional PCR cycling the resulting amplicon product is analysed at endpoint, which usually involves electrophoretic methods using fluorescent dyes to detect that the correctly sized amplicon has been produced.

PCR has had a significant impact on the diagnosis and management of infectious diseases. Early assays for detection of *Mycobacterium tuberculosis* (MTB) demonstrated PCR to be comparable to culture in terms of sensitivity, specificity and positive/negative predictive values, with results obtainable after around 6.5 hours (D'Amato *et al.*, 1995). Culture-based methods for diagnosing MTB can take up to 14 days to be detected (Pfyffer and Wittwer, 2012), highlighting the potential benefit to patient care if time-to-diagnosis can be reduced. The utility of PCR as an adaptable and versatile technique for diagnosing infectious diseases can be demonstrated across a breadth of applications. PCR can provide sensitive detection of pathogen genomic material in biological samples that are difficult to obtain, or contain low numbers of organism, including: cerebral spinal fluid (CSF), amniotic fluid, urine, saliva and respiratory secretions (Taberlet *et al.*, 1996). Adaptations of the technique such as nested PCR, which involves two sequential amplifications using different primer pairs, have been applied for PCR detection of *Plasmodium* spp in epidemiological surveys (Li *et al.*, 2014). PCR can be used to target the bacterial 16S ribosomal DNA (known as broad-range PCR) in clinical bacteriology as a pre-cursor to microbiome studies (Patel *et al.*, 2017). PCR can be effectively optimised to suit complex templates, including those that are GC rich. The technique can also be applied in multiplex (i.e. detecting more than one gene target at once) to conserve reagents, reduce time to results and infer possible relationships between targets (Henegariu *et al.*, 1997).

PCR can enable the detection of pathogen RNA by combining the technique with reverse transcription, facilitating amplification of viral RNA genomes and transcripts from viable organisms (Sheridan *et al.*, 1998, Yang and Rothman, 2004). Reverse transcription possesses the general purpose of converting RNA into complementary DNA (cDNA) (Baltimore, 1970). This is facilitated by reverse transcriptase, an RNA dependent DNA polymerase. In the context of reverse transcription PCR (RT-PCR), RNA is converted to cDNA as a more stable, RNase resistant substrate for PCR amplification. This is often performed using a primer complementary to the 3' end of the RNA template which directs the first-strand cDNA synthesis. PCR then proceeds as described above. Reverse transcription can be performed as a separate reaction, and the cDNA

subsequently added to the PCR reaction (known as two-step RT-PCR). Conversely the two reactions can take place in the same tube, ensuring that an incubation step for reverse transcription is performed prior to PCR (referred to as one-step RT-PCR). Commonly used reverse transcriptases for RT-PCR include those of the Avian Myelomatosis Virus (AMV) or the Murine Moloney Leukaemia Virus (MMLV), and a vast catalogue of commercial enzymes are available. Choice of reverse transcriptase, among other factors, is a key factor in the efficiency and success of an RT-PCR experiment (Barragán-González *et al.*, 1997). Considerations for choosing enzymes for RT-PCR are discussed in further detail in Chapter 3.

1.2.3.2. *Real-time PCR (qPCR)*

Further adaptation and evolution of conventional PCR involved the development of real-time PCR (qPCR), enabling simultaneous amplification and detection of amplicon (Yang and Rothman, 2004). The ability to detect PCR amplification in real time reduces the length of the analysis phase by eliminating the requirement for electrophoretic gels, which are necessary for conventional methods. qPCR follows the same basic principles as conventional PCR, except that the accumulation of new double stranded DNA (dsDNA) PCR product can be monitored in real time by capturing changes in fluorescent signal after each PCR cycle. This is achieved using dsDNA intercalating dyes such as SYBR® Green, or fluorescently labelled internally binding DNA probes such as hydrolysis probes. Fluorescently labelled probes, which are specific to the sequence of interest, have the benefit of improving specificity for target amplification. Probe-based qPCR assays have gained popularity for infectious disease diagnostics (Kralik and Ricchi, 2017). In addition, commercial availability of numerous fluorophores with different emission spectra for probe-based chemistries enables detection of several targets in multiplex and in real-time.

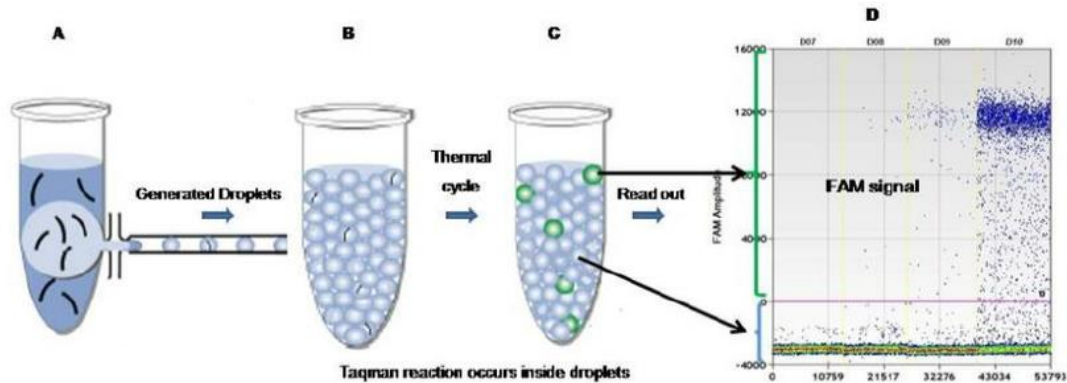
Initial detection of DNA amplification in the reaction is signalled by the point at which fluorescence is distinguishable from the background, referred to as the quantification cycle (C_q) (Huggett *et al.*, 2013). The C_q value corresponds to the PCR cycle number at which a signal was detected for the target sequence, representing a 'crossing point' or threshold for amplification. Positive amplification of the target of interest can be used qualitatively to infer presence or absence. In addition, C_q values can be used quantitatively. This is performed by comparing C_q values for an unknown sample to that obtained for a calibration standard of known quantity, which is included in the same experiment. A dilution series of the standard is constructed and analysed, and the

instrument response (Cq values) plotted against the logarithm of the input quantity (for example, in copies per reaction, or copies per μL in the initial sample). The Cq value obtained for the unknown sample can then be extrapolated against the standard curve to determine the input quantity, expressed in the same units as the calibration standard (Bustin *et al.*, 2009, Kralik and Ricchi, 2017). Accurate quantification by qPCR necessitates that the standard used for the dilution series is well characterised, free from inhibition and representative of the unknown sample matrix, where possible. qPCR has been described as the 'current gold-standard method' for quantitative analysis of nucleic acids (Nolan *et al.*, 2013). The ability to accurately quantify pathogen load by qPCR has become essential for the detection and management of numerous infections. When combined with reverse transcription, RT-qPCR has facilitated viral load quantification for pathogens such as HIV-1, hepatitis C and coronavirus which can directly influence transmission risk and clinical management of patients (Clementi *et al.*, 1993, Berger *et al.*, 1998, Gibellini, 2004, Yu *et al.*, 2020).

1.2.3.3. *Digital PCR (dPCR)*

The concept of digital PCR (dPCR) was first described in the 1990s (Morley, 2014), however the technique has predominantly emerged within the last decade as a novel method for quantification of nucleic acid (Huggett and Whale, 2013, Huggett *et al.*, 2016). dPCR involves partitioning a reaction so that a proportion of the partitions contain the nucleic acid template, and some do not. Thermal cycling commences in a similar manner to qPCR using fluorescence-based chemistries (most commonly hydrolysis probes, although dsDNA intercalating dyes can be used (Miotke *et al.*, 2014)), with individual PCR reactions occurring in each of the partitions. At end point of amplification, binary counting of positive (k) and negative (w) partitions is performed based on whether a fluorescent signal is detected or not (Figure 1.5). The average number of targets present in a partition, lambda (λ), can be calculated based on the number of negative partitions relative to the total number of analysable partitions (n) (Huggett *et al.*, 2013). The λ value can then be used to calculate the concentration of nucleic acid in the starting template, accounting for partitions that may have contained more than one nucleic acid molecule prior to cycling.

Figure 1.5: Sample partitioning, thermal cycling and detection of fluorescence that takes place during digital PCR. A total reaction volume containing template (A) is split into multiple partitions under pressure (B). Each partition hosts an individual PCR reaction (C), and the resulting fluorescent signal is detected. Partitions are categorised as positive or negative (D) (Dongngam *et al.*, 2015).



As the technique has become more popular among the scientific community, a growing number of commercial dPCR platforms have become available. These are broadly separated into those involving fixed-volume chamber-based partitioning (Fluidigm™ Biomark, Applied Biosystems/Life technologies™ QuantStudio™ 3D) and those that sequester the reaction into oil-based partitions (Bio-Rad QX200™ Droplet Digital™ PCR system, Stilla Technologies Naica). Current approaches offer between 765 and 10 million partitions that range from 5 pL to 6 nL volume per partition, depending on the platform (Rutsaert *et al.*, 2018a). dPCR has been validated for absolute quantification of DNA (Sanders *et al.*, 2011) and RNA (Sanders *et al.*, 2013) templates, and has become an attractive technique for molecular diagnostics. The method offers precise quantification of target sequence that can be achieved without the need for a standard curve (Kuypers and Jerome, 2017). dPCR can be applied to quantify targets that are present at low copy number (Huggett *et al.*, 2015), and is well suited to multiplexing to deduce complex relationships between targets in a sample (Whale *et al.*, 2016b, Taylor *et al.*, 2017). There is growing interest in using dPCR to value assign calibration materials for diagnostic qPCR assays, and in integrating dPCR into clinical workflows (Huggett *et al.*, 2015).

dPCR has a broad spectrum of potential applications within microbiology and pathogen quantification (Powell and Babady, 2018). Numerous applications for dPCR have been demonstrated within virology, particularly for rarer pathogens and those that lack suitable qPCR reference materials (Salipante and Jerome, 2019). Absolute quantification offered by dPCR has been used to explore viral load quantification compared with qPCR for HCMV (Hayden *et al.*,

2013), numerous applications within HIV-1 research (Trypsteen *et al.*, 2016), to detect rare mutations associated with drug resistance in influenza (Whale *et al.*, 2016a), and evaluate the clinical significance of chromosomally integrated human herpesvirus (Sedlak *et al.*, 2014). The utility of dPCR is also described for quantification of bacterial gene targets, such as for *Staphylococcus* spp (Kelley *et al.*, 2013, Ziegler *et al.*, 2019b), *M. tuberculosis* (Devonshire *et al.*, 2016a) and *Chlamydia trachomatis* (Roberts *et al.*, 2013). Interest in dPCR applications extends beyond viral and bacterial pathogens including; quantification of low-level fungal gene targets in neonates (Li *et al.*, 2019), detection of *Schistosoma japonicum* DNA in a range of clinical sample types (Weerakoon *et al.*, 2017) and *Ascaris lumbricoides* eggs in water sources (Acosta Soto *et al.*, 2017), as a tool to standardise quantitative studies for *Plasmodium* spp (Koepfli *et al.*, 2016) and numerous other parasitic infections (Pomari *et al.*, 2019). This diverse set of examples demonstrates the utility of dPCR in numerous fields of pathogen research, and the potential of the technique as an emerging *in vitro* diagnostic (IVD) tool.

1.2.3.4. *Isothermal nucleic acid amplification approaches*

Isothermal nucleic acid amplification methods, such as loop-mediated isothermal amplification (LAMP), transcription-mediated amplification (TMA) and nucleic acid sequence-based amplification (NASBA), form the basis of many commercial tests for clinical quantification of pathogen nucleic acids (Ginocchio, 2004). TMA, which is a popular technique for detection of *C. trachomatis* and *N. gonorrhoeae* in clinical microbiology laboratories, is well established for quantification of viruses such as HIV-1 (Oehlenschläger *et al.*, 1996, Ginocchio *et al.*, 2003, Manak *et al.*, 2016), HBV (Chevaliez *et al.*, 2017a) and HCV (Hofmann *et al.*, 2005, Chevaliez *et al.*, 2017b), using the Aptima Quant Dx (Hologic) and NucliSens (bioMérieux) tests. TMA (which is synonymous with NASBA (Singleton, 2000)) differs from qPCR in that amplification occurs at a single temperature and targets the RNA template instead of DNA. Similarly to qPCR, quantification using isothermal methods requires dilutions of a standard of known concentration against which the unknown sample will be compared. The threshold time (T_t), a similar metric to C_q for qPCR, is used for quantification of the unknown sample (Nixon *et al.*, 2014b). The instrument response for the unknown sample can be extrapolated from the standard curve, enabling the results to be reported in the desired units (e.g. copies per μL). Advantages of isothermal nucleic acid amplification methods over PCR-based approaches include the fact that

thermal cycling equipment is not required, making these techniques an attractive option for resource-limited settings. However, techniques such as LAMP have been demonstrated to be several orders of magnitude less sensitive than qPCR for quantifying viral sequences (Nixon *et al.*, 2014a). This puts LAMP at a potential disadvantage for detection and quantification of low numbers of pathogens.

1.2.3.5. Next generation sequencing (NGS)

Next generation sequencing (NGS) is an emerging genomic method that is gaining traction as a key laboratory technique for diagnosis and monitoring of infectious diseases. An increasing number of NGS methodologies have become available since the emergence of the Sanger DNA sequencing method in 1977. Improved accessibility of sequencing platforms and reducing costs have led to increased interest in applying NGS to clinical microbiology, particularly in laboratories that already have molecular capabilities. Popular approaches for NGS include Solexa HiSeq and MiSeq sequencing (Illumina, USA) and, more recently, Nanopore sequencing (Oxford Nanopore Technologies, UK) (Kulski, 2016). Most sequencing studies for infectious diseases involve targeted amplicon sequencing or whole genome sequencing (WGS). Both methods have been applied to drug resistance mutation testing and surveillance, pathogen identification, microbiome studies and genotypic characterisation (Lefterova *et al.*, 2015). WGS, which offers *de novo* assembly of genomes, has the potential to provide a broader analysis compared to amplicon sequencing, offering more information on drug resistance through a full spectrum of genes, facilitating better resolution (Brumfield *et al.*, 2020). WGS has also emerged as a new reference method for bacterial strain typing (Fitzpatrick *et al.*, 2016). Application for this purpose tends to be on an *ad hoc* basis by reference laboratories (Lewis *et al.*, 2010, Izwan *et al.*, 2015, Fang *et al.*, 2016, Alouane *et al.*, 2017, Li *et al.*, 2017), and the feasibility of adopting the technique into routine practice is still to be fully evaluated (Willems *et al.*, 2016, Venditti *et al.*, 2018). NGS technologies also hold a promising role for metagenomic analysis of clinical samples for a number of diseases (Pallen, 2014, Miao *et al.*, 2018, Dekker, 2018, Gu *et al.*, 2019). Although not routinely available in routine microbiology laboratories, NGS is used for variant detection in clinical diagnosis of hereditary disorders and genetic testing (Hartman *et al.*, 2019). Implementation may presently be limited by cost of equipment and requirement for experience in bioinformatic

analysis, however standardisation of protocols and guidance for data analysis could lead to a more rapid uptake of the technique for routine microbiology laboratories (Olson *et al.*, 2015).

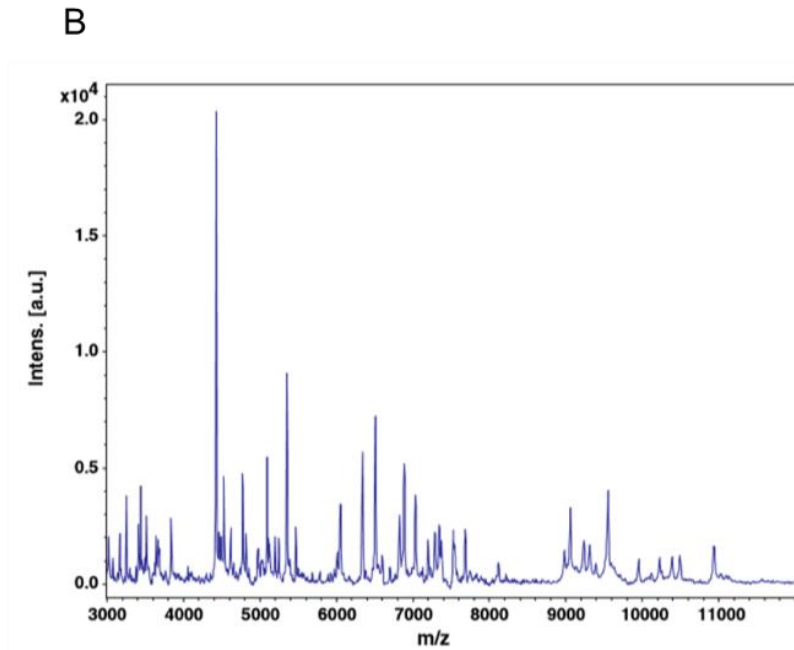
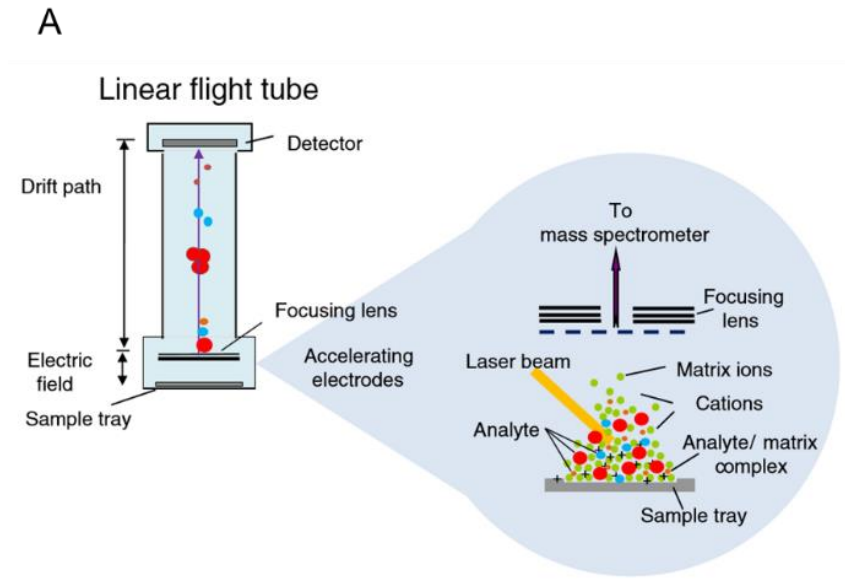
1.2.4. Proteomic analysis of pathogens

1.2.4.1. Matrix assisted laser desorption/ionisation time of flight mass spectrometry (MALDI-TOF MS)

In addition to the nucleic acid-based approaches described in Section 1.2.3, the emergence of techniques for protein analysis has contributed to shaping the diagnostic landscape in infection control. In particular, matrix-assisted laser desorption/ionisation time-of-flight mass spectrometry (MALDI-TOF MS) is a soft ionisation mass spectrometry technique that has revolutionised the identification of bacteria and fungi in clinical microbiology laboratories within the last decade (Singhal *et al.*, 2015, van Belkum *et al.*, 2017, Parchen and de Valk, 2019). Historically microbiology has relied on culture-based methodologies for species identification, characterising pathogens by their morphology and biochemistry. Whilst these methods still hold their place in the microbiology laboratory, they have been complemented by the introduction of rapid, accurate and inexpensive genomic and proteomic techniques (Marx, 2017). This has facilitated a reduction in time to diagnosis, which can be of great benefit for making urgent clinical decisions in targeting appropriate antimicrobial therapies. Bacterial species identification by MALDI-TOF MS relies on the generation of a mass spectrum containing a mixture of proteins of different masses. The proteins are co-crystallised within an organic matrix, ionised using a laser, and are subsequently separated in a vacuum on the basis of their time-of-flight; a function of their mass-to-charge (m/z) ratio. Ions from ribosomal proteins predominate in the mixture, as they are readily isolated in the acidic, organic matrix (Opota *et al.*, 2017). The ions are detected at the end of the flight tube and a mass spectrum generated for that sample; the m/z ratio is used to represent the molecular weight of the proteins in Daltons (Da) since the charge of the ions is +1 (Shah and Gharbia, 2017) (Figure 1.6). Detailed databases containing reference spectra are available against which the unknown sample can be compared, enabling species identification within minutes. The number of peaks in the unknown sample is compared to the number of peaks in the reference database and reported as a log score, which represents how well the mass spectrum of the unknown sample matches the reference spectrum.

Figure 1.6: Principles of MALDI-TOF MS. A: the co-crystallised sample-matrix is ionised by a laser beam, accelerated through the linear flight tube and detected based on time-of-flight.

B: an example mass spectrum with peaks of varying m/z values (Wieser et al., 2012).



MALDI-TOF MS has been demonstrated as a robust method for bacterial identification across a range of experimental variables, including choice of platform and culture medium (Carbonnelle *et al.*, 2012, Anderson *et al.*, 2012). Routine approaches for species identification by MALDI-TOF MS generally require organisms to be cultured prior to analysis. Bacterial colonies from cultured isolates can be directly spotted onto the MALDI target plates, or proteins may be extracted. Formic acid extraction is a commonly used approach that has been demonstrated to improve identification accuracy for some species of bacteria, such as Gram-positive cocci (Alatoom *et al.*, 2011). Some studies have also evaluated MALDI-TOF MS analysis directly from urine samples, with promising results (Ferreira *et al.*, 2011, Íñigo *et al.*, 2016). Although demonstrated to be robust for species identification, standardisation of MALDI-TOF MS protocols should still be considered within laboratory practices (Williams *et al.*, 2003). Numerous experimental factors including culture, instrument calibration and organism characteristics have the potential to influence the quality of spectra. This, combined with the quality of spectra available in the database, can impact upon the reliability of the species identification result (Croxatto *et al.*, 2012). MALDI-TOF MS methods are well optimised for identifying a range of bacterial species including carbapenem resistant *Enterobacteriaceae* (CREs) (Sakarikou *et al.*, 2017), *Staphylococcus aureus* (Wolters *et al.*, 2011) and other species of clinical relevance (Benagli *et al.*, 2011). In addition to identification of species associated with more common infections, further roles for MALDI-TOF MS have been indicated. These include development of methods and databases to characterise non-tuberculous mycobacteria (NTMs) (Mediavilla-Gradolph *et al.*, 2015) and fungi (Normand *et al.*, 2017, Gorton *et al.*, 2014). In addition, the applicability of MALDI-TOF MS has been demonstrated for detecting protein peaks associated with hypervirulence and drug resistance (Hart *et al.*, 2015, Flores-Treviño *et al.*, 2019), and detection of biomarkers additional to proteins such as peptides and lipids (Cho *et al.*, 2015, Larrouy-Maumus *et al.*, 2016). MALDI-TOF MS has also been implicated for strain typing below the species level for a number of organisms (Rafei *et al.*, 2014, Mehta and Silva, 2015, Johnson *et al.*, 2016). These examples demonstrate the breadth of potential applications for MALDI-TOF MS, highlighting an invaluable role for advanced molecular analysis in better understanding the dynamics of infection.

1.3. Improving measurement accuracy in molecular diagnosis of infectious diseases

1.3.1. Harmonising molecular measurements

1.3.1.1. Establishing metrological frameworks

Despite the widespread integration of molecular methods into diagnostics for infection, metrological concepts have been relatively slow to catch up. Measurement variability between tests, experiments and laboratories hinders the comparability of results between patients, platforms and studies. For example, diagnosis of infection with the highly contagious bacterium *Clostridium difficile* often includes blood toxin (TOX) testing to indicate symptomatic disease, and a pathogen-specific PCR to confirm the presence of the etiological agent. Indication for invasive infection is usually accepted when a patient is TOX and PCR positive. However, reliance on PCR results in lieu of TOX outcomes in some centres has been reported to lead to overdiagnosis of symptomatic *C. difficile* infection which may lead to inappropriate use of antimicrobial therapy. The lack of standardisation in data interpretation between centres may put patients at risk, highlighting the need for harmonisation of methods (Polage *et al.*, 2015). Similar issues surrounding disharmony of methods between diagnostic laboratories exist for response-based treatment of HCV infection. The approach, which is based on qPCR quantification of viral load as a marker for shortening of HCV treatment as discussed in Section 1.2.2, may not be reliable as a global indicator because of variability between assays and patients (Vermehren *et al.*, 2016). Improved harmonisation of results could be achieved through the implementation of reference measurement procedures (RMPs) and standardisation of workflows, facilitated through the establishment of metrological frameworks for infection.

The importance of measurement traceability and standardisation has been recognised in clinical diagnostic laboratories, and frameworks have been established to help laboratories achieve this. Such frameworks enable an externally validated source of quality control, ensuring that clinical laboratories are producing the most accurate measurements possible. This also means producing uncertainty values to encompass random and systematic error associated with laboratory methods, enabling confidence in measurements that underpins the quality of results for diagnostics. It is upon recommendation that the uncertainty of patient results from diagnostic

microbiological tests is known (Fuentes-Arderiu, 2002), and that laboratory-developed (i.e. non-commercial) diagnostic assays endure full and thorough validation to ensure that they are fit for purpose (Burd, 2010). National Measurement Institutes (NMIs) are designated centres responsible for leading measurement science, and play a key role in establishing and maintaining metrological frameworks to support clinical diagnostic measurements. Such institutes, including the National Measurement Laboratory (NML) in Teddington, operate at a national and international level through collaboration with other NMIs, government, industry, academia and clinical partners. The role of the NMI is to ensure traceability and quality of measurements, and to identify issues that can impact upon measurement accuracy to facilitate reliable metrics for ensuring patient safety (Braybrook and Dean, 2012). This can be facilitated through NMI engagement in international consortia for metrology in biological measurements, and participation in international comparison studies for measuring amount of substance including nucleic acids and proteins. This provides an opportunity to demonstrate measurement comparability for the most sensitive applications (Whale *et al.*, 2017, Devonshire *et al.*, 2016b, Dong *et al.*, 2020a). NMIs are also prolific in delivering EU funded projects for metrology in infection. Past projects include Infect-Met (EURAMET, 2015) and AntiMicroResist (EURAMET, 2019), demonstrating the reach of metrology within infection.

1.3.1.2. Inter-laboratory collaboration and comparison of clinical measurements

In addition to NMIs, diagnostic laboratories for clinical testing can promote harmonisation of molecular measurements from within. A platform for clinical laboratories to do this is through participation in External Quality Assessment (EQA) schemes to support harmonised reporting of results, especially those that are quantitative. This can promote improvements in metrological accuracy between laboratories through analytical quality, and through standardisation in the way results are reported – such as through the use of common nomenclature, measurement units and reference intervals (Jones, 2017). Generally, participating laboratories will receive a set of samples from an EQA provider such as INSTAND e. V. (Germany), Quality Control for Molecular Diagnostics (QCMD, UK) and the National External Quality Assessment Service (NEQAS, UK). Commercial companies such as Randox Laboratories (UK) and Bio-Rad Laboratories (USA) also co-ordinate their own EQA programs (Jones, 2017). The samples have been pre-analysed using

a reference method and have been characterised in terms of number or identity. The participating laboratory will analyse the samples using their method of choice, such as their usual diagnostic approaches in the case of clinical laboratories, and report back to the EQA provider. The results of the participants can be compared, and any outliers identified. Following interlaboratory studies for clinical biomarkers, the consensus value will be assigned an uncertainty and may be used as a clinical range for healthy versus disease states. If the uncertainty on the value is large (indicating imprecision), or the value has been skewed by inherent bias in the method, then the clinical diagnostic range is unreliable and may jeopardise patient safety. A study by Patton *et al* (2014) highlighted variability in reported results from a pilot EQA for somatic epidermal growth factor receptor (EGFR) gene mutational analysis in non-small-cell lung cancer (NSCLC). The authors speculate that variability was largely attributed to error from pre-analytical steps, which resulted in false negatives being obtained by some of the participating laboratories. In addition, lack of information given by laboratories on experimental procedures highlights the need for transparency to enable sources of error to be identified. This study highlights that there is still room for improvement within interlaboratory schemes for molecular analyses, which can improve reliability of reporting and clinical care for patients where EGFR mutation analysis is used as a first-line diagnostic test (Patton *et al.*, 2014).

An important emerging role of NMIs in inter-laboratory studies is the value assignment of test materials or calibrators that are to be included in proficiency schemes. Types of materials included in these analyses range from purified nucleic acid in buffered solution to extractable matrices containing whole organisms. Value assignment can be performed using a precise counting method, such as mass spectrometry, direct counting or dPCR. This has been demonstrated for an EQA scheme to quantify genomic RNA from SARS-CoV-2, for which reference values were provided by three NMIs using RT-dPCR as a candidate reference method (INSTAND, 2020). Prospective participants in the scheme can use this value as a benchmark for their own analyses, promoting harmonisation of measurements between laboratories that are measuring nucleic acid from SARS-CoV-2. This represents the first use of NMI-defined RT-dPCR values as reference in an EQA scheme for RNA quantification, and highlights a pivotal role for measurement harmonisation in achieving accuracy in clinical measurement of pathogen genomes. EQA participation, or more generally inter-laboratory testing, can help to validate the repeatability and

robustness of methods, or the commutability of a reference material used to calibrate clinical diagnostic approaches.

1.3.1.3. *Transparency in data reporting*

The requirement for standardisation in molecular measurements exists alongside the necessity for transparency in reporting of data to facilitate harmonisation. Although rare, misrepresentation of scientific results in published studies may occur if the data contained within them are inaccurate or lacking in scientific credibility. This can have a wider, sometimes catastrophic impact on public opinion, as well as limiting method repeatability in the lab. A well-known example of this involved the misrepresentation of results linking autism spectrum disorders (ASDs) with the measles, mumps and rubella (MMR) vaccine (Wakefield *et al.*, 1998). The report led to reduced public uptake of the vaccine, resulting in multiple epidemics of measles which can be fatal. It was later revealed that unreported contamination issues within the laboratory likely invalidated the findings of the study (Cedillo v. HHS, 2007), contributing to the retraction of the published work. Importantly this event also highlighted the importance of utilising rigorous laboratory controls, throwing a spotlight onto the role of metrology in ensuring data integrity.

Numerous guidelines have since been published to encourage author driven transparency of experimental protocols and data reliability. The purpose of these guidelines is to ensure a minimum level of quality in reported results for molecular approaches. The Minimum Information for Publication of Quantitative Real-Time PCR Experiments (MIQE) guidelines (Bustin *et al.*, 2009), a collaborative effort between molecular biology laboratories and NMIs, discusses the importance of harmonisation of qPCR data and associated terminology. The publication includes a checklist that researchers can use to ensure that their experiments meet the minimum requirements. As discussed in Section 1.2.3.2, the widespread use of qPCR and potential for disharmony between quantitative data could be problematic (Bustin *et al.*, 2013), and the significance of producing high quality qPCR data is so great that comprehensive guidance for conducting experiments has been published (Taylor *et al.*, 2019). The importance of data transparency extends to other areas of molecular diagnostics, particularly for emerging methods such as dPCR (digital MIQE) (Huggett *et al.*, 2013, The dMIQE Group and Huggett, 2020). Minimum information guidelines exist for NGS from the genomic standards consortium; Minimum Information about any x Sequence (MIxS) including Minimum Information about a Genome

Sequence (MIGS) (Field *et al.*, 2008, Bowers *et al.*, 2017), and also for molecular epidemiology (STROME-ID) and metagenomic studies (STROBE-metagenomics) of infectious diseases (Field *et al.*, 2014, Bharucha *et al.*, 2020). Data transparency is also encouraged for proteomics/mass spectrometry experiments to address reproducibility, via the Minimum Information About a Proteomics Experiment (MIAPE) and supplemental Minimum Information About a Mass Spectrometry Imaging Experiment (MIAMSIE) guidelines (Taylor *et al.*, 2007, Gustafsson *et al.*, 2018). Guidance documents of this kind are not a concept unique to molecular diagnostics, as other guidelines for reporting standards exist for randomised control trials (CONSORT) and accuracy of diagnostic tests (STARD). Reports have demonstrated that implementing these checklists improves the quality of reported data for clinical trials (Plint *et al.*, 2006, Smidt *et al.*, 2006), supporting their usefulness in maintaining data integrity is all aspects of clinical and pre-clinical research.

1.3.2. Development and characterisation of reference materials and methods

1.3.2.1. International reference standards

To ensure that measurements in molecular diagnostics are reliable, laboratory results must be traceable over space and time. This is particularly important for detection of pathogens that may be present at low levels within complex biological matrices, and for diseases that require monitoring over extended periods of time. Measurement variability in molecular diagnoses can be attributed to sources of random and systematic error. These can result from differences in instrument calibration within and between laboratories, analytical approaches and reagent production batches, as well as biological variability related to the sample type. Uncontrolled or uncharacterised measurement error can complicate measurement precision and, ultimately, accuracy. The increasing application of emerging methods for making sensitive measurements of pathogen biomarkers requires suitable quality metrics for comparing measurements and validating workflows. Furthermore, an increasing number of diagnostic results are reported as absolute values rather than relative changes, highlighting the need for the highest possible degree of accuracy (Madej *et al.*, 2010). Traceability and harmonisation of laboratory results, and

validation of new workflows, can be facilitated through the availability of stable and well characterised reference materials.

There is an urgent need for quantitative reference materials in infectious disease diagnostics. The relative lack of well characterised and traceable reference materials available for detecting, characterising and quantifying pathogens has been a limiting factor in affording measurement traceability (Fryer *et al.*, 2008, Madej *et al.*, 2010, Rampling *et al.*, 2019). Commutable reference materials could help to harmonise findings between laboratories, establish new methods, and help diagnostic laboratories maintain competency through provision of reference values, against which performance can be compared. Whilst the repertoire of available reference materials for nucleic acid quantification of pathogens has increased over the past decade, maintenance of these must continue. Development of higher-order reference materials for nucleic acid quantification in infectious diseases is required (Jing *et al.*, 2018). A higher-order reference material is one to which other measurements can be referenced because it sits high in the traceability chain (Figure 1.2), and has an established measurement uncertainty associated with its nominal value (Armbruster and Miller, 2007). A catalogue of reference materials including those for HIV-1, HCV, HCMV and Epstein Barr virus (EBV) endorsed by the World Health Organisation (WHO) exists for measuring biological activity, and for the purpose of downstream standardisation of *in vitro* diagnostic approaches. Preparation and validation of these materials is the responsibility of expert laboratories including the National Institute for Biological Standards and Control (NIBSC), Paul-Ehrlich-Institut (PEI) and Centre for Biologics Evaluation and Research (CBER). The application of the WHO-endorsed materials to diagnostic approaches enables an internationally agreed unit of measurement, the International Unit (IU), to allow worldwide comparison of data (World Health Organization, 2006).

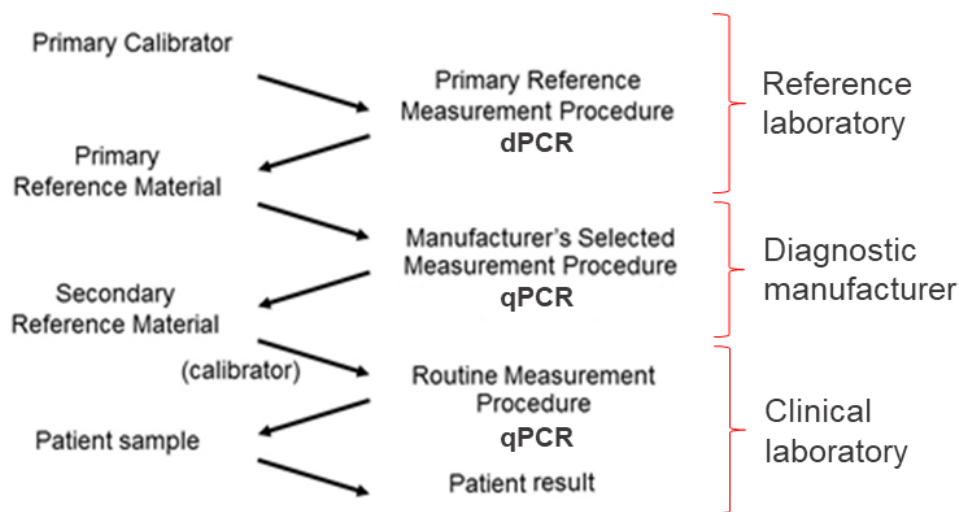
1.3.2.2. *SI traceability in infectious disease diagnostics*

SI traceability, referring to the traceability of measurements to a base unit defined by a fixed constant, is a relatively new concept to molecular diagnostics. The heterogenous nature of biological materials and lack of suitable reference methods currently limits measurements of infectious disease biomarkers being ubiquitously expressed in accordance with the SI system of units (World Health Organization, 2017b). The availability of primary reference materials for infection traceable to the SI through validated measurement procedures would further help to

standardise quantitative analyses of pathogens. This would facilitate downstream traceability for subsequent standards and calibration materials, allowing any resulting diagnostic measurements that are indirectly traceable to the SI to be comparable between studies and centres. Development of traceable methods and materials for nucleic acid analysis could be of benefit for molecular diagnostics, especially where quantification of nucleic acids directly influences clinical decisions (Katto, 2017). The approach taken for value assignment of WHO International Standards allows measurements to be standardised to the IU assigned to a primary reference material. The development of more complex materials representative of clinical samples can allow matrix effects to be factored in, and sources of measurement error to be characterised.

The concept of developing reference measurement procedures (RMPs) and SI traceable reference materials for assessing measurement trueness of biological entities in infection is emerging. Primary RMPs are intended to give SI traceability to primary reference materials, initiating the traceability chain for production of subsequent reference materials and measurements. 'Count' – expressed as the number of molecules of substance, such as copies of a nucleic acid sequence – has come to be recognized as a dimensionless SI unit. As a result, formal traceability to the SI can be established through an appropriate measurement procedure for counting the number of molecular entities (BIPM., 2019). dPCR has been applied as an RMP for DNA quantification in cancer models (Whale *et al.*, 2018), and for quantification of HCMV DNA (Pavsic *et al.*, 2017). This is fitting given the development of the first HCMV DNA plasmid standard that is traceable to the SI expressed as DNA copies per μL (Haynes *et al.*, 2013). Figure 1.7 shows a traceability chain for molecular quantification, adapted from Figure 1.2, demonstrating the role of dPCR as a RMP for qPCR quantification of clinical biomarkers.

Figure 1.7: Calibration traceability chain for quantitative molecular measurements, demonstrating the positioning of dPCR as a reference measurement procedure (RMP). Figure adapted from Gantzer (2012)

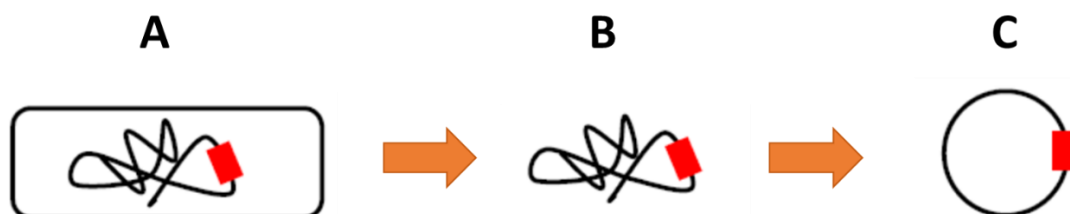


The application of dPCR as an RMP for absolute value assignment of primary reference materials could eliminate measurement bias that may be introduced by other methods, potentially providing a more accurate reference value. The emergence of SI traceability within the realm of biological standards for infectious diseases paves the way for the other disease models, and holds particular value for quantification of RNA viruses as a future application.

1.3.2.3. *Biological complexity of reference materials*

Reference materials and calibration standards for quantification of nucleic acids from pathogens exist in numerous states of varying complexity (Figure 1.8). This refers not only to primary standards at the top of the traceability chain, but also to secondary standards and those that may be produced for validating and calibrating in-house assays.

Figure 1.8: Varying complexity of microbiological standards and reference materials (Devonshire *et al.*, 2015). A material that closely resembles a complete organism within a clinical sample matrix (A) may be used to assess the full analytical workflow including extraction. In some cases, pre-extracted material such as genomic nucleic acid (B) or synthetic constructs (C) may be more appropriate options.



Many of the WHO International Standards used for quantification of nucleic acids, predominantly from viruses although some standards of this kind exist for protozoa (Padley *et al.*, 2008), are comprised of whole organism in a background of human plasma or serum. These materials (Figure 1.8 A) best represent a clinical sample matrix, and incorporate measurement uncertainty from extraction and other analytical steps in their analysis. However, samples containing biological fluids may contain more inhibitors of NAATs including nucleases that can degrade the target of interest. In addition, production of materials containing whole virus is not always possible. In the case of haemorrhagic diseases including Lassa fever and Rift Valley fever, source materials are yet to be obtained to prepare a whole virus material (Rampling *et al.*, 2019). There are also safety implications due to limited access to biosafety level (BSL) 4 facilities required to culture these viruses. Where possible, reference material providers may distribute pre-extracted genomic material for these pathogens (Figure 1.8 B), a safer option for enabling increased complexity in nucleic acid analysis. One interesting additional workaround is the inclusion of synthetic viral nucleic acid constructs encapsulated in a lentiviral envelope. These lentiviral materials contain no infectious virus and therefore enable safe handling and extraction of nucleic acid from the material. A WHO International Standard of this nature is already available for Ebola (Mattiuzzo *et al.*, 2015), and a similar material for SARS-CoV-2 is in development (SARS-CoV-2 RNA; NIBSC 19/304). In lieu of extractable material, laboratories may turn to synthetic plasmid constructs or *in vitro* RNA transcripts containing the pathogen sequence of interest (Figure 1.8 C). The use of these stable constructs benefits from standardised input quantity based on known molecular weight, contributing to accurate quantification of target sequence. Synthetic standards are a common choice of material for validating in-house assays, and may be designed by the end user

for validation against an existing primary (or secondary) reference material (Nolan *et al.*, 2013). This highlights the importance of reference material traceability at source to ensure that accurate measurements can be made based on in-house controls downstream.

1.3.3. Characterising sources of experimental variability contributing to measurement error

Characterisation of sources of experimental variability contributing to measurement error is a fundamental activity at the core of achieving accurate measurements. Essentially, understanding why measurements vary could help to prevent unnecessary error, or promote incorporation of the error into measurement uncertainty budgets. Understanding sources of random and systematic error is also essential when developing novel diagnostic approaches for molecular quantification and characterisation of pathogens. Increased measurement error, defined as the variation of measurements around the true value (Bland and Altman, 1996), can diminish measurement quality through reduced accuracy, repeatability and reliability (Coggon *et al.*, 2020). There remains a need to ensure that diagnostic tests are fit-for-purpose, necessitating stewardship for measurement reliability (Messacar *et al.*, 2017). Measurements of molecular biomarkers should be made with the highest technical accuracy (i.e. the performance of the molecular test under a defined set of conditions, including analytical sensitivity, repeatability and reproducibility) to support diagnostic accuracy (i.e. the ability of a diagnostic test to correctly detect or exclude a disease) and impact upon clinical outcomes (Šimundić, 2009). Evaluation of diagnostic tests should therefore always include an assessment of technical accuracy in determining clinical impact (Van den Bruel *et al.*, 2007).

Measurement error can be introduced due to variability in numerous pre-analytical and analytical processes. This can include sample storage and culture of organisms (pre-analytical), choice of extraction method, efficiency of enzymatic processes, stability of calibration standards (analytical), and choice of data analysis approach (post-analytical) (Narayanan, 2000, Sanders *et al.*, 2014, Adams, 2015, Bustin *et al.*, 2015, Markus *et al.*, 2018, Chávez, 2019). Sample preparation and extraction, in particular, can significantly contribute to experimental variability. Nucleic acid extraction has been demonstrated as a major contributing factor to experimental variability in studies characterising microbiomes in humans (Greathouse *et al.*, 2019). Additionally, extraction efficiency of cell-free DNA (cfDNA) from plasma has been shown to vary

by approximately 65% between specimens, as determined by qPCR quantification of a spike-in oligonucleotide control. This has been proposed as a source of bias in quantifying cfDNA levels that may be used for clinical prognosis following traumatic brain injury and stroke (O'Connell *et al.*, 2017). The authors discuss how properties of the individual specimens, including ion concentrations, pH, protein levels, and lipid content, may contribute to variability in extraction and quantification of the target sequence. This highlights the measurement challenges associated with molecular analysis of biological entities, in that varying and unpredictable levels of potential inhibitors can contribute to measurement error. Matrix-specific variability associated with DNA extraction has also been observed for qPCR analysis of food samples (Cankar *et al.*, 2006), and in viral nucleic acid quantification (Pavšič *et al.*, 2016). In addition, choice of extraction protocol can impact upon yield as the quantity of extracted material is a function of extraction efficiency, purity and intactness, which can vary by method (Olson and Morrow, 2012). This is an important consideration when assessing the impact of nucleic acid extraction method on measurement variability. This consideration is not limited to analysis of nucleic acids either, as Toh-Boyo *et al.* (2012) illustrated that sample preparation steps are key variables in MALDI-TOF MS analysis of bacterial proteins that can influence experimental reproducibility (Toh-Boyo *et al.*, 2012). Ensuring continuity in upstream methods calls for implementation of standardised approaches, which should be considered on a sample-dependent basis (Demeke and Jenkins, 2010).

1.4. Contribution to the field

Analytical accuracy in molecular measurements for diagnosis of infectious diseases can be achieved through the practice and promotion of metrology. This can involve characterisation of sources of experimental variability contributing to measurement error, development and use of reliable reference materials, establishment of metrological frameworks for infection, contribution to inter-laboratory comparisons of measurement, and transparency in data reporting. Implementation of metrological principles by clinical laboratories, NIMs, reference material producers, EQA providers, commercial manufacturers, and policy makers can help to facilitate improved accuracy in analytical measurements. This also highlights the importance of maintaining collaborative metrology networks in ensuring the development and use of appropriate diagnostic methods for managing and controlling infectious diseases. This is not only essential for the management of current endemic diseases, but for emerging diseases posing the biggest threats

to human health, including COVID-19, haemorrhagic fevers and presently unidentified pathogens of the future (World Health Organisation, 2018).

In this thesis I explore the role of emerging technologies and the significance of measurement research in molecular characterisation and quantification of pathogens. In each chapter I explore possible contributions to measurement error through evaluation of experimental variables, and the potential impact on measurement accuracy. This thesis investigates the measurement of RNA, DNA and proteins using emerging technologies for molecular quantification and characterisation of pathogen biomarkers. I examine the placing of emerging technologies for making advanced measurements and discuss their potential role as complementary methods to routine clinical management of pathogens. The work presented in this thesis complements previously published data to support the role of metrology in infectious disease diagnostics, and expands on measurement challenges specific to each of the disease models described in each chapter. This work could help to address fundamental questions surrounding analytical error in sensitive molecular measurements. As discussed in Section 1.3.3, an evaluation of the placing of these methods in molecular diagnosis of infection must include scrutiny of the inherent sources of measurement variability. Rigorous assessment of these parameters could influence the adoption of emerging techniques into clinical practices.

1.5. Thesis aims

To explore the aims of my thesis within the broad context of infectious disease diagnostics, I have focused on four distinct models for different diseases, molecular approaches and measurement challenges. Briefly, the models presented in this thesis centre around quantification of viral and bacterial nucleic acids, and qualitative analysis of bacterial proteomes for sub-species typing. Clinically, nucleic acid quantification and protein characterisation may be applied to identify and monitor infections, and for identifying transmission routes. In order to explore the analytical accuracy of these measurements, I have set out the following thesis aims:

1. To determine which experimental variables contribute to measurement error and have the potential to influence measurement accuracy.
2. To explore how metrological principles can be promoted and utilised to support the accuracy of current methods for quantification and characterisation of pathogens.

3. To establish how emerging molecular methods could improve confidence in measurements for infectious disease diagnostics and be of benefit to clinical decisions and patient outcomes.

1.6. Hypotheses

Specific hypotheses are presented for each of the results chapters to accommodate the measurement challenges associated with each section.

Chapter 3. Investigating differences between reverse transcription (RT) digital PCR methods for quantification of HIV-1 genomic RNA

HIV-1 RNA viral load is quantified in plasma of HIV positive individuals using reverse transcription quantitative PCR (RT-qPCR). Response to treatment is monitored to help prevent the development of drug resistance or viraemic relapse in these patients. Quantification of HIV-1 viral load requires viral RNA to first be converted to complementary DNA (cDNA) through reverse transcription, the efficiency of which has been shown to vary with choice of reverse transcriptase enzyme. This could impact upon the quantitative result and method sensitivity when using RT-qPCR. Discrepancies between laboratory results might lead to differences in patient management between clinical centres and could contribute to the emergence and transmission of resistance. Digital PCR (dPCR), which is an absolute nucleic acid counting method, can be used to compare the cDNA yield for different reverse transcriptases that influence subsequent HIV-1 RNA quantification.

Hypothesis: Harmonisation of quantitative measurements of HIV-1 RNA could be improved through characterisation of variability in the upstream reverse transcription process. This could support accuracy in measurement of HIV-1 RNA viral load.

Chapter 4. Calibrating quantitative measurements of HIV-1 DNA using digital PCR

Quantification of HIV DNA associated with the viral reservoir is increasingly used in research as a tool to study latent disease. Such a target could potentially be used clinically to assist with monitoring disease progression as it has been reported to correlate with viral outgrowth, and could serve as a biomarker for monitoring chronic infection. In addition to measurement of RNA viral load, qPCR is used as the method of choice for quantification of HIV DNA. Results are normalised to a human genomic target and reported as HIV DNA copies per 1,000,000 cells using a standard curve for calibration. Appropriately calibrated quantitative methods afford greater accuracy and measurement harmonisation when using qPCR to measure a specific sequence. dPCR can quantify nucleic acid in the absence of a standard curve and may have a role for accurate, clinical quantification of HIV DNA.

Hypothesis: Measurements of the HIV-1 proviral reservoir can be achieved through quantification of HIV-1 DNA. It is hypothesised that dPCR, which can quantify HIV-1 DNA without the need for a standard curve, can perform with equivalent sensitivity to qPCR and may facilitate greater measurement accuracy in determining the number of copies of HIV provirus.

Chapter 5. Quantification of methicillin resistance in *Staphylococcus* spp using digital PCR

Healthcare associated infections with methicillin-resistant *Staphylococcus aureus* (MRSA) remain a clinical concern for numerous patient groups. Commercial PCR-based methods are widely used as screening tools to detect MRSA colonisation by amplification of *mecA*, which confers methicillin resistance. Molecular quantification of bacterial load is an emerging concept that can be used to predict disease severity, and to distinguish between colonisation and invasive disease. This could include quantification of *mecA* to determine which organisms are carrying drug resistance. Digital PCR (dPCR) could enhance the performance of current molecular methods through absolute quantification of model materials for MRSA that could be used for calibration.

Hypothesis: Methods for precise DNA quantification can be applied to measure ratios of methicillin resistance genes relative to endogenous targets in MRSA and other Staphylococci. Such approaches could be applied to characterise materials used to calibrate contemporary molecular methods, supporting accuracy in quantitative measurements of MRSA.

Chapter 6. Characterising sources of experimental variability in MALDI-TOF MS strain typing and evaluating applicability of the technique to resolving nosocomial outbreaks

Colonisation and subsequent infections with drug resistant bacteria are a concern for vulnerable patient groups within the hospital setting, with outbreaks involving multi drug-resistant strains being a particular threat to patient outcome. Reliable molecular typing methods can help to trace transmission routes and manage outbreaks. In addition to current reference methods, Matrix Assisted Laser Desorption/Ionisation-Time of Flight Mass Spectrometry (MALDI-TOF MS) may have a role for making initial in-house judgements on strain relatedness. However, limited studies on method reproducibility exist for this application. This could prevent the use of MALDI-TOF MS as a reliable alternative to current genomic techniques. Rigorous assessment of sources of experimental variability and their impact on spectral acquisition could support the incorporation of MALDI-TOF MS into routine use for molecular strain typing.

Hypothesis: Standardisation of upstream workflows for protein analysis may improve reproducibility of methods for strain typing of bacteria. These approaches could be used to differentiate between bacterial strains to resolve nosocomial outbreaks, and in epidemiological studies.

2. General methods and preparation of reagents

2.1. Nucleic acid analysis

2.1.1. *Plastic-ware for nucleic acid analysis*

DNA LoBind® tubes (Eppendorf Ltd, Germany) were used for storing and diluting nucleic acids.

Tubes were certified PCR clean and free of nucleases.

2.1.2. *Oligonucleotide design*

Unless obtained from published literature or through collaborators specifically acknowledged in each chapter, PCR oligonucleotides were designed *in silico* where required. An NCBI basic local alignment search tool (BLAST, <https://blast.ncbi.nlm.nih.gov/Blast.cgi>) search was performed and relevant FASTA sequences subjected to a PrimerBlast search. Primer selections were made on the basis of melting temperature (°C), self-complementarity, amplicon size and primer dimer formation. A manual design strategy was sometimes necessary, such as for selecting specific gene regions containing particularly conserved or divergent regions. To perform manual design, sequences were aligned using MultAlin multiple sequence alignment tool (Corpet, 1988) and suitable primer and probe regions identified. Technical specifications were obtained using online data tools.

2.1.3. *Preparation of oligonucleotides for PCR*

Oligonucleotides were obtained from Sigma-Aldrich (USA), Life Technologies – Thermo Fisher Scientific (USA), Eurofins Genomics (Germany), LGC Biosearch Technologies (USA) and Integrated DNA Technologies IDT (USA). Lyophilised oligonucleotides were reconstituted in nuclease-free water (Ambion, USA), using the volume specified by the relevant manufacturer to prepare 100 µM stocks. Primers and probes were subsequently combined in a 20X working concentration, aliquoted for single use and stored at -20°C.

2.1.4. Calculating molecular weight (MW) and copy number of synthetic constructs

Molecular weight of DNA and RNA templates for nucleic acid analysis (e.g. plasmids, *in vitro* generated transcripts, genomic material) was determined by counting the respective number of nucleotides (nt) and multiplying by the average weight of a single base pair (bp) for DNA (660 g/mol) or individual nucleotide for RNA (A - 329.2 g/mol, C - 305.2 g/mol, G - 345.2 g/mol, U - 306.2 g/mol; <https://www.thermofisher.com/uk/en/home/references/ambion-tech-support/rna-tools-and-calculators/dna-and-rna-molecular-weights-and-conversions.html>; Accessed 26/09/2020). Copy number calculations were determined using Avogadro's number (6.022×10^{23}).

2.1.5. General dPCR protocol for the Bio-Rad QX200 system

The Bio-Rad QX200 Droplet Digital PCR System was the main dPCR platform utilised in this thesis. A general protocol is described here and referenced within each relevant chapter. All QX200 digital PCR (dPCR) experiments were implemented in accordance with the dMIQE2020 guidelines (The dMIQE Group and Huggett, 2020). dMIQE compliance criteria were recorded on the dMIQE checklist for each chapter (Appendix 9).

DNA, RNA or cDNA template was added to a total prepared reaction volume of 22 μ L containing PCR mastermix, sterile nuclease-free water (Ambion, USA) and specific primers and probes. Primers and probes were added to a final reaction concentration of 900 and 200 nM, respectively, unless stated otherwise. 20 μ L of this total volume was pipetted into the sample well of a DG8 cartridge, and droplets generated using a manual droplet generator, as previously described (Devonshire *et al.*, 2015). Typical thermocycling conditions were as follows: 10 minutes at 95 °C, 40 cycles of 94 °C for 30 s, and 60 °C for 1 min, followed by 98°C for 10 min and a 4 °C hold. Deviations from the standard protocol are described in the relevant chapters. The ramp rate for each step was 2°C/s. Droplets were read using the QX200 Droplet Reader, and the data were analysed using QuantaSoft versions 1.6.6.0320 & 1.7.4.0917. No Template Controls (NTCs) of nuclease-free water were employed as controls in all cases. Other specific controls are described in the relevant chapters.

2.2. Protein analysis

2.2.1. Plastic-ware for proteomic analysis

Plastic-ware for MALDI-TOF MS experiments included 50 mL Greiner centrifuge tubes, 15 mL Corning tubes and 1.5 mL microcentrifuge tubes (Eppendorf Ltd, Germany). Contact time of organic solvents with plastics was kept to a minimum to prevent leaching of plastic residues that can affect MALDI-TOF MS.

2.2.2. Preparation of 70% formic acid solution

For each MALDI-TOF MS experiment, an aqueous solution of formic acid was prepared by combining 300 μ L HPLC-grade HiPerSolv Chromanorm® water (VWR, USA) and 700 μ L formic acid (Honeywell, USA) in a 1.5 mL microcentrifuge tube. The solution was mixed by carefully inverting the tube 12 times.

2.2.3. Preparation of Bruker Bacterial Test Standard (BTS)

40 μ L of Organic Solvent (Honeywell, USA), a mixture of trifluoroacetic acid, water and acetonitrile, was added to the lyophilized BTS material. The mixture was pipetted 20 times taking care not to create air bubbles. The solution was allowed to equilibrate at room temperature for 5 minutes, followed by further pipette mixing. The tube was briefly centrifuged and stored at -20°C.

2.2.4. Preparation of Bruker α -Cyano-4-hydroxycinnamic acid (HCCA) matrix

250 μ L of organic solvent (OS) was added to the lyophilized HCCA material, which was promptly dissolved by vigorous agitation for 30 seconds. The tube was briefly centrifuged and left to equilibrate at room temperature for 30 minutes before use. Any HCCA matrix remaining following an experiment was discarded.

3. Investigating differences between reverse transcription (RT) digital PCR methods for quantification of HIV-1 genomic RNA

3.1. Introduction

3.1.1. Human immunodeficiency virus type 1 (HIV-1)

Human immunodeficiency virus type 1 (HIV-1) is a retrovirus that can cause acquired immunodeficiency syndrome (AIDS) if left untreated, leading to the eventual destruction of the host's immune system. There were approximately 37.9 million people worldwide living with HIV-1 at the end of 2018 (UNAIDS, 2019). The HIV/AIDS epidemic remains one of the longest standing epidemic diseases in human history following characterisation of the disease in 1983 (Barre-Sinoussi *et al.*, 1983). The development of highly active antiretroviral therapy (HAART) and combination ART (cART) has resulted in a dramatic reduction in the number of HIV infected individuals who progress to AIDS by preventing viral replication (Bangsberg *et al.*, 2001). Numerous classes of antiretroviral drugs are used to control HIV-1 infection, including nucleoside-analogue reverse transcriptase inhibitors (NRTIs), non-nucleoside reverse transcriptase inhibitors (NNRTIs), integrase inhibitors, protease inhibitors (PIs), fusion inhibitors, and coreceptor antagonists. They are grouped based on their mechanism of action and resistance profiles, and target different stages of the HIV-1 life cycle (Arts and Hazuda, 2012). However, despite the ability of antiretrovirals to control viral replication so that levels of circulating HIV-1 are undetectable, a vaccine or cure is yet to be available. Management of the disease relies on accurate monitoring of circulating viral RNA (viral load).

3.1.2. Clinical quantification of HIV-1 RNA viral load

HIV-1 RNA viral load (VL) is routinely quantified in the plasma of infected individuals to monitor response to antiretroviral therapy (Steinmetzer *et al.*, 2010, Pasternak *et al.*, 2013). The number of HIV-1 RNA copies per mL of plasma is used to monitor response to treatment and predict the progression of infection, or detect viraemic relapse that could be due to antiretroviral resistance (Mellors *et al.*, 1997, Gullett and Nolte, 2015). Numerous commercial platforms exist for the quantification on HIV-1 RNA which are based on reverse transcription (RT) qPCR (Amendola *et al.*, 2014, Ginocchio, 2001, Kiselina *et al.*, 2014), although RT transcription mediated

amplification (TMA) is also used (Nair *et al.*, 2016). Commonly used clinical platforms for HIV-1 RNA quantification include: RealTime HIV-1 Viral Load Assay (Abbott), COBAS® AmpliPrep/COBAS® TaqMan® v2.0 (Roche), GeneXpert® HIV-1 Viral Load (Cepheid), Aptima® RT-TMA technology for Panther system (Hologic) and VERSANT® HIV RNA 1.0 (kPCR) (Siemens) (Ochodo *et al.*, 2018). Further platforms exist for HIV-1 viral load quantification both on the market and in development (Gullett and Nolte, 2015, Ochodo *et al.*, 2018, Mazzola and Pérez-Casas, 2015). Measurement of HIV-1 viral load is mediated by reverse transcription of the genomic viral RNA, followed by nucleic acid amplification and quantification in relation to a reference standard or calibration curve. Clinical platforms utilise secondary calibrators that are traceable to the WHO 4th HIV-1 RNA International Standard (NIBSC code: 16/194) (Falak *et al.*, In preparation, World Health Organisation, 2020a).

3.1.3. Variability associated with reverse transcription and the potential impact on RNA quantification

Reverse transcriptase enzymes were first identified as part of viral replication and subsequently incorporated into molecular applications (Baltimore, 1970, Temin and Mizutani, 1970). This has enabled detection and quantification of viral RNA genomes, which has been invaluable to pathogen diagnostics. Reverse transcription prior to nucleic acid amplification can be performed in a one-step format (i.e. immediately prior to amplification in the same reaction tube) or two-step format (i.e. cDNA is generated in a separate reaction tube, an aliquot of which is then amplified and detected). Each has advantages; simplicity, rapidity, ease of optimisation and ability to multiplex one-step RT techniques, and the ability to produce large quantities of cDNA stock using two-step formats. One-step approaches tend to feature in commercial approaches owing the fact that extraction, reverse transcription and nucleic acid amplification take place within an automated system (Mazzola and Pérez-Casas, 2015). However, despite having demonstrable benefits for RNA amplification the process of reverse transcription has been shown to be inherently variable for RNA quantification (Sanders *et al.*, 2013, Sanders *et al.*, 2014, Bustin *et al.*, 2015, Miranda and Steward, 2017). This is related in part to experimental variables associated with different stages of the RT-PCR reaction, including properties of the reverse transcriptase enzymes themselves (Barragán-González *et al.*, 1997). Wild-type reverse transcriptases possess intrinsic RNase H activity to cleave RNA from the RNA:cDNA complex following polymerisation. This can

be problematic for RT-PCR of longer templates as the RNA may be degraded by RNase H activity before full-length cDNAs can be synthesized, which may lead to a heterogeneous population of cDNAs. To circumvent this and improve cDNA synthesis, many commercial recombinant enzymes have reduced or diminished RNase H activity. This has been well characterised in reverse transcriptases derived from murine Moloney leukaemia virus (MMLV) (Gerard *et al.*, 1997), although several engineered, commercial enzymes derived from avian myeloblastosis virus (AMV) are available. Enzyme processivity, RNase H activity, conversion efficiency and fidelity are also important considerations for obtaining optimal yields of cDNA, as well as performance at higher temperatures which can help denature strong secondary RNA structures (Gerard *et al.*, 2002). This can facilitate higher yields of full-length cDNA to be synthesised that better represents the RNA populations present in the starting template.

Other experimental factors including RT priming strategy, PCR priming sites and gene target, target RNA concentration and secondary structure, background RNA concentration and the presence of inhibitors can impact upon RT-PCR performance (Gerard *et al.*, 2002, Schwaber *et al.*, 2019, Kiselinova *et al.*, 2014). This implies that choice of RT approach, enzyme and kit can impact upon the quantification of HIV-1 RNA, which has been demonstrated previously for other RNA targets (Sanders *et al.*, 2013). Different commercial platforms for HIV-1 RNA quantification will almost certainly utilise different enzymes for converting RNA to cDNA for clinical samples and the calibration standard, and subsequently quantitative results will be reported relative to that method. Whilst this allows for standardised intra-laboratory measurements, differences in enzyme performance between different platforms could be reflected in discrepancies in inter-laboratory comparisons, such as for EQA schemes and clinical studies. This could influence clinical tolerance limits or threshold values between centres where quantitative bias is introduced owing to differences in reverse transcriptase conversion efficiency, leading to disharmony in inter-laboratory values.

3.1.4. The role of digital PCR for quantification of viral RNA

Most commercial platforms for HIV-1 viral load quantification apply calibrators that are traceable to a unified WHO International Standard. However, the assigned value of HIV-1 RNA in the WHO standard is reported in international units (IU) where the convention in clinical laboratories is to report in copies per mL (Prescott G *et al.*, 2017). Reporting in copies per mL is enabled after

applying a conversion factor from IU, however each of the commercial platform manufacturers report different conversion factors for this purpose (World Health Organisation, 2020a), Falak *et al* (Section 10.11.3). Better harmonisation of viral load values between platforms could be achieved through direct use of a reference standard assigned in copies per mL. In addition, characterisation of reverse transcriptase conversion efficiency between different kits and methods could help to provide better analytical accuracy in quantification. Digital PCR (dPCR) could facilitate this through absolute quantification of nucleic acid molecules. dPCR could be applied to highlight variability in RNA quantification using different reverse transcriptase enzymes, and could be developed as a reference method to value assign calibration standards. dPCR has previously been demonstrated as an SI traceable method for nucleic acid quantification (Pavsic *et al.*, 2017, Whale *et al.*, 2018), which could in turn provide SI traceability to calibration standards used to quantify HIV-1 viral load. This could facilitate harmonisation and unification of approaches, enabling better analytical accuracy in clinical methodologies.

The aims of this chapter were to investigate whether choice of reverse transcriptase enzyme impacts upon quantification of HIV-1 RNA using dPCR. Absolute quantification using dPCR eliminates the requirement for a calibration curve, and could facilitate more direct and unbiased comparisons between enzymes. Understanding absolute differences in RNA quantification using different enzymes could support characterisation of RT efficiency, which would in turn facilitate better quantitative accuracy in terms of trueness (Appendix 1). In addition, this chapter explores the development of RT-dPCR as a candidate reference method to support current approaches for quantification of HIV-1 RNA genomes. Such a method could be useful for value assignment of primary reference materials used in clinical platforms, which could facilitate better traceability for HIV-1 viral load quantification and improve measurement harmonisation.

3.2. Materials and methods

3.2.1. Study materials

3.2.1.1. Culture of cell lines

Cell culture experiments were performed by Dr Gary Morley (LGC). 8E5 (ATCC® CRL-8993™) cell pellets were obtained as recommended by ATCC (USA), described in Section 10.11.2 (Appendix 11). In addition, Jurkat (ATCC® TIB-152™) cell pellets were obtained that were cultured using ATCC recommended conditions and stored at -80°C in RNA*later* stabilization solution (Sigma-Aldrich, USA).

3.2.1.2. Extraction of RNA

Total RNA was extracted from approximately one million cells using the Qiagen RNeasy mini Kit according to the manufacturer's instructions, and eluted in a final volume of 50 µL in buffer AE (Qiagen, Germany). The concentration of each RNA extract was estimated using a NanoDrop 2000 spectrophotometer to measure 1 µL of solution (Thermo Scientific™, USA). Extracts were assigned an RNA Integrity Number (RIN) out of 10 for intactness and fragmentation using an RNA 6000 Nano Bioanalyzer kit (Agilent Technologies, USA). 8E5 total RNA was diluted to a final concentration of ~0.2 ng/µL in ~10 ng/µL Baker's yeast tRNA (Sigma-Aldrich, USA) and Jurkat total RNA was diluted to a final concentration of ~5 ng/µL in 1X TE (Sigma-Aldrich, USA). Diluted RNA was divided into 20 µL single use aliquots and stored at -80°C.

3.2.1.3. Synthetic construct for comparison of reverse transcriptase enzymes

A region of the human immunodeficiency virus type 1 (HXB2) HIV1/HTLV-III/LAV reference genome (NCBI accession number K03455.1) was selected (positions 1 to 5,619) for generation of a synthetic RNA test molecule. The region included gene sequences for the 5' LTR, *pol*, *gag* and *vif*. The 5,619 bp DNA insert, along with a T7 RNA polymerase promoter sequence and *Xma*I restriction site (Appendix 2), was cloned into a standard pEX-A2 vector by Eurofins genomics

(Germany). Gene insertion in the correct orientation was confirmed by Sanger sequencing by Eurofins.

3.2.1.4. *In vitro transcription of synthetic RNA*

One microgram of the HXB2 plasmid (Section 3.2.1.3) was linearised with 0.4 units/ μL *Xma*I, 1X CutSmart buffer (New England Biolabs, USA) and nuclease-free water in a final reaction volume of 50 μL for 1 hour at 37 °C. This was followed by purification using the QIAquick PCR purification kit according to the manufacturer's instructions (Qiagen, Germany), with elution into 50 μL elution buffer. Linearisation was assessed using the 2100 Bioanalyzer with DNA 7500 series II kit (Agilent Technologies, USA), and the DNA concentration was estimated using the Qubit 2.0 fluorometer with the dsDNA HS Assay Kit (Invitrogen, USA). To generate positive sense strand RNA *in vitro* transcription (IVT) was performed using the MEGAscript T7 kit (Life Technologies, USA) containing 7.5 mM of each of ATP, CTP, GTP and UTP, 1X Reaction Buffer, 2 μL T7 enzyme mix and 8 μL of plasmid, with incubation at 37 °C for 4 hours. This was followed by incubation with TURBO DNase (Life Technologies, USA) at 37°C for 15 minutes. The reaction was purified using the RNeasy Mini Kit for RNA clean up protocol (Qiagen, Germany), which included an additional on-column DNase treatment with an RNase-free DNase set (Qiagen, Germany). IVTs were eluted into 50 μL RNase-free water. Transcribed RNA concentration was estimated using the Qubit RNA HS Assay Kit (Invitrogen, USA) and NanoDrop 2000. RNA was diluted 10- and 100-fold in The RNA Storage Solution (Ambion, USA) and assessed using the 2100 Bioanalyzer with RNA 6000 Nano kit (Agilent Technologies, USA), which also provided an approximate RNA concentration in ng/ μL . HXB2 IVT transcripts were diluted to approximately 10,000,000 copies per μL in 5 ng/ μL Jurkat total RNA carrier, divided into 20 μL single use aliquots and stored at -80 °C.

3.2.1.5. *Total HIV-1 genomic RNA reference material*

Total HIV-1 genomic RNA extract was obtained from the National Institute for Biological Standards and Control (NIBSC, UK). The virus strain had previously been used to prepare the 3rd and 4th HIV-1 WHO International Standards (Morris and NIBSC, 2019) (personal communication). RNA extraction was performed by Clare Morris (NIBSC) using a QIAamp UltraSens Virus Kit (Qiagen, Germany), having demonstrated inactivation of the virus following heating to 60°C for 1

hour. The RNA was transported from NIBSC to NML on dry ice and stored at -80°C on arrival. The material was analysed by RT-dPCR following the basic approach described in Section 2.1.5 using a One-Step RT-ddPCR Advanced Kit for Probes (Bio-Rad, USA) and an assay targeting the HIV-1 *gag* gene (Bosman *et al.*, 2015). Units of the material were gravimetrically prepared to a concentration of ~188 copies of HIV-1 *gag* per μL in ~5 ng/ μL human Jurkat total RNA (Ambion, USA) based on RT-dPCR.

3.2.1.6. *Whole viral External Quality Assessment (EQA) materials*

A total of 11 materials were obtained from INSTAND e.V. (Germany) that were part of INSTAND EQA Schemes 360 and 382 (2018; <https://www.istand-ev.de>; accessed on 22/07/20). Three of the materials were part of a previous scheme (June 2017), for which the quantitative results were known. The remaining 8 materials were for the March 2019 scheme, for which the results were blinded and are yet to be published. The materials were certified as being non-infectious HIV-1 virus in plasma, making them suitable to be handled at biosafety level 2 (BSL 2). Total RNA was extracted using a QIAmp viral nucleic acid kit (Qiagen, Germany) by following the manufacturer's protocol. Briefly, samples were reconstituted in 1.1 mL nuclease-free sterile water. 200 μL of this solution was extracted using the Qiagen kit, and resulting RNA was eluted in 62 μL volume. Duplicate units of the March 2019 materials were extracted across two days, and the resulting RNA was analysed immediately by RT-dPCR (Section 3.2.4). A negative control, where the extraction protocol was followed with no sample input, was included for each experiment.

3.2.2. *Assays for quantification of HIV-1 RNA*

3.2.2.1. *Oligonucleotide sequences*

Sequence information for the HIV-1 specific primers and probes is given in Table 3.1. Incompatibility has been reported between the Bio-Rad Advanced One-step RT-ddPCR kit for probes and standard dual-labelled hydrolysis probes (Pinheiro-de-Oliveira *et al.*, 2019). Based on these findings, a custom double-quenched probe for the LTR-*gag* assay was obtained from LGC BioSearch technologies (USA) for use with the one step RT advanced kit. Additional oligonucleotide sequences used for interlaboratory comparison of HIV-1 RNA quantification are given in Table 3.2.

Table 3.1: Primer and probe sequences for HIV-1 detection.

Assay target	Genbank accession	Name	5' to 3' *	Source
HIV-1 <i>pol</i>	K03455.1	Forward	GCA CTT TAA ATT TTC CCA TTA GTC CTA	(Strain <i>et al.</i> , 2013)
		Reverse	CAA ATT TCT ACT AAT GCT TTT ATT TTT TC	
		Probe	FAM – AAG CCA GGA ATG GAT GGC C – MGBNFQ	
Long Terminal Repeat – <i>gag</i> junction of HIV-1 (HIV-1 LTR- <i>gag</i>)	K03455.1	Forward	GCC TCA ATA AAG CTT GCC TTG A	(Busby <i>et al.</i> , 2017)
		Reverse	GGC GCC ACT GCT AGA GAT TTT	
		Probe	FAM – TGT GAC TCT GGT AAC TAG AGA TCC CTC AGA C – BHQ1	
		Double quenched probe	FAM – TCT GAG GGA-BHQnova™-TCT CTA GTT ACC AGA GTC ACA – BHQ1	Custom design (LGC BioSearch)
HIV-1 <i>gag</i>	K03455.1	Forward	TGG GTA AAA GTA GTA GAA GAG AAG GCT TT	(Bosman <i>et al.</i> , 2015)
		Reverse	CCC CCC ACT GTG TTT AGC AT	
		Probe	FAM – TCA GCA TTA TCA GAA GGA G – MGBEQ	

* Refer to page 23 for abbreviations relating to fluorescent dyes and quenchers.

Table 3.2: Primers and probes used in interlaboratory analysis of HIV-1 RNA materials

Assay target	Genbank accession	Name	5' to 3' *	Source
HIV-1 <i>gag</i>	K03455.1	Forward	AGT RGG GGG ACA YCA RGC AGC HAT GCA RAT	(Kondo <i>et al.</i> , 2009)
		Reverse	TAC TAG TAG TTC CTG CTA TRT CAC TTC C	
		Probe	FAM – AT CAA TGA R -ZEN™- G ARG CTG CAG AAT GGG A- IABkFQ	
HIV-1 <i>pol-vif</i>	K03455.1	Forward	TTT GGA AAG GAC CAG C	(Lim <i>et al.</i> , 2016)
		Reverse	CTG CCA TCT GTT TTC CAT A	
		Probe	HEX – TGG AAA GGT -ZEN™- GAA GGG GCA GT – IABkFQ	

* Refer to page 23 for abbreviations relating to fluorescent dyes and quenchers.

3.2.2.2. Assay verification

The LTR-*gag* (single and double-quenched versions) and *pol* and assays were verified using a 5-point dilution series of the plasmid DNA (pDNA) construct coding the HXB2 RNA transcript. Input concentration ranged from 10,000 to 1 copy per μL . The aim of the experiment was to assess assay linearity and compare quantitative estimates obtained using single versus double fluorescence quenching chemistries. Samples were analysed in triplicate reactions by uniplex assay (i.e. one assay per reaction) containing 5 μL DNA per reaction, using ddPCR Supermix for Probes without dUTP (Bio-Rad). The *gag* (Bosman *et al.*, 2015) assay was verified using a 4-point dilution series of the HXB2 RNA transcript from 1,000 to 10 copies per μL . 5 μL of RNA transcript was analysed using the One-Step RT-ddPCR Advanced Kit for Probes (Bio-Rad, USA). The *gag* and *pol-vif* EQA assay duplex (Table 3.2) was then compared by RT-dPCR with the *gag* (Bosman *et al.*, 2015) assay using the HXB2 RNA transcript. Quadruplicate reactions were analysed and differences in copies per μL compared. In addition, a single dilution of plasmid DNA was included in triplicate alongside the HXB2 RNA transcript to compare performance for DNA and RNA templates.

3.2.3. Evaluation of reverse transcriptase kits for absolute quantification of RNA by dPCR

The performance of different reverse transcriptase kits was compared by digital PCR (dPCR). A total of 4 kits were chosen which are listed in Table 3.3. All reverse transcriptase enzymes were recombinant MMLV in origin. Prior to reverse transcription (RT), RNA templates (*in vitro* transcribed RNA at a concentration of 10,000 copies per μL , or 0.2 ng per μL of $8\text{E}5$ total RNA) were heated to 65°C for 5 minutes and then quenched on ice for 1 minute to denature secondary structures. For the two-step protocols, RT was performed on a DNA Engine Tetrad (Bio-Rad, USA), and resulting cDNA was stored at -80°C . All RT experiments included controls without reverse transcriptase added (RT negative) to monitor plasmid DNA contamination.

Table 3.3: Reverse transcriptase enzymes and kits used in the study

Product	Supplier	Catalogue number	Format
FIREScript RT cDNA synthesis kit	Solis BioDyne	06-15-00050	Two-step
Maxima First Strand cDNA Synthesis Kit for RT-qPCR	Thermo Scientific™	K1641	Two-step
SuperScript™ III Reverse Transcriptase	Invitrogen™	18080093	Two-step
One-Step RT-ddPCR Advanced Kit for Probes	Bio-Rad	1864021	One-step

3.2.3.1. *FIREScript RT cDNA synthesis kit*

RT was performed as per the manufacturer's recommended standard protocol. A final concentration of 2 µM oligo dT primer, 2 µM random primers, 0.2 µM of either HIV LTR-*gag* or HIV *pol* reverse primer (Table 3.1), nuclease-free water, 2 µL RNA sample and the remaining reagents were combined in a 0.2 mL tube in a final volume of 20 µL. Reaction conditions were 50°C for 30 minutes and termination of the reaction at 85°C for 5 min.

3.2.3.2. *Maxima First Strand cDNA Synthesis Kit for RT-qPCR*

RT was performed as per the manufacturer's recommendations. In addition, 0.2 µM of either HIV LTR-*gag* or HIV *pol* reverse primer was added along with 2 µL RNA sample in a final volume of 20 µL. Reaction conditions were 50°C for 30 minutes and termination of the reaction at 85°C for 5 min.

3.2.3.3. *SuperScript™ III Reverse Transcriptase*

The following reagents were combined in a 0.2 mL tube: 0.2 µM of either HIV LTR-*gag* or HIV *pol* reverse primer, 2 µM oligo dT primer and 2 µM random primers (both Solis BioDyne, Estonia), 10 mM dNTP mix, 1x First Strand sample buffer, 2 U/µL RNase inhibitor, 10U/µL SuperScript III reverse transcriptase, 5mM DTT (all Invitrogen™, USA), nuclease-free water (Ambion, USA) and

2 μL RNA template to a final volume of 20 μL . Reaction conditions were 55°C for 30 minutes and termination at 70°C for 15 minutes.

3.2.3.4. One-Step RT-ddPCR Advanced Kit for Probes

The reaction was performed as per the manufacturer's recommendations, with an initial RT step at 47.5°C for 60 minutes followed by thermocycling as described below. The primers and probes used are given in Table 3.1. Of note, a custom double-quenched HIV-1 LTR-*gag* probe, was used with this kit in place of the standard LTR-*gag* probe.

3.2.4. General protocol for RNA quantification by dPCR

Following reverse transcription using the two-step or one-step protocols, dPCR was performed as described in Section 2.1.5 using the QX200™ droplet digital PCR system (Bio-Rad, USA). 2 μL cDNA (or 2-5 μL RNA for the one-step protocol) was added to a total reaction volume of 20 μL . Thermocycling conditions were as follows: 10 minutes at 95 °C, 40 cycles of 94 °C for 30 s, and 58 °C for 1 min, followed by 98°C for 10 min and a 4 °C hold. A partition volume of 0.85 nL was used to calculate copy number concentration (Bio-Rad, USA).

For the EQA analysis, 7 μL RNA was added to a total volume of 20 μL containing the One-Step RT-ddPCR Advanced Kit for Probes (Bio-Rad, USA), nuclease-free water (Ambion, USA) and the oligonucleotides described in Table 3.2. In these experiments, each probe was added to a final concentration of 250 nM. Cycling conditions were reverse transcription for 60 minutes at 50°C, 10 minutes at 95°C followed by 45 cycles of 95°C for 30 seconds and 55°C for one minute. The remaining steps were as described in Section 2.1.5. A partition volume of 0.834 nL was used to calculate copy number concentration (Corbisier *et al.*, 2015).

3.2.5. Evaluating the sensitivity of different reverse transcriptase enzymes by RT-dPCR

The respective sensitivities of the Maxima First Strand cDNA Synthesis Kit and Bio-Rad One-Step RT-ddPCR Advanced Kit were evaluated. Briefly, a dilution series of the HXB2 RNA transcript was prepared gravimetrically ranging from ~250 to ~0.1 copies per μL estimated using Qubit. 2 μL each dilution was added to duplicate RT reactions in a total volume of 20 μL (Maxima), or into RNase-free water to a final volume of 20 μL (Bio-Rad one-step). 2 μL of either cDNA or

diluted RNA transcript, respectively, was then added to the dPCR reaction as described above in a total of ten reactions per dilution. The *pol* assay was used for both reverse transcriptase kits.

3.2.6. Data analysis

Data from dPCR experiments were subject to threshold and baseline setting in QuantaSoft version 1.7.4.0917 (Bio-Rad), and were exported as .csv files to be analysed in Microsoft Excel 2010. The average number of copies per droplet (λ) was calculated as described previously (Whale *et al.*, 2016a). Differences in copies per μL were compared for statistical significance using a Student's t-test.

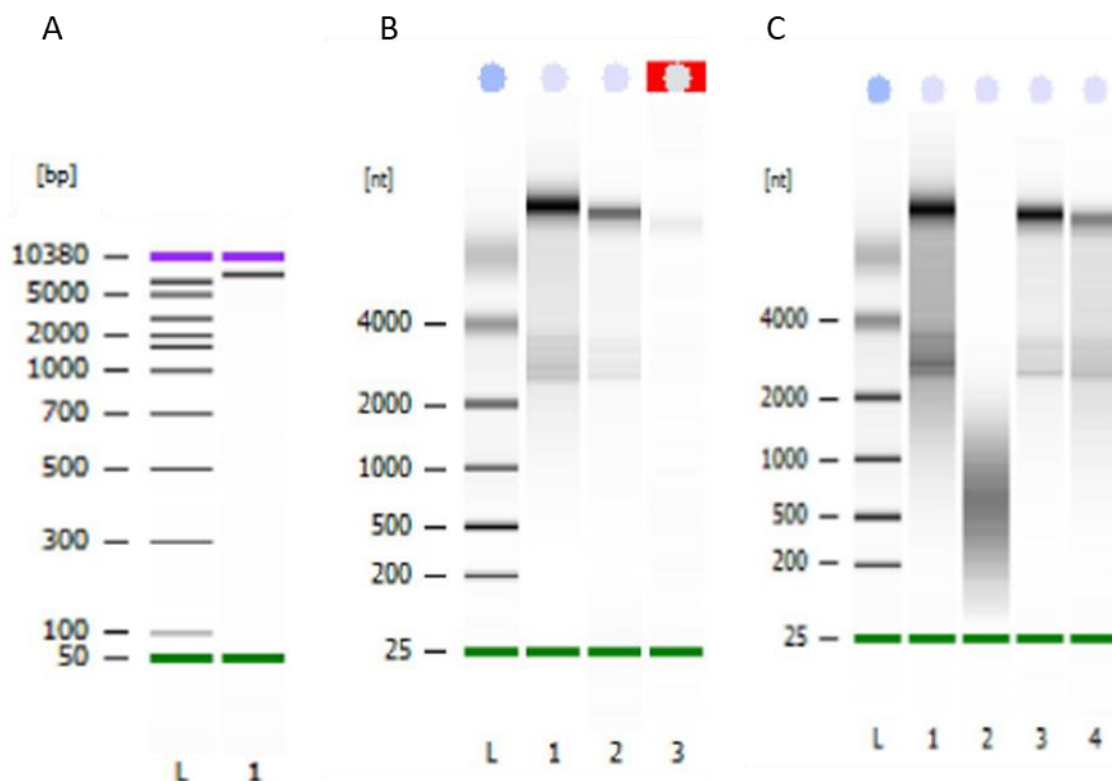
3.3. Results and discussion

3.3.1. *Design and in vitro transcription of a synthetic HIV-1 RNA molecule for characterisation of reverse transcription (RT) dPCR*

The HXB2 synthetic transcript was designed so that positive sense RNA representative of the HIV-1 genome could be transcribed using the anti-sense strand of DNA as a template. This was achieved by designing the molecule with a promoter sequence of T7 RNA polymerase upstream of the start of the sequence (7 to 24 bp; Appendix 2). A *Xma*I restriction site at positions 5,652-5,657 bp enabled linearisation of the DNA plasmid in preparation for *in vitro* transcription (Figure 3.1 A). Of note, the molecule was designed with additional promoter and restriction site sequences, namely *Bsp*HI restriction site (1-6 bp), *Not*I restriction site (25-32 bp) and a T3 RNA polymerase promoter site in reverse complement orientation (5,657-5,675 bp). The respective purposes of these sites was to enable the fragment to be fully excised from the plasmid vector using *Bsp*HI if desired, and to enable transcription from the sense DNA strand using T3 RNA polymerase and *Not*I should the orientation of the gene insert in the plasmid vector be found to be incorrect.

Following synthesis and subsequent visualisation on the Agilent 2100 Bioanalyser, the *in vitro* RNA molecule was estimated to be 6,000 nt, which is slightly larger than the expected size of 5,632 nt (Figure 3.1 B). The reason for this observation is unclear, and although not performed on this occasion, an additional larger RNA ladder could be analysed in parallel with the RNA transcript to confirm the expected fragment size (e.g. Millennium™ RNA Markers, Ambion, USA). Figure 3.1 B also shows unexpected additional bands at approximately 2,800 to 3,000 nt that may represent secondary RNA structures. This was unlikely as, prior to visualisation, templates were denatured at 70°C for 2 minutes and immediately quenched on ice. To mitigate against the possibility of resistant secondary structures fresh aliquots of the fragment were subjected to a further heat denaturation step at 95°C with little to no effect. Lane 2 (Figure 3.1 C) shows that 95°C heat denaturation of the neat RNA transcript appeared to severely impact upon the integrity of the RNA, with almost complete fragmentation observed. Lanes 1, 3 and 4 show that, despite additional heating, the unexpected lower bands were still observed.

Figure 3.1: Bioanalyzer 2100 gel-like images depicting (A) linearised plasmid DNA expected at 8,125 bp visualised using a DNA7500 kit (B) *in vitro* transcribed RNA visualised using a RNA6000 nano kit. The three lanes represent neat [1], 10-fold [2] and 100-fold [3] dilutions of the RNA (C) heat denaturation of the neat RNA [lanes 1 & 2] and a 10-fold dilution [lanes 3 & 4] at 70 [1 & 3] and 95°C [2 & 4]. L indicates the molecular weight ladder for each kit.

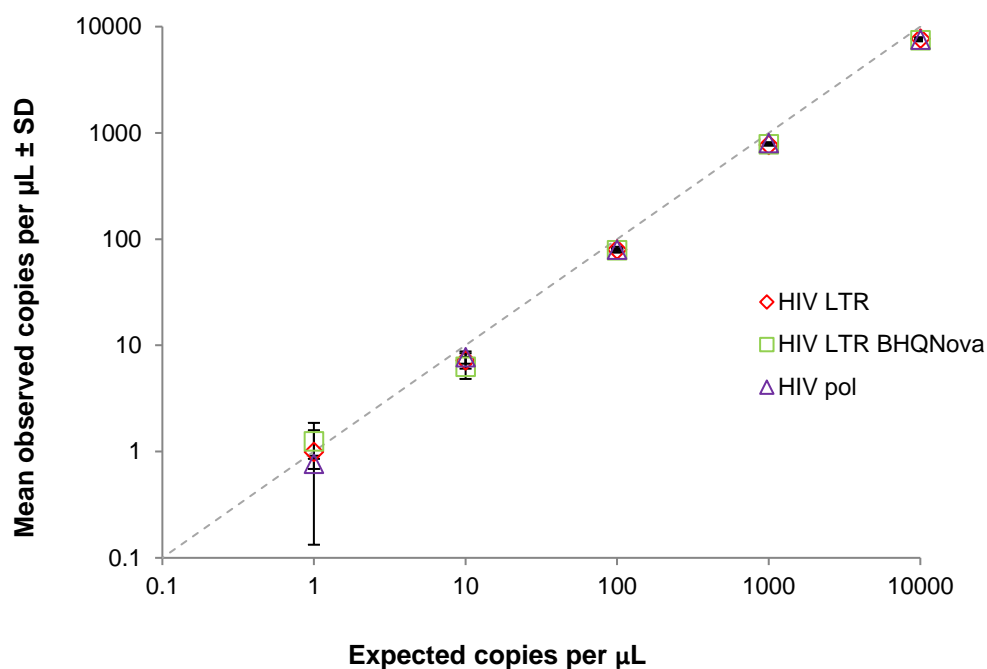


It is possible that the unexpected products are truncated structures generated during *in vitro* transcription. This can occur due to numerous factors including runs of single bases and the presence of cryptic promoter or terminator sites, causing the T7 RNA polymerase to stop generating RNA. Although a more thorough heat denaturation step was shown to have little effect (Figure 3.1 C), the presence of highly resistant RNA secondary structures related to this particular sequence still cannot be ruled out. Extensive *in silico* analysis of RNA folding was not performed for this molecule, although could reveal sequence regions that are highly susceptible to complex folding. Further investigation to explain this observation was not explored in this thesis, however additional work could include sequencing of all products following agarose gel excision to identify their origin. The ~6,000 nt HXB2 *in vitro* transcript was taken forward for use in this study, accepting that heterogenous populations of transcripts or secondary structures could impact upon RNA quantification.

3.3.2. Verification of dPCR assays for comparing RT kits

The assays that were to be used for the RT kit comparison were verified for digital PCR using HXB2 plasmid DNA, which was used to generate the *in vitro* transcribed RNA molecule. Verification was to ensure that the assays were performing with good linearity across a dilution series and whether quantitative values were comparable between assays for plasmid DNA. In addition, a comparison between the performance of the single and double quenched LTR-*gag* probes could be made in this way. Figure 3.2 illustrates that the initial assays evaluated for this study were capable of quantification down to 1 plasmid DNA copy per μL . At the lowest point of the dilution series, precision was notably poorer which is characteristic of PCR amplification at this low level of quantification (Quan *et al.*, 2018). Analysis of assay linearity is a valuable tool for assessment of new assays by digital PCR to identify any template concentration related effects, or inhibition. Assay validation holds additional importance for qPCR where quantification of unknown samples relative to a standard curve can be highly biased by non-linearity in a dilution series. Figure 3.2 shows that the assays performed comparably in terms of quantification of the respective gene targets in the DNA plasmid. This is demonstrated by a 1:1 ratio between the LTR-*gag* and *pol* gene copy numbers, which is expected since they are on the same molecule of DNA. In addition, a 1:1 ratio was observed between copy numbers measured using the single and double-quenched LTR-*gag* probes.

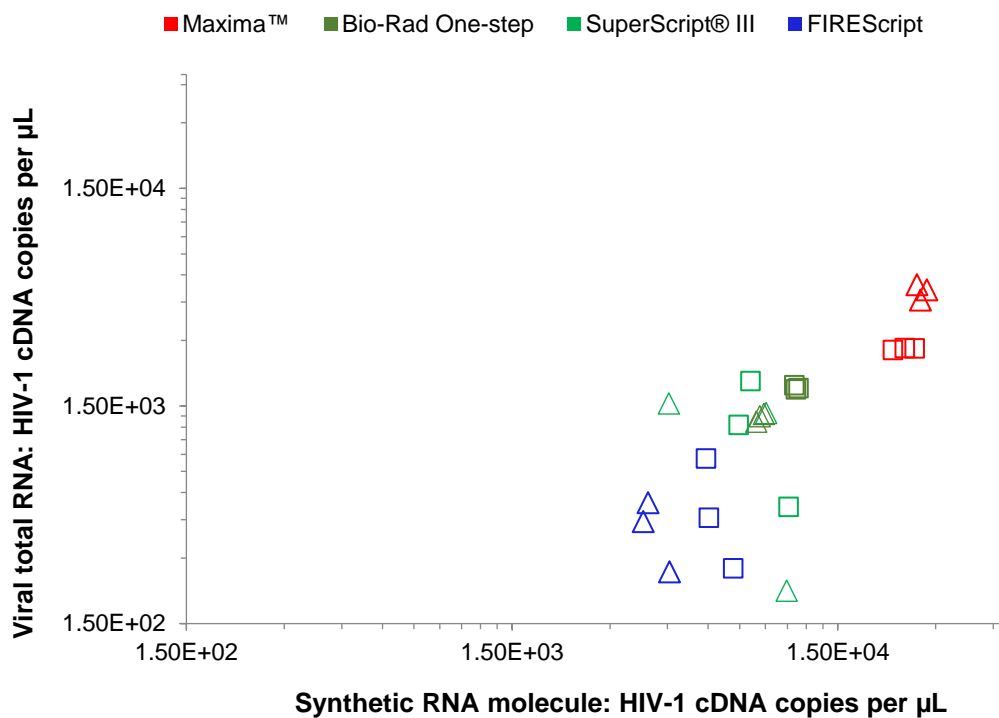
Figure 3.2: Digital PCR verification of single and double-quenched HIV LTR-gag and pol assays using plasmid DNA. Error bars represent standard deviation. The dashed line represents equivalence.



3.3.3. Comparison of different kits for performing reverse transcription using dPCR

Four commercially available reverse transcriptase kits (Table 3.3) were compared in terms of their cDNA conversion efficiency. The comparison was performed using *in vitro* transcribed HXB2 RNA template, the initial input quantity of which was standardised to ~10,000 copies per µL using a Qubit 2.0 fluorometer. Reverse transcription was performed either in a one-step or two-step format, and the resulting cDNA was quantified by digital PCR. The four enzymes were then applied to total RNA extracted from the 8E5 cell line input at a standardised concentration of 0.2 ng per µL to evaluate the impact of template complexity on reverse transcription.

Figure 3.3: Comparison of RT kits for total RNA and synthetic RNA. HIV-1 cDNA copy number was found to be dependent on assay target as well as RT kit. Δ HIV-1 *pol* assay \square HIV-1 LTR-*gag* assay. Each data point represents a single RT-dPCR replicate.



HIV-1 cDNA copies per μL were found to differ significantly between the four kits - up to ~6-fold in some cases. Furthermore, differences in cDNA copies per μL were observed between the two assay targets chosen (LTR-*gag* and *pol*) (Figure 3.3). The assays were demonstrated to be equivalent in performance when applied to plasmid DNA (Figure 3.2), suggesting that the observed differences were not necessarily due to assay performance. The kits were ranked in order of cDNA copy number, and the Maxima kit was found to give the greatest yield for both the HXB2 molecule and the 8E5 total viral RNA. The Bio-Rad one step was found to exhibit the least amount of variability between replicate measurements for both assays, whereas more variability was observed for the other kits. This is an important consideration when choosing a kit for the most sensitive quantitative estimates, as high variability introduced by the RT kit will likely further inflate stochastic effects for measurements at low copy number (such as for HIV viral load). It is unsurprising that two-step RT formats exhibit higher variability, particularly at low levels, owing to increased pipetting steps and requirement for dilution of cDNA template prior to analysis.

Figure 3.3 shows that the Maxima kit provided the highest estimation out of the four kits in terms of RNA concentration. The reasons for the observed differences in copy number are unclear,

however it was possible that the reverse transcriptase in this kit was highly efficient at converting RNA to cDNA. Another possibility was that the RNase H activity is ineffective at cleaving the initial RNA template, and so more than one cDNA copy was generated per RNA molecule. RNase H has been shown to possess sequence-specific preferences for cleavage of the RNA:DNA complex in reverse transcription, particularly for HIV-1 *in vivo* (Kielinski *et al.*, 2017). These findings suggest that variability could exist within the RNase H activity inherent to numerous commercial RT kits. cDNA copy numbers measured by dPCR were used to estimate the concentration of the stock HXB2 RNA molecule concentration, assuming a 1:1 RNA to cDNA conversion ratio. These values were compared with the orthogonal methods used to estimate initial RNA concentration in the IVT stock.

Figure 3.4: Comparison of copy numbers per μL for the four reverse transcriptase kits compared with orthogonal methods: NanoDrop (black), Qubit (dark grey) and Bioanalyser (light grey) for the LTR-gag (red) and pol (pink) assays. Error bars represent standard deviation.

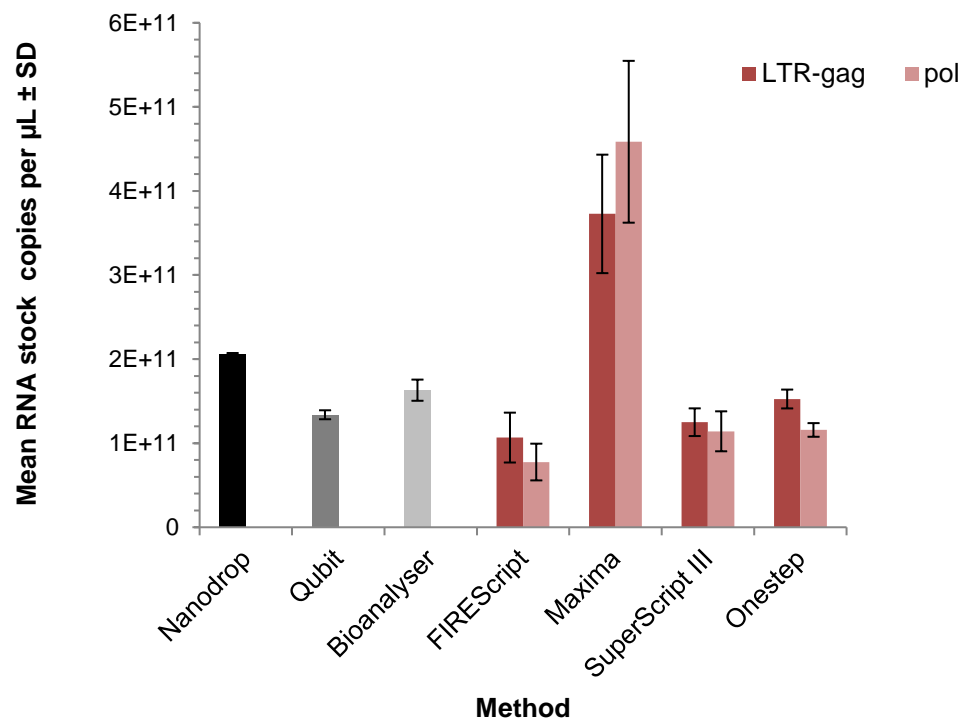


Figure 3.4 shows a comparison of RNA copies per μL between the four reverse transcriptases tested and the orthogonal methods used to quantify the HXB2 molecule following *in vitro* transcription. These were the NanoDrop 2000 spectrophotometer which estimates nucleic acid quantification using ultraviolet (UV) spectrophotometry; the Qubit 2.0 which binds nucleic acid using an intercalating dye; and the BioAnalyser 2100 which performs capillary electrophoresis in

a chip-based format. The Maxima kit was found to yield an estimation of RNA copy number that was up to 2.2-fold higher than the NanoDrop, which often inflates estimations of concentration due to being unable to distinguish between RNA and DNA at 260 nm absorbance (Koetsier and Cantor, 2019). This raises further questions over the kinetics of the Maxima kit, and whether misrepresentation of RNA copy number was indeed being observed.

3.3.3.1. *Assessing the analytical sensitivity of RT dPCR*

The Maxima two-step kit and the Bio-Rad one-step kit were chosen to evaluate the analytical sensitivity and linearity of RT dPCR. An additional aim was to investigate RT efficiency for the two kits by challenging the 1:1 RNA:cDNA conversion hypothesis discussed previously. Amplification and detection of a single molecule of RNA by dPCR, following conversion to a single molecule of cDNA, should be possible following this assumption. A dilution series from ~250 to ~0.1 copies per μL of RNA stock solution (corresponding to ~50 to ~0.02 cDNA copies per reaction) based on Qubit fluorometric analysis was gravimetrically constructed using the HXB2 synthetic RNA fragment in a background of human Jurkat cell RNA carrier. A total of 20 μL of cDNA or diluted RNA was analysed as ten separate dPCR reactions (each containing 2 μL template per reaction) and expressed as copies of HIV *pol* per μL (in the 20 μL sample volume). The results were \log_{10} transformed and compared with the expected cDNA copies per μL . The *pol* assay was chosen because it was common to all RT kits tested in this study, as opposed to the LTR-*gag* assay which possessed different quenching moieties depending on which kit was used.

Figure 3.5: \log_{10} transformed observed versus expected cDNA copies per μL for the HIV pol assay using (a) Maxima two-step and (b) Bio-Rad one-step kits. The dashed line represents equivalence.

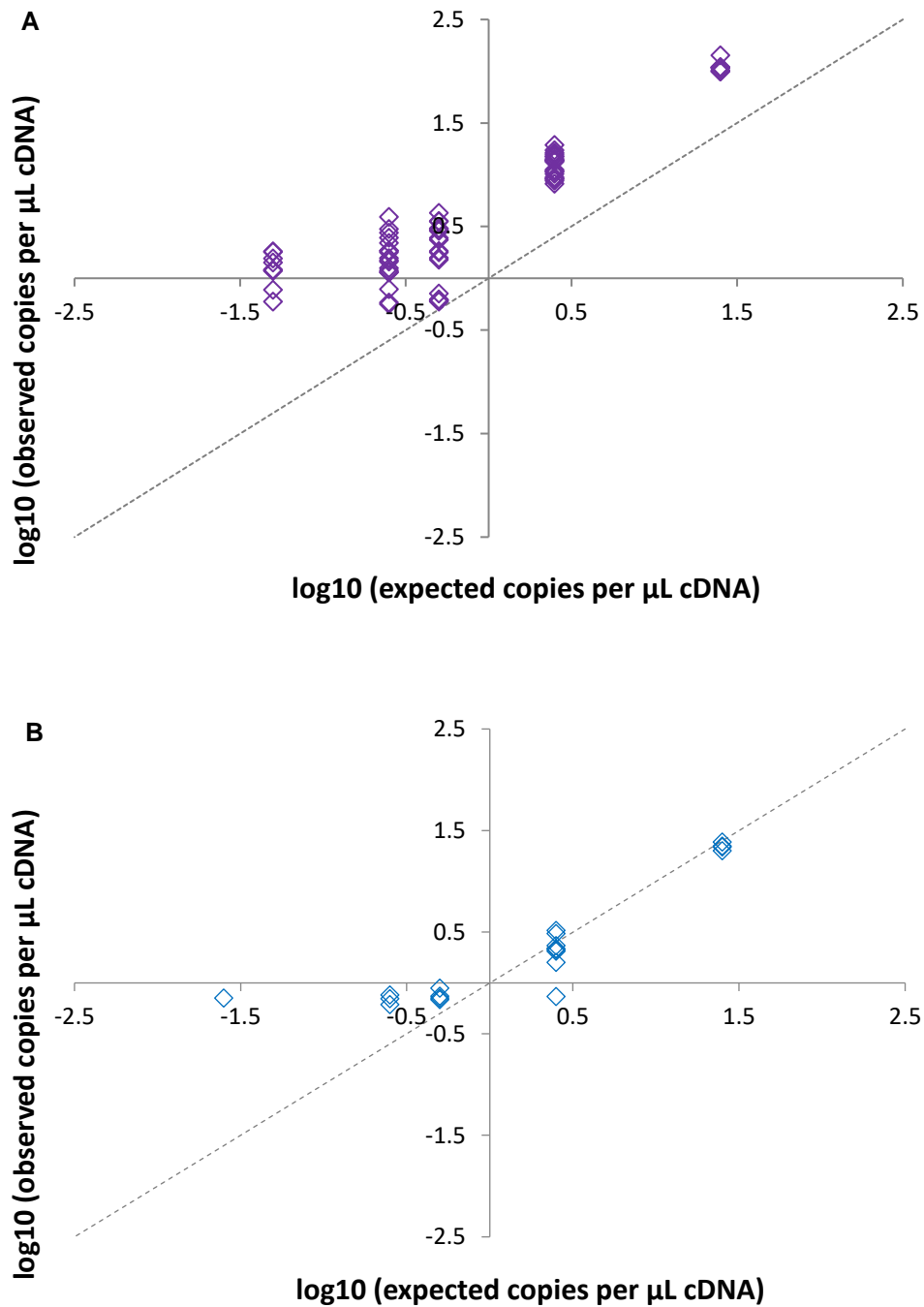


Figure 3.5 shows that the Bio-Rad one step kit was technically capable of detecting lower cDNA copy numbers (corresponding to 0.025 copies per μL RNA input) compared with the Maxima kit (corresponding to 0.05 copies per μL RNA input). However, when assessing the technical sensitivity of a method measurement uncertainty estimates play a key role in analytical confidence. Whilst lower dilutions in the series were detected using the Bio-Rad kit, only 1 technical replicate out of 10 produced a signal. The limit of detection (LOD), often defined as the concentration at which 95% of technical replicates produce a positive signal, can be used to

determine analytical sensitivity. Whilst the LOD of dPCR has been described as corresponding to detection of a single molecule in a single partition (Quan *et al.*, 2018), a formal statistical estimation of sensitivity cannot reliably be based on the presence of one out of ten positive replicates. A more robust estimation of the LOD would include data for a higher number of replicates, which may be a reciprocal of the expected input copy number (Strain *et al.*, 2013). The sensitivity of the Bio-Rad kit in this study was proposed as < 25 copies per μL , and <0.25 copies per μL for the Maxima kit based on 100% of replicates containing the target template. Ten NTC replicates were included in each experiment, none of which gave a positive signal for HIV RNA. Additional replicate experimental runs would provide further statistical confidence for formal LOD estimates. A limitation of these experiments is that false positive amplification associated with the HIV *pol* assay at the lowest dilution points for the Bio-Rad one-step kit made it difficult to set a cut-off between clusters of positive and negative droplets. This presented challenges for differentiating between true and spurious positives (Appendix 3). For this reason, the baseline quantity (i.e. the number of positive droplets in the no template control and carrier wells) was subtracted from the number of positive droplets counted per reaction in the test material. This may have caused a reduction in the perceived sensitivity of the Bio-Rad one step RT dPCR kit using this assay. False positive amplification has been described in other studies utilising dPCR for HIV DNA quantification (Jones *et al.*, 2014).

The theoretical 1 cDNA copy per reaction in this study corresponded to the third dilution point in Figure 3.5 (expected $-0.3 \log_{10}$ cDNA copies per μL). At this dilution 100% and 40% of replicate wells for the Maxima and Bio-Rad kits, respectively, contained amplified target. Both kits continued to demonstrate amplification past this point, which enabled detection of cDNA target past the point of theoretical 1 copy per reaction. This is likely attributed to sampling dynamics from the 20 μL total reaction. However, the Maxima kit demonstrated amplification in a high proportion of reaction wells below the theoretical 1 copy per reaction which may indicate that a greater cDNA yield is being detected. It is unclear whether this reflects the true RT efficiency of the Maxima kit, and further work should aim to investigate this. A similar strategy to the one implemented in this study was applied by (Schwaber *et al.*, 2019) to characterise RT efficiency for transcriptomics. A limitation of this kind of approach is that reliance on one method to assign input quantity to synthetic transcripts prior to dPCR could introduce error into measurements through any inaccuracies, and potentially invalidate calculations for RT efficiency.

3.3.3.2. *Considerations for selecting reverse transcriptase kits for HIV RNA quantification*

The benefit of using an *in vitro* transcribed molecule for the comparison of different reverse transcriptase kits compared with total RNA is that input copy numbers of HIV sequence are easier to estimate than when using HIV present in total cellular RNA extracts. Pure RNA concentration can be measured using non-specific optical methods such as fluorometric or spectrophotometric methods and copy number calculated based on the known molecular weight of the synthesized molecule. This can be more complicated for HIV total RNA where multiply spliced and un-spliced versions of varying lengths may exist. This could be overcome by using full-length sequenced transcripts from pure cultured HIV virus; a resource that was unavailable for this work. Using the *in vitro* transcribed molecule to compare reverse transcriptases by dPCR led to the following preliminary conclusions; (i) variability in efficiency to convert RNA to cDNA exists between different commercially available reverse transcriptases. This was true between three different enzymes present in two-step format, and additionally between these enzymes and a one-step kit. This manifested as different yields of cDNA copy number from a standardised input of RNA, suggesting that the conversion rate varies between kits. (ii) sequence-specific effects should be taken into consideration when comparing RNA copy numbers as different dPCR assays can generate significantly different values. This is particularly relevant for quantifying HIV genomes which can be highly divergent, making assay design and selection difficult (Carneiro *et al.*, 2017). (iii) ease of use, cost and labour should be considered. Whilst the high yields and enhanced sensitivity offered by the Maxima two-step kit may be an attractive option, there are numerous advantages to using a one-step RT kit over a two-step format. Some of these advantages include preservation of cDNA copy number and minimisation of measurement uncertainty by removing additional dilution steps, ease of standardisation and overall simplicity; advantages which may lend themselves to supporting HIV-1 viral load quantification in a clinical diagnostic setting.

The factors that can influence RT-dPCR quantification of HIV-1 RNA, including RT format and assay sequence, were taken into consideration for the subsequent section of this chapter. An externally specified approach was applied to a set of EQA materials to evaluate additional factors affecting HIV-1 RNA quantification, which included RNA extraction and inter-laboratory effects.

The purpose of this was to assess RT dPCR as a method for value assigning reference materials to support clinical quantification of HIV-1 viral load.

3.3.4. Application of RT-dPCR to EQA materials for HIV-1 RNA quantification

3.3.4.1. Characterisation of assays and materials

Inter-laboratory EQA assessment of HIV-1 RNA quantification helps to ensure that measurements performed by different laboratories are comparable, robust and accurate. RT-dPCR can be applied as a precise and sensitive method for nucleic acid quantification. Two assays were stipulated for an inter-laboratory comparison of RT-dPCR HIV-1 RNA quantification; targeting HIV *gag* and *pol-vif* to be assayed in duplex (Table 3.2). The performance of these assays was compared with those previously evaluated in this study. The assays described so far were tested on synthetic material derived from the HXB2 reference genome, and RNA extracted from the 8E5 cell line. To explore the performance of RT-dPCR for analysis of additional HIV-1 sequences that represent a wider repertoire of samples, pre-extracted RNA was obtained from a whole viral material resembling the WHO HIV-1 RNA International Standard (Section 3.2.1.5). An additional assay was introduced as a reference control for these experiments; HIV *gag* (Bosman) (Table 3.1). This additional assay was introduced at this stage owing to a deletion in the sequence for the HIV-1 NIBSC control material at the LTR region that was identified *in silico* (Gall *et al.*, 2014). A comparison of the HIV *gag* (Bosman) assay with the HIV LTR-*gag* assay by one-step RT dPCR using triplicate replicates of the HXB2 transcript showed that there was no significant difference in the number of copies per μL (HIV *gag* = 1135.5 copies per μL (SD 27.7), HIV LTR-*gag* = 1083.4 copies per μL (SD 28.7)) ($p = 0.087$). Following this the *gag* and *pol-vif* duplex was compared with the HIV *gag* (Bosman) assay using the HXB2 transcript. There was found to be no significant difference between the two HIV *gag* assays ($p = 0.26$), however the Bosman *gag* and *pol-vif* assays were found to give significantly different quantitative values ($p = 0.00039$) (Figure 3.6a). To investigate this further, the assay duplex was applied to plasmid DNA containing the HXB2 sequence in parallel with the RNA molecule and analysed by RT-dPCR.

Figure 3.6: The HIV gag (Bosman) and HIV gag (Kondo)/pol-vif assay duplex was applied to (a) the HXB2 synthetic RNA transcript and the viral RNA extract. A comparison was performed between (b) the HXB2 RNA transcript and the corresponding DNA plasmid.

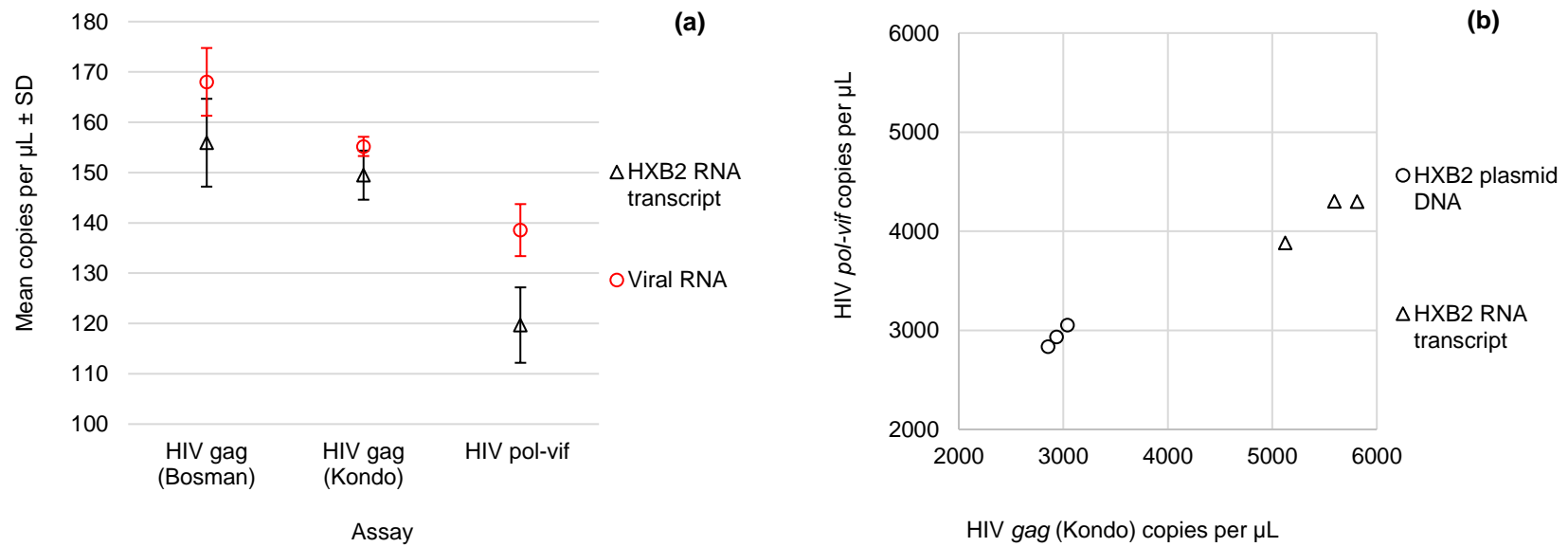
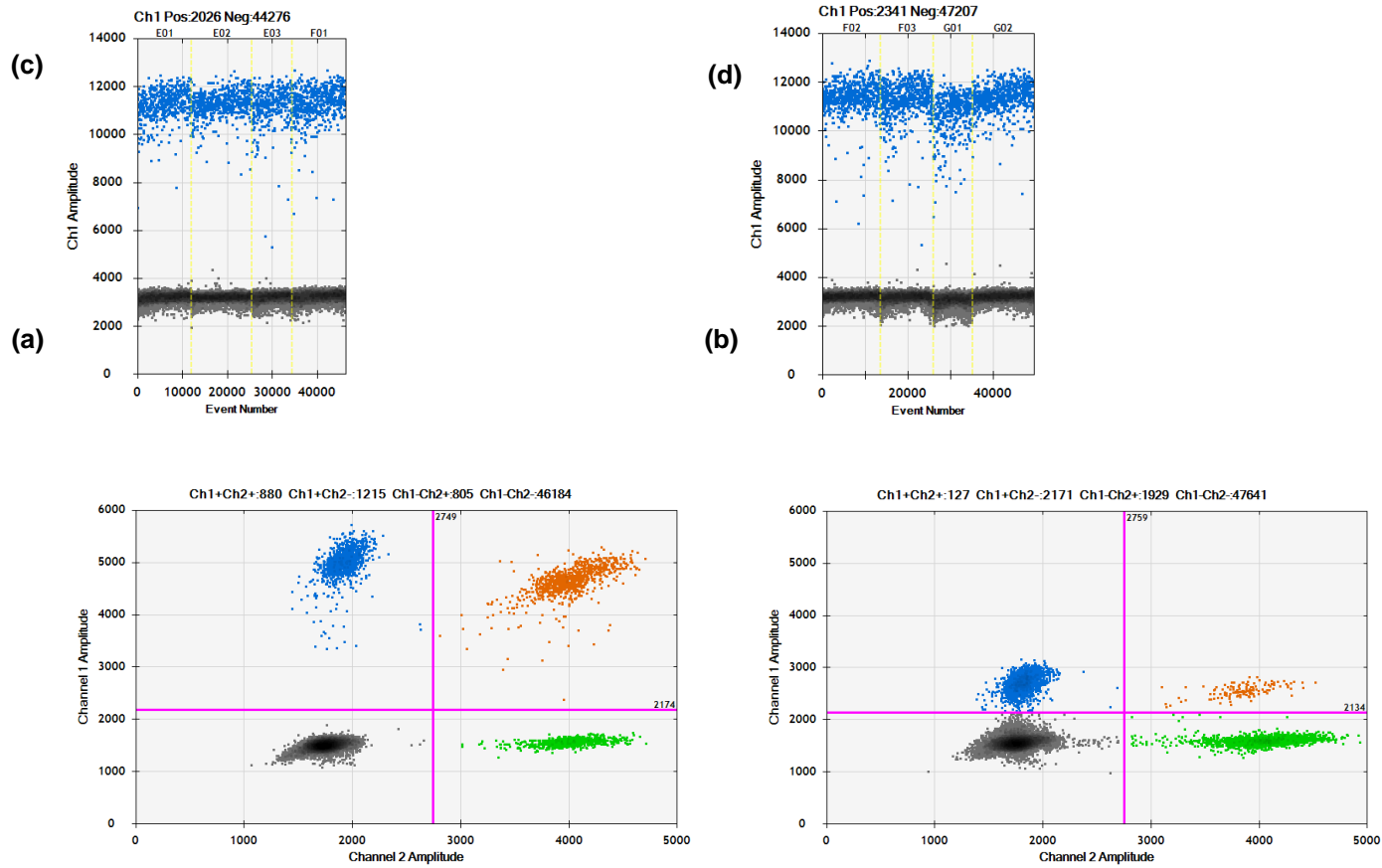


Figure 3.7: QX200 dot plots showing the HIV gag (Bosman) assay applied to (a) the HXB2 RNA molecule and (b) the viral RNA extract and the HIV gag (Kondo)/pol-vif duplex applied to (c) the synthetic HXB2 RNA molecule and (d) the viral RNA extract. Blue dots represent partitions containing HIV gag target, green dots represent HIV pol-vif.



Analysis of plasmid DNA revealed that there was no significant difference in copy number between the two assays ($p=0.64$), however when the assays were compared for RNA they were significantly different ($p=0.0037$) (Figure 3.6b). This indicates an assay-dependent effect associated with conversion of RNA to cDNA via reverse transcription, and suggests that any differences in RT conversion efficiency are related to the reverse transcription step and not necessarily PCR.

For the whole viral RNA material a statistically significant difference in copy number was observed between both HIV *gag* assays (Figure 3.6a) ($p=0.014$). Following *in silico* analysis of the published sequence of NIBSC-1, it was found that there were three mismatches between the probe and degenerate reverse primer of the Kondo *gag* assay (2 substitutions and 1 insertion). Figure 3.7d shows dPCR dot plots with reduced peak resolution in the FAM channel (compared with Figure 3.7c), which corresponds to the HIV *gag* (Kondo) assay. In contrast Figure 3.7a & b show that the peak resolution for the HIV *gag* (Bosman) assay, which has perfect sequence homology with both materials, is comparable between the two templates. The finding of mismatched primers, combined with the observed deletion in the HIV LTR region of the NIBSC1 sequence, raises important questions surrounding assay design for highly heterogeneous and divergent HIV-1 sequences. *In vivo*, HIV reverse transcriptase is able to switch between the two copies of single stranded RNA for dsDNA synthesis. Therefore, if the copies are heterogeneous a chimeric DNA molecule may be produced, resulting in the eventual production of genetically novel virions (Hu and Hughes, 2012). The high degree of sequence heterogeneity in HIV-1 viral sequences can be problematic for assay design and ultimately affect quantitative results (Bosman *et al.*, 2018, Rutsaert *et al.*, 2018b).

3.3.4.2. Analysis of test EQA materials

The Bio-Rad one step RT dPCR kit, offering more simplicity for setup and higher precision over other formats including two-step RT, was chosen for the analysis of RNA extracted from the EQA materials. To test the suitability of the chosen extraction method, RT kit and assay duplex the full workflow was performed once for a set of three test EQA materials (Section 3.2.1.6). The HXB2 *in vitro* transcribed RNA molecule was chosen as an RT-dPCR positive control.

Figure 3.8: Copies per μL for the gag and pol-vif assays and the expected values from the 2017 EQA scheme.

Upper and lower expected values are based on 95% confidence intervals given by the scheme providers.

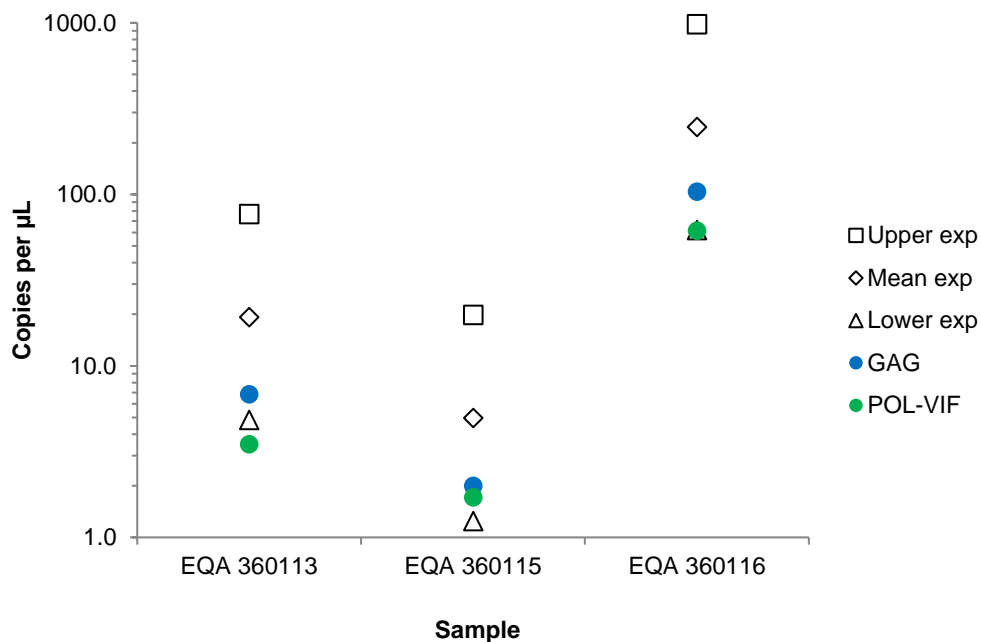


Figure 3.8 shows that the copies per μL observed for each material were towards the lower end of the expected range, with the HIV *pol-vif* value for EQA 360113 falling just outside. These data are based on a single experiment, and further experimental replicates are necessary to be able to assign any statistical confidence to the values. However, based on comparisons of different assays for RT dPCR using the same kit it (Figure 3.3) is unsurprising that differences exist between the two assay targets due to sequence-specific effects. For this reason, it seems prudent to report copy numbers for the individual assays as opposed to an average of the two. The HIV *gag* (Kondo) assay was chosen to represent the copy number estimations for these materials since it had previously been shown to give comparable copy numbers to the *gag* (Bosman) assay using the HXB2 positive control.

3.3.4.3. *Intra-laboratory analysis of EQA materials for HIV RNA quantification*

The method was subsequently applied to materials from a current EQA inter-laboratory study (Section 3.2.1.6). Extraction was performed on duplicate units across two days (one unit per day), with each extract analysed in triplicate by RT dPCR. The results were expressed as copies of HIV *gag* per μL , and the HXB2 RNA fragment was included as a positive control for dPCR.

Figure 3.9: HIV RNA EQA intra-laboratory results. (a) Copies of HIV gag per μL for 8 EQA samples across two extraction batches represented on a logarithmic scale. (b) Mean copies gag per μL are plotted against %CV indicative of an inverse relationship between the two.

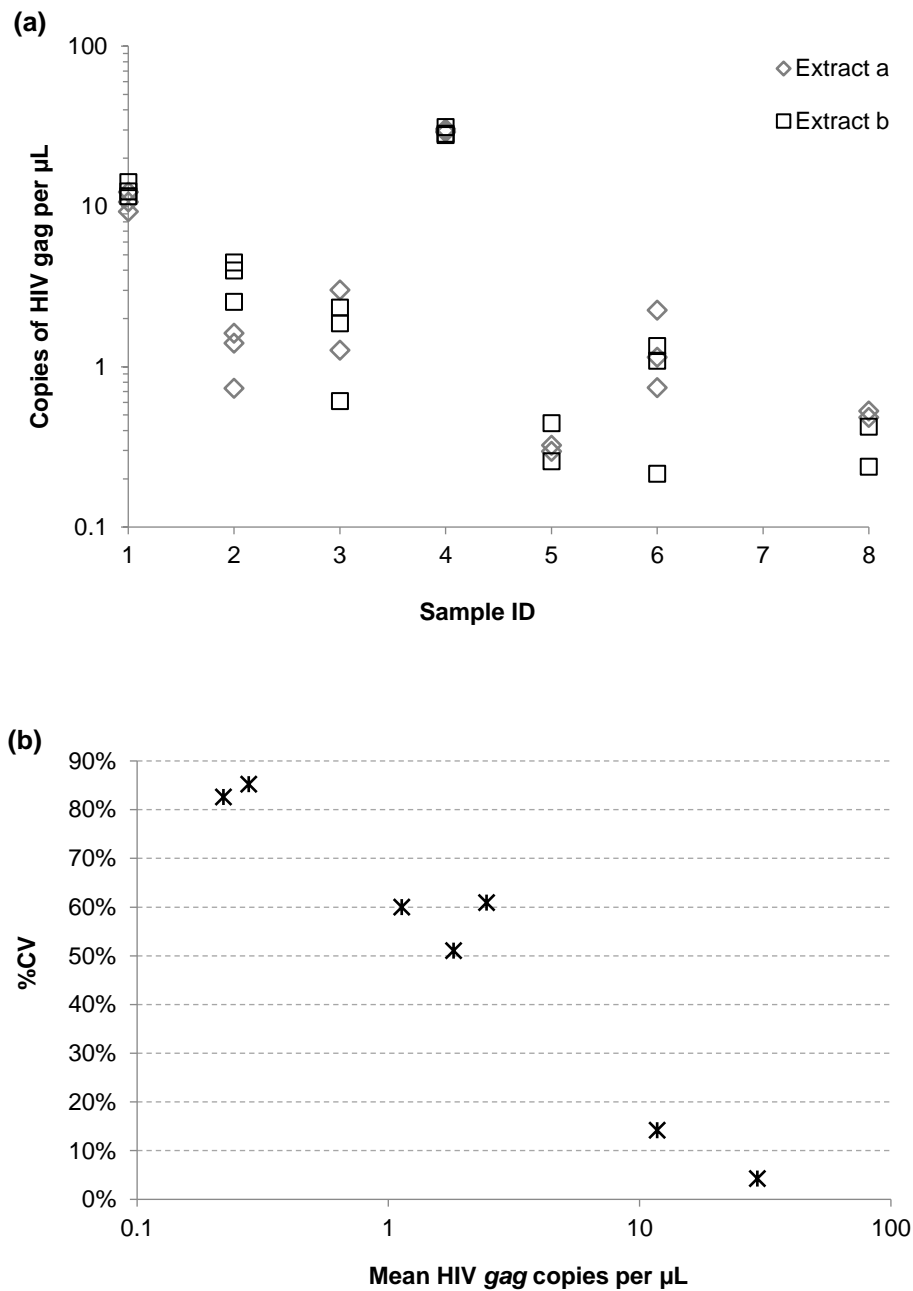


Figure 3.9a shows copy number estimates for HIV *gag* across duplicate extraction batches, which ranged from 0.2 (sample 6) to 31.3 (sample 4) copies per μL . One sample (7) was found to contain no HIV *gag* target across 6 dPCR replicates. Figure 3.9b illustrates an inverse relationship between HIV *gag* copy number and % CV indicating higher variability in quantification in the lowest concentration samples. Of these (samples 5 & 8), no HIV RNA was detected in 2 out of 6 dPCR replicates indicating a degree of dropout. This is likely owing to sampling effects at the

lower concentrations. An important consideration when determining the extent of variability in EQA materials is what the wider impact could be on participant results in terms of measurement error. Effects related to extraction batch, RT kit choice, assay and the low concentration of HIV molecules in the lower samples could result in variability in quantitative estimates of HIV-1 RNA copy number. The impact of RNA extraction efficiency and variability was not extensively explored as part of this thesis, although a comparison of the performance of different extraction kits on HIV-1 RNA quantification in the EQA samples was performed as part of the wider collaborative study (Falak *et al.*, Section 10.11.3). The study demonstrated up to ~17-fold differences in RNA copy number quantification between different extraction kits. The QIAmp viral nucleic acid kit (Qiagen) was chosen for the interlaboratory comparison study based on these experiments performed by Dr Samreen Falak. Further work to evaluate the impact of RNA extraction method on dPCR quantification of HIV RNA could help to characterise measurement error, which in turn could impact upon clinical quantification. Better measurement precision in inter-laboratory EQA schemes may afford better result outputs from clinical laboratories, which could in turn enable greater confidence in treatment decisions for patients on antiretroviral therapy.

3.3.4.4. Inter-laboratory analysis of EQA materials for HIV RNA quantification

The analysis of the EQA materials discussed in Section 3.3.4.3 was also performed by another NMI; Physikalisch-Technische Bundesanstalt (PTB), Germany. This enabled an inter-laboratory comparison of HIV-1 RNA copy number quantification using RT-dPCR contributing to INSTAND EQA Schemes 360 and 382 (2018; <https://www.istand-ev.de>; accessed on 22/07/20).

Figure 3.10: dPCR results obtained by two NMI for the EQA samples. Bars show the acceptance range based on the consensus value from all quantitative results for the respective sample for the whole INSTAND EQA scheme, including calibration using the 4th WHO International Standard. Blue symbols represent PTB dPCR results, black symbols represent NML dPCR results. Figure based on data provided by NML, PTB and participants of Virus Genome Detection HIV-1 (RNA) Program 1 (360) and the Virus Genome Detection-HIV-1 (RNA) additional Training Program 2 (382) (INSTAND) of the 2019 EQA scheme (Section 10.11.3; Appendix 11).

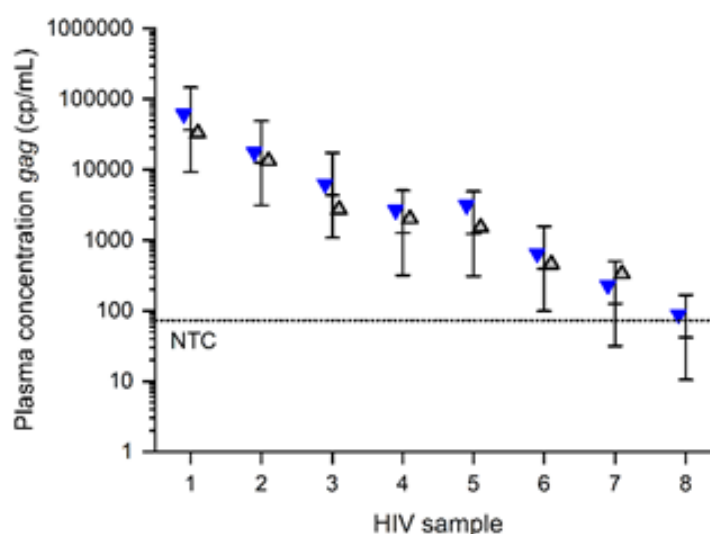


Figure 3.10 shows overall good agreement between the HIV-1 *gag* RT-dPCR results for the two NMIs which are within the acceptance range, indicating that RT-dPCR performed comparably to other methods implemented in the EQA scheme. In addition, RT-dPCR provided absolute quantification of HIV-1 RNA copies per mL without the requirement for conversion from the WHO Standard (reported in IU per mL). The 8th sample in Figure 3.10, which was shown by PTB to contain approximately 100 HIV RNA copies per mL, represents sample 7 in Figure 3.9a for which no HIV RNA copies were reported by NML. The results for this sample, which lie around the limit of detection of the assay, demonstrate how detection of low copy samples may be missed by some laboratories leading to discrepancies in reporting for the schemes where results fall outside of the consensus range. Clinical quantification of HIV-1 RNA viral load is performed by different laboratories using different platforms and techniques (Section 3.1.2), highlighting the importance of ensuring measurement harmonisation between laboratories and studies. The work presented here demonstrates how RT-dPCR, which does not require a calibration curve or conversion between IU and copies per mL, may have a role in providing reference values for EQA schemes.

This could support measurement accuracy, and help to identify results that deviate from EQA consensus values, promoting measurement confidence. This can be a valuable tool in demonstrating reliability of results for HIV-1 RNA viral load quantification (Senechal and James, 2012).

3.3.5. RT-dPCR analysis of clinical samples from HIV-1 positive individuals

Improved measurement accuracy in HIV-1 RNA quantification (including plasma viremia and cell-associated RNA) could help with harmonisation of patient results between studies and clinical centres. In this study, dPCR quantification demonstrated that differences in RNA copy number estimates can arise from choice of reverse transcriptase kits, different assays, and potentially RNA extraction method. Another possible cause for variability in quantitative results could be related to sequence diversity in the virus itself where multiple HIV-1 subtypes may exist within an individual patient (Redd *et al.*, 2013). There is interest in applying dPCR as a sensitive and precise method for direct clinical quantification of HIV-1 RNA, which may be equivalent or even superior to qPCR owing to better tolerance of primer-probe mismatches (Kiselinova *et al.*, 2014, Sedlak *et al.*, 2017). Future work could aim to investigate the role of RT-dPCR in direct clinical quantification of HIV viral load in samples obtained from patients. dPCR could also facilitate further investigations into RT efficiency, which would provide a better understanding of differences in RNA viral load quantification obtained using different kits and platforms.

3.4. Conclusions

Several factors can influence quantitative estimates of HIV-1 RNA, including choice of reverse transcriptase enzyme and choice of assay. This can introduce measurement error and could introduce bias between laboratories where different platforms or kits are used. Digital PCR can be applied as an absolute quantification method for investigating discrepancies between reagents, assays, and materials. In this chapter dPCR highlighted that up to ~6-fold differences in quantitative values can exist between different commercial reverse transcriptases, which was assay dependent. This was demonstrated using a standardised input of synthetic RNA transcript. dPCR could be used to evaluate and correct for RT efficiency, which could help to eliminate quantitative bias where different RT kits are used. RT-dPCR was also applied to different HIV-1

RNA materials, including whole viral genomic RNA sequences, to highlight how sequence diversity in viruses obtained from different sources can result in quantitative differences. In addition to evaluating RT efficiency and the impact of choice of reverse transcriptase, this chapter demonstrated that RT-dPCR exhibits good inter-laboratory reproducibility for analysis of EQA samples and could be considered as a candidate reference method for HIV-1 RNA quantification. Further work should aim to explore the role of RT-dPCR as a potential RMP that could be used to value assign reference materials and influence EQA acceptance ranges. Ironically, this must include further evaluation of the impact that variable RT efficiency may have on the application of the reference method. This could help to harmonise quantitative results between different laboratories and improve confidence in measurements of HIV-1 RNA, which could ultimately improve clinical measurement accuracy of viral load.

4. Calibrating quantitative measurements of HIV-1 DNA using digital PCR

4.1. Introduction

4.1.1. *The proviral reservoir: a barrier to curing HIV-1*

Although immense progress has been made in the response to the HIV epidemic, the disease remains a global concern (Bekker *et al.*, 2018). Improved access to testing, effective antiretroviral therapy (ART) and sensitive molecular methods to monitor RNA viral load have contributed to controlling the disease. However, a current barrier to curing HIV-1 infection is the presence of the latent viral reservoir. Following entry into the host cell the HIV-1 RNA genome is subject to reverse transcription into double stranded (ds) DNA for integration into the host chromosome. The integrated DNA acts as a template for transcription of new viral RNA, utilising the host's cellular mechanisms as part of the viral life cycle (Craigie and Bushman, 2012). The integrated DNA copy of the HIV-1 genome, along with an un-integrated portion, is widely thought to contribute to the viral reservoir comprised of latently infected CD4+ T-lymphocytes and other cells (Kiselinova *et al.*, 2016, Avettand-Fenoel *et al.*, 2016). Following discontinuation of (ART) latently infected cells, which are not targeted by current therapies (Lorenzo-Redondo *et al.*, 2016), have the potential to become activated leading to the release of progeny virions (Richman *et al.*, 2009, Bruner *et al.*, 2016). Accurate quantification of the latent reservoir using highly sensitive methods could assist with the development of latency reversal strategies to eliminate infection (Margolis *et al.*, 2016, Spivak and Planelles, 2018), or allow HIV positive individuals the opportunity to reduce their intake of antiretroviral medicines through accurate monitoring of the proviral reservoir (The BREATHER Trial Group, 2016). The absence of HIV-1 DNA in patient samples could be a useful indicator of functional cure from infection. To date, two individuals that were previously HIV positive have been declared as having no measurable virus in their blood following stem cell transplantation (Gupta *et al.*, 2019). These examples demonstrate a real-world requirement for the application of robust and reliable protocols to quantify HIV-1 DNA.

4.1.2. *Quantification of HIV-1 DNA*

qPCR quantification of HIV-1 DNA is increasingly being performed as a biomarker of the viral reservoir (Bruner *et al.*, 2015, Rouzioux and Avettand-Fenoël, 2018). Quantification of HIV-1 DNA has been suggested to play a role in predicting disease progression and the potential for viral

rebound through association with plasma viral load and CD4 T cell count (Williams *et al.*, 2014). Total HIV-1 DNA has additionally been shown to correlate with viral outgrowth assays (VOAs) used to determine the size of the replication competent viral reservoir (Kiselinova *et al.*, 2016). HIV-1 DNA (total and unintegrated) can be detected in the absence of circulating plasma viral RNA (Hatano *et al.*, 2009, Mexas *et al.*, 2012), making the molecule an attractive biomarker for monitoring infection dynamics. HIV-1 DNA quantification may be a useful parameter for clinical follow-up, following measurement at treatment initiation and at a suitable time-point post-initiation (Mortier *et al.*, 2018).

Quantification of HIV-1 DNA by qPCR is reported as number of copies per million cells. This is through the use of a calibration curve containing an HIV-1 gene along with a host reference target. The 8E5 cell line is a popular choice (Avettand-Fenoel *et al.*, 2009, Beck *et al.*, 2001, McFall *et al.*, 2015, Surdo *et al.*, 2016) that is reported to contain one HIV-1 genome per diploid cell (Folks *et al.*, 1986, Deichmann *et al.*, 1997, Desire *et al.*, 2001). Unlike for HIV-1 RNA viral load monitoring no WHO International Standard currently exists for HIV-1 DNA qPCR quantification, and accurate measurement relies on reported assumptions about the 8E5 calibration standard. In order to maintain reproducibility between experiments and ensure that data are comparable between laboratories and studies, materials used to calibrate qPCR must be stable and commutable. The impact of variability in qPCR studies for HIV-1 DNA quantification is often ignored, making it difficult to compare data between studies (Strain *et al.*, 2013). In addition, measurements of HIV-1 DNA are often at the lower end of the dynamic range of qPCR. Very small viral reservoirs have been characterised in peripheral blood of HIV positive individuals, that are often indistinguishable from background signals (Gálvez *et al.*, 2020, Strain and Richman, 2013). It is therefore necessary that well characterised materials and methods for making highly sensitive measurements are available for quantification of HIV-1 DNA associated with the latent reservoir (Hatano *et al.*, 2009, Mexas *et al.*, 2012).

4.1.3. A role for dPCR in HIV-1 DNA quantification

Interest is growing in the application of dPCR for direct quantification of HIV-1 DNA (Bosman *et al.*, 2015, Eriksson *et al.*, 2013, Henrich *et al.*, 2012, Jones *et al.*, 2014, Strain *et al.*, 2013). In contrast to qPCR, dPCR can provide sensitive, absolute measurements without the need for a standard curve (Sedlak and Jerome, 2013). dPCR has been reported to have enhanced precision

and better tolerance to primer-probe mismatches compared to qPCR; a desirable attribute for measuring highly variable HIV-1 sequences (Strain *et al.*, 2013, Rutsaert *et al.*, 2018a). Precise measurements could facilitate accuracy in HIV-1 DNA quantification by reducing experimental error. dPCR has also demonstrated equivalent sensitivity to qPCR for HIV-1 DNA quantification, indicating the potential utility of the technique for quantifying small viral reservoirs (Henrich *et al.*, 2012). The work presented in this chapter aimed to compare qPCR and dPCR for HIV-1 DNA quantification in a cohort of clinical samples. dPCR was demonstrated in Chapter 3 to offer precise quantification of HIV-1 RNA which was highly reproducible between laboratories, and may also be a suitable technique for HIV-1 DNA quantification. It is hypothesised that dPCR can perform with equivalent sensitivity to qPCR. dPCR can quantify nucleic acid without the need for a calibration curve, which may afford better inter-laboratory reproducibility through comparison of absolute measurements. The work presented in this chapter could help to establish a role for dPCR in quantification of HIV-1 DNA.

4.2. Materials and methods

4.2.1. Study materials

4.2.1.1. Patient samples

Peripheral blood mononuclear cell samples (PBMC) were obtained from HIV-positive individuals as part of a recently published clinical trial comparing Short Cycle Therapy (SCT) with continuous antiretroviral therapy. The original study had received appropriate ethical committee approval (EudraCT number 2009-012947-40) (The BREATHER Trial Group, 2016). Each sample was given a unique study identifier and provided as extracted DNA, which was stored at -20°C until required.

4.2.1.2. Cell lines

8E5 cell materials (Folks *et al.*, 1986) were obtained from three separate sources and designated Standard 1, Standard 2 and Standard 3. Standards 1 and 2 were obtained as pre-extracted DNA from two different clinical diagnostics laboratories and had been used for research on HIV nucleic acids. Standard 3 was obtained as cryo-preserved cells from the American Type Culture Collection (ATCC® CRL-8993™).

4.2.2. Culture of 8E5 'Standard 3' cells

Culture of the 8E5 'Standard 3' cells was performed by Dr Gary Morley (LGC). One vial of 8E5 'Standard 3' cells (ATCC® CRL-8993™) was taken from liquid nitrogen and thawed at 37°C for 1-2 minutes. 500 µL of cells was removed from the vial for culture and the remaining 300 µL (approximately 2.4×10^6 cells) retained for DNA extraction. The cells were cultured in growth medium containing RPMI 1640 (ATCC® 30-2001™) plus 10% foetal bovine serum (ATCC® 30-2020™) at 37 °C in the presence of 5% CO₂, as recommended by ATCC. A batch suspension culture was maintained between 2.0×10^5 and 1.0×10^6 cells per mL for four successive passages in triplicate (representing three separate culture flasks). Cell pellets were obtained representing each passage, estimated to contain between 1.0×10^6 and 4.0×10^6 cells per mL. Cell pellets were stored at -80°C for approximately 1 month prior to DNA extraction.

4.2.3. DNA extraction

DNA extraction for the PBMC samples was performed by Dr Bridget Ferns (UCLH). Briefly, DNA was extracted on the QIA Symphony platform (Qiagen, Germany) using the DSP Virus/Pathogen Mini Kit (Qiagen, Germany) as recommended by the manufacturer. Extracts were eluted in 60 μ L of buffer AVE (Qiagen, Germany) and stored at -20 °C prior to analysis.

DNA was extracted from the 8E5 Standard 3 cell pellets (containing between 1×10^6 and 6×10^6 cells per pellet) from each culture passage using the QIAamp DNA Blood Mini Kit (Qiagen, Germany). Supplemental to the manufacturer's protocol, extracts were treated with 4 μ L of RNase A (Qiagen, Germany) prior to the addition of lysis buffer. Final elution volume was 200 μ L in buffer AE (Qiagen, Germany). The concentration of the 8E5 cell line DNA extracts (Standard 1, 2 and 3) was estimated using a Qubit 2.0 fluorometer (Invitrogen™, USA).

4.2.4. PCR assays

Assays targeting the HIV LTR-*gag* junction or HIV *pol* gene (Table 3.1) were used to measure HIV DNA copies, and PDH (Busby *et al.*, 2017) or RNase P (Table 4.1) (Devonshire *et al.*, 2014b) to measure the number of reference gene copies. The PDH probe was adapted for digital PCR (dPCR) from a previously unpublished version used for qPCR (5'-JOE-CCCCCAGATACACTTAAGGGATCAACTCTTAATTGT-TAMRA-3'). dPCR and qPCR assays were utilised in duplex format, and the number of HIV DNA copies detected was normalised to one million cells using PDH or RNase P reference targets. Of note, the LTR-*gag* assay reverse primer site allows amplification of a single LTR region at the 5' end of the HIV-1 genome, rather than both the 5' and 3' LTR sequences (Zhang *et al.*, 1998).

Table 4.1: Primer and probe sequences for detection of human reference genes

Assay target	Genbank accession	Name	5' to 3' *	Source
Pyruvate Dehydrogenase (PDH)	NG_016860.1	Forward	TGA AAG TTA TAC AAA ATT GAG GTC ACT GTT	(Busby <i>et al.</i> , 2017)
		Reverse	TCC ACA GCC CTC GAC TAA CC	
		Probe	VIC - CCC CCA GAT ACA CTT AAG GGA – MGBNFQ	
RNase P (RNase P)	NC_000014.8	Forward	GCG GAG GGA AGC TCA TCA G	(Devonshire <i>et al.</i> , 2014b)
		Reverse	GGA CAT GGG AGT GGA GTG ACA	
		Probe	VIC - CAC GAG CTG AGT GCG – MGBNFQ	

* Refer to page 23 for abbreviations relating to fluorescent dyes and quenchers.

4.2.5. qPCR analysis of clinical samples

qPCR analysis of 18 PBMC sample extracts was performed by Dr Bridget Ferns (UCLH) using an Applied Biosystems® 7500 Real-Time PCR System. Experiments were implemented in accordance with the MIQE guidelines (Bustin *et al.*, 2009). Compliance criteria for these experiments are available (Busby *et al.*, 2017). To prepare a qPCR calibration curve consisting of ~50,000 to ~5 HIV DNA copies per reaction (assuming 1 HIV DNA copy per 8E5 cell), DNA extracted from the 8E5 cell line (Standard 1) was serially diluted using a tenfold dilution series in nuclease-free water containing 5 µg/ mL polyA RNA carrier (Qiagen, Germany). 20 µL of each clinical sample extract was added to a total reaction volume of 50 µL and analysed once as a single replicate. The reaction mix contained 1x QuantiTect Multiplex PCR Master Mix (with ROX dye) (Qiagen, Germany), sterile nuclease-free water and the PDH/HIV LTR-*gag* duplex assay. Primer and probe concentrations were 0.1 µM of PDH and HIV LTR-*gag* primers and PDH probe, and 0.2 µM of the HIV LTR-*gag* probe. Thermocycling conditions were: 15 minutes at 95 °C, then 45 cycles of 94 °C for 60 s and 60 °C for 60 s. Data were analysed using Applied Biosystems SDS v1.4 analysis software.

4.2.6. Digital PCR basic protocol

Duplex format dPCR experiments were implemented in accordance with the dMIQE guidelines (The dMIQE Group and Huggett, 2020). Two dPCR instruments were utilised during the study; the RainDrop® Digital PCR System (RainDance Technologies, USA) and the QX200™ Droplet Digital™ PCR System (Bio-Rad, USA). Positive (k) and negative (w) partitions (defined in Section 1.2.3.3) were selected for the RainDrop® and QX200™ manually using ellipse or quadrant gating, respectively, as recommended by the manufacturer using the instruments' software.

For dPCR using the RainDrop® instrument, 5.5 µL DNA extract (from approximately 55,000 cells) was added to a total master reaction volume of 55 µL containing 1x TaqMan® Genotyping Master Mix (Applied Biosystems™, USA), 1x droplet stabiliser (RainDance Technologies, USA), sterile nuclease-free water (Ambion, USA) and the chosen primer assay duplex. 50 µL of reaction mix was pipetted into a RainDrop® Source chip and oil emulsion droplets were generated (Milbury *et al.*, 2014) and cycled on a Tetrad PTC-225 Thermal Cycler (Bio-Rad, USA). Thermal cycling conditions were: 10 minutes at 95 °C, 45 cycles of 95 °C for 15 s and 60 °C for 60 s, 10 minutes at 98 °C and a 10 minute hold at 12 °C. A ramp rate of 0.5 °C/sec was maintained for all stages

of thermal cycling. Following PCR amplification, droplets were read on the RainDrop® Sense and the data analysed with RainDrop® Analyst II. A partition volume of 0.005 nL was used to calculate copy number concentration (Milbury *et al.*, 2014).

For the QX200™ Droplet Digital PCR System 5.5 µL DNA extract was added to a master reaction volume of 22 µL containing 1X ddPCR Supermix for Probes without dUTP (Bio-Rad, USA), sterile nuclease-free water and the selected assay duplex. The remaining steps of the protocol are described in Section 2.1.5. QuantaSoft version 1.6.6.0320 was used for data analysis. A partition volume of 0.85 nL was used to calculate copy number concentration (Bio-Rad, USA). No template controls (NTCs) were included in all PCR experiments.

4.2.6.1. *Digital PCR analysis of clinical samples*

5 µL (equivalent to approximately 50,000 cells) of the 18 PBMC extracts were analysed once as a single replicate using the RainDrop® dPCR platform as described above. The samples were amplified using the PDH/HIV LTR-*gag* duplex assay. NTCs of HIV-1 negative whole blood extracts and sterile nuclease-free water (Ambion, USA) were included as controls. The extracts were coded and the dPCR operator had no prior knowledge of the qPCR results on the same samples. dPCR analysis of the patient samples was also performed using the Bio-Rad QX200 digital PCR system.

4.2.6.2. *Digital PCR characterisation of 8E5 cells*

The Standard 1, 2 and 3 8E5 DNA extracts were assessed using the RainDrop® platform with duplex primer sets to PDH/HIV LTR-*gag*, PDH/HIV *pol* and RNase P/HIV LTR-*gag*. Results were confirmed using the QX200™ platform and the PDH/HIV LTR-*gag* assay duplex. For the Standard 3 cells all four culture passage extracts to a Cumulative Population Doubling (cPD) of ~10, and the initial passage zero extract, were analysed using both RainDrop® and QX200™ instruments with the PDH/HIV LTR-*gag* duplex assay.

4.2.6.3. *Effect of different 8E5 calibrator sources on qPCR analysis of clinical samples*

Three different 8E5 cell standards (1, 2 and 3) were utilised simultaneously as calibrators in the same run for analysis of an additional seven HIV-positive clinical sample PBMC extracts from the clinical trial (The BREATHER Trial Group, 2016). qPCR was performed at UCLH by Dr Bridget Ferns as described in Section 4.2.5 and the PDH/HIV LTR-*gag* assay duplex was applied. HIV DNA copies were calculated per million cells using either the published quantity of 1 HIV DNA copy per 8E5 calibrator for all three different 8E5 sources or, alternatively, the quantity determined using dPCR during the present study.

4.2.7. **Data Analysis**

Data from dPCR and qPCR experiments were subject to threshold and baseline setting in the relevant instrument software and were exported as .csv files to be analysed in Microsoft Excel. For dPCR experiments the average number of copies per partition (λ) was calculated as described previously (Whale *et al.*, 2016a). dPCR and qPCR analyses of the clinical samples were compared by using a paired t-test on the \log_{10} transformed HIV DNA copies per million cells. The number of HIV DNA copies per 8E5 cell was calculated using the ratio of measured HIV copies to reference gene copies.

4.3. Results and Discussion

4.3.1. Measurement of HIV-1 DNA in patient samples by dPCR and qPCR

dPCR and qPCR were compared for quantification of HIV-1 DNA. All samples were positive for HIV DNA by qPCR, and HIV DNA was detected in 15/18 and 12/18 extracts using the RainDrop and QX200 dPCR instruments. Raw HIV DNA copy numbers measured by dPCR were up to 31-fold (Sample 15) and 680-fold (Sample 4) lower than qPCR for the RainDrop and QX200, respectively (Table 4.2a). The number of HIV DNA copies was normalised to one million cells by calculating the ratio of HIV DNA to PDH reference gene copies for each sample. Normalisation improved the agreement between dPCR and qPCR, with 2.7-fold and 46.1-fold differences in HIV DNA copy numbers observed for the respective platforms (Table 4.2b). However, discrepancies in HIV DNA quantification remained between the techniques. Some discrepancies are likely due to differences in methodological workflow, including differences in template input volume (Approximately 5 μ L for dPCR compared with 20 μ L for qPCR). This could explain the absence of HIV DNA target in some dPCR-analysed samples that were positive by qPCR, particularly those that were shown to be low concentration using the latter method. This presents a potential limitation of dPCR, with low sample volume as a barrier to amplification of low copy targets (Whale *et al.*, 2013). However, the observation of low or no raw HIV DNA copies using dPCR was relevant for samples that contained high concentrations of HIV DNA by qPCR (Sample 4, 5, 11, 12, 15, 17), suggesting other causative factors than sample volume. In addition, the HIV DNA copies per million cells presented in Table 4.2b were found to be up to 19.6-fold different between the two dPCR platforms ($p=0.01$) which warranted further investigation.

Table 4.2: Number of HIV DNA copies measured in single replicates of 18 clinical samples using qPCR and the two dPCR platforms. (a) Raw HIV DNA copies measured by qPCR, RainDrop® dPCR and QX200™ dPCR. (b) HIV DNA copies normalised to million cells for the three methods. Approximate input volumes for dPCR refer to the volume loaded into the cartridge prior to droplet generation.

(a)	Raw HIV DNA copies per reaction		
	qPCR	RainDrop®	QX200™
<i>Method</i>			
<i>Reaction volume (µL)</i>	50	~50	~20
<i>Sample volume (µL)</i>	20	~5	~5
Sample 1	22	0	0
Sample 2	204	7	6
Sample 3	263	31	5
Sample 4	2041	77	3
Sample 5	2824	110	0
Sample 6	2	0	2
Sample 7	11	2	0
Sample 8	358	20	13
Sample 9	16	3	2
Sample 10	3	0	0
Sample 11	1569	116	0
Sample 12	109	4	2
Sample 13	171	12	4
Sample 14	52	4	2
Sample 15	2497	81	0
Sample 16	108	12	8
Sample 17	392	16	2
Sample 18	185	16	7

(b)	HIV DNA copies per million cells		
	qPCR	RainDrop®	QX200™
<i>Method</i>			
<i>Reaction volume (µL)</i>	50	~50	~20
<i>Sample volume (µL)</i>	20	~5	~5
Sample 1	80	0	0
Sample 2	579	215	181
Sample 3	724	784	141
Sample 4	1660	704	36
Sample 5	3590	1496	0
Sample 6	10	0	79
Sample 7	38	76	0
Sample 8	1780	915	539
Sample 9	40	76	43
Sample 10	21	0	0
Sample 11	1100	721	0
Sample 12	100	47	25
Sample 13	1460	1023	229
Sample 14	473	358	123
Sample 15	1670	776	0
Sample 16	1710	1700	803
Sample 17	657	296	34
Sample 18	1050	896	333

4.3.2. Investigating discrepancies between the two dPCR systems

Several samples that were found by qPCR and RainDrop® dPCR to contain HIV DNA returned a low or even negative result by QX200™ dPCR. These samples are listed in Table 4.3.

Table 4.3: Samples flagged as discrepant following the qPCR-dPCR-dPCR comparison. (a) Raw QX200™ dPCR data for HIV and PDH targets for all 18 samples. Saturation of partitions is indicated by a PDH lambda (λ) greater than or equal to 4.0 (highlighted red). λ values were calculated by subtracting the natural logarithm (LN) of the number of partitions containing no target (w) from LN of the total number of partitions accepted by QuantaSoft for that sample (i.e. positive plus negative partitions in this instance, n). (b) Raw HIV DNA copies per reaction for the 'saturated' samples for each of the three techniques. QX200™ dPCR results are given before and after template dilution.

(a)	Total accepted partitions (n)	HIV positive partitions (k)	PDH positive partitions (k)	PDH negative partitions (w)	PDH λ^*
Sample 1	13739	0	12942	797	2.8
Sample 2	14505	4	13784	721	3.0
Sample 3	14395	3	13686	709	3.0
Sample 4	14288	2	14281	7	7.6
Sample 5	14565	0	14551	14	6.9
Sample 6	14036	1	11511	2525	1.7
Sample 7	11550	0	10296	1254	2.2
Sample 8	12645	7	11020	1625	2.1
Sample 9	13861	1	13281	580	3.2
Sample 10	11918	0	9285	2633	1.5
Sample 11	13916	0	13796	120	4.8
Sample 12	12580	1	12550	30	6.0
Sample 13	12143	2	9177	2966	1.4
Sample 14	15613	1	10461	5152	1.1
Sample 15	15049	0	15045	4	8.2
Sample 16	15656	5	8650	7006	0.8
Sample 17	13966	1	13717	249	4.0
Sample 18	14412	4	11741	2671	1.7

* Average number of molecules per partition.

(b)	qPCR raw HIV DNA copies per reaction	RainDrop® raw HIV DNA copies per reaction	QX200™ raw HIV DNA copies per reaction (before dilution)	Dilution factor applied for re-analysis	QX200™ total raw HIV DNA copies in 22 µL (after dilution)
Sample 4	2041	77	3	5.5	79
Sample 5	2824	110	0	5.5	100
Sample 11	1569	116	0	7.3	86
Sample 12	109	4	2	7.3	4
Sample 15	2497	81	0	8.8	39
Sample 17	392	16	2	5.5	15

The highlighted samples in Table 4.3a were observed to contain highly concentrated genomic DNA, reflected by the high λ values for PDH target for these samples (where each dPCR partition contained, on average, 4 or more molecules of DNA). This also coincided with limited amplification of the HIV-1 DNA target. Saturation of the dPCR partitions introduces bias towards the PDH target and lowers the probability that HIV molecules will also be observed in the available partitions (Quan *et al.*, 2018). dPCR quantification obeys Poisson statistics, where the rate of occurrence for detecting a molecule of DNA containing a particular sequence is estimated (Gart, 1975). To improve the rate of occurrence and therefore detection of HIV-1 DNA in the six challenging samples, each extract was diluted in nuclease-free water up to a volume of 22 μ L and analysed over quadruplicate reaction wells. The dilution factor for each sample is given in Table 4.3b. This resulted in the differences in HIV copy number between the two platforms no longer being significant ($p=0.55$). This saturation effect was not observed for the RainDrop system, possibly owing to the increased reaction volume (50 μ L rather than 20 μ L for the QX200, therefore allowing more dilution of the sample), and the higher number of available partitions (10 million rather than 23,000). This allows better partitioning of the highly concentrated genomic DNA, meaning that the minority HIV DNA molecules have a better probability of being detected. The increased reaction volume attributed to the RainDrop instrument, and the large number of partitions that can subsequently be generated per well, enables this platform to benefit from a broad dynamic range.

The linear dynamic range was demonstrated to be approaching that of qPCR using the HIV LTR-*gag* assay described in Table 3.1 (Jones *et al.*, 2016). Highly concentrated, viscous genomic DNA has been shown to alter droplet volume in emulsion-based dPCR, which can impact upon nucleic acid quantification (Hindson *et al.*, 2011). The review by Rutsaert *et al.* (2018) also articulates the challenges facing emulsion-based digital PCR as a tool to quantify minority targets in a concentrated background, such as HIV DNA in human gDNA. The authors discuss in particular the difficulties for threshold setting to accurately quantify minority targets, and the problems for droplet formation that can be introduced by highly viscous genomic DNA (Rutsaert *et al.*, 2018a). This also introduces a potential challenge when measuring two targets that exist at opposing ends of the dynamic range of the instrument; a situation that requires careful planning for future experiments to ensure that both targets have equivalent λ values. These findings are relevant for approaches that seek to incorporate dPCR into routine diagnostics, particular for trace detection of minority targets in a rich background of genomic DNA.

4.3.3. Investigating the discrepancies between dPCR and qPCR quantification of HIV DNA

Owing to the analytical challenges presented when quantifying HIV-1 DNA in the clinical samples using the QX200 dPCR system, only the values obtained using the RainDrop were carried forward to investigate the discrepancies between qPCR and dPCR. Overall, there was a good correlation of HIV DNA copies per million cells between dPCR and qPCR (Figure 4.1) ($R^2 = 0.87$). However, despite this agreement the dPCR results were approximately 60% of the qPCR results; a statistically significant difference ($p = 0.02$). As aforementioned, reduced sample input volume for dPCR may provide insight into this discrepancy. However, whilst this would account for observed differences in raw HIV copy number, plotted results are normalised to the number of PDH copies and reported as a ratio. This suggests that there may be an alternative hypothesis for the cause of the observed discrepancies.

4.3.3.1. Digital PCR characterisation of the 8E5 cell line

Calibration of qPCR for quantification of the clinical samples was performed using DNA extracted from the 8E5 cell line, which is widely reported to contain one integrated HIV provirus per diploid cell (Folks *et al.*, 1986, Deichmann *et al.*, 1997, Desire *et al.*, 2001, Quillent *et al.*, 1993, McFall

et al., 2015, Jaafoura *et al.*, 2014, Beck *et al.*, 2001, Ghosh *et al.*, 2003). Whilst this is taken to be an assured characteristic of the cell line, inaccuracies in the nominal number of HIV proviruses per 8E5 cell could bias quantitative results and may be the cause of the ~30% difference between the qPCR and dPCR estimates. To determine the absolute number of HIV DNA copies per cell, dPCR was applied to DNA extracted from the 8E5 cell line to determine the number of HIV DNA copies per diploid cell. Initially, the source of 8E5 DNA used to calibrate the qPCR analysis of the 18 samples (Standard 1) was analysed using the RainDrop® dPCR platform. The cells contained approximately 0.6 HIV DNA copies per cell, rather than the reported ratio of one. This result was confirmed on the QX200 dPCR platform, and using additional assays targeting a different HIV gene (*pol*) and human reference target (RNase P) to rule out the possibility that the observed finding was due to under-quantification with the LTR-*gag* assay, or an over estimation of the number of PDH copies. These findings clearly indicated that '8E5 Standard 1' contains less than one HIV DNA copy per cell. The HIV DNA copies measured in the 18 clinical samples by qPCR were recalculated from the 8E5 standard curve assuming the dPCR value of ~0.6, and the discrepancy between dPCR and qPCR measurements of HIV DNA was no longer statistically significant ($p = 0.42$) (Figure 4.1). These data suggest that the number of HIV DNA copies in the 18 samples was over-estimated by qPCR as the result of inaccuracies in the standard 1 calibration curve.

To further explore whether these findings were unique to this particular source of 8E5 DNA, the same dPCR approach was applied to additional standards from two separate institutes (Standard 2 and Standard 3). Standard 3 exhibited a similar ratio of HIV DNA per cell to Standard 1 (~0.8 HIV DNA copies per cell), whereas Standard 2 demonstrated even greater loss of HIV DNA (~0.02 HIV DNA copies per cell). The three 8E5 standards are compared in Figure 4.2a. Furthermore, 8E5 Standard 3 had been cultured to a cumulative population doubling (cPD) of approximately 10 (Roth, 1974). Cells were sampled at 5 distinct time-points representing each passage (P0-P4), providing an opportunity to evaluate whether progressive loss of HIV DNA from the 8E5 cell line occurred with serial passage. Analysis of the DNA extracts on the RainDrop and QX200 using the PDH/HIV LTR-*gag* assay duplex demonstrated that HIV DNA quantity decreased in culture, from ~0.8 to 0.6 HIV DNA copies per cell (Figure 4.2 b & c).

Figure 4.1: Comparison between qPCR and dPCR measurements of HIV DNA copies per million cells for 18 PBMC samples. Red markers are where qPCR results were calculated assuming one HIV DNA copy per 8E5 cell. Blue markers are where qPCR results were calculated assuming 0.6 HIV DNA copy per 8E5 cell. Samples in which HIV DNA was not detected are not plotted. The dashed line represents equivalence.

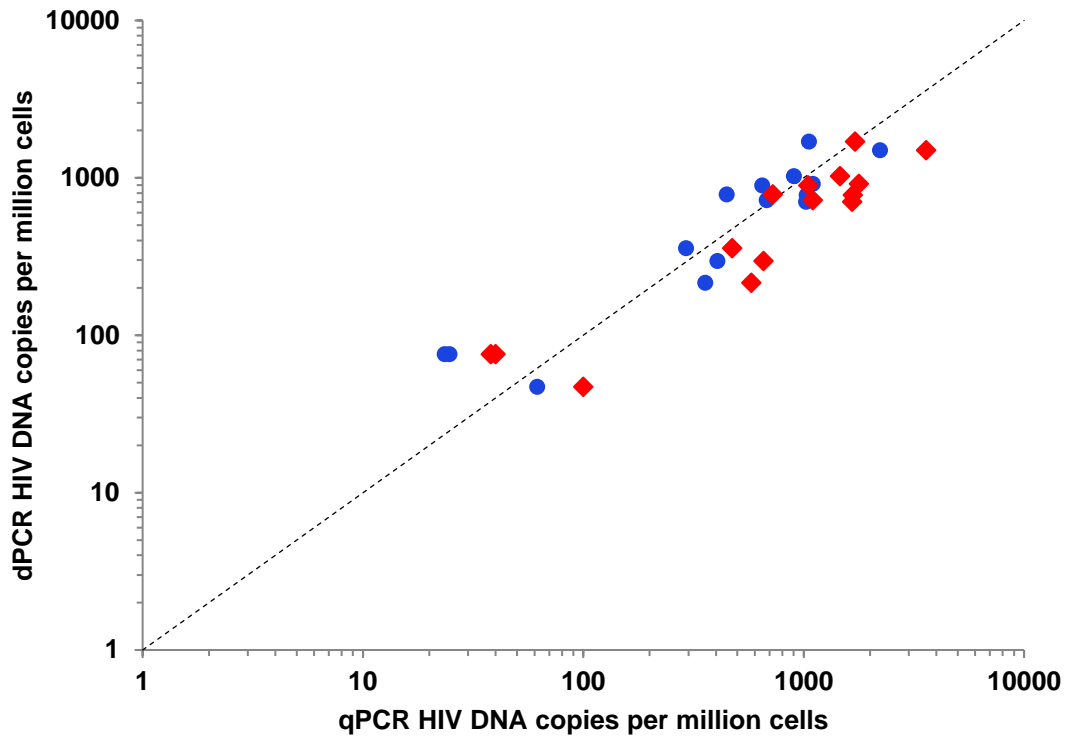
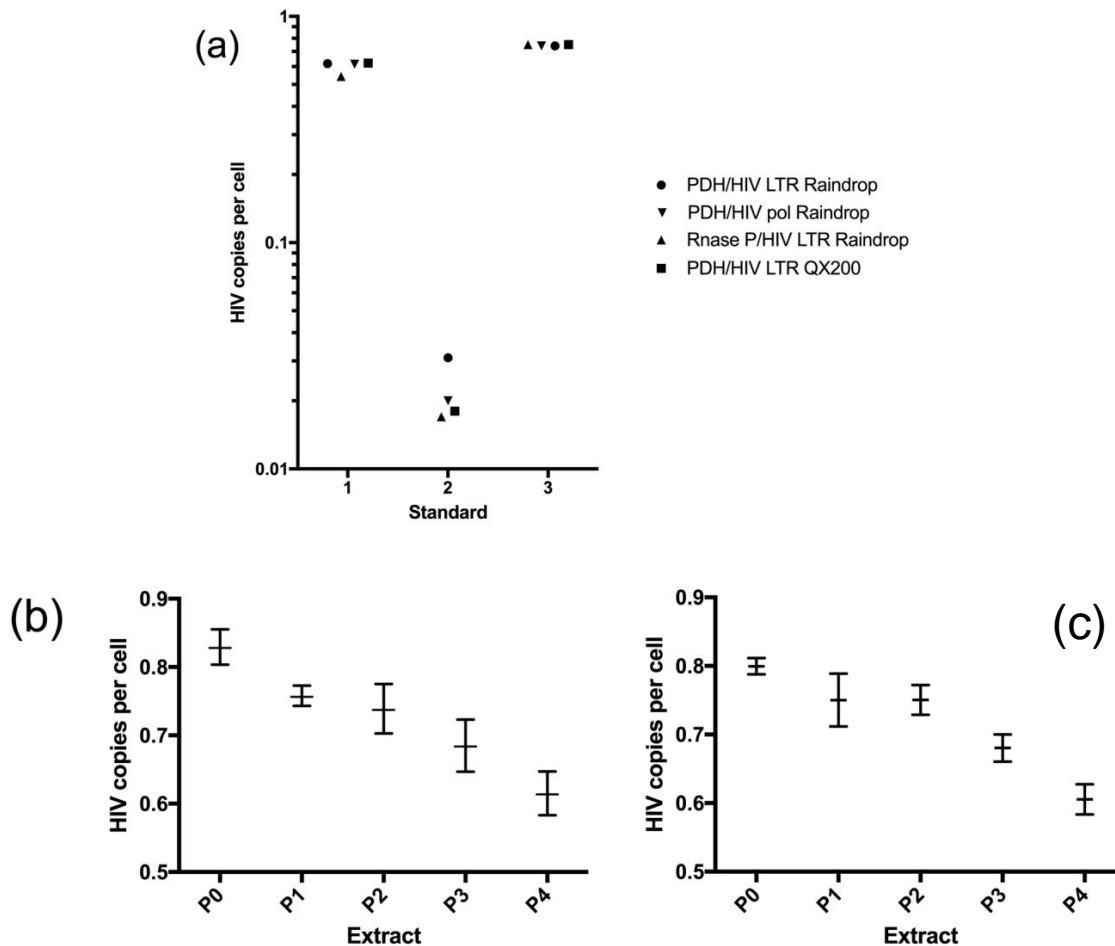


Figure 4.2: HIV DNA copies per cell determined by dPCR for three different 8E5 cell line sources. (a) Comparison of 8E5 Standards 1, 2 and 3 on the RainDrop® and QX200 platforms. (b) Effect of serial culture on HIV DNA content per cell for 8E5 Standard 3 measured using the RainDrop® dPCR platform (c) Effect of serial culture on HIV DNA content per cell for 8E5 Standard 3 measured using the QX200™ dPCR platform. Mean values with standard deviations are plotted (Busby *et al.*, 2017).



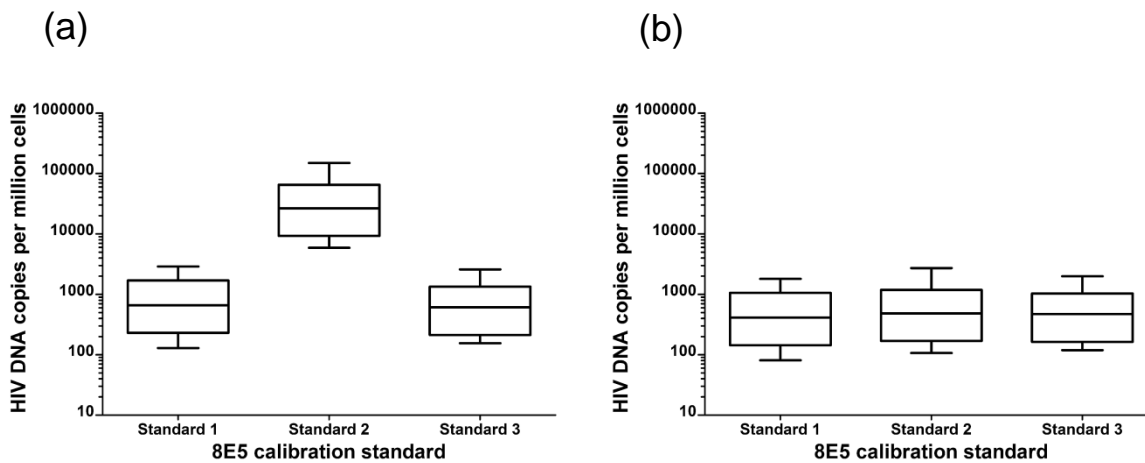
The mechanism of this apparent loss of HIV DNA from 8E5 cells in culture is unclear, although the presence of a contaminating human cell line could result in an increased number of human genomes and therefore skew the ratio of HIV DNA per cell (i.e. copies of PDH or RNase P). However, intra-species determination by short tandem repeat (STR) analysis was performed on the Standard 3 cells by the supplier prior to culture. STR profiling is a technique developed for forensic analyses that enables cell identification through PCR-based amplification of polymorphic STR loci (Masters *et al.*, 2001). The unique DNA profile for Standard 3 was concordant with the cell line specification, suggesting that no contaminating cell lines were present. Coincidentally, a recently published study also identified heterogeneous loss of HIV nucleic acid from different

sources of 8E5 cells at various passages using RNA FISH:FLOW analysis (Wilburn *et al.*, 2016). The authors suggest that the integration of HIV DNA into a region of the human genome containing fragile sites (13q14-q21) may be relevant to the loss of viral DNA from the cells, and could be the result of selective pressure on the cells during culture. In the case of Standard 2, no data were provided on the number of passages this sample had been subjected to upon dPCR analysis, but it is hypothesised that these cells were at a high passage.

4.3.3.2. Evaluating the impact of the 8E5 calibrator on qPCR quantification HIV DNA

To empirically determine the impact of varying quantities of HIV nucleic acid in different sources of the 8E5 calibrator on qPCR HIV DNA quantification, 7 PBMC samples that were separate from the original 18 were analysed and calibrated against standard curves constructed from 8E5 Standards 1, 2 and 3. Results were expressed in HIV DNA copies per million cells. When the reported 'one HIV genome per 8E5 cell' was assumed the results calibrated against Standard 1 and Standard 3 demonstrated no significant bias, but HIV DNA quantities calculated using the 'Standard 2' calibrator were approximately 50 times higher (Figure 4.3a). However, when the dPCR-determined HIV DNA copy number per extract for the three calibrators was applied, complete concordance of results was observed between the three sources of 8E5 calibrator (Figure 4.3b).

Figure 4.3: Median HIV DNA copies per million cells of seven clinical samples assayed by qPCR and calibrated using 8E5 Standards 1, 2 and 3 (boxplots shown with interquartile and range). (a) Calculated assuming one HIV DNA copy per 8E5 cell for all three Standards. (b) Calculated using the dPCR-determined number of HIV DNA copies per cell for each of the three different sources of 8E5 (Busby *et al.*, 2017).



dPCR value assignment of the three sources of 8E5 cell line DNA revealed that inaccuracies in the calibrator can bias qPCR quantification of HIV DNA. qPCR is likely to remain the method of choice for quantifying HIV DNA as the technique is well established in diagnostic laboratories. However, in order for quantitative qPCR results to be reliable an accurate calibration curve is essential (Bustin *et al.*, 2009). dPCR holds significant value for characterizing reference materials used to quantify nucleic acids, as has been demonstrated for other model systems (Bhat and Emslie, 2016, Devonshire *et al.*, 2016a, White *et al.*, 2015). This indicates a potential role for the method in further supporting qPCR quantification of HIV DNA where instability has been identified in the calibration material. Since passage number had a likely impact on cell line stability, fresh aliquots of the 8E5 cell line should be obtained and the HIV DNA copy number per cell verified by dPCR prior to commencement of studies quantifying HIV DNA by qPCR. This will ensure that laboratories obtain reproducible results that are comparable between diagnostic centres.

4.3.3.3. Application of cell lines for calibration of qPCR quantification of HIV-1 DNA

As demonstrated in this work, issues exist surrounding the genetic stability of the 8E5 cell line used to calibrate qPCR measurements of HIV-1 DNA. Additional cell lines either containing HIV-

1 genetic material or able to produce whole virions exist; namely, the J-lat 10.6 (Jordan *et al.*, 2003), J1.1 (Perez *et al.*, 1991), U1 (Folks *et al.*, 1987) and the ACH-2 cell lines (Clouse *et al.*, 1989, Folks *et al.*, 1989). In contrast to the 8E5 cell line, these materials are capable of producing infectious viral particles and so safety issues should be considered when choosing which calibrator to use. A review of the current literature on quantification of HIV-1 DNA demonstrates that the 8E5 cell line is most commonly used for constructing a standard curve. Table 4.4 lists numerous studies utilising qPCR for HIV-1 DNA quantification that cite the use of an HIV-1 infected cell for standard curve calibration. There are limited reports of genetic instability in cell lines other than 8E5, however one study demonstrated evidence of ongoing replication within ACH-2 cells during passaging which resulted in an increase in HIV-1 copies per cell (Sunshine *et al.*, 2016). In addition, the article by Telwatte *et al* (2019) highlights how HIV-producing cell lines differ from each other in their mechanisms governing viral latency. The authors recommend that these differences be taken into consideration when choosing cell lines for HIV research (Telwatte *et al.*, 2019). In the context of HIV-1 DNA quantification, dPCR value assignment of commonly used HIV-producing cell lines could help to promote harmonisation of results obtained between studies, regardless of which cell line is used. This could enable better data comparability between studies looking to quantify HIV-1 DNA, which could in turn promote greater confidence in measurement of the HIV latent reservoir.

Table 4.4: Variety of materials used to calibrate quantification of HIV-1 DNA in the literature.

Material	Number of articles citing use for qPCR calibration	Source
8E5 cell line	12	(Avettand-Fenoel <i>et al.</i> , 2009, Beck <i>et al.</i> , 2001, Desire <i>et al.</i> , 2001, Ghosh <i>et al.</i> , 2003, Jaafoura <i>et al.</i> , 2014, Kabamba-Mukadi <i>et al.</i> , 2005, McFall <i>et al.</i> , 2015, Shiramizu <i>et al.</i> , 2005, Sonza <i>et al.</i> , 2001, Surdo <i>et al.</i> , 2016, Thomas <i>et al.</i> , 2019, Gibellini, 2004)
ACH-2 cell line	3	(O'Doherty <i>et al.</i> , 2002, Chun <i>et al.</i> , 1997a, Ostrowski <i>et al.</i> , 2015)
U1 cell line	4	(Bosman <i>et al.</i> , 2015, Saha <i>et al.</i> , 2001, Thomas <i>et al.</i> , 2019, Chun <i>et al.</i> , 1997a)
J-lat 10.6 or J1.1 cell lines	1	(Thomas <i>et al.</i> , 2019)
Papers citing another calibrator* for HIV-1 DNA measurement	5	(Kellogg <i>et al.</i> , 1990, Gibellini, 2004, Butler <i>et al.</i> , 2001, Casabianca <i>et al.</i> , 2007, Malnati <i>et al.</i> , 2008)

*'another calibrator' includes in-house HIV infected cell lines additional to those described here, and plasmid constructs. The literature search was carried out using the following terms: hiv dna; real-time pcr; qPCR; quantitative; standard curve; 8E5; ACH-2; U1; J-lat; j1.1; plasmid.

4.3.3.4. *General use of cell lines for qPCR calibration*

Numerous studies indicate that over passaged, potentially contaminated and unstable cell lines are responsible for poor or unreproducible laboratory results, inaccurate data and financial loss. Issues with cells lines in research tend to focus on inconsistencies in culture or in gene expression. However, genetic instability in laboratory cell lines is well documented and generally considered to be an issue for research due to the unpredictably changing chromosomal structure of the cells. This is the case because the majority of research cell lines are derived from immortalised cancer cells, the chromosomal content of which tends to be both abnormal and variable within a cell population (Geraghty *et al.*, 2014). This becomes a particular issue where cell lines are being used to calibrate qPCR for the most sensitive measurements of low-level targets, such as the 8E5 cell line. A degree of stewardship over the use of cell lines for quantitative nucleic acid research may be of benefit to the scientific community, affording more reliable and reproducible results that could impact upon clinical decisions. In the context of the 8E5 cell line for HIV DNA quantification, the cell line may benefit from DNA sequencing to further characterise the integrated HIV provirus and identify any defects that may be causing the reported loss of HIV copy number. Further work should also include analysis of extended passage of this cell line, since the data presented in Figure 4.2 demonstrates that HIV DNA copy number decreased with culture within a limited period of time. With this in mind it would be prudent to provide information such as passage number when sharing cell line calibrators between laboratories (Hughes *et al.*, 2007). Digital PCR could also be applied as a reference method to verify the copy numbers of particular targets in cell lines used to calibrate qPCR.

4.3.4. *Comparison of qPCR and dPCR for HIV DNA quantification*

Alongside qPCR, there is increased interest in the role of dPCR as an alternative method for sensitive quantification of HIV-1 DNA in clinical and pre-clinical studies (Anderson and Maldarelli, 2018, Rutsaert *et al.*, 2018a, Trypsteen *et al.*, 2016). dPCR is a precise method with a dynamic range demonstrated to be approaching that of qPCR (Jones *et al.*, 2016). The work presented in this chapter provides an opportunity to explore some of the relative advantages and limitations of the two techniques (Table 4.5).

Table 4.5: Attributes and limitations of the techniques evaluated in this study for HIV DNA quantification.

'qPCR' and 'dPCR' refer to the specific protocols described in this chapter, although other protocols and platforms exist for these techniques.

Method	Attributes	Limitations
qPCR	Well characterized in-house clinical protocol	Quantitative estimates can be biased by inaccuracies in standard curve
	Large sample input volume (20 µL), increasing probability of detection of minority targets	Inaccuracies in calibration curve can be difficult to identify without a well characterised reference standard or method
	Multiplex format can be applied	
	Medium sample throughput (96 samples per run)	
QX200™ dPCR	Absolute quantification of single copy targets in multiplex format	Limitations on input sample volume owing to number of available partitions (up to ~23,000 per reaction well)
	Medium sample throughput (96 samples per run)	
	Closed system i.e. only specific Bio-Rad reagents can be used. This can be considered as both an advantage, where approaches can be standardized to a single kit, and a limitation where scope to explore and optimize protocols is limited.	
RainDrop® dPCR	Absolute quantification of single copy targets in multiplex format	Limited sample throughput (8 samples per run)
	Large number of partitions generated in each reaction well (up to ~10 million)	
	Open system i.e. a range of reagents can be used with this platform, with recommendations available from the manufacturer. This is both advantageous, where scope exists to explore numerous options and protocols, and a limitation where there is a risk of a lack of standardization.	

Issues surrounding the impact of limited sample input volumes for dPCR quantification of HIV DNA have been described previously (Strain *et al.*, 2013). Typically, a 50 μL qPCR reaction can measure $\sim 20 \mu\text{L}$ of sample. This $20 \mu\text{L}$ aliquot, which may be run in triplicate reactions and taken from 60-100 μL DNA extract, facilitates a high probability of capturing the HIV DNA molecules that may be present in that extract. In contrast, commonly used dPCR platforms including the Bio-Rad QX200 only have capacity for a lower volume of sample. Initial preparation for a QX200 dPCR experiment typically involves pipetting 5 μL of sample into a $20 \mu\text{L}$ total reaction volume prior to partitioning. Calculations of expected copy numbers are based on the assumption that the entire $20 \mu\text{L}$ reaction volume is emulsified into droplets, which is usually not the case, and that all of these partitions pass the necessary quality criteria. Therefore, a considerable proportion of the reaction volume and sample are lost to the so called 'dead volume' as illustrated in Table 4.6. This puts the QX200 at a disadvantage to qPCR in terms of sampling an equivalent volume. A higher number of replicates are required for dPCR to analyse an equivalent volume of sample to qPCR, representing more 'hands-on time' for setup along with increased consumable requirements and costs. As well as contributing to copy number calculations, the number of partitions accepted per QX200 dPCR reaction (Section 1.2.3.3) is a metric of run quality where less than 10,000 partitions is usually considered to be a quality failure (Whale *et al.*, 2017). Accepted partition count depends on numerous factors; poor droplet handling and improper reaction mix preparation are usually to blame for low counts (Bulletin-6407). Automatic generators are available (AutoDG, Bio-Rad), however there is less user control over how the droplets are handled by the robot. Factors intrinsic to the sample type can also influence droplet generation, including the presence of inhibitors and high quantities of genomic DNA. Notwithstanding, controlling the number of accepted partitions in a reaction is challenging and not always predictable, which potentially limits the role of the QX200 dPCR platform for clinical quantification of HIV DNA.

Table 4.6: Approximate reaction and sample volumes analysed and lost depends on the number of accepted partitions per reaction well using the QX200™ dPCR platform. The maximum number of partitions (23,981) is based on the assumption that all 20 µL reaction volume is converted into droplets, and assuming a partition size of 0.834 nL (Corbisier et al., 2015). The values given for ‘accepted number of partitions per reaction’ are examples based on typical experiments performed in this study.

Number of accepted partitions per well (n)	Approximate sample volume analysed per well (µL) assuming 5 µL initial input	Approximate total reaction volume analysed per well (µL)	Reaction volume lost based on accepted partition count (µL)	Percentage of reaction lost to ‘dead volume’	Number of QX200 dPCR replicate wells per sample per experiment required to equal 20 µL (used in qPCR)
23,981	5.0	20.0	0.0	0%	4
18,000	3.8	15.0	5.0	25%	5
15,000	3.1	12.5	7.5	37%	6
10,000	2.1	8.3	11.7	58%	10

4.3.5. Sensitive estimations of the size of the HIV proviral reservoir normalised to one million cells

The widely adopted convention for reporting quantitative estimates of the proviral reservoir is to normalise HIV DNA copy numbers to one million cells (Avettand-Fenoel *et al.*, 2009). A review of the literature suggests that the use of this denominator is largely historical, and possibly related to the adaptation of molecular approaches from cell culture assays. Measurement of tissue culture infective dose (TCID) is historically reported per million PBMCs (Daar *et al.*, 1991, Ho *et al.*, 1989), along with viral outgrowth assays for estimating the size of the replication competent HIV reservoir (Henrich *et al.*, 2017). Studies utilising transposable elements for HIV integration assays estimate that approximately one million Alu repeats are present in the human genome, enabling precise quantification of integrated forms of HIV DNA normalised to one million cells (Chun *et al.*, 1997a). Furthermore the average number of latently infected cells containing replication competent virus in an individual has been estimated at approximately one million (Chun *et al.*, 1997b), inferring that HIV DNA estimates per million cells could be indicative of the size of the total reservoir.

Absolute quantification by dPCR in this chapter revealed that very small numbers of HIV DNA copies could be detected in samples from HIV positive individuals (Table 4.2a). Sample 7, which contained 2 raw copies per reaction by RainDrop dPCR, contained 11 copies by qPCR. Differences in sample input volumes contributing to this difference have already been discussed (Section 4.3.1). However, when raw HIV DNA copies were normalised to one million cells dPCR shows almost twice as many copies as qPCR (76 compared to 38, respectively). Similar results were also observed for Sample 9. This could be misleading about the respective performances of qPCR and dPCR, and may hide true copy numbers in a sample in the presence of high background DNA concentrations. Table 4.3 shows that both of these samples exhibited PDH (reference gene) λ values of greater than 2.0, indicating that they may be approaching the limits of precision in terms of HIV DNA quantification in a background of concentrated genomic DNA. Discordances between dPCR and qPCR were also observed for other samples, where technically sensitive measurements of low levels of HIV DNA were obtainable by dPCR (Sample 2, Sample 14). However, normalisation of these samples to one million cells resulted in disagreement between the techniques which gives the impression that the methods possess different sensitivities. Whilst normalisation of data in this way generally facilitates comparison between

techniques, technical and biological limitations could lead to measurement error and prevent comparability of results.

Normalising two unrelated targets, i.e. HIV DNA relative to human genomic targets, as an absolute metric for quantifying the HIV reservoir could introduce bias within and between individuals, as well as between laboratories. Differences in PCR assay dynamics, diurnal changes in blood counts (Jones *et al.*, 1996), and differences in reporting of CD4+ cell counts between labs (Sax *et al.*, 1995) may all contribute to measurement error. In addition, choice of reference target must also be considered as copy numbers for different genes can vary within an individual (Devonshire *et al.*, 2014a). Combined with potential bias introduced by instability in the qPCR calibrator discussed in Section 4.3.3.2, these issues suggest that the convention of reporting HIV DNA copies per million cells may require review in the future. This denominator could contribute to discrepancies between studies where low-level samples are masked by the cellular content. Normalisation of HIV-1 DNA copy numbers quantified per million cells could respectively inflate or diminish the estimated copy number in a sample when the ratio is calculated relative to low or high concentrations of host DNA. Reporting of absolute copy numbers of HIV DNA and host genomic targets in place of normalised values could provide a more accurate estimate, especially where analytical sensitivity of a method is being investigated.

4.4. Conclusions

Clinical quantification of HIV-1 DNA could be a valuable tool in monitoring how individuals infected with HIV-1 are managed and treated by estimating the size of the viral reservoir. The availability of methods capable of sensitive and precise quantification could permit greater confidence in measurements of low levels of HIV-1 DNA. In this chapter qPCR, the current method of choice for HIV-1 DNA quantification, and dPCR were compared. The two approaches were generally shown to perform comparably for a cohort of 18 clinical samples. However, numerous analytical factors were found to contribute to measurement error for the two methods leading to discordances between results. Sample volume of dPCR may have a limiting role for detection compared to qPCR, and the convention of normalising HIV-1 DNA copy numbers to one million cells may skew estimates of the viral reservoir using both methods. In addition dPCR, which can quantify nucleic acid in the absence of a standard curve, revealed instability in the 8E5 cell line qPCR calibrator which biased quantitative estimates. Bias was eliminated following re-calculation

of results to the dPCR assigned value, allowing harmonisation of measurements between different batches of the calibration standard. dPCR may have a role in supporting qPCR quantification of HIV-1 DNA through value assignment of calibration materials, which could improve measurement reproducibility between laboratories and studies. Further work addressing the sensitivity of dPCR could help to establish a role for direct quantification of HIV-1 DNA in patient samples to support clinical use.

5. Quantification of methicillin resistance in *Staphylococcus spp* using digital PCR

5.1. Introduction

5.1.1. Methicillin resistant *Staphylococcus aureus* (MRSA)

In 2017 the World Health Organisation (WHO) published the global priority pathogens list (global PPL); a list of bacteria for which urgent research and development for new antibiotics is required (World Health Organization, 2017a). The list was constructed to help prioritise research efforts focussed on these pathogens as increasing levels of antimicrobial resistance threaten to jeopardise human health. It has been suggested that by 2050, 10 million people will die every year due to infections with antimicrobial resistant organisms unless a global effort to develop new treatments is escalated (O'Neill, 2014). Organisms are categorised into three groups: medium, high and critical priority. Methicillin resistant *Staphylococcus aureus* (MRSA) is a member of the high priority group. Staphylococci are Gram-positive organisms that are ubiquitous colonisers of human skin, nasal passages and axillae. In some instances, staphylococci can cause invasive disease resulting in soft tissue infections and disseminated disease. The genus is broadly divided into coagulase positive species including *S. aureus*, and coagulase negative species (Foster, 1996). Coagulase-positive organisms possess the ability to coagulate blood plasma, allowing bacteria to persist within colonised tissue and therefore contributing to pathogenesis (McAdow *et al.*, 2012). Active disease caused by *S. aureus* has historically been successfully treated using β -lactam antibiotics. However, antimicrobial resistance to these drugs, including penicillin and methicillin, has been documented in *S. aureus* since the 1960s. Subsequent, widespread emergence of methicillin resistance has necessitated the introduction of other antimicrobial classes to treat infections with this ubiquitous organism (David and Daum, 2017).

5.1.2. Colonisation and infection with MRSA

Approximately one third of the global population are colonised with *S. aureus* (Hassoun *et al.*, 2017), and about 1 in 30 people in the UK are colonised with methicillin resistant *S. aureus* (MRSA) (NHS, 2017). Colonisation of the skin and nasal passages with MRSA can lead to soft tissue infections that are difficult to treat. Complications of disseminated MRSA include bone and joint infections, endocarditis and sepsis (Hassoun *et al.*, 2017). Patients are screened for MRSA

carriage upon or prior to admission into hospital, such as for elective surgical procedures (Coia *et al.*, 2006, Mehta *et al.*, 2013). A positive result for MRSA can result in lengthy decolonisation protocols, delays to procedures and potential isolation to prevent spreading the organism. This may be troublesome for patients awaiting surgery, or those that experience prolonged hospital stays as a result. Infection with MRSA can be particularly problematic for neonates in intensive care (Nelson and Gallagher, 2012), transplant patients (Liu *et al.*, 2018) and those who are generally immunocompromised. Appropriate treatment of infections with MRSA is necessary to prevent further transmission along with associated morbidity and mortality, and usually involves administration of second-line antibiotics including vancomycin and linezolid (Welte and Pletz, 2010). Rare, but serious complications associated with MRSA treatment have been reported such as myelosuppression resulting from linezolid treatment (Gorchynski and Rose, 2008) and haemolytic anaemia after off-label treatment with ceftaroline (Verdecia *et al.*, 2019). This highlights the need for accurate detection of MRSA, particularly when administering treatment regimens that may carry significant side effects.

5.1.3. Molecular diagnosis of MRSA and the clinical relevance of coagulase-negative staphylococci (CoNS)

Molecular approaches including qPCR are utilised for detecting MRSA colonisation. Numerous commercial tests are available, including the BD MAX™ MRSA Assay (Becton Dickinson), LightCycler® MRSA Advanced Test (Roche) and the GeneXpert® MRSA range (Cepheid) (Aydiner *et al.*, 2012, Yam *et al.*, 2013, Lee *et al.*, 2017). Many assays target the SCCmec cassette, a mobile genetic element which contains the *mecA* gene that confers methicillin resistance by producing an altered penicillin-binding protein (PBP2a) (Fishovitz *et al.*, 2014). The cassette integrates at a known locus within open reading frame X (*orfX*) in *S. aureus* (Huletsky *et al.*, 2004, Ito *et al.*, 2014), and is referred to as the staphylococcal cassette chromosome mec (SCCmec)-*orfX* right-extremity junction (MREJ). The assays available can be applied directly to clinical specimens where other species may be present since they only target MRSA (Huletsky *et al.*, 2004). However, there are limitations associated with these techniques; firstly, the primer sequences used to amplify MREJ are patented and therefore proprietary, which limits the availability for clinical microbiology laboratories to incorporate them into in-house assays. This region is also prone to high levels of recombination, which could cause MRSA colonisation or

infection to be missed when only these assays are used (Hill-Cawthorne *et al.*, 2014). In addition, false positives can occur owing to the presence of 'empty cassette variants' of *S. aureus*, where the *mecA* gene has been excised from the otherwise intact SCCmec cassette and could lead to misclassification of these isolates which are phenotypically methicillin sensitive (Lee *et al.*, 2017). False positives could cause patients to be isolated unnecessarily, or surgical procedures to be delayed. Furthermore, other opportunistic organisms that can also harbour *mecA* may be missed. This includes coagulase negative staphylococci (CoNS), such as *Staphylococcus epidermidis* (Becker *et al.*, 2014). Although generally regarded as non-pathogenic, such organisms have been increasingly recognized in central nervous system shunt infections, native or prosthetic valve endocarditis, urinary tract infections, and endophthalmitis as well as in bloodstream infections (Kelley *et al.*, 2013, Méric *et al.*, 2018). The majority of commercial platforms targeting the *S. aureus* specific MREJ will not detect DNA sequences for CoNS. As a result, clinical microbiology laboratories resort to developing in-house qPCR assays for detection of multiple targets including *mecA*, *S. aureus* targets and those specific to CoNS (Kim *et al.*, 2013).

5.1.4. A role for DNA quantification in managing MRSA infections

Current in-house and *in vitro* diagnostic (IVD) assays for MRSA diagnosis are generally qualitative. In addition to detection, quantification of MRSA (which has not yet been integrated into routine diagnostic workflows) could be of benefit for management of infections. Heavy bacterial load, particularly MRSA colonisation in the nasal passage, has been suggested to be a risk factor for invasive disease (White, 1963, Kalmeijer *et al.*, 2000). In addition, high bacterial load from the nares may be indicative of colonisation of additional body sites, which in turn could predict the effectiveness of decolonisation procedures (Mermel *et al.*, 2011). Changes in bacterial load could be used for monitoring response to treatment, and could contribute to setting thresholds for colonisation versus disease states in patients. The latter has been demonstrated for other organisms, where nasopharyngeal bacterial load has been suggested as a marker of invasive disease in children with suspected pneumococcal infection. Individuals with invasive infection were distinguishable from control groups based on a cut-off value of 6.5 log₁₀ genome copies per mL (Brotons *et al.*, 2017).

Existing in-house qPCR approaches could be used to quantify methicillin-resistant organisms in samples. Determination of genome copy numbers could be used to accurately calculate ratios

between *mecA* and host genomic targets to determine the number and nature of drug resistant organisms present. Such an approach could be used to precisely determine which species is harbouring methicillin resistance. This could be of particular use in scenarios where *S. aureus* is co-colonised with CoNS, which can also carry the *mecA* gene and exhibit methicillin resistance. Measuring the bacterial load of the drug-resistant population could be of benefit to managing patients with MRSA infections, including targeted treatment strategies and monitoring of patients with heavy colonisation.

5.1.5. A role for digital PCR in quantifying MRSA DNA

As demonstrated in Chapter 4, qPCR approaches for quantifying gene targets can be limited by bias introduced through inaccurate calibration materials. dPCR was demonstrated in Chapters 3 and 4 to offer precise absolute quantification of DNA and RNA in the absence of a calibration curve. In addition, dPCR was shown to be useful in value assigning reference materials used to calibrate qPCR approaches. Since quantification of MRSA DNA is an emerging concept, dPCR could be applied for absolute quantification of *mecA* and species-specific targets to support qPCR approaches through value assignment of calibration materials. dPCR has been implemented in studies assessing the relationship between magnitude of bacterial DNA load and bloodstream infections/sepsis (Ziegler *et al.*, 2019a, Ziegler *et al.*, 2019b), also indicating a potential clinical role for the technique. The work presented in this chapter describes the development of a multiplex dPCR approach that could be used to determine which *Staphylococcus* species is carrying resistance by comparing the ratio of *mecA* to host genomic targets. This is demonstrated through the characterisation of candidate reference materials that could be used to support qPCR assays, and through direct quantification applied to clinical samples. Accurate quantification of MR-*Staphylococcus* spp could improve diagnostic specificity to assist with patient management through administering appropriate antimicrobial therapies, improving infection control strategies and limiting the need for isolation, representing an overall reduction in healthcare costs.

5.2. Materials and methods

5.2.1. Study materials

5.2.1.1. ATCC genomic DNA controls

The following materials were obtained as pre-extracted genomic DNA from the American Type Culture Collection (ATCC, USA): methicillin resistant *Staphylococcus epidermidis* (MRSE; 35984D-5), *Staphylococcus aureus* subsp. *aureus* Rosenbach both methicillin resistant (MRSA; BAA-1556D-5) and sensitive (MSSA; BAA-1718D-5). Nucleic acid concentration was estimated using a Qubit® 2.0 fluorometer and a dsDNA BR Assay Kit (Invitrogen™, USA). DNA was stored at -80°C upon receipt.

5.2.1.2. Whole bacterial cell materials

Whole cell bacterial materials were prepared by LGC Microbiology Proficiency Testing (United Kingdom) and Helios University Clinic Wuppertal (Germany). The materials were provided as units of lyophilised organisms. The suite of materials included units of methicillin resistant and sensitive *S. aureus* (MRSA and MSSA, respectively) and *S. epidermidis* (MRSE and MSSE, respectively), including mixtures of these which were prepared based on estimated colony forming units (CFU) per mL following colony counting at each centre. The materials were stored at +4°C upon receipt.

5.2.1.3. Residual clinical DNA extracts

Residual DNA extracts from 22 culture-negative primary clinical samples, submitted to the Department of Microbiology at Great Ormond Street Hospital for Children NHS Foundation Trust (GOSH), were obtained for validation of the dPCR method. The residual extracts were surplus to requirements having already been analysed as part of the routine diagnostic service at GOSH. 10 µL of each extract was analysed in a total reaction volume of 28 µL by the Department of Microbiology using qPCR. Extracted DNA was stored at -20°C upon receipt. The qPCR result was blinded prior to dPCR analysis, and any clinical sample identifiers had been removed prior to receipt of the samples.

5.2.2. Optimisation of a protocol for DNA extraction from bacteria

A comparison of DNA extraction protocols was performed using lyophilised whole cell MSSA material. The comparison included the following kits: DNeasy® blood and tissue kit (Qiagen, Germany); Wizard® Genomic DNA Purification Kit (Promega, USA); E.Z.N.A® Bacterial DNA Kit (Omega Bio-Tek, USA). DNA was extracted in accordance with the manufacturer's instructions which included an enzymatic bacterial cell lysis step. Enzymes were added to the following final concentrations prior to incubation: 20 mg/ mL lysozyme (DNeasy® blood and tissue kit), 2 mg/ mL lysostaphin and lysozyme mixture (Wizard® Genomic DNA Purification Kit), 5 mg/ mL lysozyme (E.Z.N.A® Bacterial DNA Kit). Triplicate units of material were extracted on three different days (three units per day) for each kit, along with extraction negative controls which contained no sample input. DNA yield was quantified using a Qubit® 2.0 fluorometer and the dsDNA HS Assay (Invitrogen™, USA) and by digital PCR (dPCR) using the QX200 droplet digital PCR system (Bio-Rad, USA).

5.2.3. Oligonucleotides

Table 5.1: Primer and probe sequences for detection of *Staphylococcus* spp

Target	Genbank accession	Assay	Oligo Name	Sequence (5'-3')	Source
Gene conferring methicillin resistance in <i>Staphylococcus</i> spp.	CP043916	<i>mecA</i>	Forward	TTA GAT TGG GAT CAT AGC GTC ATT AT	Primer sequences: (Pierpont, 2016) Probe sequence: (Nihonyanagi <i>et al.</i> , 2012)
			Reverse	AAT TCC ACA TTG TTT CGG TCT AAA A	
			Probe	FAM-CCA GGA ATG CAG AAA GAC CAA AGC ATA CA-BHQ1	
Coagulase gene specific to <i>Staphylococcus aureus</i>	AB436985	<i>coA</i>	Forward	GTA GAT TGG GCA ATT ACA TTT TGG AGG	(O'Sullivan <i>et al.</i> , 2014)
			Reverse	CGC ATC TGC TTT GTT ATC CCA TGT A	
			Probe	HEX or Cy5** -TAG GCG CAT TAG CAG TTG CAT C-BHQ1	
<i>Staphylococcus epidermidis</i> species specific gene	U23713	<i>femA</i>	Forward	TGC AGG GAG CTA TGC GGT TCA ATG	Present study
			Reverse	CGC CAG CAT CTT CAG CAT CTT CAC	
			Probe	HEX-CCA TGT TCA ATT GCA TAG TTA ATC ATC T-BHQ1	

* Refer to page 23 for abbreviations relating to fluorescent dyes and quenchers. ** the *coA* probe was labelled with HEX for analysis using the QX200 system (Bio-Rad, USA) and Cy5 using the Naica system (Stilla, France).

5.2.3.1. *Staphylococcus epidermidis femA* assay design

Suitable candidate sequences for assay design were searched in Genbank (Clark *et al.*, 2016). Sequences were aligned using MultAlin (Corpet, 1988) to ensure sufficient diversity from related species *in silico*. A portion of the *S. epidermidis femA* gene (Accession: U23713) was identified that was suitable for the design of a 119 bp amplicon (positions 1,398 to 1,516). Forward and reverse primers were designed to the sense and anti-sense DNA strands, respectively, and a dual-labelled hydrolysis probe designed to the anti-sense strand. *In silico* specificity of the assay for *S. epidermidis* was confirmed using NCBI Blast, and later verified by dPCR. The intended amplicon shared 100% homology and coverage with 22 sequences for *S. epidermidis* deposited in GenBank with an e-value of 7e-54. Four additional entries shared 100% coverage of the amplicon, but with 2 single nucleotide mismatches (one of which is in the reverse primer region of the amplicon).

5.2.4. **Quantification by digital PCR**

5.2.4.1. *Dynamic range of assays*

The dynamic ranges of the assays (Table 5.1) were tested using the QX200™ droplet digital PCR system (Bio-Rad) following the general protocol described in Section 2.1.5. QuantaSoft version 1.7.4.0917 was used for data analysis. Serial dilutions were prepared for the MRSA and MRSE ATCC genomic DNA control materials over a 5-log interval linear range from 1.68E+04 to 1.68E-01 copies per µL (based on quantitative estimates obtained following analysis using the Qubit dsDNA BR Assay Kit). Each dilution point was tested in a single experiment in triplicate reactions. 7.7 µL of DNA template was added to a total prepared volume of 22 µL including 1X ddPCR™ Supermix for Probes without dUTP (Bio-Rad, USA). DNA was analysed using two assay duplexes (i.e. two assay targets in one reaction): *mecA* and *coA* for MRSA, and *mecA* and *femA* for MRSE.

5.2.4.2. *dPCR quantification of methicillin resistance in genomic DNA admixtures*

MRSA and MRSE ATCC genomic DNA were mixed to a 1:1 copy number ratio based on the Qubit so that each reaction contained an equivalent number of *Staphylococcus* genomes and *mecA* targets per μL (750, 75 and 7.5 copies per μL input concentration estimated using Qubit) of the respective genomic targets (*coA* and *femA*). A dilution series was constructed by diluting the 1:1 mixture 10-fold in nuclease-free water (Ambion, USA) and analysed using the assay duplexes. This was followed by separate dilution series of MRSA genomic DNA (5-point range from 400 to 10 copies per μL) in a constant background of MSSA and MSSE DNA (200 copies per μL). Copy number calculations from the previous dPCR experiments were used for input quantities. Specificity of the assays was confirmed using MSSA and MSSE genomic DNA, and no template controls were included containing nuclease-free water. The DNA mixtures were initially analysed using the QX200™, and subsequently using the Naica System™ for Crystal Digital™ PCR.

5.2.4.3. *General protocol for the Naica System™ for Crystal Digital™ PCR*

5.5 μL of DNA template was added to a total prepared reaction volume of 27.5 μL containing Perfecta Multiplex qPCR ToughMix (Quanta Biosciences, USA), sterile nuclease-free water (Ambion, USA), 20X stock of each primer probe mix and 0.1 μM fluorescein (VWR, USA). Fluorescein solution was prepared by weighing out fluorescein sodium salt (VWR, USA) and solubilising in nuclease-free water (Ambion, USA) to a stock concentration of 200 μM . A working stock of 2 μM fluorescein was prepared in nuclease-free water for use as a reference dye. 25 μL of total reaction volume was applied to a Sapphire chip (version 2) which was loaded into the Naica Geode. Partitioning was achieved under 950 mbar of pressure at 40°C for 12 minutes as described in (Madic *et al.*, 2016). Typical PCR cycling conditions were 95°C for 10 minutes followed by 60 cycles of 95°C for 30 seconds and 60°C for 30 seconds. A final decompression step back to atmospheric pressure and room temperature was performed for 33 minutes. Chips were scanned using the Naica Prism and Crystal Reader software version 2.1.6. The following

parameters were applied; focus 0.9 mm, exposure time for blue channel 45 ms, green channel 125 ms, red channel 25 ms. Data were analysed using Crystal miner software version 2.1.6. An initial experiment was performed to compensate spill over of the three reporter dyes into each channel. This involved inclusion of a single positive control (MRSA or MRSE genomic DNA) for each channel (red, green, blue corresponding to Cy5, HEX and FAM, respectively) and a negative control (nuclease-free water). The bespoke compensation matrix file was applied to successive experiments using the assay triplex in Crystal Miner and Crystal Reader software. A partition volume of 0.59 nL was used to calculate copy number concentration (Stilla, France).

5.2.5. Inter-laboratory analysis of whole bacterial cell materials

Units of lyophilised materials containing varying quantities and mixtures of methicillin resistant and sensitive *Staphylococcal* species were analysed as part of an inter-laboratory study involving three national measurement institutes. The participating institutes were National Measurement Laboratory (NML, UK), National Institute of Biology (NIB, Slovenia) and Physikalisch-Technische Bundesanstalt (PTB, Germany). Lyophilised materials were reconstituted in 1 mL of sterile nuclease-free water (Ambion, USA) and incubated at ambient temperature for 30 minutes. The entire 1 mL suspension was transferred to a 2 mL DNA Lo-Bind tube and pelleted by centrifugation. DNA was extracted from the pelleted material using the Qiagen® DNeasy blood and tissue kit described in Section 5.2.2. PolyA RNA carrier (Roche, Switzerland) was included at a concentration of 0.27 µg/ µL in lysis buffer (AL). Extracts were eluted in 100 µL Qiagen elution buffer (AE) and stored at 4°C. DNA extraction of triplicate units per material was performed across three separate days (three units per day), followed by a single dPCR experiment per extraction batch. dPCR was performed on the QX200™ system in duplex. 5.5 µL of each extract was added to a prepared volume of 22 µL and analysed in triplicate reactions. A partition volume of 0.85 nL was used to calculate copy number concentration (Bio-Rad, USA). MRSA and MRSE genomic DNA controls were included in the dPCR experiment along with extraction negatives (i.e. eluates from the extraction process but without sample added) and no-template controls (nuclease-free water).

5.2.6. dPCR analysis of clinical isolates

The 22 residual DNA extracts from primary clinical isolates (Section 5.2.1.3) were analysed by dPCR using the QX200™ droplet digital PCR system and Naica System™ for Crystal Digital™ PCR. A single replicate of each sample was analysed using the assay duplexes or in triplex on the QX200 and Naica platforms, respectively. MRSA, MRSE, MSSA and MSSE genomic DNA controls were included along with no-template controls. 5.5 µL total volume of template was added to prepared volumes of 22 µL for the QX200 and 27.5 µL for the Naica.

5.2.7. Data analysis

Data from dPCR experiments were subject to threshold and baseline setting in QuantaSoft version 1.7.4.0917 (Bio-Rad, USA) and Crystal miner software version 2.1.6 (Stilla, France), and exported as .csv files to be analysed in Microsoft Excel 2010. The average number of DNA copies per partition (λ) were calculated from these data as described in (Whale *et al.*, 2016a). Statistical significance was calculated within 95% confidence using Student's t-test, and agreement between groups was assessed using Bland Altman analysis.

5.3. Results and discussion

5.3.1. Method development

5.3.1.1. Assay specificity

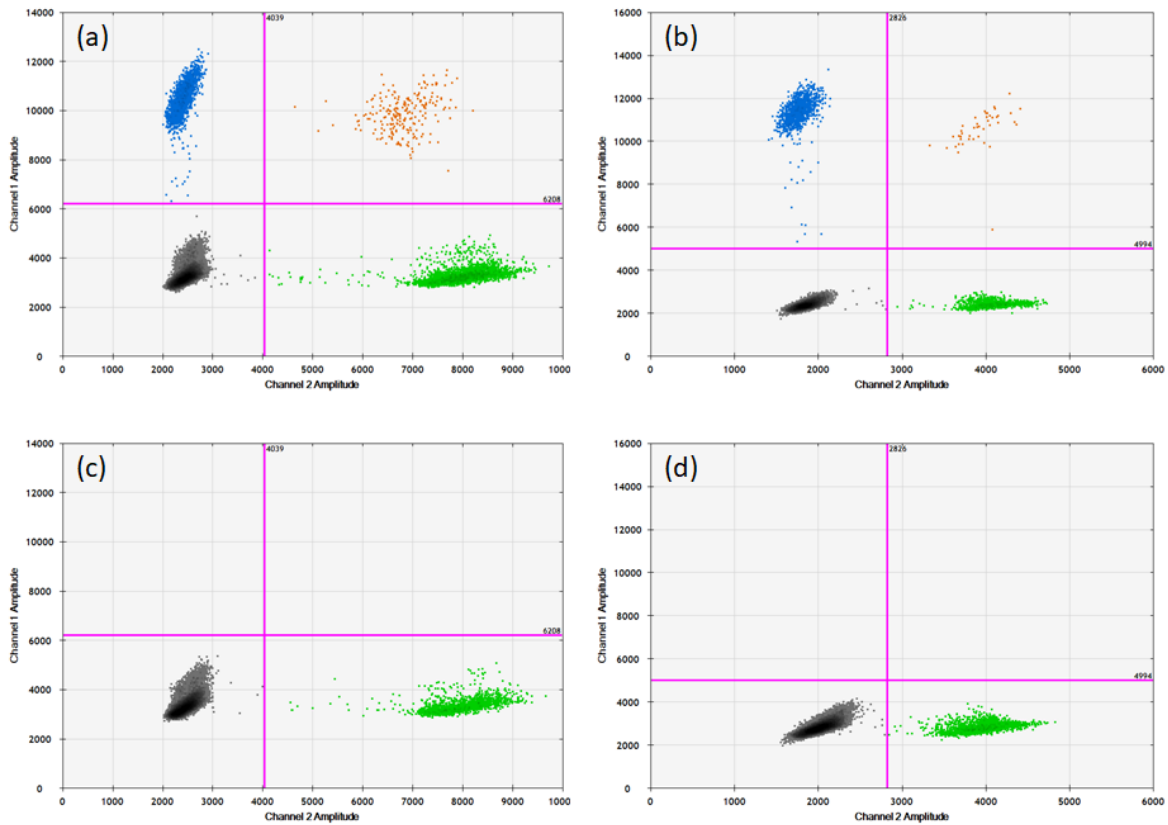
Specificity of the oligonucleotides listed in Table 5.1 was verified by analysing genomic DNA materials for MRSA, MSSA, MRSE and MSSE using the QX200™ droplet digital PCR system. The average number of input copies per μL calculated for each assay target is given in Table 5.2. The *mecA* assay sequence is common to both methicillin-resistant *S. aureus* and *S. epidermidis*.

Table 5.2: Copies per μL for each of the assays analysed in duplex using genomic DNA as template.

Organism	Assay target average copies per μL (SD)		
	<i>mecA</i>	<i>coA</i>	<i>femA</i>
MRSA	389.0 (8.7)	377.6 (18.9)	0.0
MSSA	0.0	171.8 (13.4)	0.0
MRSE	631.4 (19.0)	0.0	631.5 (43.7)
MSSE	0.0	0.0	198.6 (19.0)

Table 5.2 shows that, for the methicillin-resistant DNA templates, *mecA* and the respective species-specific gene were detected. However, in each of the methicillin-sensitive templates only the species-specific gene was detected demonstrating specificity of the *mecA* assay for the resistance gene target. These data also demonstrate that there is no detectable cross reactivity between the *coA* and *femA* assays that are specific for *S. aureus* and *S. epidermidis*, respectively. Figure 5.1 depicts the QX200 dPCR dot plots corresponding to the results shown in Table 5.2. *mecA* was detected in both MRSA and MRSE, but not in the methicillin-sensitive counterparts.

Figure 5.1: Digital PCR dot-plots showing detection of (a) *mecA* & *coA* and (b) *mecA* & *femA* using MRSA and MRSE ATCC genomic DNA controls, respectively; (c) and (d) represent MSSA ATCC genomic DNA and MSSE extract, respectively. Blue dots represent presence of FAM-labelled target (*mecA*), green dots represent HEX-labelled targets (*coA* & *femA*), orange dots represent both targets present in a droplet, grey dots represent no amplification.



5.3.1.2. Dynamic range

For methicillin resistant staphylococci, the ratio of *mecA* gene copy numbers to species-specific copy numbers is expected to be 1 (Bode *et al.*, 2012). dPCR quantification can exploit this ratio to indicate which organism is carrying methicillin resistance. Dynamic range of the assay duplexes was assessed using a 6-point dilution series of each gDNA material in triplicate, whilst simultaneously assessing the fidelity of the 1:1 hypothesis.

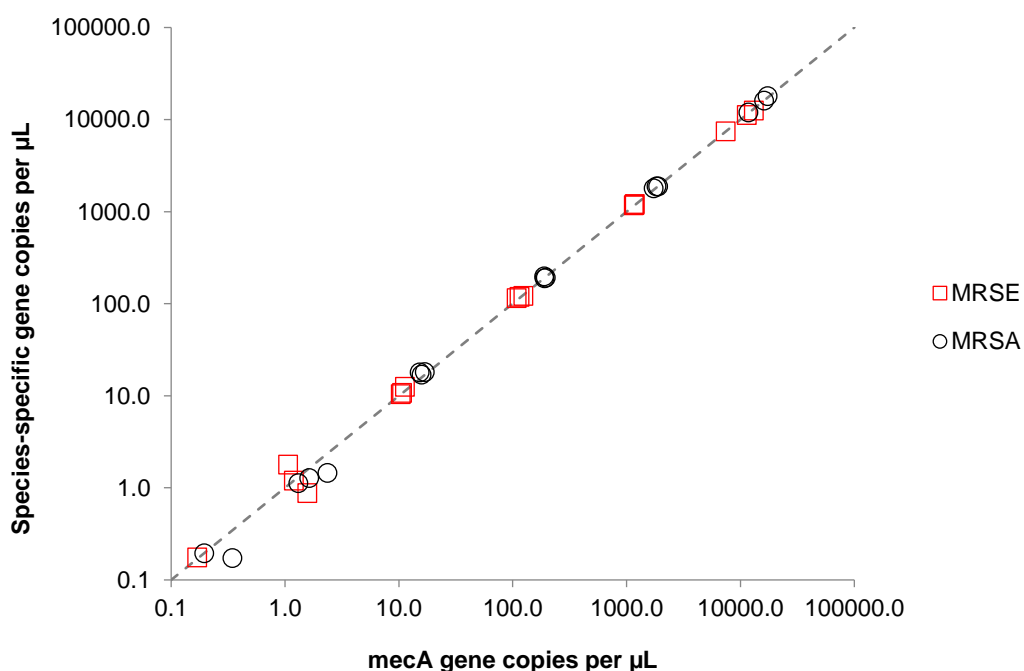
Table 5.3: Dynamic range of assays for analysis of (a) MRSA and (b) MRSE ATCC genomic DNA. Results are expressed as copies per μL in the neat extract.

(a) Sample	<i>mecA</i> positive partitions (k)	Mean <i>mecA</i> λ	Mean <i>mecA</i> copies per μL	<i>coA</i> positive partitions (k)	Mean <i>coA</i> λ	Mean <i>coA</i> copies per μL	Ratio <i>mecA:coA</i> copies per μL
MRSA S1	16049	4.5	15073.4	16065	4.6	15298.0	1.0
MRSA S1	15744			15763			
MRSA S1	16889			16885			
MRSA S2	7955	0.5	1822.0	8129	0.5	1845.2	1.0
MRSA S2	7612			7732			
MRSA S2	7584			7526			
MRSA S3	1009	0.1	191.8	995	0.1	192.6	1.0
MRSA S3	1057			1107			
MRSA S3	1097			1075			
MRSA S4	91	0.0	16.0	107	0.0	17.7	0.9
MRSA S4	98			105			
MRSA S4	74			79			
MRSA S5	7	0.0	1.8	6	0.0	1.3	1.4
MRSA S5	13			8			
MRSA S5	9			7			
MRSA S6	1	0.0	0.2	1	0.0	0.1	1.5
MRSA S6	0			0			
MRSA S6	2			1			

(b) Sample	<i>mecA</i> positive partitions (k)	Mean <i>mecA</i> λ	Mean <i>mecA</i> copies per μL	<i>femA</i> positive partitions (k)	Mean <i>femA</i> λ	Mean <i>femA</i> copies per μL	Ratio <i>mecA:femA</i> copies per μL
MRSE S1	13387	3.2	10669.1	13330	3.1	10397.3	1.0
MRSE S1	15008			15014			
MRSE S1	16864			16831			
MRSE S2	5766	0.3	1173.0	5800	0.4	1184.6	1.0
MRSE S2	5460			5479			
MRSE S2	5613			5698			
MRSE S3	591	0.0	115.8	625	0.0	118.2	1.0
MRSE S3	646			668			
MRSE S3	683			667			
MRSE S4	60	0.0	10.8	60	0.0	11.2	1.0
MRSE S4	66			73			
MRSE S4	54			54			
MRSE S5	6	0.0	1.3	10	0.0	1.3	1.0
MRSE S5	9			5			
MRSE S5	7			7			
MRSE S6	0	0.0	0.1	0	0.0	0.1	1.0
MRSE S6	0			1			
MRSE S6	1			0			

Table 5.3 shows that both assay duplexes (*mecA* in combination with either *coA* or *femA*) were able to quantify less than 1.0 copy per μL , although not all replicate reactions at this dilution (S6) gave a positive signal. Precision of dPCR decreases in proportion with target concentration copy number, where there is increased stochasticity and reduced sampling of target (Bulletin-6407, Depez *et al.*, 2016). The aim of this work was not to formally establish the limit of detection (LOD) of these assays, negating the requirement for high replication in this respect. However, the sensitivity of the assays may be estimated to be between 1.0 and 2.0 copies per μL based on the results in Table 5.3 since target DNA was quantified in all three dPCR replicates at this level. For dilution points S1-S5, the ratio between *mecA* and the species-specific gene target was between 0.9 and 1.4 (mean and mode = 1.0). Additionally, Figure 5.2 illustrates that there was good linearity between the *mecA* assay and the species-specific assays for both MRSA and MRSE across the dynamic range. These data support the hypothesis that the methicillin-resistant species for which the ATCC genomic DNA has been tested contain one *mecA* target per genome, and that this assumption retains fidelity across the dynamic range analysed in these experiments. The ability to determine which species is carrying resistance at the lowest end of the dynamic range could support the application of this model where sensitive quantification may be required in instances of low bacterial load.

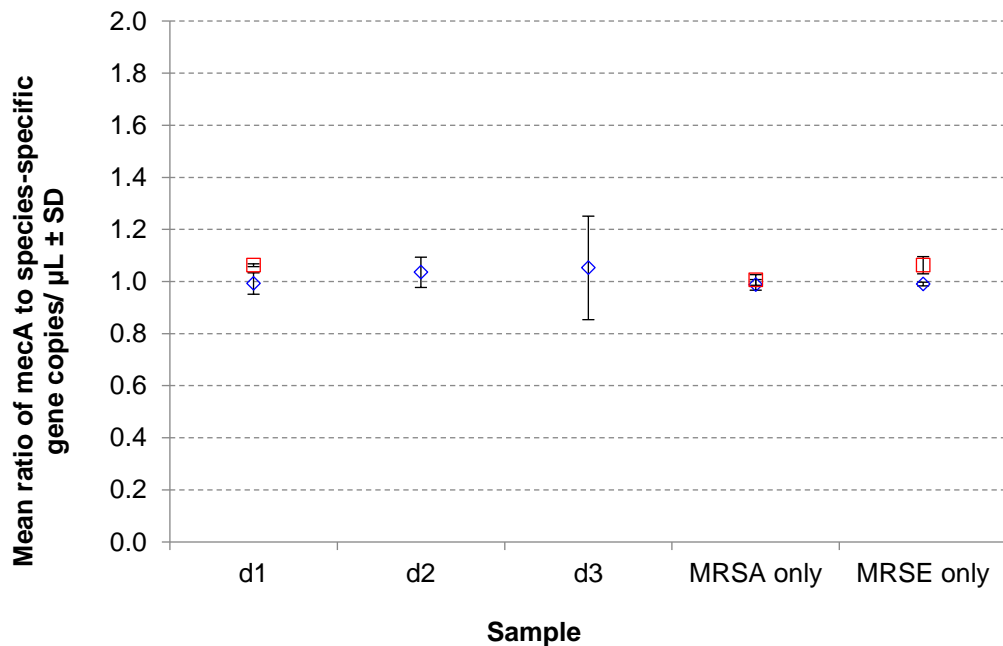
Figure 5.2: Dynamic range for MRSA and MRSE expressed as *mecA* versus species-specific gene (*coA* for MRSA, *femA* for MRSE). The dashed line represents equivalence.



5.3.1.3. Application of assays to genomic DNA admixtures

Dilutions of 1:1 copy number ratio ad-mixtures of MRSA and MRSE ATCC genomic DNA (based on measurement of the stock copy numbers using Qubit, Section 5.2.4.2) were analysed in duplex by dPCR using the QX200 platform, and subsequently in triplex using the Naica System™ for Crystal Digital™ PCR (Stilla Technologies). The copy numbers for *mecA* were compared with the summed copy numbers for *coA* and *femA* in samples d1, d2 and d3. Figure 5.3 demonstrates that the ratio of *mecA* copies per μL to the summed *femA* and *coA* copies per μL for dilution 1 (d1) was 1.0 (QX200) and 1.1 (Naica).

Figure 5.3: Mean ratio of *mecA* copies per μL relative to the species-specific gene targets (*coA* and *femA* for MRSA and MRSE, respectively) measured using the QX200™ (blue markers) and Naica™ (red markers) dPCR platforms. For samples d1, d2 and d3, copy numbers for *mecA* were compared to the summed copy numbers for *coA* and *femA*. For the MRSA and MRSE only controls, *mecA* copy numbers were compared directly to *coA* or *femA*, respectively. The expected ratio in all cases is 1.0.



The ratios for d2 and d3 (10- and 100-fold dilutions from d1) were 1.0 and 0.9, respectively. These latter two dilutions were not analysed on the Naica platform. These data suggest that the dPCR approach can be applied to mixtures of methicillin resistant *Staphylococcus* species to demonstrate the 1:1 copy number hypothesis, which is repeatable across different dPCR

platforms. Standard deviation was higher at lower copy numbers (d3), as expected where increased measurement uncertainty is observed in dPCR quantification at low level.

To challenge the 1:1 copy number hypothesis further, a dilution series of MRSA ATCC genomic DNA was constructed in a background of MSSA and MSSE genomic DNA and analysed using the QX200 platform. The experiment demonstrated proof-of-principle for quantifying *mecA* in a background of methicillin-sensitive organisms, which could be representative of clinical scenarios involving co-colonisation of methicillin resistant and sensitive *Staphylococcus* spp.

Figure 5.4: dPCR quantification of *mecA* where MRSA is present alongside (a) MSSA and (b) MSSE. *mecA* copies per μL correlates with % MRSA relative to a constant copy number concentration (200 copies per μL) of methicillin sensitive population.

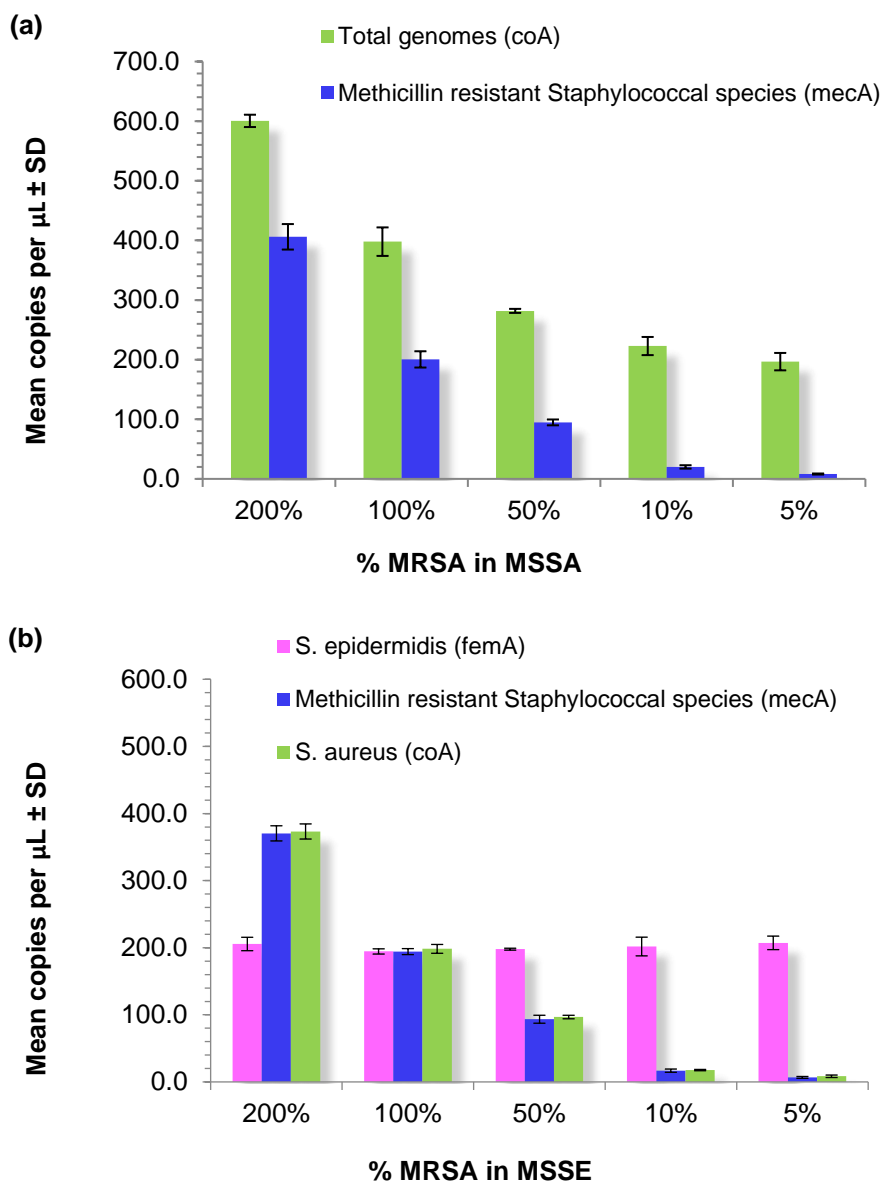


Table 5.4: Mean copies per μL for each dilution point depicted in Figure 5.4. The observed % abundances based on the copy number ratios for each of the assays correlate strongly with the expected values.

Nominal abundance MRSA in methicillin sensitive species (%)	MRSA in MSSA				MRSA in MSSE			
	Total genomes (<i>coA</i> copies per μL)	<i>mecA</i> copies per μL	MSSA (<i>coA</i> copies per μL)	Observed abundance MRSA in MSSA (%)	<i>mecA</i> copies per μL	<i>coA</i> copies per μL	<i>femA</i> copies per μL	Observed abundance MRSA in MSSE (%)
200	600.5	406.0	194.5	209	370.4	373.2	205.6	180
100	397.9	200.4	197.5	101	194.2	198.3	194.5	100
50	281.8	94.7	187.0	51	93.4	96.7	197.9	47
10	222.8	20.1	202.8	10	16.8	17.6	201.8	8
5	196.6	8.2	188.5	4	6.7	8.4	207.3	3

Figure 5.4a shows decreasing concentrations of *mecA* gene target (associated with methicillin resistance), alongside decreasing concentrations of *coA* gene target (associated with *S. aureus*). By comparing the copy numbers of *mecA* and *coA*, and assuming that each MRSA genome contains one *mecA* gene, the *coA* copy numbers arising from both the MRSA and MSSA populations were calculated. Table 5.4 shows how the % abundance of MRSA in a background of MSSA was estimated; the observed values correlated strongly with the expected values. The same principles were applied for estimating abundance of MRSA in a background of MSSE (Figure 5.4b). Calculating % abundance of MRSA in this case was more simplistic since the background species is both methicillin sensitive and involving a different gene target. Once again, the observed values for % abundance MRSA in MSSE correlated strongly with the expected values. These data demonstrate the dPCR duplex approach to be fit-for-purpose for quantifying *mecA* as a marker for methicillin resistance in MRSA when the organism was present alongside other genomes, using genomic DNA.

5.3.1.4. *Optimisation of DNA extraction*

A method comparison was performed to establish the optimal approach for extraction of genomic DNA from *S. aureus* organism. Variability in DNA extraction efficiency can impact upon downstream molecular applications (McOrist *et al.*, 2002). Three commercial kits were selected, and DNA was extracted from units of lyophilised MSSA. This organism was chosen since the *coA* species-specific assay was the most established at the time of the experiments. The *coA* assay was applied to the extracts for dPCR analysis of DNA yield, and Qubit fluorometric quantification was performed as an orthogonal approach.

Figure 5.5: DNA extraction was performed on lyophilised MSSA organisms using three commercial kits. DNA yields expressed as *coA* copy number per μL were compared using dPCR and Qubit. Plotted results are based on triplicate technical measurements performed on three extraction replicates, obtained across triplicate experiments (3 extracts per day). The dashed line represents the expected copies per μL based on CFU estimates performed during material preparation (1 genomic copy = 1 CFU) (EURAMET, 2019).

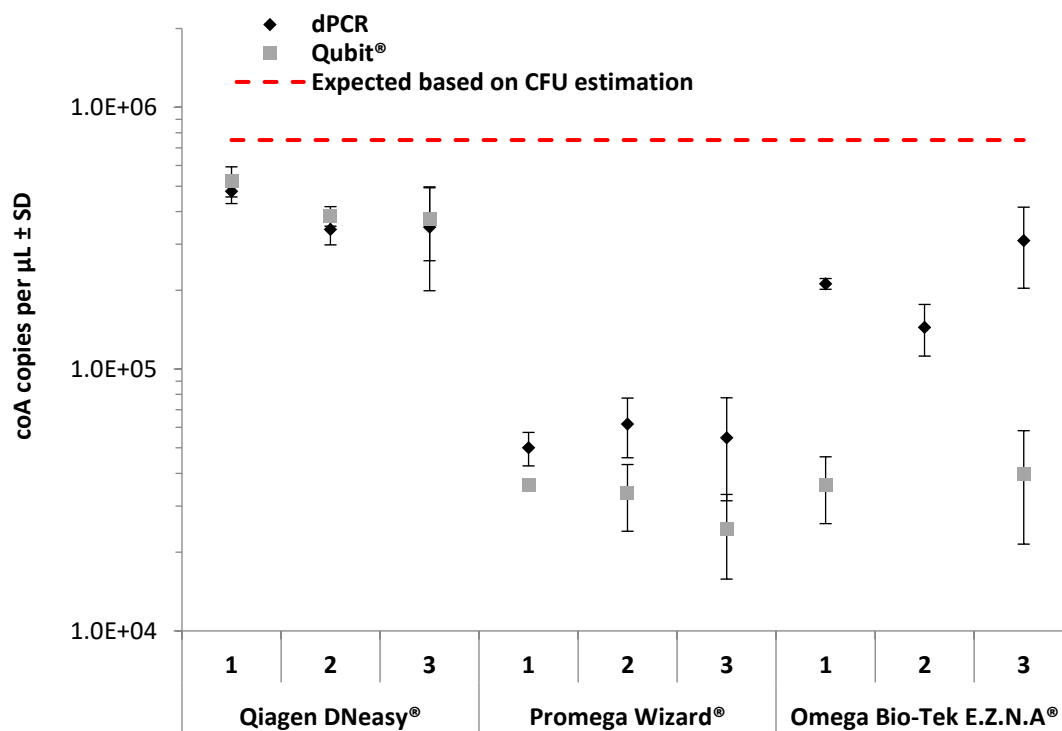


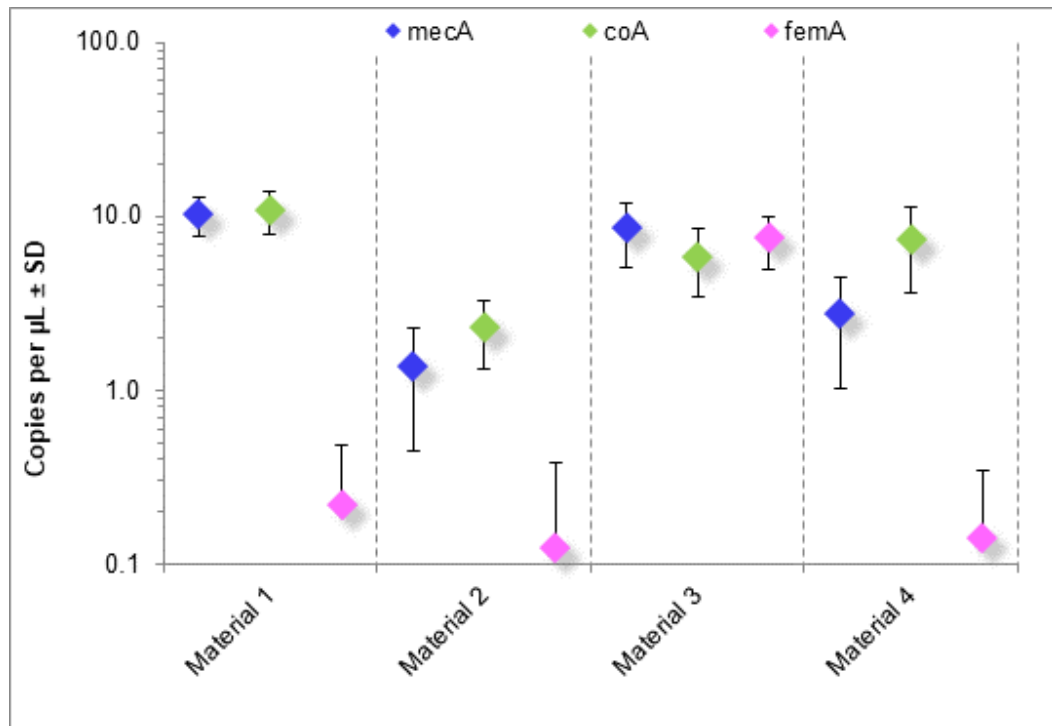
Figure 5.5 shows that the Qiagen DNeasy approach gave the greatest DNA yield when analysed using both dPCR and Qubit, and that estimated *coA* copies per μL were close to the expected value based on CFU estimation. The Promega Wizard approach yielded the lowest *coA* copy numbers by dPCR, but the Omega E.Z.N.A kit demonstrated greater variability between dPCR and Qubit estimates of DNA yield. The intra-laboratory precision across all extraction replicates across three days for each method was: Qiagen (CV 27%), Promega (CV 28%), Omega (CV 41%). dPCR precision within-extract (three replicates per sample per dPCR experiment) for the three methods was never greater than 8%, highlighting how the DNA extraction step introduced variability to quantitative estimates. Based on these data the Qiagen kit was chosen as the optimal method which yielded the greatest quantity of DNA and offered the best precision compared to the other kits. For each extraction approach, an enzymatic lysis step was performed which included incubation with lysozyme. This helps to disrupt the peptidoglycan cell wall present in

Gram-positive bacteria, enabling more effective isolation of DNA (Gill *et al.*, 2016). Different input concentrations of enzyme are stipulated for each kit, which could be a factor contributing to the differences in yield observed between the three methods.

5.3.2. Intra-laboratory analysis of whole bacterial cell materials

The optimised DNA extraction protocol (Qiagen DNeasy) and verified duplex dPCR workflows were applied to units of whole bacterial cell materials to evaluate the approach for analysis of more complex matrices. The units, which represent candidate reference materials that could be used to calibrate qPCR, contained varying quantities of methicillin resistant and sensitive organisms. The suite of materials also included mixtures of these. DNA was extracted from multiple units on three separate days and dPCR performed using the *mecA/coA* and *mecA/femA* assay duplexes.

Figure 5.6: dPCR quantification of methicillin resistance (*mecA*), *S. aureus* (*coA*) and *S. epidermidis* (*femA*) in the four test materials. The materials were identified as a high (Material 1) and a low (Material 2) concentration MRSA, MRSE in a background of MSSA (Material 3), and MRSA in MSSA (Material 4) by comparing the copy number ratios for each gene target. Materials 3 and 4 represent more challenging mixtures that could be representative of clinical scenarios involving co-colonisation of organisms.



The materials were identified as a high (Material 1) and a low (Material 2) concentration MRSA, MRSE in a background of MSSA (Material 3), and MRSA in MSSA (Material 4) by comparing the copy number ratios for each gene target (Figure 5.6). Materials 3 and 4 were more challenging mixtures representative of possible clinical scenarios involving co-colonisation of organisms.

Mean reported copy numbers ranged from ~1.4 to ~10.8 copies per µL across all units and assays. The %CV values ranged from 26-67% which corresponded to *mecA* copy numbers in Material 1 and Material 2, respectively. This shows an increasing trend from the variability exhibited by this extraction kit in Figure 5.5 and supports the observation that, when applied to more complex matrices incorporating DNA extraction into the workflow, increasing variability may be observed in dPCR quantitative estimates. This was more pronounced for the materials that contained lower concentrations of *Staphylococcus* genomic DNA. Reduced precision could impact upon the performance of the approach when attempting to compare copy number ratios to determine which species is exhibiting methicillin resistance. In addition, copy numbers of *femA* that were below the suggested sensitivity of the assays (1.0 to 2.0 copies per µL, Section 5.3.1.2)

were detected in Materials 1, 2 and 4 throughout the experiments indicating the presence of *S. epidermidis*. The detection of this organism was unexpected in these particular materials, and the reason for its presence is unclear. Potential contamination with skin flora may have occurred in the preparation of the materials, which is feasible since *S. epidermidis* contributes to normal skin flora (Widerström, 2016). It could also represent cross-contamination between materials, highlighting the importance of good laboratory practices to prevent spurious contamination.

5.3.3. Inter-laboratory study of method reproducibility

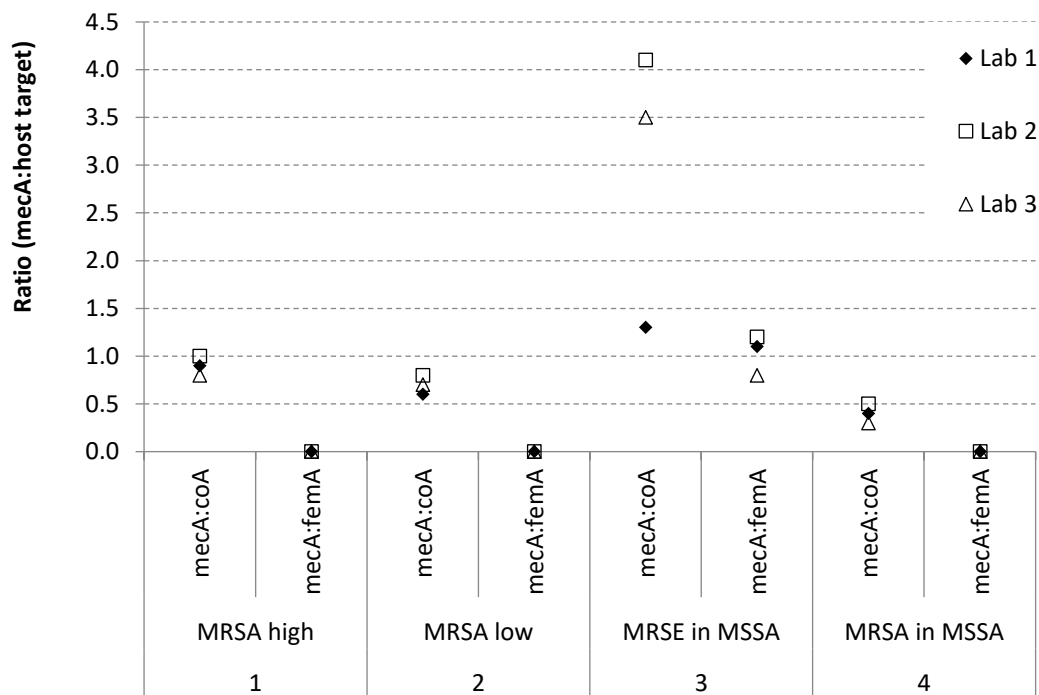
The candidate reference materials described Section 5.3.2 were incorporated into an inter-laboratory comparison to assess the reproducibility of the DNA extraction and dPCR approach. The results of such studies could further support the use of dPCR for development of candidate reference materials and international standards for quantification of MRSA genomes. Inter-laboratory approaches involving dPCR have previously been described and used to validate primary reference methods for quantification of cancer biomarkers (Whale *et al.*, 2017), and used to support commercial methods for quantitative diagnosis of Tuberculosis (Devonshire *et al.*, 2016a).

The work presented in this chapter demonstrates that the dPCR assays performed well when using genomic DNA materials to determine the ratio of *mecA* to host genomic targets, and that good measurement precision was observed. However, measurement precision declines when DNA extraction is introduced into the workflow for analysis of more complex matrices and is further reduced between different laboratories. Table 5.5 shows that laboratory 2 consistently reported the highest copy numbers, and laboratory 3 the lowest with laboratory 1 as the intermediate. Laboratory 1 reported the highest overall measurement uncertainty, and laboratory 2 the lowest. Calculated uncertainties account for triplicate extraction units replicated in each dPCR experiment. Further work should aim to establish the cause of variability in copy number observed between the three laboratories, including the DNA extraction step. Efforts to standardise the extraction step between laboratories could help to develop the approach for value assignment of reference materials for quantification of methicillin resistance in staphylococci.

Table 5.5: Copies per μL reported from three laboratories obtained for four different materials. Each value represents the concentration obtained from the extraction of three different units of each material across three different days and triplicate reactions analysed using dPCR. Relative standard uncertainties are shown expressed as a percentage. N/A: not applicable, LOQ: limit of quantification, n.d.: not detected (EURAMET, 2019).

Material	Duplex	Target	Mean concentration of target (copies per μL) reported by Laboratory					
			Lab 1	Uncertainty (%)	Lab 2	Uncertainty (%)	Lab 3	Uncertainty (%)
(1) MRSA high	1	<i>mecA</i>	10.20	12	21.17	7	6.16	11
		<i>femA_SE</i>	<LOQ	N/A	<LOQ	N/A	n.d.	N/A
	2	<i>mecA</i>	10.08	13	21.37	8	5.90	13
		<i>coA</i>	11.61	8	21.64	8	7.20	11
(2) MRSA low	1	<i>mecA</i>	1.42	19	2.48	1	1.02	6
		<i>femA_SE</i>	<LOQ	N/A	<LOQ	N/A	n.d.	N/A
	2	<i>mecA</i>	1.37	22	2.51	1	0.96	7
		<i>coA</i>	2.26	20	3.05	1	1.38	9
(3) MRSE in MSSA	1	<i>mecA</i>	8.13	30	29.43	13	4.28	16
		<i>femA_SE</i>	7.23	25	24.72	11	5.04	14
	2	<i>mecA</i>	7.87	28	28.51	13	4.28	16
		<i>coA</i>	5.92	25	7.00	3	1.22	12
(4) MRSA in MSSA	1	<i>mecA</i>	2.78	34	5.88	1	1.09	7
		<i>femA_SE</i>	<LOQ	N/A	<LOQ	N/A	0.52	6
	2	<i>mecA</i>	2.57	34	5.76	2	1.16	8
		<i>coA</i>	7.15	33	12.66	3	4.13	11

Figure 5.7: Ratio of *mecA* to species-specific (host) gene targets for the four materials for each of the laboratories

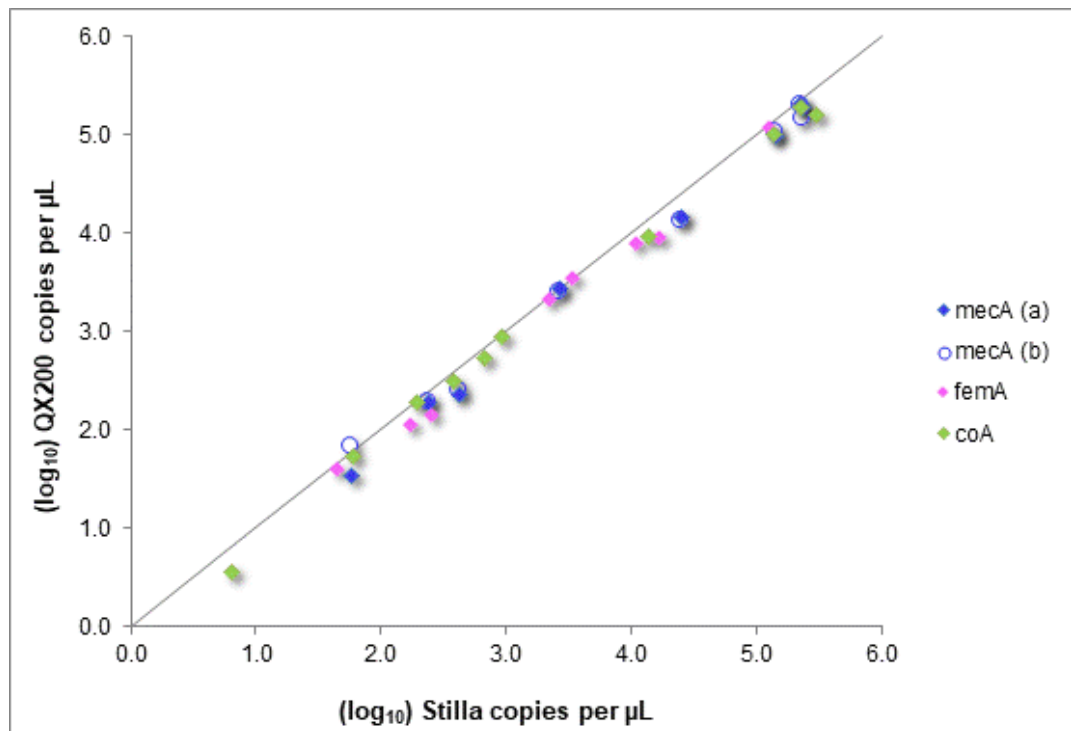


To test the 1:1 copy number ratio model, the respective ratios of *mecA* to host genomic targets were calculated for each of the materials and labs. Figure 5.7 shows that, for the high MRSA Material 1, copy number ratios were between 0.8 and 1.0 for the three labs. However, in comparison Material 2 (low MRSA) copy number ratios were between 0.6 and 0.8. This was similar to Material 4 (MRSA in MSSA), where copy number ratios were between 0.3 and 0.5. These findings could highlight potential limitations of the model when applied to low copy number materials, especially those that contain mixtures of sensitive and resistant organisms. Material 3, a mixture of MRSE in a background of MSSA, proved to be more complicated with high variability in copy number ratios between the three labs (1.3 – 4.1 for *mecA:coA*). The *mecA:femA* copy number ratio range was 0.8 to 1.2, which better aligns with the 1:1 model. dPCR holds a potential role in value assignment of candidate reference materials for quantification of methicillin resistance in *Staphylococcus* spp. However, further work is required to evaluate the reliability of the approach presented here for determining which species is carrying resistance by comparing *mecA* copy numbers relative to host genomic targets, particularly at low copy numbers in complex whole cell materials requiring DNA extraction.

5.3.4. Analysis of clinical isolates

An additional aim in this chapter was to evaluate the role for dPCR in direct quantification of methicillin resistant organisms in clinical samples. The dPCR approach was applied to a cohort of residual DNA extracts from samples that had previously been analysed by qPCR at Great Ormond Street Hospital for Children NHS Foundation Trust. The samples were analysed using the QX200 and Naica dPCR platforms. Figure 5.8 shows that the \log_{10} transformed copy numbers for the extracts measured using the *mecA*, *femA* and *coA* assays were well correlated between the two platforms ($r=1$ for all assays). Agreement between methods was investigated using a Bland-Altman analysis (Appendix 4) and found to agree between the two platforms with 95% confidence.

Figure 5.8: \log_{10} transformed copy number concentrations for the 22 clinical isolates analysed using the Bio-Rad QX200 and Stilla Naica dPCR platforms. Note that *mecA* (a) and *mecA* (b) refer to the value returned for *mecA* when measured in duplex with *coA* and *femA*, respectively, using the QX200. The assay targets were analysed in triplex using the Naica platform, so a single value is plotted for *mecA*.



The dPCR copy numbers for each of the assay targets are presented in Table 5.6. In some cases, copy numbers were reported for the three assay targets that were around the proposed limits of detection of the assays (1.0 to 2.0 copies per µL). dPCR is capable of detecting single molecules of nucleic acid. However, the existence of partitions exhibiting fluorescent signal that are difficult

to classify as positive or negative are often described for dPCR (Quan *et al.*, 2018). These may be referred to as ‘false positives’ and may be the result of poor assay design, spurious amplification or adventitious contamination. It is unclear whether the low copy targets in this study represented true positives, or adventitious contamination as discussed above. Owing to this and the fact that a formal LOD was not established for the assays, any samples returning values below 2 copies per μL were deemed to be ‘not quantified’ and were not plotted in Figure 5.8.

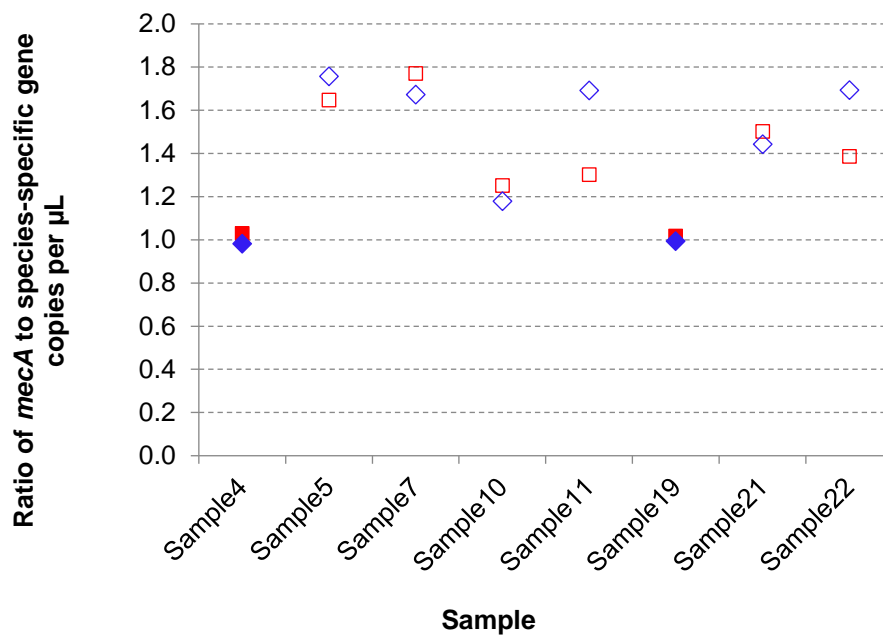
Table 5.6: Analysis of clinical isolates on the Naica and QX200 dPCR platforms. Assays were applied in triplex (all three assays in one reaction) and duplex (two in one reaction) on the respective platforms.

Sample	Naica (copies per μL)			QX200 (copies per μL)			
	<i>mecA</i>	<i>femA</i>	<i>coA</i>	<i>mecA</i>	<i>femA</i>	<i>mecA</i>	<i>coA</i>
Sample1	0.0	0.0	0.0	0.0	0.0	0.0	0.0
Sample4	140802.1	1.9	136986.5	104898.1	0.0	96981.2	98787.8
Sample5	422.7	256.6	0.8	253.9	144.5	232.7	0.0
Sample6	0.7	0.0	0.4	0.0	0.0	0.9	0.4
Sample7	226007.1	127631.6	0.0	198973.0	118974.1	207232.4	0.0
Sample8	1.2	0.0	196.8	0.0	0.0	0.0	190.4
Sample9	0.0	1.2	0.4	0.0	0.0	0.0	1.6
Sample10	2727.3	2177.8	0.0	2532.8	2149.3	2771.0	0.0
Sample11	58.8	45.2	0.0	69.2	40.9	33.9	0.0
Sample12	0.3	0.6	61.2	0.0	0.0	0.0	54.7
Sample13	0.0	0.3	663.8	0.0	0.0	0.0	540.2
Sample14	0.0	0.0	297876.0	0.0	0.0	0.0	156214.3
Sample15	0.0	1.0	376.6	0.0	0.0	0.0	317.6
Sample16	0.0	1.8	13945.1	0.0	0.0	0.0	9186.8
Sample17	0.0	10761.7	0.0	0.0	7774.6	0.0	0.0
Sample18	0.0	0.0	931.1	0.0	0.0	0.0	876.5
Sample19	231212.3	0.0	227279.7	146711.3	0.0	188917.5	190206.4
Sample21	25288.7	16839.4	0.0	13038.9	9035.4	14415.9	0.0
Sample22	237.3	171.2	0.3	190.2	112.3	188.5	0.0
Sample23	0.0	0.0	6.4	0.0	0.0	0.0	3.6
Sample24	0.0	0.0	0.0	0.0	0.0	0.3	0.0
Sample25	0.0	3354.9	0.0	0.0	3556.6	0.0	0.0

Lower than expected copy numbers of *femA* relative to *mecA* were calculated for the 6 MRSE samples (56-80% of the *mecA* copy number for the Naica system, 57-85% of the *mecA* copy number for the QX200). MRSE ATCC genomic DNA, which was included as a positive control for both platforms, exhibited the expected ratio of *femA* to *mecA* copy numbers (~1:1). The ratios

between *mecA* and *coA/femA* correlated between the two platforms ($r = 0.82$). The ratios are plotted in Figure 5.9. *mecA:coA* ratios for MRSA samples were 1.0 when analysed on both platforms.

Figure 5.9: Ratios between *mecA* and *coA/femA* for samples identified as MRSA and MRSE. QX200 (blue markers), Naica (red markers). Filled markers represent MRSA, unfilled represent MRSE. Expected ratio of *mecA* to host genomic targets is 1.0.



The reasons for the observed *mecA:femA* ratios may include: 1) a heterogeneous population of *S. epidermidis* present in the samples, some of which may not contain the primer or probe sequences used in this study. Assay specificity was tested *in silico*, although this does not rule out potential sequence mismatches in the samples. Multilocus sequence typing (MLST) illustrates that a considerable degree of diversity exists for this organism which has been described previously (Jamaluddin *et al.*, 2008, Du *et al.*, 2013, Jolley *et al.*, 2018). Further work to investigate a potential mismatch could include sequencing of the *femA* gene in this cohort of samples. Of note, although digital PCR has been demonstrated to have relative insensitivity to primer-probe mismatches compared to other techniques such as qPCR, a reduction in quantitative estimates has still been observed for dPCR analysis of HIV-1 DNA (Strain *et al.*, 2013) and hepatitis A virus (Persson *et al.*, 2019) where mismatches exist. 2) Presence of additional *mecA* cassette(s). *S. epidermidis* has been reported to act as reservoir for and can transfer *mecA* to *S. aureus* (Najar-

Peerayeh *et al.*, 2014), however there is limited evidence as to whether the organism can harbour more than one *mecA* gene at once. 3) The presence of other methicillin resistant coagulase-negative staphylococci (MRCoNs), which could be investigated through culture, MALDI-TOF MS or using PCR.

5.3.4.1. Comparison of dPCR and qPCR results

Absolute quantification of the three gene targets by dPCR enabled the samples to be identified as MRSA (n=2), MRSE (n=6), MSSA (n=8) and MSSE (n=2). Four of the samples were classified as not quantified (NQ). Table 5.7 shows a comparison of the qPCR findings and the dPCR interpretation based on the copy numbers presented in Table 5.6.

Table 5.7: Comparison of qPCR and dPCR interpretations following analysis of 22 residual DNA extracts from clinical samples. qPCR data were obtained as part of the routine diagnostic service provided by the Department of Microbiology at Great Ormond Street Hospital for Children NHS Foundation Trust. NQ – not quantified, which was defined when copy number was < 2 cp/μL. ND – not done.

Sample	16S broad-range PCR	<i>S. aureus</i> PCR	<i>mecA</i> PCR	dPCR interpretation	Comment
Sample1	<i>Staphylococcus capitis</i>	ND	ND	Negative/NQ	qPCR & dPCR agree
Sample4	ND	+	+	MRSA	qPCR & dPCR agree
Sample5	<i>S. epidermidis</i>	ND	ND	MRSE	<i>mecA</i> detected by dPCR
Sample6	ND	+	+	Negative/NQ	
Sample7	<i>S. epidermidis</i>	ND	ND	MRSE	<i>mecA</i> detected by dPCR
Sample8	ND	+	-	MSSA	qPCR & dPCR agree
Sample9	ND	+	-	Negative/NQ	
Sample10	<i>S. epidermidis</i>	ND	ND	MRSE	<i>mecA</i> detected by dPCR
Sample11	<i>S. epidermidis</i>	ND	ND	MRSE	<i>mecA</i> detected by dPCR
Sample12	ND	+	-	MSSA	qPCR & dPCR agree
Sample13	ND	+	-	MSSA	qPCR & dPCR agree
Sample14	ND	+	+	MSSA	Discrepant
Sample15	ND	+	-	MSSA	qPCR & dPCR agree
Sample16	ND	+	-	MSSA	qPCR & dPCR agree
Sample17	<i>S. epidermidis</i>	ND	ND	MSSE	qPCR & dPCR agree
Sample18	ND	+	-	MSSA	qPCR & dPCR agree
Sample19	ND	+	+	MRSA	qPCR & dPCR agree
Sample21	<i>S. epidermidis</i> ; <i>Staphylococcus hominis</i>	ND	ND	MRSE	<i>mecA</i> detected by dPCR
Sample22	<i>S. epidermidis</i>	ND	ND	MRSE	<i>mecA</i> detected by dPCR
Sample23	ND	+	-	MSSA	qPCR & dPCR agree
Sample24	<i>S. epidermidis</i>	ND	ND	Negative/NQ	
Sample25	<i>S. epidermidis</i>	ND	ND	MSSE	qPCR & dPCR agree

Sample 1 was determined to be *S. capitis* which was not assayed for by dPCR. Sample 14 was identified by qPCR as MRSA, but by dPCR as MSSA. It was deemed that this could be due to a labelling error, and the sample is pending return to GOSH for re-analysis by qPCR. Out of the four samples that were classified as negative/NQ by dPCR, two (Samples 6 and 9) returned a positive qPCR result. In addition, Sample 24 was defined as *S. epidermidis* by qPCR but may also represent a low concentration sample which returned a 'negative/NQ' result by dPCR. As discussed in Section 5.3.4, a dPCR 'negative/NQ' result was determined based on the proposed sensitivity of the assays, although a more thorough investigation is required to formally establish LOD. Furthermore, qPCR may be benefitting from enhanced sensitivity in this scenario owing to the larger volume of sample that was used for analysis (10 µL compared to up to 5 µL for dPCR). Some samples were revealed by dPCR as being MRSE, whereas the qPCR interpretation was MSSE as the samples were not tested for *mecA*. Hospital schemes such as CQUIN (Public Health England, 2019) are implemented for reducing nosocomial cases of MRSA colonisation, and so detection of this species could likely be prioritised over methicillin resistant CoNS during clinical testing. This may explain why testing MSSE samples for the *mecA* target was 'not done' by qPCR.

5.3.4.2. Co-colonisation of *S. aureus* with CoNS

The role of dPCR in quantification of MRSA DNA has been explored previously (Kelley *et al.*, 2013, Luo *et al.*, 2017), however it is yet to be implemented into clinical workflows. Analysis of residual clinical extracts demonstrates how the dPCR approach described in this chapter could be applied in the clinical diagnosis of infections with methicillin resistant *Staphylococcus* spp. Multiplex dPCR approaches such as that offered by the Naica platform could enable detection of several gene targets in a single reaction, which could save on time, reagents and cost by streamlining current workflows. Furthermore, the approach could be applied to resolve cases where co-colonisation of methicillin sensitive and resistant organisms is suspected.

dPCR analysis provided absolute quantitative values which could be used to determine which *Staphylococcus* species is exhibiting resistance. Detection of methicillin resistance in CoNS such *S. epidermidis* could be important as this organism can act as a carrier of the *mecA* cassette and transfer to *S. aureus* and other species. Evidence exists suggesting that MRSA can co-colonise with MSSA and CoNS (Shaw *et al.*, 2013). Although no mixtures of resistant and sensitive staphylococci were identified in the cohort of residual clinical extracts, the data presented in this

chapter infer the potential for the dPCR method in the analysis of mixed clinical samples. Further work could involve analysis of a broader cohort of isolates derived from primary clinical samples (i.e. nasal swabs) to determine the prevalence of mixed staphylococcal infections, and to establish whether dPCR can assist in resolving complex scenarios where genetic elements conferring drug resistance have the potential to be transferred between organisms. This could potentially reduce the time to diagnosis of infections with methicillin resistant staphylococci.

5.4. Conclusions

In this chapter, the utility of quantifying methicillin resistance in MRSA and other Staphylococcal species was assessed. A digital PCR (dPCR) approach, which can enable precise DNA quantification in the absence of a standard curve, was developed. dPCR showed promise for value assigning candidate reference materials that could be used to support qPCR detection of MRSA. However, limitations associated with DNA extraction efficiency were found to potentially inflate measurement error associated with the use of whole bacterial cell materials. The dPCR approach was comparable with qPCR for detecting methicillin resistant species in clinical extracts. dPCR offered simplicity over the qPCR approach for precise quantification of multiple gene targets at once. This chapter demonstrates that quantification of MRSA, and other organisms that can carry methicillin resistance, can be achieved by comparing the ratios of *mecA* copies to genomic targets. This approach could be applied to better understand the dynamics of infection with these pathogens. Accurate quantification of these species could be a useful tool for monitoring bacterial load in response to treatment and predicting disease severity. This could represent an overall benefit to patient management and healthcare costs by streamlining current workflows, improving infection control strategies and reducing further transmission of MRSA.

6. Characterising sources of experimental variability in MALDI-TOF MS strain typing and evaluating applicability of the technique to resolving nosocomial outbreaks

6.1. Introduction

6.1.1. Nosocomial transmission of bacterial infections

Nosocomial transmission, colonisation and subsequent infection with organisms that can exhibit drug resistance poses a significant threat to global public health. This is of particular significance for hospitalised patients, including those within Intensive Care Units (ICU), on oncology wards and those that are immunocompromised (Haque *et al.*, 2018). Organisms including *Acinetobacter baumannii*, *Pseudomonas aeruginosa* and *Enterobacteriaceae* that develop resistance to carbapenem antibiotics are of critical concern for global health (World Health Organization, 2017a). Carbapenems are a class of β -lactam antibiotic that possess a broad spectrum of activity against pathogenic organisms, and are often reserved as a 'last-line' antibiotic (Papp-Wallace *et al.*, 2011). Carbapenem resistant organisms (CROs) acquire the means to produce carbapenemase enzymes that break down the antibiotics, rendering them ineffective. Resistance is often acquired through horizontal gene transfer of mobile genetic elements (Pagano *et al.*, 2016). Resistant organisms can transfer these mobile elements to otherwise susceptible organisms, propagating multi-drug resistance throughout the hospital setting. CROs, along with drug-resistant Gram-positive bacteria such as *Staphylococcus aureus*, are responsible for an increasing number of difficult-to-treat respiratory tract, soft tissue and bloodstream infections (Dryden *et al.*, 2015). Risk factors for becoming colonised by these organisms, which could result in bacteraemia, include length of hospital stay, ICU admission, having an intravenous catheter or ventriculoperitoneal (VP) shunt, having surgery or having a ventilator fitted (Baran *et al.*, 2008, Blanco *et al.*, 2017, Graffunder and Venezia, 2002, Chi *et al.*, 2012). Minimising transmission of these organisms amongst vulnerable patient cohorts undergoing long hospital stays is crucial. The availability of reliable methods for determining transmission routes and tracing outbreaks can help to improve infection control strategies, streamline antimicrobial therapy and reduce patient morbidity.

6.1.2. Molecular strain typing of bacteria

Molecular strain typing enables organisms isolated from patients to be compared in terms of transmission route, timeline and geographic location to ascertain whether there is a common ancestor or point of origin (Dijkshoorn *et al.*, 2000). The ability to strain type bacteria associated with nosocomial acquisition and infection enables routes of transmission to be traced, outbreaks to be monitored and the effectiveness of control measures to be evaluated (Ranjbar *et al.*, 2014). Molecular typing analyses are usually performed by a specialist reference laboratory using genomic techniques including pulsed-field gel electrophoresis (PFGE), multiple locus variable number of tandem repeat analysis (MLVA) and multi locus sequence typing (MLST) (Pourcel *et al.*, 2011, Oberle *et al.*, 2016, Singhal *et al.*, 2015, Adzitey *et al.*, 2013, Salipante *et al.*, 2015). As discussed in Section 1.2.3.5, laboratories have also taken on whole genome sequencing (WGS) as a reference method for strain typing in recent years. WGS can provide a broad analysis, offering information on drug resistance and a full spectrum of genes, facilitating better resolution between strains of bacteria. However, access to the method for some laboratories remains largely limited by cost.

Limitations exist for other strain typing approaches, despite the methods being well established. Protocols described for PFGE can take up to 4 days to complete, which could increase the time taken to receive results to infer or rule out an outbreak (Sharma-Kuinkel *et al.*, 2016). In addition, disharmony between approaches could limit comparability of typing results between strains, hospitals, and geographical locations. For example, two MLST schemes exist for strain typing of *A. baumannii*, referred to as the 'Oxford' (Bartual *et al.*, 2005) and 'Pasteur' (Diancourt *et al.*, 2010) schemes. Issues with these schemes have been identified including inconsistencies in which genes are sampled for typing, limited use of the bacterial chromosome and discrepant primer sequences (Hamidian *et al.*, 2017). The two schemes have been found to yield different strain typing results at an international level (Tomaschek *et al.*, 2016). Interest has grown in repurposing techniques that are already well established within clinical microbiology laboratories for strain typing organisms from a range of species. Implementation of these approaches using standardised workflows could yield typing results that are reproducible between centres, and could save time and resources.

6.1.3. Matrix Assisted Laser Desorption/Ionisation-Time of Flight Mass Spectrometry (MALDI-TOF MS) as a method for strain typing

Matrix-assisted laser desorption/ionisation time-of-flight mass spectrometry (MALDI-TOF MS) has revolutionised identification of bacterial species within the last decade (Singhal *et al.*, 2015, van Belkum *et al.*, 2017, Parchen and de Valk, 2019), and is widely adopted within diagnostic microbiology laboratories. In addition, the technique shows promise for molecular strain typing of bacteria and has been successfully implemented to resolve nosocomial and foodborne outbreak-associated bacterial strains (Christner *et al.*, 2014, Barbuddhe *et al.*, 2008, Stephan *et al.*, 2011, Egli *et al.*, 2015, Steensels *et al.*, 2017, Mencacci *et al.*, 2013). The possession of existing MALDI-TOF capabilities by most diagnostic microbiology laboratories presents an opportunity for in-house epidemiological analysis. However, there is limited evidence supporting the robustness of MALDI-TOF MS in this context, and conflicting evidence exists suggesting that MALDI-TOF MS is unreliable and unsuitable for strain typing some species (Ghebremedhin *et al.*, 2017, Sousa *et al.*, 2015, Rim *et al.*, 2015).

Numerous experimental factors are known to affect the performance of MALDI-TOF MS including upstream sample preparation, data acquisition and analysis (Williams *et al.*, 2003). MALDI-TOF MS has been criticised as a method for routine strain typing as being limited by poor reproducibility (Albrethsen, 2007), insufficient discriminatory power (Lasch *et al.*, 2014) and limited guidance for data interpretation (Spinali *et al.*, 2015). Investigation into the sources of experimental variability and better characterisation of measurement bias in MALDI-TOF MS protocols could help to demonstrate that the method is reliable for strain typing bacteria. This in turn could facilitate adoption of the technique as an in-house method for bacterial strain typing and outbreak surveillance. Laboratories with in-house capability could more rapidly obtain typing data that could influence clinical decisions, such as isolating high-risk patients, reviewing infection control procedures or altering treatment regimens.

In this chapter, the experimental robustness of MALDI-TOF MS for bacterial typing was explored by evaluating numerous stages in the protocol that can introduce variability and influence a typing result. Demonstrating sufficient data reproducibility could facilitate adoption of MALDI-TOF MS strain typing where instrumentation is already present in microbiology laboratories. The MALDI-TOF MS typing method was applied to clinical organisms (*A. baumannii* and *S. aureus*) collected during outbreaks at the Royal Free London NHS Foundation Trust. An outcome of this work was

to evaluate the discriminatory power of MALDI-TOF MS for differentiating between strains within an outbreak in comparison to existing reference methods. MALDI-TOF MS strain typing could provide better discrimination than existing genomic methods, and could be quicker than outsourcing typing to reference laboratories to confirm or rule out hospital outbreaks.

6.2. Materials and methods

6.2.1. Study materials

6.2.1.1. Clinical isolates

Isolates were collected between 2014 and 2015 at the Royal Free London NHS Foundation Trust as part of the routine microbiological diagnostic service. This included 18 isolates of multi drug resistant (MDR) *Acinetobacter baumannii* associated with a multi-ward outbreak, collected from 15 patients. The outbreak was associated with a single surgery ward (ward A) however patients had migrated between 15 wards over the two year period (wards B-L), including an intensive/critical care unit (ICU/CCU) and an outpatient department (OPD). Length of stay on ward A varied between 1 and 184 days. In addition, 8 isolates of methicillin resistant *Staphylococcus aureus* (MRSA) associated with an outbreak in a neonatal unit at the hospital were collected. Antimicrobial susceptibility testing (AST) was implemented for all isolates according to EUCAST breakpoint guidelines as part of routine testing (Brown *et al.*, 2015). AST was performed using a BD Phoenix™ platform (Becton Dickinson, USA) and minimum inhibitory concentrations (MICs) were established using ETEST® AST reagent strips (bioMérieux, France). A clinical isolate of NDM *Klebsiella pneumoniae* was also selected for a comparison of different culture conditions. Species identities of the isolates were confirmed using the MALDI-TOF Microflex (Bruker UK) following the manufacturers protocol. Isolates were assigned a unique study identifier to remove patient information (e.g. MBT16-001) (Appendix 5).

6.2.1.2. Commercial reference strains

Commercially available *Staphylococcus aureus* subsp. *aureus* Rosenbach reference strains (MRSA ATCC® 29213™, MRSA ATCC® 43300™ and MSSA ATCC® 25923™) were obtained, corresponding to ID numbers: MBT16-070, MBT16-071 and MBT16-072, respectively.

6.2.2. Bacterial culture

All isolates were recovered from storage at -80°C onto pre-poured Columbia blood agar (CBA) containing 5% horse blood (ThermoFisher Scientific, USA) and incubated aerobically at 37 °C for 24 hours. Where required, a second passage was performed by streaking a single colony onto

160

fresh pre-poured Colombia blood agar (CBA) containing 5% horse blood (Thermo Fisher Scientific, USA) and incubating at 37°C for a further 24 hours to ensure that a pure culture was obtained. All organisms were stored at -80°C in Cryobank™ tubes (Thermo Scientific, USA) containing cryopreservation medium.

6.2.3. Reference laboratory strain typing of isolates

As part of the routine microbiological service, *A. baumannii* isolates were sent on nutrient agar slopes to Public Health England (PHE, UK) for reference laboratory characterisation. Pulsed-field gel electrophoresis (PFGE) and variable number tandem repeat (VNTR) profiling was performed at four loci (1, 10, 845,3468) (Turton *et al.*, 2009, Pourcel *et al.*, 2011). All 18 isolates were classified as belonging to European clone II lineage OXA-23 clone 1. PFGE data and VNTR profiles are included in Appendix 6. Isolate MBT16-062 was not sent to the reference laboratory but was included in this study for prospective analysis. MALDI-TOF MS strain typing analysis was performed blind to the reference laboratory typing results.

6.2.4. General protocol for formic acid extraction of proteins from bacterial cells

For each isolate being tested, 300 µL of HPLC-grade water was added to a 1.5 ml microcentrifuge tube. Enough single colonies were selected to fill a 1 µL sterile plastic loop (Fisher Scientific, USA), which was transferred to the tube containing the HPLC-grade water. The biomass was emulsified in the water, and homogenous cell suspension produced by gentle mixing. 900 µL absolute ethanol was added to each tube and mixed by vigorous agitation followed by brief vortexing. The tubes were centrifuged for 2 minutes at 13,000 rpm in a microcentrifuge to remove residual ethanol and cell pellets allowed to dry at room temperature. Dried pellets were re-suspended in a 50:50 mixture of 70% aqueous formic and acetonitrile (Honeywell, USA) and thoroughly mixed by pipetting. The volume added was relative to the size of the dried pellet as recommended by the manufacturer. The mixture was vortexed and tubes centrifuge for 2 minutes at 13,000 rpm in a microcentrifuge ready for MALDI-TOF MS analysis.

6.2.5. Spectral acquisition for strain typing using MALDI-TOF MS

Detailed protocols for reagent preparation for MALDI-TOF MS can be found in Section 2.2. Isolates were recovered from -80°C onto pre-poured blood agar and incubated aerobically at 37

°C for 24 hours. Proteins were extracted as described in Section 6.2.4. Strain typing was performed using a MALDI-TOF Microflex LT (Bruker UK) according to the Bruker MALDI Biotyper protocol which has been described elsewhere (Holzknecht *et al.*, 2018). Measurements were obtained using flexControl software (version 3.4). Replicate spots of extracted protein solution were overlaid with 1 µL fresh α -Cyano-4-hydroxycinnamic acid (HCCA) matrix (Bruker UK), allowed to air dry, and each spot measured in triplicate. Spectra were recorded in positive linear mode within the range of 2 and 20 kDa, capturing peak position (m/z) for each protein present and the associated peak intensity value in arbitrary units (a.u.). Peaks with intensity values above the nominal threshold of 500 a.u. were included in the analysis. External calibration of each MALDI typing experiment was through measurement of Bacterial Test Standard (BTS) solution (Bruker UK). Where applicable, Minimum Information About a Proteomics Experiment (MIAPE) criteria for MALDI-TOF MS experiments are described in Appendix 10.

6.2.6. Characterising sources of variability in sample preparation for MALDI-TOF MS typing

6.2.6.1. Variability from culture-subculture cycle

Spectra were obtained from organisms at different stages of the culture-subculture cycle (Section 6.2.2). The stages were as follows:

- (i) Fresh colonies of *K. pneumoniae* were recovered from a new Cryobank™ bead per MALDI-TOF MS experiment, representing one culture cycle of 24 hours duration.
- (ii) Three different agar plates from the same initial bead sub-cultured onto fresh Colombia Blood agar every 24 hours followed by immediate analysis, representing three culture-subculture cycles.
- (iii) A single culture cycle lasting 72 hours, with measurements recorded every 24 hours with no sub-culture.

MALDI-TOF MS spectra were analysed in FlexAnalysis software (Bruker UK); peak positions were visually observed and recorded, including the presence or absence of expected peaks along with peak 'shifts' between 2 and 20 kDa.

6.2.6.2. *Variability from formic acid protein extraction*

6.2.6.2.1. *Preparation of a 0.5 McFarland standard*

MRSA reference strain ATCC® 29213™ was cultured as described in Section 6.2.2. 1-2 colonies were selected from the agar plate and re-suspended in 3 mL glass vial containing 0.9% sterile saline ensuring thorough mixing. The optical density (OD) of the solution was measured using a WPA CO8000 cell density meter (Biochrom Ltd., UK) and the concentration adjusted to give a value of 0.1, which is roughly equivalent to a McFarland 0.5 standard (~10⁸ colony forming units (CFU) per mL) (McFarland, 1907). Colony counting of the suspension was performed by serially diluting to ~10¹ CFU per mL following a previously described approach (Miles *et al.*, 1938).

6.2.6.2.2. *Comparison between two biomass collection and delivery methods*

To prepare the 0.5 McFarland suspension for protein extraction, a 1 mL aliquot of the McFarland solution was pelleted at 13,000 rpm in a microcentrifuge for 3 minutes. The supernatant was removed and 300 µL HPLC grade water added. The extraction protocol was continued as described in Section 6.2.4. A 1 µL filled loop of bacteria (approximately 2-3 colonies per loop) was prepared in parallel and proteins extracted.

6.2.6.2.3. *Varying volumes of extraction reagents*

Varying volumes of 70% formic acid (FA) and acetonitrile (ACN) at a 50:50 ratio were added to each of 0.5 McFarland and the 1 µL-loop cell pellets. 60, 80 or 100 µL total volume of extraction reagent was added to the dried cell pellets following removal of ethanol. The cells pellets were homogenised into suspension and centrifuged. Mass spectra were analysed in FlexAnalysis (Bruker) and m/z peak lists exported for analysis in MS Excel.

6.2.6.3. *Assessing day-to-day stability of the bacterial test standard (BTS)*

BTS was prepared as described in Section 2.2.3. The freshly reconstituted vial contents were spotted five times on a MALDI target plate, allowed to dry, and then overlaid with HCCA. The MALDI Biotyper method was performed for each spot measured in triplicate, and the remaining BTS stored at -20°C. The process was repeated over a total of three days using the same vial of

BTS. Mass peak lists were exported from FlexAnalysis software for analysis in MS Excel. The presence of the expected mass peaks (m/z), along with ionisation efficiency represented by peak intensity (a.u.) was compared across the three days.

6.2.7. Assessing peak intensity at different stages of the typing protocol

The MALDI Biotyper protocol was applied to 18 clinical isolates of *A. baumannii* (Section 6.2.1). The stages of the protocol investigated were defined as (i) technical – where spectra were acquired from individual spots of protein extract in triplicate and treated as distinct datasets (ii) co-crystallisation – separate 1 μ L spots of protein extract deposited on a MALDI target plate in triplicate and overlaid with HCCA matrix and (iii) temporal – the day-to-day variability between experiments, incorporating sub-culture of isolates onto fresh agar. Mass spectra were exported from FlexAnalysis (Bruker UK) for peak matching in BioNumerics 7.6 (Applied Maths, Belgium). Peak profiles were exported for analysis in MS Excel; intensities for each peak class were normalised to the total intensity for each spectra, and a mean, SD and relative standard deviation (rsd) of peak intensity calculated for selected peaks. Following an initial experiment, the protocol was repeated for the same isolates after one year in storage at -80°C .

6.2.8. Data handling and analysis of typing spectra

6.2.8.1. Bruker FlexAnalysis method

Spectra were processed as described in the MALDI Biotyper protocol using the MBT_standard.FAMSMETHOD in FlexAnalysis (version 3.4). Peaks were detected using a centroid algorithm within a 2.0 m/z width range. Baseline subtraction and curve smoothing were performed using TopHat and SavitzkyGolay algorithms, respectively. Replicate spectra were visually inspected and any peaks below 500 arbitrary units (a.u.), or deviating outside of a mass tolerance of $\sim\pm 0.025\%$ of the estimated m/z value, were excluded. MALDI 'biotypes' were allocated for strain typing analyses based on the presence or absence of biomarker peaks. A biomarker peak was assigned as such if the following criteria were satisfied: (i) above 500 a.u. for at least two out of three technical replicate spectra (ii) at least 5.0 m/z (Da) difference from peaks of a similar size (iii) present for at least one but not all of the isolates.

6.2.8.2. *Bioinformatics software*

Processed spectra files (referred to as mzXML files) were exported from FlexAnalysis for each isolate for analysis in BioNumerics software (Applied Maths, Belgium. Version 7.6) and Clover MS data analysis software (Clover BioSoft, Spain. <http://www.clovermsdataanalysis.com/>, accessed 09/08/2020). Analysis using Clover MS data analysis software was performed by Gema Mendez-Cervantes (Clover BioSoft, Spain). Peak matching was performed in each program based on m/z data with a constant tolerance of 0.5, linear tolerance of 300 parts per million (ppm) and a detection rate of 50 new peak classes per spectra. For strain typing, similarity matrices were generated based on the Pearson correlation coefficient and isolates clustered using the unweighted pair group method with arithmetic mean (UPGMA). The cophenetic correlation between isolates was calculated and expressed as a percentage on the resulting dendrograms.

6.2.9. *Whole genome sequencing and phylogenetic analysis*

Whole genome sequencing analysis was performed by Dr Ronan Doyle (GOSH) as described in Section 10.11.4 (Appendix 11). Briefly, DNA was extracted from all isolates as previously described (Shaw *et al.*, 2019). 50 ng of DNA was prepared using NEBNext Ultra II FS DNA Library Prep Kit for Illumina (New England Biolabs, USA) and post-PCR clean-up was carried out using Ampure XP beads (Beckman Coulter, UK). Library size was validated using the Agilent 2200 TapeStation with Agilent D1000 ScreenTape System (Willoughby, Australia) and 75bp paired-end reads were sequenced on a NextSeq 550 system (Illumina, USA). Fastq files containing paired end sequences for each isolate were screened against all complete *A. baumannii* reference genomes found on NCBI Refseq database using Mash (Ondov *et al.*, 2016) to identify the closest matching reference sequence. The best matching genome was *A. baumannii* strain BAL062 (Accession: NZ_LT594095) and all samples were mapped to this reference using BBmap (Bushnell, 2014). Single nucleotide variants (SNVs) were called against the reference using FreeBayes (Garrison and Marth, 2012) and variants were only taken forward if (i) read depth >5, (ii) mapping quality >30, (iii) base quality >20, (iv) alternate read frequency >80%, (v) if there were >2 reads on both strands and (vi) >2 reads with variant present at both the 5' and 3' ends of the fragments. Variant positions were also masked if not present at >5 read depth in 90% of samples. Possible recombination sites were identified and masked using Gubbins (Croucher *et al.*, 2015)

and a maximum likelihood phylogenetic tree was inferred from the aligned variant sites using RAxML under the GTRCAT model (Stamatakis, 2014).

6.3. Results and Discussion

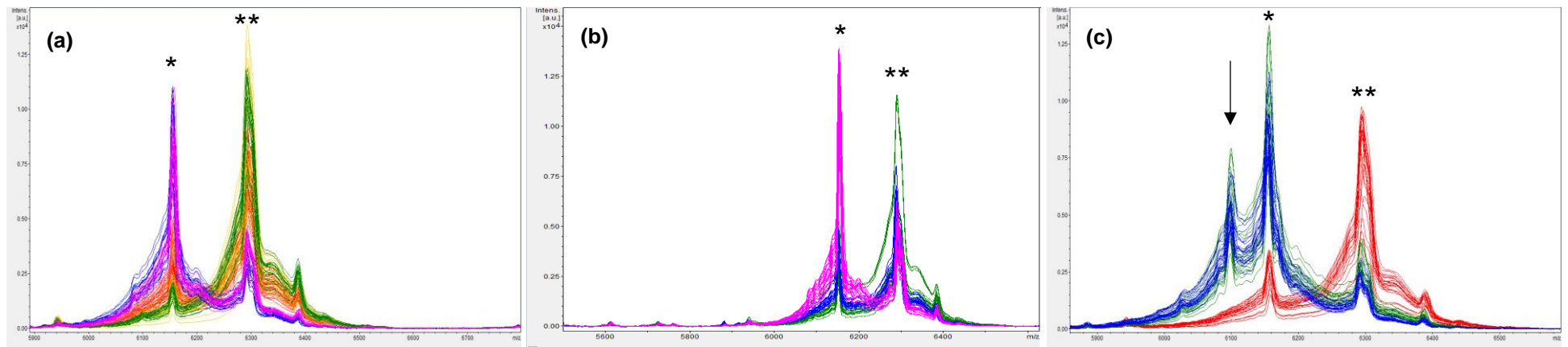
6.3.1. Part 1: Evaluating sources of variability in the MALDI-TOF MS strain typing protocol

6.3.1.1. *Variability in spectra attributed to sample preparation*

6.3.1.1.1. *Culture-subculture cycle and phase of bacterial growth*

MALDI-TOF MS spectra used for bacterial strain typing can vary depending on cell culture (Sauget *et al.*, 2017). This variable was investigated for the Bruker Biotyper protocol to ensure that spectra obtained between multiple culture passages, Cryobank™ storage beads and experiments were repeatable. Homogeneity of spectral profiles within each storage tube, which contains approximately 25 Cryobank™ beads available for bacteria to adhere to, was assessed. Heterogeneity of bacterial clones could exist within a storage tube as a result of recombination, spontaneous mutations and horizontal gene transfer (Robertson and Meyer, 1992). This could result in organisms within a population exhibiting different protein profiles adhering to different beads and might introduce bias when characterising protein spectra using MALDI Biotyping, depending on the bead selected. The organism *K. pneumoniae* was chosen for this investigation because a high number of mass peaks were observed within the 2-20 kDa range (Appendix 7), providing good resolution for the analysis.

Figure 6.1: (a) Comparison of spectra between six individual Cryobank™ beads; condition i (Section 6.2.6.1). (b) Comparison of spectra obtained for three fresh cultures from a single Cryobank™ bead with fresh sub-culture every 24 hours; condition ii (Section 6.2.6.1). (c) Example of changes to mass spectra plots for condition iii (Section 6.2.6.1). Spectra in red represent organisms at 24 hours; green and blue spectra represent organisms at 48 and 72 hours, respectively. Common peaks were observed at approximately 6150 (*) and 6300 (**) m/z. Note the presence of an additional peak at 6100 m/z (indicated by the arrow) after 48 and 72 hours that is absent at 24 hours, and absent in (a) and (b).



Visual interpretation indicated that spectra obtained for individual freshly recovered beads (Section 6.2.6.1, condition i) were comparable to one another. This included characteristic peaks at approximately 6150 and 6300 m/z (Figure 6.1a). In addition, the impact of daily subculture originating from a single bead on MALDI-TOF MS typing spectra was explored (condition ii). Figure 6.1b shows that spectra were also comparable between each culture, with the same characteristic peaks being observed in Figure 6.1a. These initial findings suggest that homogeneity of profiles obtained from different Cryobank beads within a tube are comparable to spectra obtained from fresh sub-culture of organisms from a single initial bead.

A time course experiment was performed using a single agar plate containing established colonies originating from a single bead that was not sub-cultured and analysed across three days (condition iii). Figure 6.1c shows that, when the culture was analysed at 48 and 72 hours, a new peak was observed at 6100 m/z that was not observed in the initial spectra obtained after 24 hours in culture when cells are growing exponentially. These changes in mass spectra may represent the expression of new proteins as the result of an organism's adaptation to a changing chemical environment (Arnold *et al.*, 1999). Changes to protein spectra related to bacterial cell senescence have been suggested to relate to inconsistencies in mass peak spectra (Egli *et al.*, 2015), highlighting the importance of obtaining spectra from bacteria at a defined point in their growth cycle. These data suggest that changes in protein spectra can result when bacteria are under stress, possibly due to nutrient depletion (Poole, 2012). Cultured cells should therefore be used for MALDI-TOF MS typing when they have been incubated for no longer than 24 hours at 37°C. It has also been noted that experiments performed using different batches of culture medium can result in variable expression of bacterial proteins, which could lead to discordant results between typing experiments (Jabbour and Snyder, 2014). This highlights the importance of ensuring that common reagents batch numbers are utilised between repeat experiments to ensure that comparable results are obtained. Incorporation of MALDI-TOF MS strain typing into the workflow of a busy microbiology laboratory should take these findings into consideration when assessing the feasibility of performing such analyses in-house.

6.3.1.1.2. Formic acid extraction of proteins

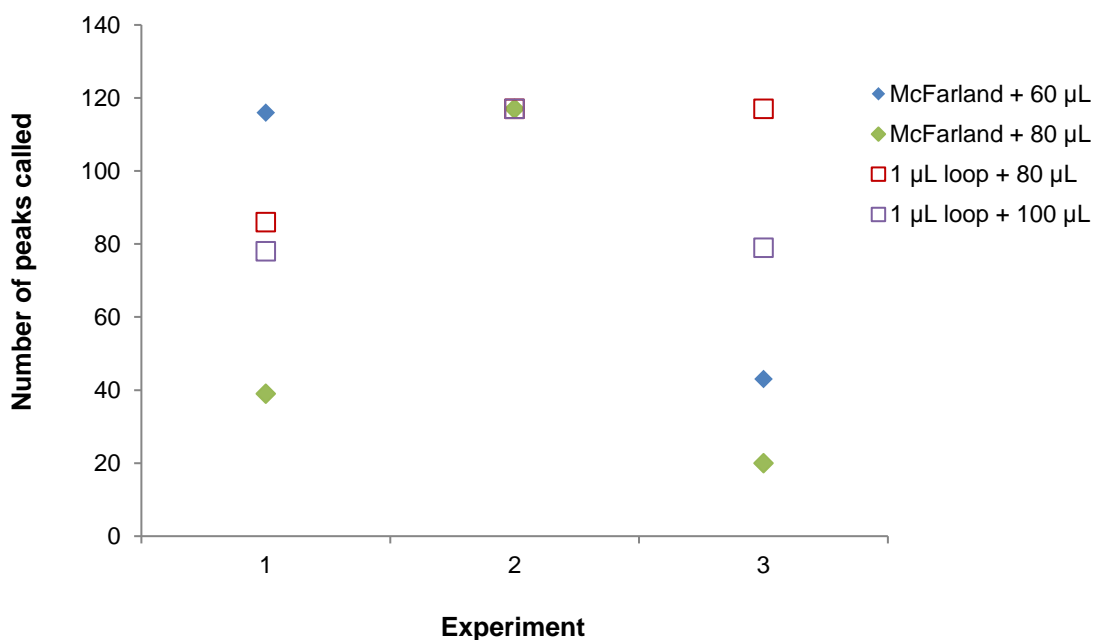
To extract proteins from bacterial cells for MALDI-TOF MS typing analysis, added volumes of extraction reagents must be proportional to cell pellet size following centrifugation. This process is based on visual interpretation (Section 6.2.4). Misjudgement of the volume required could influence the final concentration of bacterial cells in the extraction mixture, and the subsequent number of extracted proteins that are deposited on the MALDI target plate. Variability in bacterial cell concentration in the extraction mixture has been shown to affect the quality and reproducibility of MALDI-TOF MS spectra (Williams *et al.*, 2003). An investigation was performed to compare the effect of varying the input amount of biomass as either a 1 μL filled sterile loop, or a bacterial suspension made up to a 0.5 McFarland standard. Proteins were extracted from the 1 μL loop or 0.5 McFarland inputs using different volumes of extraction reagents to make the final bacterial suspension more or less concentrated prior to analysis on the MALDI target plate. The volumes of reagent chosen were tailored to the amount of biomass input, which gave different sized pellets owing to varying initial input CFU per mL (Table 6.1).

Table 6.1: Bacterial cell concentration was shown to impact upon the number of peaks that were identified in MALDI-TOF MS spectra. Note that lower volumes were added to the 0.5 McFarland pellets, which were smaller than with the 1 μL loop pellets owing to lower initial input CFU per mL.

Sample input	Estimated concentration of cells in pellet ($\times 10^8$ CFU per mL)	Reference	Volume of extraction reagent added (μL)	Number of peaks called
0.5 McFarland pellet	~1.5	(Kralik <i>et al.</i> , 2012)	60	270
			80	137
1 μL loop pellet	~2-3	(Lodish <i>et al.</i> , 2000)	80	320
			100	274

Table 6.1 shows that the 1 μL loop input method yielded greater numbers of peaks when compared to the 0.5 McFarland standard method. This finding is unsurprising given that greater numbers of bacteria were present in the 1 μL loop pellet initially, providing a greater quantity of extracted proteins for MALDI-TOF MS analysis. Furthermore, bacterial concentrations were lower owing to greater volumes of extraction reagent which resulted in fewer peak calls. This was observed for both the 0.5 McFarland pellet and the 1 μL loop input method. In the case of the 0.5 McFarland pellet this manifested in a 2-fold difference in number of peaks called. These findings support the hypothesis that the concentration of bacterial cells, associated with either the biomass input method or the volume of extraction reagent added, influences the number of potential peak calls that can be made. This could bias interpretation of spectra for typing where peaks that may represent strain-specific biomarkers are omitted from the analysis. In addition, Figure 6.2 shows that there was inter-experimental variability in the number of peak calls for each of the extraction conditions (17 to 88 %CV across the four different conditions). This suggests that variability from the extraction step could influence MALDI-TOF MS spectra obtained from different experiments, further confounding the reproducibility of MALDI-TOF MS for strain typing.

Figure 6.2: Inter-experimental variability in the number of peaks called for different concentrations of bacterial cell preparations. Key: \square 1 μL loop + volume of extraction reagent (μL) \blacklozenge 0.5 McFarland standard + volume of extraction reagent (μL).



Although both biomass input methods represent 'standardised' quantities, these data support the importance of maintaining further rigour in extraction approaches between typing experiments, where biomarker peaks could be lost due to varying concentrations of bacterial proteins in solution. Optimising the concentration of bacteria present in the matrix can ensure that high quality MALDI-TOF MS spectra are yielded from whole cell preparations (Williams *et al.*, 2003). Figure 6.2 indicates that the 1 μ L loop input method was less variable than the 0.5 McFarland standard in terms of number of peaks called, and that this method should be used for performing MALDI-TOF MS typing experiments. The data also suggests that using a more concentrated solution of bacterial cells for protein extraction yields more reproducible numbers of peaks, despite the subjectivity associated with the preparation method. Quantitative approaches for standardising input protein concentrations could be of benefit for obtaining reproducible spectra for typing, such as Bradford or UV absorption (De Mey *et al.*, 2008). However, incorporation of these approaches into the MALDI Biotyper workflow would require further characterisation and optimisation.

6.3.1.2. *Peak intensity as a metric for evaluating robustness of replicate spectra*

6.3.1.2.1. *Evaluating inter-experimental variability in peak intensity for a standardised protein solution*

The number of mass peaks per spectra can vary across experiments for proteins extracted from freshly cultured organisms (Figure 6.2). Peak classification by MALDI-TOF MS largely relies upon peak intensity to establish thresholds for acceptance of a peak. Peak intensity, or peak height, is reported to be a useful indicator of ionisation efficiency (Duncan *et al.*, 2016), and could be highly indicative of the matrix-to-analyte interactions unique to an experiment along with laser energy, crystal morphology and detector performance (Wang *et al.*, 2016). In a review by Albrethsen (2007) it was reported that peak intensities varied by up to 26% (Given as %CV) between studies that published precision data for protein profiling by MALDI-TOF MS (Albrethsen, 2007). This suggests that peak height can vary considerably between experiments and could introduce bias when discriminating between isolates based on the presence or absence of peak classes. The MALDI Biotyper protocol was applied to the Bruker bacterial test standard (BTS), a solution of 8

characterised bacterial proteins used to calibrate the MALDI-TOF MS detector, over three days to evaluate the impact of inter-experimental variability on peak intensity.

Figure 6.3: Evaluating variability in peak intensity and the stability of the bacterial test standard (BTS) across three days. Mean peak intensity is plotted for the summed 15 replicate spectra per day.

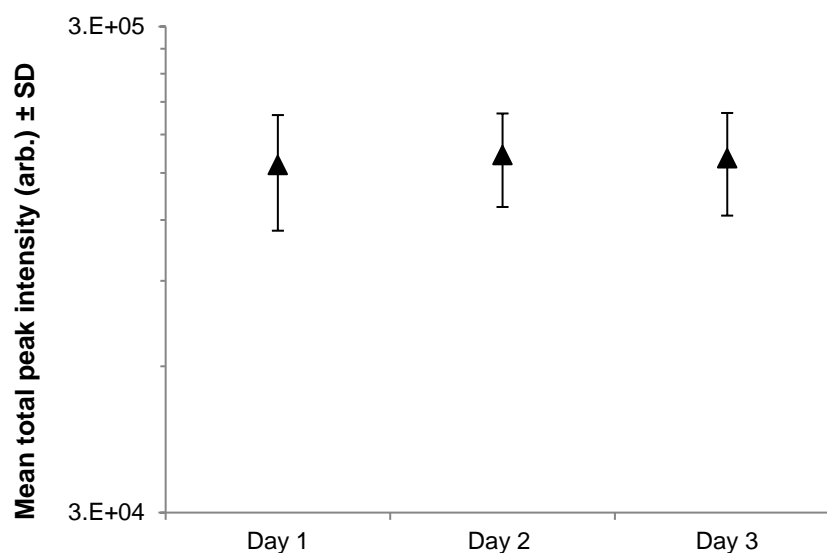


Figure 6.3 shows the mean peak intensity summed for 15 technical replicates per day. There was no significant difference in total intensity across the three days by one-way ANOVA ($p = 0.86$), suggesting that ionisation efficiency was equivalent between the triplicate experiments for the bacterial test standard. This experiment also demonstrated stability of a single vial of BTS that was analysed across the three days, which included two freeze-thaw cycles. This could represent a financial benefit to microbiology laboratories potentially implementing the technique where costly reagents can be conserved across multiple typing experiments.

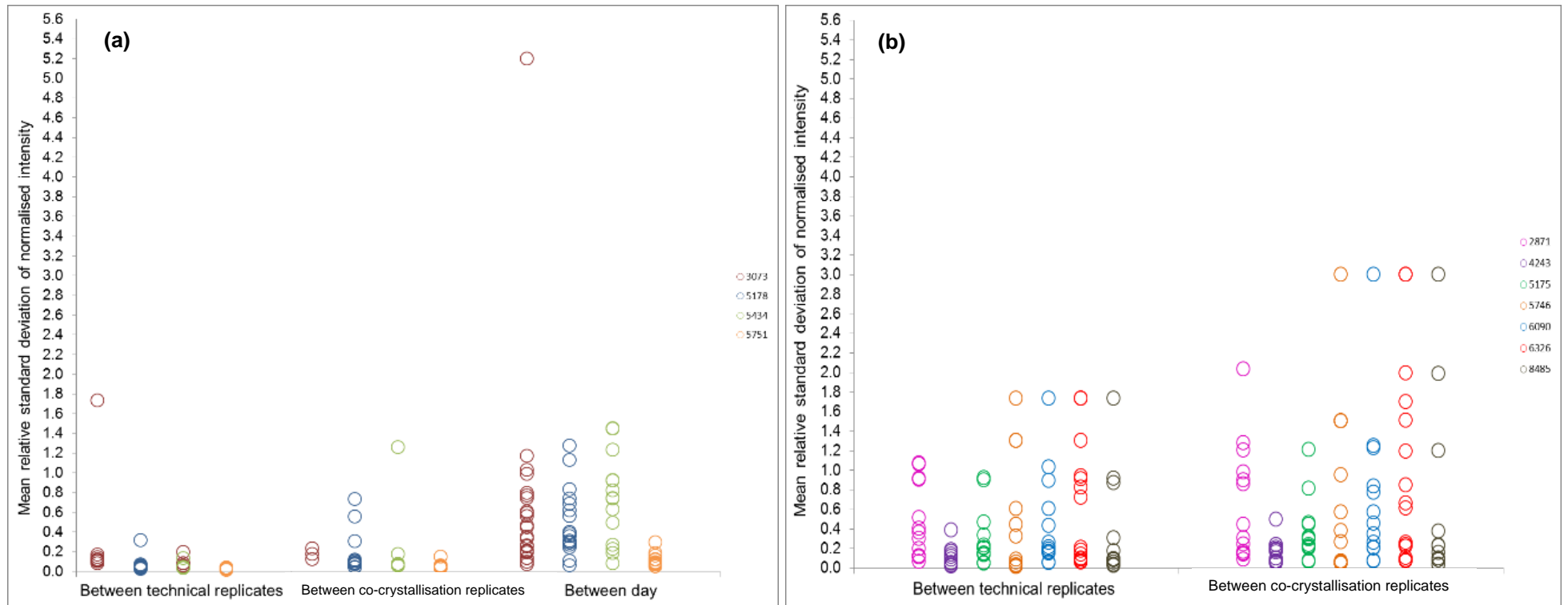
6.3.1.2.2. Variability in peak intensity for clinical isolates

A cohort of 18 clinical *A. baumannii* isolates associated with an outbreak in a surgery ward at the Royal Free London NHS Foundation Trust were selected for typing using MALDI-TOF MS. Variability in peak intensity, the chosen metric for robustness of spectra both within and between typing experiments, was evaluated for these isolates. In the context of strain typing, better reproducibility of spectra might result in improved resolution for sub-species differentiation owing to more reliable, better quality spectra containing potential biomarker peaks for discrimination (Kang *et al.*, 2017, Schumaker *et al.*, 2012, Sauget *et al.*, 2017). Spectra were imported from

FlexAnalysis into BioNumerics 7.6 for the calculation of peak metrics, which were later used to generate strain comparisons for typing (Chapter 6.3.2). Mean relative standard deviation (rsd) was calculated for replicate spectra for selected peak classes to represent the variability in peak intensity at various stages of the typing protocol. Two peaks were selected for the comparison that may represent species-specific biomarkers i.e. that were detected in the spectra of all 18 clinical isolates (m/z 5178 and m/z 5751). In addition, two peaks that might represent strain-specific biomarkers (i.e. present in some, but not all, of the isolates) were chosen; m/z 3073 and 5433.

Figure 6.4 shows that for all peak classes included in the comparison, mean rsd was lowest between technical replicates (i.e. replicate ionisations) of MALDI-TOF MS typing spectra and increased between co-crystallisation replicates (i.e. replicate sample spots overlaid with matrix). Mean rsd was greatest between different days which represent replicate experiments. This effect was more pronounced for some peak classes than others. Maximum mean rsd ranged from 0.32 (technical) to 1.27 (temporal) for m/z 5178 compared to m/z 5751, which ranged from 0.036 (technical) to 0.29 (temporal) mean rsd. When the typing experiment was repeated for the isolates after one year in storage at -80°C , the same effect was observed between technical and co-crystallisation replicates; however, temporal replicates were not included in this analysis (Figure 6.4b). To include a more comprehensive analysis of the variability across the whole spectra after one year in storage, a total of 7 peaks were chosen which included some of the same peaks selected for the initial analysis (Figure 6.4a). Mean rsd was higher for the isolates analysed after one year, however this analysis was performed following freeze-thawing of isolates and using different reagent batches which could introduce additional variability for typing. Viability and, indirectly, stress response of organisms can be affected during freezing due to the formation of ice crystals which can rupture cell membranes (Koh, 2013). This could therefore impact upon the peak classes that are identified for MALDI-TOF MS strain typing.

Figure 6.4: Evaluating variability in peak height at (a) different stages of MALDI-TOF MS typing of *A. baumannii* isolates and (b) repeated after one year in storage at -80°C . Each coloured marker represents an isolate of *A. baumannii*. Keys contain lists of the m/z peaks chosen for the comparison.



Variability in peak intensity increased as a function of time, and suggests that different stages of the MALDI Biotyper protocol including long-term storage of isolates could influence ionisation efficiency (Arnold *et al.*, 1999). Other factors might include: 1) the ionisation mechanisms of particular mass peaks, which could vary with molecular weight and protein conformation 2) differences in sample-matrix co-crystallisation between (as well as within) replicate spots in an experiment 3) differences in preparation and extraction of samples between days, which was demonstrated in Section 6.3.1.1.2 to influence the number and nature of peak classes observed. Variability in spectral acquisition between experiments could become problematic when trying to assign biomarker status to certain peak classes that are not reliably classified, resulting in poor reproducibility when experiments are repeated on different days or by different laboratories.

6.3.1.3. Choice of data analysis method for MALDI-TOF MS strain typing

Choice of data analysis method can impact upon how spectra are interpreted and reported for strain typing (Spinali *et al.*, 2015). The following section aims to address this by comparing the two different data analysis approaches that were used for performing strain typing of the clinical cohort of *A. baumannii* described above.

6.3.1.3.1. Bruker FlexAnalysis method

The Bruker FlexAnalysis method, described in the Bruker Biotyper strain typing protocol, involves visual inspection and subsequent classification of mass peaks. This approach has been described previously for strain typing with varying levels of success (Oberle *et al.*, 2016, Holzkecht *et al.*, 2018). Following acquisition of spectra, the Bruker FlexAnalysis approach was used to assign MALDI 'types' to the 18 *A. baumannii* isolates based on presence or absence of particular peak classes that had been assigned biomarker status (Table 6.2).

Table 6.2: MALDI-TOF MS peak classes identified as potential biomarkers for strain typing isolates of *A. baumannii* using the Bruker FlexAnalysis method. Shaded boxes indicate the presence of a peak, blank boxes represent absence.

Isolate	Peak class (m/z)			
	2256	2585	5434	5448
MBT16-003			■	
MBT16-005		■		
MBT16-008			■	
MBT16-011		■		
MBT16-015				
MBT16-016	■		■	
MBT16-018		■	■	
MBT16-025	■		■	
MBT16-029	■		■	
MBT16-030	■		■	■
MBT16-031			■	
MBT16-033	■		■	■
MBT16-039		■		
MBT16-040	■		■	■
MBT16-042	■		■	
MBT16-059	■		■	
MBT16-060	■		■	
MBT16-062	■		■	

There are several limitations associated with this method of interpreting spectra for strain typing bacteria; analysis is based on non-normalised spectral data, which may result in subjective classification of peaks owing to variable baseline signals between spectra. Furthermore, it is difficult to determine whether these peaks represent strain-specific biomarkers since the method is time consuming and relies on subjective interpretation. Since the analysis is highly labour intensive, requiring manual processing of data and visual interpretation of peak profiles, there is potential for analyst error which could bias a typing result and lead to unsupported conclusions. For the technique to become accessible to busy clinical microbiology laboratories, an element of automated data handling might be of benefit to enable objective interpretations of spectra to be made for strain analysis.

6.3.1.3.2. *Bioinformatics approaches*

Access to bioinformatic software could be of benefit for interpreting MALDI-TOF MS strain typing data by offering more objectivity, ease of data handling and the ability to normalise data for accurate assignment of peak classes (Spinali *et al.*, 2015, Oberle *et al.*, 2016). This could improve the downstream analysis workflow by limiting operator hands-on time and potentially enhance strain typing resolution through better discrimination of biomarker peaks. Furthermore, hierarchal cluster analyses can be performed based on similarity matrices calculated in the software (Vranckx *et al.*, 2017). These can be used to estimate and visualise the degree of relatedness between isolates of related and unrelated strains. Spectra obtained for the 18 *A. baumannii* isolates were analysed using BioNumerics (Applied Maths, version 7.6) and Clover MS Data Analysis Software (Clover BioSoft) and the breadth of peaks identified compared with the FlexAnalysis method. Each of these software programs can access peak data for the entire spectrum rather than just a handful of subjectively chosen peaks. Automated processing, normalisation and peak matching algorithms are applied, and further downstream analyses such as hierarchal clustering can be performed.

Table 6.3: UniProtKB/Swiss-Prot search results for *A. baumannii* (Tax ID: 470) performed using TagIdent tool (<https://web.expasy.org/tagident/>) compared with the full range of peaks for the 18 isolates classified using each method. MW range for the search was 2 to 9 kDa. Presumed matched ribosomal proteins (Da) and corresponding m/z peaks (± 20 Da) detected using each approach are highlighted in green.

MW (Da)	Protein	Peaks identified using the FlexAnalysis method	Peaks assigned in BioNumerics	Peaks assigned in Clover MS Data Analysis Software
2805	Aspartate 1-decarboxylase beta chain.	2256	2150	2256
2938	Coenzyme PQQ synthesis protein A.	2585	2873	2585
3980	Phosphatidylserine decarboxylase alpha chain. {ECO:000025...	5434	3073	3073
3996	Phosphatidylserine decarboxylase alpha chain. {ECO:000025...	5448	3317	3723
4265	50S ribosomal protein L36.		3338	4245
5175	50S ribosomal protein L34.		3444	5178
5189	50S ribosomal protein L34.		3723	5434
5462	UPF0391 membrane protein A1S_3910.		4245	5448
6090	50S ribosomal protein L33.		4257	5751
6642	50S ribosomal protein L30.		4267	5771
7080	50S ribosomal protein L32.		4492	8487
7402	50S ribosomal protein L35.		5034	
7435	50S ribosomal protein L29.		5178	
7719	Sec-independent protein translocase protein TatA.		5434	
8360	ATP synthase subunit c.		5751	
8451	30S ribosomal protein S21.		5772	
8492	Translation initiation factor IF-1.		6094	
8669	Acyl carrier protein.		6330	
8992	30S ribosomal protein S18.		7439	
			8490	
			8723	
			8984	
Total number of peaks identified for strain analysis		4	22	11

Peaks identified for strain analysis were recorded for the three data analysis methods in parallel with a putative protein search using TagIdent Tool (ExpASY) (Gasteiger *et al.*, 2005). Peaks identified by MALDI-TOF MS and analysed using the three methods correlated with the protein repertoire returned following the TagIdent search (Table 6.3). 0, 5 and 2 peak classes corresponding with ribosomal subunit proteins were returned following analysis using the FlexAnalysis, BioNumerics and Clover methods, respectively. The fact that more peaks identified using these analysis approaches matched with the proteins deposited in public databases suggests that the latter two (bioinformatic) methods could provide better discrimination of potential biomarker peaks for differentiating between bacterial strains. In addition, the observation that at least twice as many discernible peaks were identified using the bioinformatic methods compared with the FlexAnalysis approach indicates that these methods could provide better resolution and objectivity for strain typing. Current commercially available software programmes for analysis of MALDI-TOF MS spectra have been criticised for being biased towards only the most abundant and reproducible peaks, potentially limiting the resolution of MALDI-TOF MS for strain typing (Sindt *et al.*, 2018). However, bioinformatic methods also appear to offer relative ease in the data analysis workflow over the visual method. Further work to explore the capability of additional commercial software for data analysis, such as the ClinProTools™ software (Bruker), could be of benefit for future studies on spectra-based typing methods. In addition, the availability of affordable or open-access software programs could allow MALDI-TOF MS strain typing to be accessible to hospitals and microbiology laboratories.

6.3.1.4. Practical implications of variability in the MALDI-TOF MS strain typing workflow

To strain type bacteria using MALDI-TOF MS, characteristic spectra of predominantly ribosomal proteins that are representative of a particular clone, strain or lineage are generated. The spectra could then be compared with a custom database of strains previously characterised in-house to identify or rule out potential outbreaks. Reliable identification is therefore dependent on spectra being reproducible and representative of the organism in question (Oberle *et al.*, 2016). Studies suggest that the quality and reproducibility of MALDI-TOF MS fingerprints can be influenced by sample preparation steps, matrix choice and instrumental performance, among other factors (De Bruyne *et al.*, 2011, Zhang *et al.*, 2014). Highly variable acquisition of spectra could bias the

capture of a particular protein contained within the spectra, which may result in misleading profiles being obtained for an isolate. In addition, spectra obtained between different extraction batches and different experiments can exhibit variability rendering the typing data as unreliable (Steensels *et al.*, 2017).

Figure 6.5: Workflow for spectral acquisition from bacteria using MALDI-TOF MS. The central arrow represents the overall experimental process from bacterial isolate to characteristic mass spectrum for that organism. Peripheral branches represent various stages of the experimental process that have the potential to introduce variability. Aspects addressed in this chapter are highlighted in green.

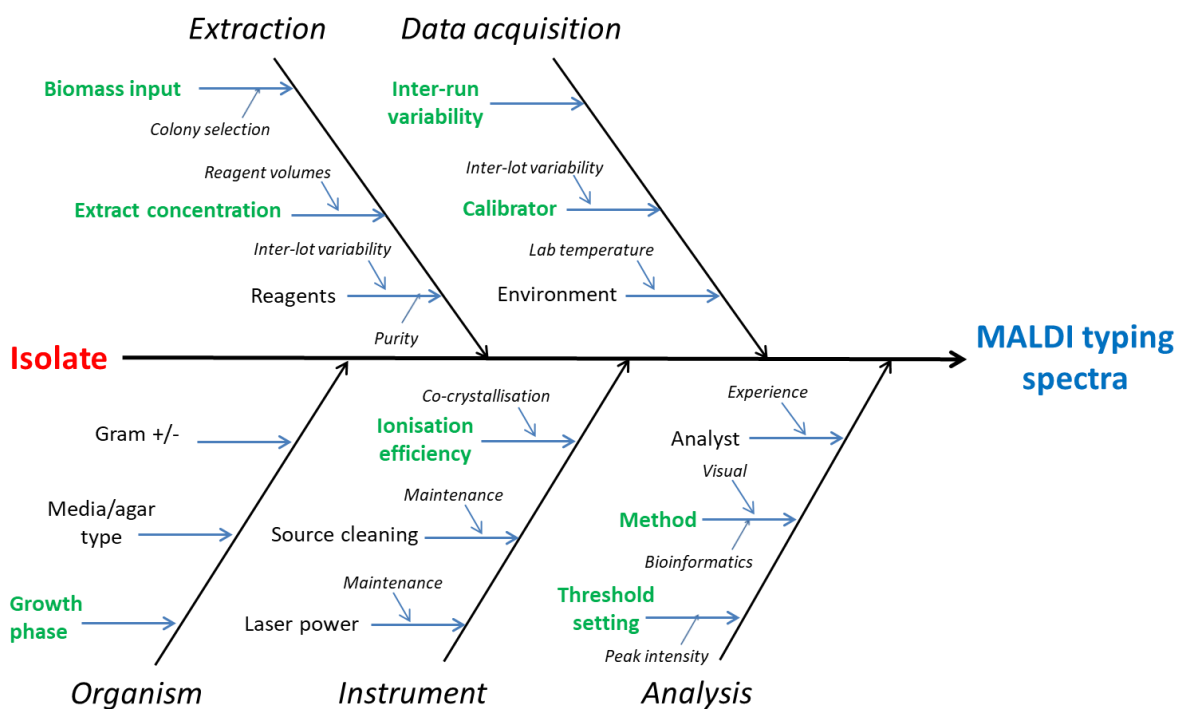


Figure 6.5 illustrates the workflow for obtaining a characteristic mass spectrum for a particular isolate, and highlights the aspects that can influence spectral acquisition at each step. The steps of the experimental workflow highlighted in green were investigated in this chapter. It was found that variability associated with each of these steps can introduce measurement error in spectral acquisition, which can influence whether a peak is called or not and subsequently bias a typing result. Analysis of isolates at different growth stages, unsuitable protein extraction, choice of data analysis tool and inter-experimental effects contribute to random and systematic error associated with the MALDI-TOF MS typing approach. It is worth noting that the variables highlighted in Figure 6.5 are not exhaustive and many other variables in the protocol could be candidates for

future exploration. The review by Sauget *et al* (2017) explores the placing of MALDI-TOF MS for strain typing bacteria, discussing the numerous variables that can influence a typing result. The authors suggest that, whilst MALDI-TOF MS presents as a promising tool for strain clinically relevant typing bacteria, improved control over the upstream processes of the workflow including sample preparation are needed (Sauget *et al.*, 2017).

6.3.2. Part 2: Can MALDI-TOF MS be used to strain type bacteria?

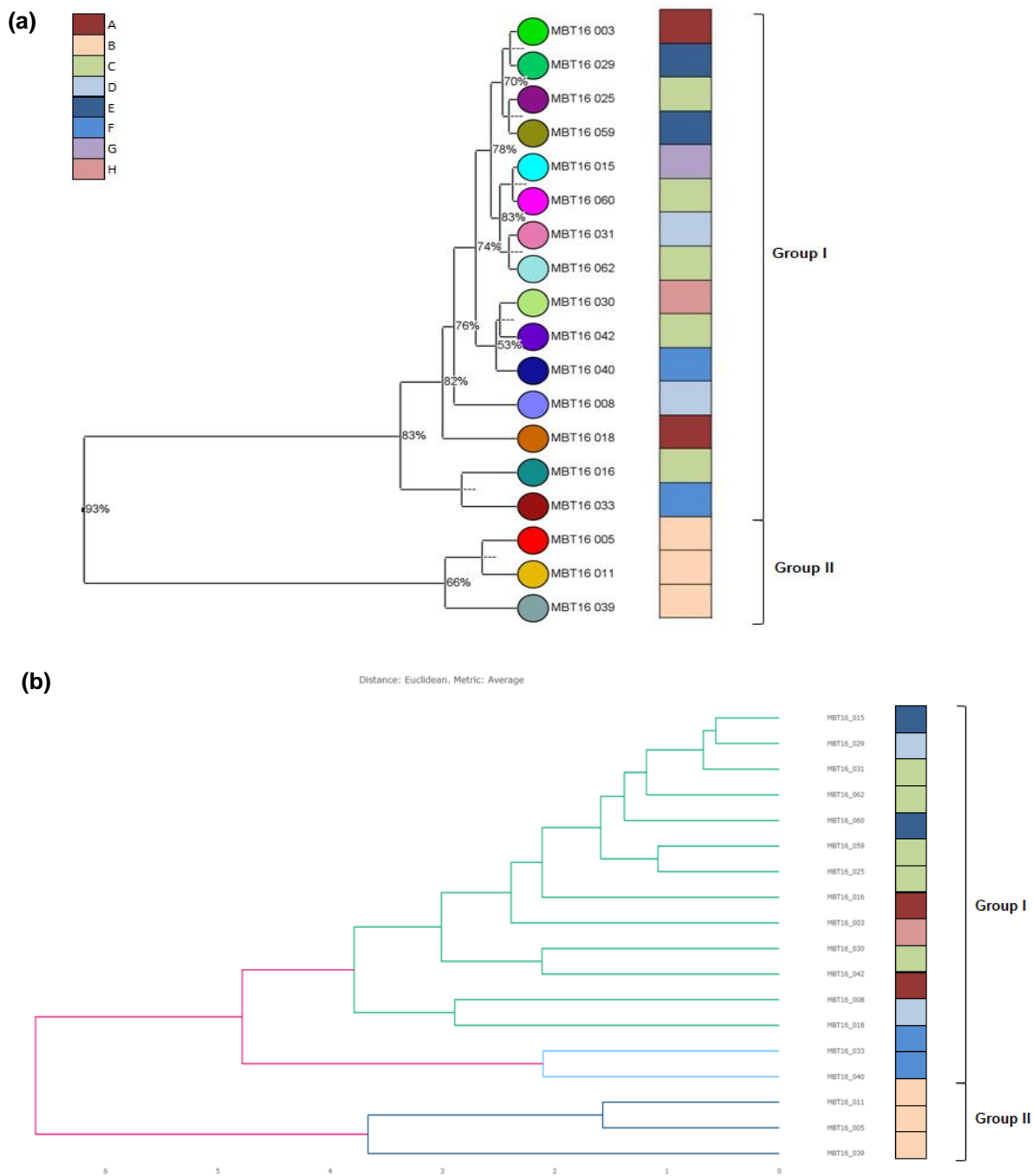
6.3.2.1. MALDI-TOF MS strain typing of *Acinetobacter baumannii*

Part 1 (Section 6.3.1) of this chapter examines the sources of variability associated with MALDI-TOF MS as a method for strain typing bacteria. It was found that different aspects of the protocol can influence the number and range of mass peaks that are identified. To investigate how the variables discussed in Part 1 may influence performance of MALDI-TOF MS typing of clinical samples, the Bruker Biotyper protocol was applied to the cohort of *A. baumannii* isolates (n=18) and compared with the reference laboratory findings. All isolates were classified as being identical in terms of strain (OXA-23 clone 1) by the reference laboratory (Appendix 6). The Bruker FlexAnalysis and two separate bioinformatics software programmes were applied for analysis peaks. 27 spectra were included for each isolate across a total of three days to provide high replication and infer greater confidence in measurements of protein biomarkers.

Table 6.4: Bruker MALDI Biotyper groups assigned to each of the 18 *A. baumannii* isolates based on presence or absence of visually chosen mass to charge (m/z) peak classes.

MALDI Biotype	Isolate
A	MBT16-003
A	MBT16-008
B	MBT16-005
B	MBT16-011
B	MBT16-039
C	MBT16-016
C	MBT16-025
C	MBT16-042
C	MBT16-060
C	MBT16-062
D	MBT16-018
D	MBT16-031
E	MBT16-029
E	MBT16-059
F	MBT16-033
F	MBT16-040
G	MBT16-015
H	MBT16-030

Figure 6.6: Hierarchical clustering of *A. baumannii* isolates calculated in (a) BioNumerics and (b) Clover MS data analysis software using UPGMA based on MALDI-TOF MS spectra. The isolates clustered into two main groups: Group I and Group II. The coloured key represents the 8 MALDI Biotypes listed in Table 6.4 (Groups A-H). Note: For (a) cophenetic correlation is indicated at base of each node (Section 10.11.4; Appendix 11).



The Bruker FlexAnalysis approach revealed four peaks that satisfied the inclusion criteria for strain typing (Table 6.2), and the isolates were grouped into a total of 8 classes representing different 'MALDI Biotypes' (Table 6.4). Two of the isolates (MBT16-015 [G] and MBT16-030 [H]) were classified as unique Biotypes since their spectral profiles did not match with any of the other

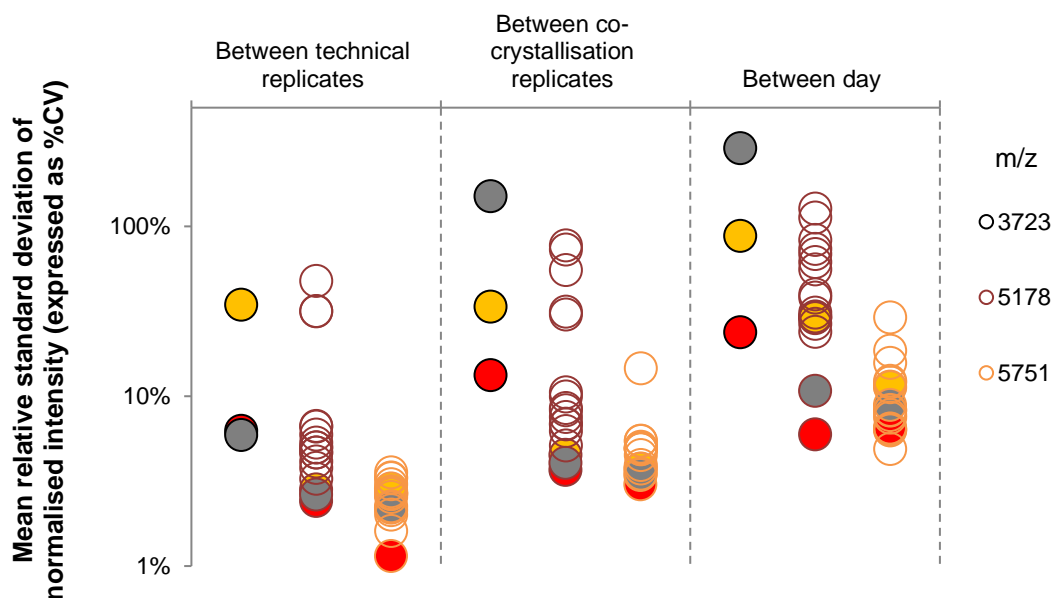
isolates. Following baseline subtraction and curve smoothing in FlexAnalysis, the pre-processed spectra were imported into BioNumerics 7.6. Spectra were summarised for each isolate and clustered using the unweighted pair group method with arithmetic mean (UPGMA). Two main clusters were identified using this method; designated Group I and Group II (Figure 6.6a). Of note, the isolates that clustered into Group II using the BioNumerics analysis method also fell within the same MALDI Biotype 'group B' designated in Table 6.4 (isolates MBT16-005, MBT16-011 & MBT16-039). This finding was confirmed when the same spectra were clustered using Clover MS data analysis software (Figure 6.6b).

Overall, there was poor correlation of the MALDI Biotypes with the UPGMA clusters generated in the bioinformatics software programmes. The exception to this is the group of three isolates which formed a distinct cluster for the three analysis methods. The FlexAnalysis method was based on non-normalised spectral data which may result in subjective classification of peaks owing to variable baseline signals between spectra. Analysis was performed on a small number of peak classes; 4 out of approximately 9 observable peaks per spectra. Similar numbers of mass peaks for *A. baumannii* have been observed previously (Sousa *et al.*, 2015, Jeong *et al.*, 2016), which potentially limits the usefulness of the FlexAnalysis method for strain typing this organism due to the limited resolution offered. However, analysis using bioinformatics software allows access to peak data for entire spectra, applies pre-defined peak height normalisation algorithms and removes subjectivity from visual peak calling. This could help to more reliably distinguish peaks that may represent strain-specific biomarkers in future studies of this nature.

6.3.2.1.1. *Peak intensity as a metric for discrimination of peak classes using MALDI-TOF MS typing*

The Group II/MALDI Biotype B isolates clustered together using both the Bruker FlexAnalysis and bioinformatic methods and could represent a diverse group of organisms. These isolates could possess mass peaks that offer better typing resolution, or are more reproducible, therefore enabling more consistent clustering between the three analysis methods. Peak intensity for the Group II/MALDI Biotype B isolates was examined to determine whether better reproducibility of spectra enables improved strain typing resolution.

Figure 6.7: Variability in peak height at different stages of the MALDI-TOF MS typing protocol. The 'Group II/MALDI Biotype B' isolates are represented by the following coloured spots: Red – MBT16-005, Yellow – MBT16-011, Grey – MBT16-039. Unfilled spots represent the other 15 isolates. m/z 5178 and 5751 represent peak classes common to all isolates; m/z 3723 represents a peak only observed for the Group II/MALDI Biotype B isolates following analysis in BioNumerics (Section 10.11.4; Appendix 11).



For peaks that were shared among the 18 *A. baumannii* isolates (m/z 5178 and 5751 determined using BioNumerics), the Group II isolates exhibited the lowest relative standard deviation (rsd) compared to the other isolates (< 0.30 rsd, 30% CV) (Figure 6.7). This finding could suggest that better reproducibility between spectra for these peak classes permitted discrimination of these isolates from the rest of the cohort. However, when this approach was applied to a peak at m/z 3723, identified by BioNumerics as unique to these three isolates, the mean rsd was up to 10-fold higher indicating a decrease in reproducibility between peak height values. Regardless of peak class there was an overall trend of increasing variability in peak height at progressive stages of the experiment protocol, with technical replicates exhibiting the lowest variability and between-day replicates exhibiting the highest. These findings support the data presented in Figure 6.4. Further work comparing variability of peak intensity at progressive stages of the MALDI Biotyper protocol should be extended to additional peak classes and other isolates in this cohort. This could enable a more detailed understanding of how the inherent variability in the protocol can influence reproducibility of spectra, and as a result, resolution for typing.

6.3.2.1.2. *Potential identification of a nosocomial transmission event*

MALDI-TOF MS bioinformatics analysis approaches clustered the isolates into two groups, with the 'Group I' isolates appearing to be closely related. All 18 isolates were classified by reference laboratory VNTR profiling as belonging to European clone II lineage OXA-23 clone 1 (Appendix 6). Therefore, any observed differences such as different peak classes assigned to different isolates could be representative of the typical diversity between isolates of the same strain (Ueda *et al.*, 2015). However, 3 of the 18 isolates were classified as being separate from the main group by all of the MALDI analysis methods (respectively denoted as Group II /MALDI Biotype B by bioinformatics & Bruker FlexAnalysis method). Sufficient diversity could exist between groups I & II to indicate that they are not identical and possibly not from the same transmission route. Epidemiological data associated with this outbreak were obtained in order to explore the hypothesis that two strains may, in fact, exist in this cohort.

The outbreak in question was identified as being associated with a single surgical ward, multiple beds of which were inhabited by the patients during this time period (Appendix 8). Patients had also spent time on numerous other wards of varying specialties within the hospital including intensive care units. There were overlaps in time in which patients stayed on ward A, presenting possible opportunities for transmission to occur. It is worth noting that for the three 'Group II/MALDI Biotype B' isolates, MBT16-005 and MBT16-039 were obtained from the same patient. MBT16-011 was obtained from another individual who stayed on ward A in the same male 4-bedded bay during this time period. MDR *A. baumannii* was identified first in patient 4, followed by patient 2 thirteen days later. As a follow-up to this work the 18 isolates were also sequenced by WGS to evaluate genomic relatedness of the organisms using an alternative method, and to determine whether the three isolates in question remained divergent from the main group.

Figure 6.8: WGS SNV analysis compared with MALDI Biotype (Section 10.11.4; Appendix 11).

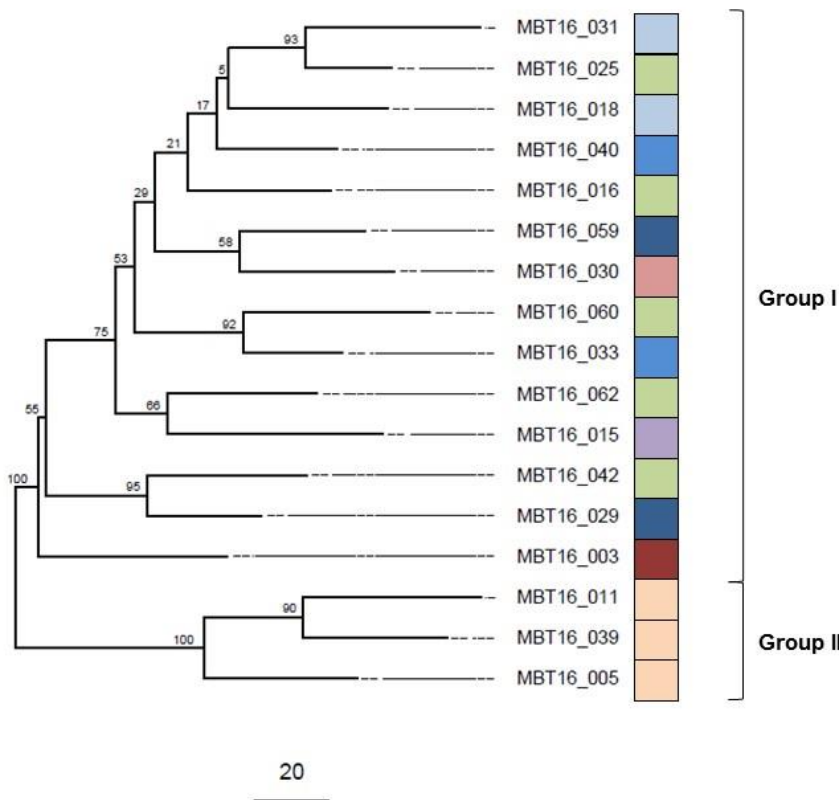


Figure 6.8 indicates that, similarly to BioNumerics and Clover MS data analysis software, WGS SNV analysis clustered the three *A. baumannii* isolates into a group that was distinct from the other isolates in the cohort (labelled as Group II). Similarly to Figure 6.6, there was little correlation between the WGS clustering and MALDI Biotype ID for the Group I isolates. This may further support the hypothesis that any observed differences between these isolates are within the realms of typical diversity for isolates of the same strain. These data, in combination with epidemiological information, provide evidence that the Group II isolates represent an incidental transmission event between two patients within ward A. This event is separate from the main outbreak cluster yet occurred at the same time. This finding could have implications for future infection control strategies where isolated transmission events can be disassociated from larger outbreaks.

6.3.2.2. MALDI-TOF MS strain typing of *Staphylococcus aureus*

As illustrated in Table 6.2, MALDI-TOF MS typing of *A. baumannii* may be limited by the fact that a small number of peaks could be distinguished as strain-specific biomarkers. This is reflected in several publications suggesting that MALDI-TOF MS is unsuitable for strain typing this organism due to insufficient discriminatory power (Ghebremedhin *et al.*, 2017, Sousa *et al.*, 2015, Rim *et al.*, 2015). In contrast, the utility of MALDI-TOF MS for successful sub-typing of *Staphylococcus aureus* lineages has been described (Steensels *et al.*, 2017, Lindgren *et al.*, 2018, Wolters *et al.*, 2011). This suggests that success of MALDI-TOF MS strain typing is dependent on the organism in question, and better resolution may be obtained for genera other than *Acinetobacter* sp. To test this hypothesis, the performance of the Bruker Biotyper protocol was evaluated for 8 clinical isolates of methicillin-resistant *S. aureus* that were associated with a nosocomial outbreak on a neonatal ward, alongside 3 ATCC reference strains. The isolates were tested using a single experimental workflow (similarly to the *A. baumannii* isolates) and data analysed using the Bruker FlexAnalysis and BioNumerics approaches.

Using the Bruker FlexAnalysis method for data handling, 13 peak classes were identified as potential strain-specific biomarkers (Table 6.5). In terms of resolution for strain typing, more than three times the number of peaks could be identified for *S. aureus* in comparison with *A. baumannii*, where only 4 biomarker peaks were assigned (Table 6.2). This highlights how species-specific differences could influence resolution and therefore the ability of the method to reliably characterise relatedness between strains. The mass peaks identified for *S. aureus* in Table 6.5 enabled the classification of isolates into five MALDI Biotyper groups (Table 6.6). These groups were then used in a comparison with UPGMA clustering analysis performed using BioNumerics (Figure 6.9).

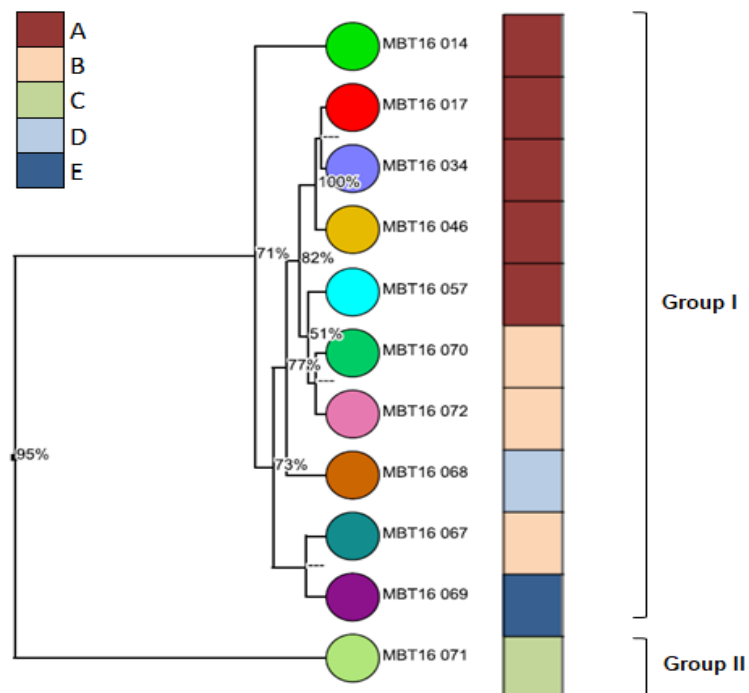
Table 6.5: Biomarker peak classes for strain typing *Staphylococcus aureus* isolates identified using the Bruker FlexAnalysis Biotyper approach. Shaded boxes represent the presence of a peak, blank represents absence.

Peak class (m/z)													
Isolate	4496	4511	5420	5432	5440	5508	5525	6578	6700	6890	7186	7420	7570
MBT16-014	■				■		■	■	■	■		■	
MBT16-017							■	■	■	■			
MBT16-034							■	■	■	■			
MBT16-046							■	■	■	■			
MBT16-057							■	■	■	■			
MBT16-067													
MBT16-068												■	■
MBT16-069		■										■	
MBT16-070													
MBT16-071		■	■	■		■	■	■	■	■	■	■	■
MBT16-072					■		■	■	■	■			

Table 6.6: Bruker MALDI Biotyper groups assigned to each of the 11 *S. aureus* isolates based on presence or absence of visually chosen peak classes.

MALDI Biotype	Isolate
A	MBT16-014
A	MBT16-017
A	MBT16-046
A	MBT16-057
A	MBT16-034
B	MBT16-067
B	MBT16-070
B	MBT16-072
C	MBT16-071
D	MBT16-068
E	MBT16-069

Figure 6.9: Hierarchical clustering of *S. aureus* isolates calculated in BioNumerics using UPGMA based on MALDI-TOF MS spectra. The key represents the 5 MALDI Biotypes listed in Table 6.6 (Groups A-E). Cophenetic correlation is indicated at base of each node.



UPGMA cluster analysis identified two groups of isolates, denoted Group I and Group II (Figure 6.9). There was some correlation between the Bruker FlexAnalysis and bioinformatics analyses, although the FlexAnalysis method appeared to inflate the number of groups present compared to BioNumerics. MBT016-071 stood out as divergent for both methods. This isolate represents a reference strain that is likely to be divergent from the other isolates in this cohort. However, the two other reference strains that were included in the analysis (MBT16-070 and MBT16-072) appeared to cluster with the clinical strains in Group I. Of note, reference laboratory *spa* typing data (Koreen *et al.*, 2004) were available for four of the isolates (MBT16-014, MBT16-017, MBT16-046 and MBT16-057) which clustered together in Group I/MALDI Biotype A; these isolates were identified as *spa* type 07-23-21-16-34-33-13. Typing data are unavailable for the remaining four clinical isolates, making it difficult to draw comparisons between MALDI-TOF MS and reference laboratory typing methods. Care must be taken at this stage not to speculate on the ability of MALDI-TOF MS to correctly differentiate between related and unrelated strains in this cohort. However, these initial data suggest that MALDI-TOF MS typing (combining two data analysis methods) can distinguish between clinical and reference isolates of *S. aureus* in a limited setting. Further work should include a greater number of isolates from multiple outbreaks to include a highly diverse cohort of organisms which could be compared with reference laboratory typing data including *spa* typing.

6.3.2.3. The potential for integration of MALDI-TOF MS typing into routine clinical diagnostics

The work presented in Section 6.3.1: Part 1 of this chapter demonstrates that variability is inherent to numerous stages of the MALDI-TOF MS typing protocol, and could influence a strain typing result. Technical (i.e. intra-spot) reproducibility of the MALDI-TOF MS typing protocol employed in this study was demonstrated to be superior compared to the sample-matrix co-crystallisation step (i.e. inter-spot), and between days. However, whilst every effort can be made to ensure that a standardised workflow is followed (for example, ensuring that organisms are cultured to a set point in their life cycle at the time of analysis and that freshly prepared reagents are used throughout), typing spectra can lack reproducibility and reliability. This must be taken into consideration if the technique would be used to compare strains from different outbreaks, hospitals, or even geographical regions. Furthermore, the work presented in this chapter

demonstrates that different approaches to analysis and interpretation of spectral data can influence a typing result. Whilst the Bruker FlexAnalysis approach might be more accessible to clinical diagnostic laboratories since the software modules are included with the instrument, the analysis workflow is labour intensive and relies on subjective interpretation. Whilst bioinformatics software programmes may offer more objectivity owing in part to a more automated workflow, most of these come at cost and may require specialist training. It has been argued that inclusion of all peaks within entire spectra, as calculated using commercial bioinformatics programmes, could influence sub-species typing analysis because not all peaks will be attributed to strain or clonal differences, therefore potentially over-embellishing the perceived spectra and biasing hierarchal clustering analyses (Ueda *et al.*, 2015). The authors of this study discuss an approach for increasing specificity of the peak calling approach for typing by excluding peak classes that could bias the analysis i.e. those that are species specific and common to all isolates. Other software programmes, such as ClinProTools, exist for analysis of MALDI-TOF MS spectra that have been applied for sequence typing of clinical MRSA isolates (Wang *et al.*, 2018).

Section 6.3.2: Part 2 of this chapter presents an evaluation of MALDI-TOF MS for discriminating between organisms belonging to different strains for two different species; *A. baumannii* and *S. aureus*. Peaks that may potentially be used as strain-specific biomarkers were identified using MALDI-TOF MS, and the technique showed promise for identifying unique organisms within each of the cohorts that is supported by epidemiological and typing data. However, limited context is available since the sample cohorts are small, contain groups of closely related organisms and do not all have reference laboratory typing data available. In addition, the MALDI-TOF MS matrix used in this study could hinder typing of organisms including *A. baumannii* since greater heterogeneity can be observed in ribosomal proteins over 10 kDa (Hortin, 2006). Matrices such as sinapinic acid are better suited for higher molecular weight proteins compared with HCCA. The results presented in this chapter suggest that, regardless of whether standardisation of experimental protocols could yield more reproducible spectra, the resolution of MALDI-TOF MS for strain typing bacteria may be limited. The method has been demonstrated in this work, and elsewhere (Oberle *et al.*, 2016), by rigorous evaluation of sources of experimental error to have the potential for technical robustness. Such robustness has clearly supported the widespread application of MALDI-TOF MS for species identification in routine diagnostics. However, the work

presented here does not fully satisfy the hypothesis that MALDI-TOF MS could become an alternative approach for strain typing bacteria in the routine diagnostic setting at this stage.

6.4. Conclusions

MALDI-TOF MS is an appealing technique for bacterial strain typing in the advent of nosocomial outbreaks, and could be readily accessible to the majority of clinical diagnostic laboratories. However, measurement error is introduced at different stages of the experimental protocol, which may impact upon resolution when assigning biomarker status to peaks. Variability in spectral acquisition is introduced during culture of organisms, protein extraction and data analysis workflow, which can be observed both intra- and inter-experimentally. Culture and sample preparation stages affect peak intensity, which correlates with ionisation efficiency. Variability in ionisation efficiency increases with the progressive stages of the protocol, suggesting that whilst high replication (technical, co-crystallisation and temporal) serves to ensure a robust workflow, care should be taken when interpreting spectra obtained over time as peaks that could be used as strain specific biomarkers could be lost. Furthermore, measurement variability and subsequent biases could result in the appointment of epidemiological significance where none exists in reality (or vice versa). Bioinformatic solutions can remove subjectivity of visual peak calling and offer a less intensive workflow than the Bruker FlexAnalysis method. MALDI-TOF MS strain typing showed promise in identifying potentially unique isolates in two different bacterial models. However, further work on a larger cohort of more diverse organisms is required to establish whether MALDI-TOF MS typing is appropriate for incorporation into routine practice. In-house applicability of MALDI-TOF MS as an initial epidemiological screening tool prior to reference laboratory typing could help to reduce the time taken to make clinical decisions whilst awaiting reference laboratory results, providing an economic overall benefit to patient care.

7. Final discussion

7.1. Experimental variability impacts upon accuracy of molecular measurements of pathogen biomarkers

In Chapters 3, 4, 5 and 6, aspects of experimental workflows that can impact upon the accuracy of molecular measurements were evaluated. Upstream processes were assessed for emerging molecular techniques that could be used to support contemporary diagnostic methods. Accurate measurement of molecular biomarkers for infectious diseases including nucleic acids and proteins permits detection, identification, and quantification of pathogens. This enables monitoring of responses to treatment, prediction of disease severity and outcomes, tracing and controlling disease outbreaks and profiling of organisms to strengthen future responses to pathogenic threats. Understanding the causes of measurement error could improve robustness of methods and allow them to be more reproducible, and enable better harmonisation of results between laboratories. Exploration of these themes is timely, given the fundamental role of molecular diagnostics in line with increasing emergence of global epidemics - including the advent of the COVID-19 pandemic. Discussions surrounding the importance of standardising molecular tests for SARS-CoV-2, namely RT-qPCR, and addressing sources of technical error to promote measurement accuracy have come to light (Huggett *et al.*, 2020a, Dong *et al.*, 2020b, Bustin and Nolan, 2020, Woloshin *et al.*, 2020). These discussions highlight how measurement research can help to promote analytical accuracy in molecular testing, which can assist in the management of existing and emerging infectious diseases.

7.1.1. Sample preparation and extraction of nucleic acids and proteins

Experimental variability in the analysis of nucleic acids and proteins can contribute to measurement error, which can bias interpretation and subsequent reporting of data. In Chapter 5, sample preparation and extraction were identified as contributors to experimental variability in the quantification of *Staphylococcus* spp genomes. Intra- (Figure 5.6) and inter- (Table 5.5) laboratory variability in quantitative estimates of methicillin resistant and sensitive organisms was introduced. This manifested in up to a 7-fold increase in variability following DNA extraction from whole bacterial cells compared to dPCR analysis of pre-extracted genomic DNA (Figure 5.4). Nucleic acid yield has been shown to vary following extraction as a result of differences within

and between extraction protocols (Olson and Morrow, 2012). Previous studies have also suggested that variability is introduced by fragmentation and degradation of nucleic acid during extraction, which has the potential to reduce quantitative accuracy (Sedlackova *et al.*, 2013). This can occur due to physical shearing during pipetting or vortexing of samples, or through chemical shearing (Klingström *et al.*, 2018). Nucleic acids are also vulnerable to degradation by nucleases that can be present in the sample, and in the laboratory environment. The organism *Staphylococcus aureus* features an extracellular nuclease that acts as a virulence factor in infection (Kiedrowski *et al.*, 2014), and it could be hypothesised that this contributes to degradation of nucleic acids isolated from this organism following extraction. Specific challenges also exist when extracting bio-molecules from samples containing Gram positives such as *S. aureus*, which has a peptidoglycan cell wall that requires additional processing to liberate cellular components (Şahin *et al.*, 2016). Similar challenges have been described for extraction of biomolecules from organisms that are phenotypically mucoid such as *K. pneumoniae*. These organisms can be resistant to pelleting by centrifugation, which may interfere with sample preparation (Domenico *et al.*, 1992, Brinkworth *et al.*, 2015, Xiao *et al.*, 2011).

In addition to extraction of nucleic acids, sample-specific challenges were demonstrated in Chapter 6 to be relevant for the extraction of proteins. Variability in the extraction step was demonstrated in Figure 6.2, where different biomass input quantities and unstandardised quantities of extraction reagents resulted in varying numbers of peaks for bacterial strain typing. The sample collection methods used (a solution of cells in saline equivalent to a 0.5 McFarland standard and a 1 µL loop-full of bacterial colonies) rely on subjective interpretation and are limited in their abilities to produce homogenous solutions containing consistent numbers of bacterial cells. Efforts have been made to enhance the quality of spectra obtained during MALDI-TOF MS analysis of bacteria through improved sample preparation. Additional sample preparation steps, such as the addition of glass beads during protein extraction to obtain more homogenous solutions, can improve ID spectra for a range of bacteria including mucoid Gram negatives (Zhou *et al.*, 2017). Standardisation of protocols in MALDI TOF MS analysis, including the extraction step, could help to improve reproducibility for MALDI TOF typing experiments (Oberle *et al.*, 2016).

Considerations surrounding the extraction of molecular analytes within infectious diseases are not limited to bacteria. Further complications can arise when extracting from biological fluids that

contain target which may be present at low levels and be highly fragmented, as can be the case for viruses. Nucleic acids from viral pathogens such as HIV-1, which features in Chapters 3 and 4, require extraction from blood and plasma. Yield and integrity of nucleic acid extracted from plasma samples has been shown to vary considerably between protocols, with pre-analytical variability in handling of plasma samples notably affecting analytical results (Markus *et al.*, 2018). As discussed above, some of this variability was attributed to fragmentation of cfDNA; a phenomenon associated with this type of analysis that is more commonly utilised in cancer liquid biopsy studies (Bronkhorst *et al.*, 2019). In the context of infection, DNA fragmentation has been demonstrated to be a particular issue for quantification of viruses such as human cytomegalovirus (HCMV) (Boom *et al.*, 2002). In addition, interest in utilising cfDNA as a biomarker for infection with *M. tuberculosis* has been described (Fernandez-Carballo *et al.*, 2019) indicating the need for careful consideration when selecting DNA isolation protocols for development of these type of assays. Variability in nucleic acid extraction from samples containing viruses was not extensively explored in this thesis. However, it is worth mentioning that efforts have been made to optimise extraction protocols for clinical analysis of HIV-1 which features prominently in Chapter 3 (Verhofstede *et al.*, 1996). Modern extraction protocols for isolating HIV-1 RNA for viral load testing are largely automated; a technology that lends itself to high throughput capabilities required of diagnostic laboratories. However, despite automated approaches for sample preparation and extraction becoming commonplace in clinical laboratories, challenges can arise owing to limited opportunities for manual troubleshooting in the event of erroneous results (Tan and Yiap, 2013).

7.1.2. Efficiency of enzymatic processes for molecular biology

Enzymatic processes are widely utilised within molecular diagnostics, involving DNA/RNA polymerases, restriction endonucleases and reverse transcriptases (Rittié and Perbal, 2008). Enzymes work most efficiently within specific temperature and pH ranges, which vary depending on the enzyme. Any variations in reaction conditions can alter the efficiency of enzymatic reactions (Zippelius *et al.*, 2000). This could become problematic when enzymatic processes are required for accurate and sensitive quantification of low levels of target, such as for HIV-1 RNA viral load quantification (Levesque-Sergerie *et al.*, 2007). In Chapter 3, the efficiency of different reverse transcriptases for converting HIV-1 RNA to cDNA were evaluated using RT-dPCR.

Quantitative estimates of HIV-1 copy numbers varied between enzymes, which were dependent on the assay sequence used (Figure 3.3). Differences in copy number estimates due to variability in enzymatic processes could result in inaccuracies in reported HIV-1 RNA copy numbers following RT PCR. Ideally, a reverse transcriptase enzyme would be 100% efficient at converting RNA to cDNA, enabling all viral genomes to be converted, amplified during PCR and detected. However, variability in the reverse transcription step has been described previously at magnitudes great enough (differences of up to 100-fold) to warrant caution over maintenance of data validity (Bustin *et al.*, 2015). Variability in reverse transcription efficiency is a widely acknowledged complication associated with RNA quantification (Bustin and Nolan, 2004, Sanders *et al.*, 2013, Zucha *et al.*, 2019). This merits consideration when utilising the technique in diagnostic approaches to permit the highest degree of measurement accuracy for the most sensitive applications. The findings in Chapter 3 support those of Okello *et al.*, (2010), who performed a comparative RT-qPCR analysis of 11 commercially available reverse transcriptase enzymes addressing their sensitivity for quantification of low copy numbers of HIV-1 RNA. The authors describe how although some enzymes were sufficiently sensitive, they lacked reproducibility and suffered reduced overall amplification efficiency. Comparisons were made based on qPCR, which relies on an accurate and stable calibration curve to make relative estimates of copy number concentration in a sample (Okello *et al.*, 2010). RT-dPCR can provide absolute copy number estimations of HIV-1 RNA based on a standardised input of RNA (Figure 3.4). This may allow enzyme efficiency to be evaluated, and could improve the accuracy of qPCR calibration curves by factoring this in.

Technical challenges exist that are inherent to quantification of viral RNA genomes, including those of HIV-1, influenza, and SARS-CoV-2. RNA is susceptible to hydrolysis by highly stable RNase enzymes, and clinical quantification requires careful consideration surrounding its handling and storage (Relova *et al.*, 2018). Efficient reverse transcription represents a key aspect of analytical accuracy in RNA quantification. Facilitating an understanding of the fundamental sources of measurement error related to key steps in clinical molecular approaches could help to ensure data traceability, reliability, and quality. Studies employing strategies similar to those presented in Chapter 3 have been applied to assess reverse transcription efficiency for transcriptomics experiments using dPCR (Sanders *et al.*, 2013, Schwaber *et al.*, 2019). Concurrent with the work presented in this thesis, the authors discuss how reverse transcription

can be strongly influenced by choice of gene sequence, and advocate for the inclusion of RNA standards in quantitative RT-PCR experiments.

7.1.3. Variability in analysis and interpretation of molecular data

Reproducible data analysis workflows are necessary to ensure accurate interpretation of results for molecular diagnostics. Variability could arise from differences in analyst experience, lack of guidance in data handling, and storing large volumes of complex data that are challenging to handle. Ensuring consistency in data analysis between laboratories, such as through standardised workflows, could help to ensure that results are interpreted in a reproducible manner. In Chapter 4, measurement bias was evidenced for qPCR quantification of HIV-1 DNA when following the assumption that the 8E5 cell line calibrator contained one integrated copy of HIV-1 DNA per cell. dPCR characterisation of three different sources of this cell line, and subsequent re-calculation of qPCR estimates, enabled harmonisation of qPCR results for quantification of HIV-1 DNA calibrated against an 8E5 cell line standard curve (Figure 4.3). This work illustrates how empirical characterisation of reference standards, combined with guidance on how qPCR is calibrated using these standards, could improve measurement accuracy through better comparability between results. Future work briefly discussed in Chapter 4 would also aim to address the adopted convention of normalising HIV-1 DNA copies to one million cells, which could skew estimates of HIV-1 total DNA contributing to the viral reservoir.

In addition to nucleic acid analysis, there is an increased need for reproducible analysis pipelines to interpret the large and complex data outputs from proteomic techniques such as MALDI-TOF MS (Kulkarni *et al.*, 2018, Kim *et al.*, 2018). In Chapter 6, choice of data analysis method was shown to impact upon peak classification and subsequent strain profiling using MALDI-TOF MS. Analyses using bioinformatics software programmes including BioNumerics were compared to the Bruker FlexAnalysis approach, the latter method involving user interpretation of mass spectra. MALDI-TOF MS spectral profiles, which are analogue in nature, are visually inspected to ascertain which peaks may represent strain-specific biomarkers. Differences in how isolates were classified in terms of 'Biotype' were observed between the two methods attributed to the relative degrees of subjectivity in the approaches (Table 6.2, Table 6.3). In addition, the FlexAnalysis method was found to be more laborious to perform in this study, which possibly contributes to a high user error rate in comparison to the bioinformatics approaches. Little information is available in terms of user

guidance from which MALDI-TOF MS data analyses could benefit (Spinali *et al.*, 2015). Efforts have been made to develop tools for reproducible analysis of spectral data, such as that produced during MALDI experiments (Palarea-Albaladejo *et al.*, 2018, Veselkov *et al.*, 2018). The study by Mitchell *et al.* (2015) suggested that a major component of variability in MALDI-TOF MS analyses relates to the algorithms used for binning of raw data in TOF experiments, and proposed that such issues could be circumvented by applying a spectrum averaging approach. The authors suggest that this approach could be readily incorporated into existing automated acquisition software to enhance the performance of MALDI-TOF MS (Mitchell *et al.*, 2015). Further studies introducing novel matrix-mining workflows for analysis of spectral data have been conducted to facilitate reproducibility in MS results (Zhvansky *et al.*, 2019). Standardised approaches to data analysis can help to make results more reproducible between analysts, experiments, and laboratories. Understanding sources of error introduced during the data analysis step could also assist in the development of new methods for molecular diagnosis of infections.

7.2. Development of reference methods and materials holds a key role in promoting measurement accuracy

Clinical quantification of nucleic acids from pathogens is performed using techniques such as qPCR. This requires a standard curve to be constructed from a reference material containing a known quantity of the target of interest. Measurement error associated with the calibration curve will be reflected in quantitative estimates for clinical samples, highlighting the importance of using a stable calibration standard where the target quantity can be assured with a high degree of confidence. In Chapter 4, the impact of instability in qPCR calibration materials was explored for quantification of HIV-1 proviral DNA. dPCR analysis of the widely used 8E5 cell line revealed a previously undetected loss of HIV-1 DNA from the cells which was exacerbated by culture (Figure 4.2). This instability, which was heterogeneous between different sources of the cell line, contributed to measurement error when quantifying HIV-1 DNA in clinical samples due to bias introduced by the calibration curve (Figure 4.1). The differences observed between three sources of 8E5 cell line DNA could be representative of different calibration standards used by laboratories for quantification of HIV-1 DNA. dPCR value assignment of the three standards permitted recalculation of HIV-1 DNA copy numbers in clinical samples, allowing harmonisation of results (Figure 4.3). Harmonisation of quantitative estimates between standards, laboratories or studies

would permit better comparability of data. In the context of Chapter 4, this could provide greater confidence in measurements of HIV-1 DNA to predict correlations with the size of the proviral reservoir, the impact of treatment cessation and, potentially, cure.

The requirement for stable, high quality reference standards to facilitate accuracy in qPCR measurements has been discussed (Röder *et al.*, 2010, Lin *et al.*, 2011, Nolan *et al.*, 2013). Better accessibility of reference standards could permit better harmonisation of quantitative findings between laboratories to demonstrate method reproducibility (Pavsic *et al.*, 2015, Devonshire *et al.*, 2016a). dPCR has been implicated for supporting existing qPCR-based quantitative diagnostic methods through characterisation of reference materials used for standard curve calibration (Bhat and Emslie, 2016). dPCR could be used to assign copy number values to existing reference materials, such as the 8E5 cell line for HIV-1 DNA quantification in Chapter 4. Similarly, the technique could be used as a reference method to characterise novel materials for nucleic acid quantification during their development. In Chapter 5, novel materials that could be used to support current contemporary approaches for diagnosis of MRSA were introduced and analysed using dPCR. These consisted of lyophilised units of bacteria (*Staphylococcus* spp) that could potentially be developed as candidate reference materials. However, despite the precision offered by dPCR quantification, variability in DNA extraction efficiency was suspected to lead to low intra- and inter-laboratory reproducibility between quantitative values. Further work to evaluate the experimental variables contributing to measurement error for these materials could aid their development as quantitative reference materials. In Chapter 3, RT-dPCR was also evaluated as a reference method for quantification of HIV-1 RNA that could be used to value assign prospective reference materials. Analysis of whole viral EQA materials by two National Measurement Institutes (NMIs) demonstrated good intra- and inter-laboratory reproducibility, supporting the development of RT-dPCR as reference method for this application (Figure 3.10). However, issues surrounding analysis of samples containing low concentrations of HIV-1 RNA could hinder reporting of results where there is a high incidence of molecular dropout (Whale *et al.*, 2013).

Despite these challenges, the findings in Chapters 3, 4 and 5 illustrate a potential role for dPCR to value assign nucleic acid reference materials and characterise issues such as cell line instability and sequence heterogeneity. This could make dPCR a valuable tool for development of reference materials for new and emerging infectious diseases that could be used to harmonise

results of molecular testing. The role of dPCR in the value assignment of reference materials has been described for numerous pathogenic organisms including HCMV, *E. coli*, BK and JC viruses (Kuypers and Jerome, 2017), genetically modified organisms (Dobnik *et al.*, 2018) and plasmid standards (Sivaganesan *et al.*, 2018), and for cancer variants including KRAS (Whale *et al.*, 2018, Dong *et al.*, 2018, He *et al.*, 2019). The precision of dPCR could help to characterise measurement uncertainty values assigned to materials. Large measurement uncertainty ranges on reference standards could limit measurement confidence, which could impact upon quantitative accuracy when analysing unknown test samples.

There is a pressing need for biologicals and reference materials for molecular analysis of infectious diseases, along with suitable methods to characterise them ready for the end user. In addition to standards for nucleic acid quantification, availability of suitable materials for qualitative analyses are also important because they enable processes to be monitored for quality (i.e. positive and negative controls). This is important for spectral techniques, including MALDI-TOF MS, where characteristic profiles are generated within defined measurement tolerances calibrated using a standard solution. Any inaccuracy in the standard could invalidate or bias the test sample results, potentially reducing the accuracy and reproducibility of the spectral data. The role of qualitative reference materials for molecular diagnosis of infection was not extensively studied in this thesis, though there remains a need to ensure their availability. Efforts to develop, characterise and promote the use of reference materials for infectious diseases are underway (Morris *et al.*, 2019). Emerging molecular methods can present as useful tools to develop reference materials where pathogens are novel or emerging, or where assays and methodologies lack thorough standardisation (Mattiuzzo *et al.*, 2019).

7.3. Advanced molecular approaches can support measurement accuracy for current diagnostic methods, and may hold a future role for direct analysis of clinical samples

Chapters 3, 4 and 5 demonstrated that dPCR, an emerging method for precise quantification of nucleic acid, can be utilised to explore sources of error in quantification of pathogens and improve measurement accuracy. This includes the role of dPCR for value assignment of reference materials that can be used to calibrate current methods. However, the desire to implement advanced molecular methods for direct analysis of patient samples is prevalent within the field of

infectious disease diagnostics. Methods offering high sensitivity, increased throughput, high resolution for comprehensive analyses of genomes and proteomes, and the potential for improved measurement accuracy may present as attractive options for analysing complex samples (Gwinn *et al.*, 2017).

Chapters 4 and 5 examined the applicability of dPCR for direct analysis of clinical samples. Interest in this application has increased owing to the analytical sensitivity, declining running costs and perceptions of the accuracy of dPCR results (Bizouarn, 2014). dPCR can offer precise measurements, quantification independent of a calibration curve, intra and inter-laboratory reproducibility and the potential for sample analysis without the need for nucleic acid extraction (Kuypers and Jerome, 2017). However, the work presented in these chapters (along with Chapter 3) has highlighted the sources of measurement error specific to dPCR that are introduced by variability within the methodology, along with biological variability from the sample. Issues surrounding reduced sample volumes may limit accuracy and therefore hinder uptake of the technique, particularly for measurement of low-level targets. False positive amplification in dPCR reactions has also been reported as a potential limitation compared to other methods (Strain *et al.*, 2013, Rutsaert *et al.*, 2018b). False positives are often attributed to contamination of a reaction with positive control template. However, in some cases there could be other reasons such as coalescence of oil emulsion droplets (Sreejith *et al.*, 2018) or improper assay design (Quan *et al.*, 2018).

Chapters 4 and 5 respectively demonstrated that dPCR analysis of residual clinical extracts containing HIV-1 DNA and *Staphylococcus* spp targets was comparable to qPCR. However, additional work utilising a larger sample cohort and demonstrating a clear advantage of the technique over qPCR is required before suggestions can be made towards its incorporation into routine practices. This may be within reach since the commercialisation of the IVD/CE-IVD QXDx BCR-ABL %IS Kit for dPCR quantification of BCR-ABL fusion transcripts in patients with Chronic Myeloid Leukaemia (CML) (Chung *et al.*, 2020). In line with current opinion (Huggett *et al.*, 2015), dPCR is promoted in this thesis as an available tool for supporting current clinical methods through characterisation of reference materials and inter-laboratory comparisons. This can offer improvements to the accuracy of clinical measurements in patient samples.

In contrast to dPCR, MALDI-TOF MS is already widely utilised in clinical diagnostics as a reproducible method for species identification (Mellmann *et al.*, 2009). The work presented in

Chapter 6 aimed to characterise the applicability of the technique for sub-species strain analysis to help resolve nosocomial outbreaks. The method was demonstrated in Section 6.3.1 to be inherently variable owing to culture and sample preparation steps, which could contribute to poor strain typing performance. As presented in Section 6.3.2, MALDI-TOF MS typing potentially revealed a distinct cluster in a group of *A. baumannii* isolates that were classified as being the same strain based on VNTR profiling. The MALDI-TOF typing result, supported by epidemiological data and whole genome sequencing, suggests that MALDI-TOF MS could have a supporting role in discriminating between different strains of bacteria. However, the strain typing results lacked reliability which may be attributed to poor repeatability of spectra. This, combined with limited availability of reference isolates available for the typing comparison, limits the use of MALDI-TOF MS for sub-species analysis of clinical isolates in this work. Advocating steps towards reproducibility in MALDI-TOF MS analyses could improve the uptake of the method for the most precise and sensitive applications (O'Rourke *et al.*, 2016).

8. Concluding remarks and future work

The 'perfect' diagnostic tool has been described as one which is rapid, specific, sensitive, easy to perform and interpret, cost-effective and high throughput (Chen *et al.*, 2018). Many of these criteria are underpinned by the ability of the diagnostic method to perform measurements that are of the highest possible analytical accuracy. In a metrological sense, measurement accuracy might imply that the method exceeds the necessary standards for measurement precision and sources of bias are minimised, enabling the highest degree of measurement trueness. Defining the sources of error that can impact upon measurement trueness in analytical processes can help to ensure that measurements of pathogen biomarkers for diagnosis of infection are accurate. The work presented in this thesis illustrates for different molecular techniques and diseases that measurement error is introduced at various stages of the workflow including: pre-analytical variables such as sample preparation and extraction, variability in data analysis, unstable reference materials and inherent variability in certain sample types. The themes explored in this thesis support the hypothesis that no one aspect of an experimental workflow is the ultimate contributor to making the most accurate measurements.

Molecular approaches capable of making advanced measurements of nucleic acids and proteins, such as dPCR, MALDI-TOF MS and NGS, are becoming highly sought after for analysis of pathogens in clinical samples. Whilst these approaches may offer advantages over currently used methodologies, laboratories must adopt stringent practices for characterising performance before incorporating them into routine workflows. Rigorous assessment can help to identify stages in experimental protocols that can introduce variability and, subsequently, measurement error into analytical methods. These approaches can themselves be applied to support existing methods in infectious disease diagnostics, such as through characterisation of reference materials used for calibration. Improved accuracy in molecular measurements of pathogens could be facilitated by laboratories that strive to 1) evaluate sources of experimental variability, such as extraction or enzyme efficiency, that contribute to measurement error and subsequently inform decisions on the best reagents or protocols to use, 2) strive to use well characterised reference materials that are of the highest quality to enable proper calibration and verification of methods, 3) take advantage of advanced methodologies to complement current workflows through characterisation of reference materials, or as orthogonal approaches. This will help to ensure method reliability

and facilitate confidence in measurements, which could permit greater measurement accuracy for the most sensitive applications.

This thesis contributes to the field by exploring measurement challenges for quantifying and characterising pathogen biomarkers for different diseases. Each chapter discusses how these challenges can be met, through the application of methods capable of making advanced measurements. The work also demonstrates the importance of standardised methodologies, data transparency and harmonisation of results that will strengthen collaborative efforts in achieving the most accurate measurements of pathogens. Future developments leading on from this work could include: further interlaboratory collaboration for measuring nucleic acids and proteins to develop quantitative reference standards for molecular testing, including for SARS-CoV-2, empirical characterisation of the intermediate precision of qPCR and dPCR to further define their respective roles in measurement of the HIV-1 proviral reservoir, and further exploration of the analytical accuracy associated with methods for making advanced measurements of pathogen biomarkers, including NGS and FTIR. Furthermore, the metrological themes presented in this thesis can be applied to challenge current and future threats within infection. This includes detecting antimicrobial resistance (AMR), identifying sepsis, and controlling future outbreaks, epidemics and pandemics, as well as applications for non-infectious diseases including precision medicine for cancer. Ultimately, facilitating measurement accuracy in disease diagnostics holds the most benefit to patient care, quietly contributing to improving and sustaining global human health.

9. References

- Acosta Soto, L., Santísima-Trinidad, A. B., Bornay-Llinares, F. J., Martín González, M., Pascual Valero, J. A. & Ros Muñoz, M. 2017. Quantitative PCR and Digital PCR for Detection of *Ascaris lumbricoides* Eggs in Reclaimed Water. *BioMed Research International*, 2017, 7515409.
- Adams, E. R. 2015. Molecular Diagnostics – Current Research and Applications. *Clinical Infectious Diseases*, 60, 1877-1877.
- Adzitey, F., Huda, N. & Ali, G. R. R. 2013. Molecular techniques for detecting and typing of bacteria, advantages and application to foodborne pathogens isolated from ducks. 3 *Biotech*, 3, 97-107.
- Akdogan, A. 2018. Introductory Chapter: Metrology. *In: Akdogan, A. (ed.) Metrology*. IntechOpen.
- Alatoom, A. A., Cunningham, S. A., Ihde, S. M., Mandrekar, J. & Patel, R. 2011. Comparison of direct colony method versus extraction method for identification of gram-positive cocci by use of Bruker Biotyper matrix-assisted laser desorption ionization-time of flight mass spectrometry. *J Clin Microbiol*, 49, 2868-73.
- Albrethsen, J. 2007. Reproducibility in protein profiling by MALDI-TOF mass spectrometry. *Clin Chem*, 53, 852-8.
- Amato, J. C. & Galvez, E. J. 2015. *Physics from Planet Earth - An Introduction to Mechanics: An Introduction to Classical Mechanics*, CRC Press.
- Amendola, A., Marsella, P., Bloisi, M., Forbici, F., Angeletti, C. & Capobianchi, M. R. 2014. Ability of two commercially available assays (Abbott RealTime HIV-1 and Roche Cobas AmpliPrep/Cobas TaqMan HIV-1 Version 2.0) to quantify low HIV-1 RNA Levels (<1,000 copies/milliliter): comparison with clinical samples and NIBSC working reagent for nucleic acid testing assays. *J Clin Microbiol*, 52, 2019-26.
- Ameta, G., Rachuri, S., Fiorentini, X., Mani, M., Fenves, S. J., Lyons, K. W. & Sriram, R. D. 2011. Extending the notion of quality from physical metrology to information and sustainability. *Journal of Intelligent Manufacturing*, 22, 737-750.
- Anderson, E. M. & Maldarelli, F. 2018. Quantification of HIV DNA Using Droplet Digital PCR Techniques. *Curr Protoc Microbiol*, 51, e62.
- Anderson, N. W., Buchan, B. W., Riebe, K. M., Parsons, L. N., Gnacinski, S. & Ledebor, N. A. 2012. Effects of Solid-Medium Type on Routine Identification of Bacterial Isolates by Use of Matrix-Assisted Laser Desorption Ionization–Time of Flight Mass Spectrometry. *Journal of Clinical Microbiology*, 50, 1008-1013.
- Armbruster, D. & Miller, R. R. 2007. The Joint Committee for Traceability in Laboratory Medicine (JCTLM): a global approach to promote the standardisation of clinical laboratory test results. *The Clinical biochemist. Reviews*, 28, 105-113.
- Arnold, R. J., Karty, J. A., Ellington, A. D. & Reilly, J. P. 1999. Monitoring the Growth of a Bacteria Culture by MALDI-MS of Whole Cells. *Analytical Chemistry*, 71, 1990-1996.
- Arts, E. J. & Hazuda, D. J. 2012. HIV-1 antiretroviral drug therapy. *Cold Spring Harbor perspectives in medicine*, 2, a007161-a007161.

- Avettand-Fenoel, V., Chaix, M. L., Blanche, S., Burgard, M., Floch, C., Toure, K., Allemon, M. C., Warszawski, J., Rouzioux, C. & French Pediatric Cohort Study, A.-C. O. G. 2009. LTR real-time PCR for HIV-1 DNA quantitation in blood cells for early diagnosis in infants born to seropositive mothers treated in HAART area (ANRS CO 01). *J Med Virol*, 81, 217-23.
- Avettand-Fenoel, V., Hocqueloux, L., Ghosn, J., Cheret, A., Frange, P., Melard, A., Viard, J. P. & Rouzioux, C. 2016. Total HIV-1 DNA, a Marker of Viral Reservoir Dynamics with Clinical Implications. *Clin Microbiol Rev*, 29, 859-80.
- Aydiner, A., Lüsebrink, J., Schildgen, V., Winterfeld, I., Knüver, O., Schwarz, K., Messler, S., Schildgen, O. & Mattner, F. 2012. Comparison of two commercial PCR methods for methicillin-resistant *Staphylococcus aureus* (MRSA) screening in a tertiary care hospital. *PLoS one*, 7, e43935-e43935.
- Baltimore, D. 1970. RNA-dependent DNA polymerase in virions of RNA tumour viruses. *Nature*, 226, 1209-11.
- Bangsberg, D. R., Perry, S., Charlebois, E. D., Clark, R. A., Roberston, M., Zolopa, A. R. & Moss, A. 2001. Non-adherence to highly active antiretroviral therapy predicts progression to AIDS. *AIDS*, 15, 1181-1183.
- Baran, G., Erbay, A., Bodur, H., Öngürü, P., Akıncı, E., Balaban, N. & Çevik, M. A. 2008. Risk factors for nosocomial imipenem-resistant *Acinetobacter baumannii* infections. *International Journal of Infectious Diseases*, 12, 16-21.
- Barbuddhe, S. B., Maier, T., Schwarz, G., Kostrzewa, M., Hof, H., Domann, E., Chakraborty, T. & Hain, T. 2008. Rapid identification and typing of listeria species by matrix-assisted laser desorption ionization-time of flight mass spectrometry. *Appl Environ Microbiol*, 74, 5402-7.
- Barragán-González, E., López-Guerrero, J. A., Bolufer-Gilabert, P., Sanz-Alonso, M., De la Rubia-Comos, J. & Sempere-Talens, A. 1997. The type of reverse transcriptase affects the sensitivity of some reverse transcription PCR methods. *Clin Chim Acta*, 260, 73-83.
- Barre-Sinoussi, F., Chermann, J. C., Rey, F., Nugeyre, M. T., Chamaret, S., Gruest, J., Dautquet, C., Axler-Blin, C., Vezinet-Brun, F., Rouzioux, C., Rozenbaum, W. & Montagnier, L. 1983. Isolation of a T-lymphotropic retrovirus from a patient at risk for acquired immune deficiency syndrome (AIDS). *Science*, 220, 868-71.
- Bartual, S. G., Seifert, H., Hippler, C., Luzon, M. A., Wisplinghoff, H. & Rodriguez-Valera, F. 2005. Development of a multilocus sequence typing scheme for characterization of clinical isolates of *Acinetobacter baumannii*. *J Clin Microbiol*, 43, 4382-90.
- Beck, I. A., Drennan, K. D., Melvin, A. J., Mohan, K. M., Herz, A. M., Alarcon, J., Piscoya, J., Velazquez, C. & Frenkel, L. M. 2001. Simple, sensitive, and specific detection of human immunodeficiency virus type 1 subtype B DNA in dried blood samples for diagnosis in infants in the field. *J Clin Microbiol*, 39, 29-33.
- Becker, K., Heilmann, C. & Peters, G. 2014. Coagulase-Negative Staphylococci. *Clinical Microbiology Reviews*, 27, 870-926.
- Bekker, L.-G., Alleyne, G., Baral, S., Cepeda, J., Daskalakis, D., Dowdy, D., Dybul, M., Eholie, S., Esom, K., Garnett, G., Grimsrud, A., Hakim, J., Havlir, D., Isbell, M. T., Johnson, L., Kamarulzaman, A., Kasaie, P., Kazatchkine, M., Kilonzo, N., Klag, M., Klein, M., Lewin,

- S. R., Luo, C., Makofane, K., Martin, N. K., Mayer, K., Millett, G., Ntusi, N., Pace, L., Pike, C., Piot, P., Pozniak, A., Quinn, T. C., Rockstroh, J., Ratevosian, J., Ryan, O., Sippel, S., Spire, B., Soucat, A., Starrs, A., Strathdee, S. A., Thomson, N., Vella, S., Schechter, M., Vickerman, P., Weir, B. & Beyrer, C. 2018. Advancing global health and strengthening the HIV response in the era of the Sustainable Development Goals: the International AIDS Society. *The Lancet*, 392, 312-358.
- Benagli, C., Rossi, V., Dolina, M., Tonolla, M. & Petrini, O. 2011. Matrix-Assisted Laser Desorption Ionization-Time of Flight Mass Spectrometry for the Identification of Clinically Relevant Bacteria. *PLoS ONE*, 6, e16424.
- Berger, A., Braner, J., Doerr, H. W. & Weber, B. 1998. Quantification of viral load: clinical relevance for human immunodeficiency virus, hepatitis B virus and hepatitis C virus infection. *Intervirology*, 41, 24-34.
- Bharucha, T., Oeser, C., Balloux, F., Brown, J. R., Carbo, E. C., Charlett, A., Chiu, C. Y., Claas, E. C. J., de Goffau, M. C., de Vries, J. J. C., Eloit, M., Hopkins, S., Huggett, J. F., MacCannell, D., Morfopoulou, S., Nath, A., O'Sullivan, D. M., Reoma, L. B., Shaw, L. P., Sidorov, I., Simner, P. J., Van Tan, L., Thomson, E. C., van Dorp, L., Wilson, M. R., Breuer, J. & Field, N. 2020. STROBE-metagenomics: a STROBE extension statement to guide the reporting of metagenomics studies. *Lancet Infect Dis*, 20, e251-e260.
- Bhat, S. & Emslie, K. R. 2016. Digital polymerase chain reaction for characterisation of DNA reference materials. *Biomolecular Detection and Quantification*.
- BIPM. 2019. The International System of Units (SI). In: Bureau international des poids et mesures (ed.) 9th edition ed.
- Bizouarn, F. 2014. Clinical applications using digital PCR. *Methods Mol Biol*, 1160, 189-214.
- Blanco, N., Harris, A. D., Rock, C., Johnson, J. K., Pineles, L., Bonomo, R. A., Srinivasan, A., Pettigrew, M. M., Thom, K. A. & the, C. D. C. E. P. 2017. Risk Factors and Outcomes Associated with Multidrug-Resistant *Acinetobacter baumannii* upon Intensive Care Unit Admission. *Antimicrobial agents and chemotherapy*, 62, e01631-17.
- Bland, J. M. & Altman, D. G. 1996. Statistics notes: Measurement error. *BMJ*, 312, 1654.
- Bloom, D. E. & Cadarette, D. 2019. Infectious Disease Threats in the Twenty-First Century: Strengthening the Global Response. *Frontiers in immunology*, 10, 549-549.
- Bode, L. G., van Wunnik, P., Vaessen, N., Savelkoul, P. H. & Smeets, L. C. 2012. Rapid detection of methicillin-resistant *Staphylococcus aureus* in screening samples by relative quantification between the *mecA* gene and the SA442 gene. *J Microbiol Methods*, 89, 129-32.
- Boom, R., Sol, C. J. A., Schuurman, T., Van Breda, A., Weel, J. F. L., Beld, M., Ten Berge, I. J. M., Wertheim-Van Dillen, P. M. E. & De Jong, M. D. 2002. Human cytomegalovirus DNA in plasma and serum specimens of renal transplant recipients is highly fragmented. *Journal of clinical microbiology*, 40, 4105-4113.
- Bosman, K. J., Nijhuis, M., van Ham, P. M., Wensing, A. M., Vervisch, K., Vandekerckhove, L. & De Spiegelaere, W. 2015. Comparison of digital PCR platforms and semi-nested qPCR as a tool to determine the size of the HIV reservoir. *Sci Rep*, 5, 13811.

- Bosman, K. J., Wensing, A. M. J., Pijning, A. E., van Snippenberg, W. J., van Ham, P. M., de Jong, D. M. C., Hoepelman, A. I. M. & Nijhuis, M. 2018. Development of sensitive ddPCR assays to reliably quantify the proviral DNA reservoir in all common circulating HIV subtypes and recombinant forms. *Journal of the International AIDS Society*, 21, e25185.
- Bowers, R. M., Kyrpides, N. C., Stepanauskas, R., Harmon-Smith, M., Doud, D., Reddy, T. B. K., Schulz, F., Jarett, J., Rivers, A. R., Eloie-Fadrosch, E. A., Tringe, S. G., Ivanova, N. N., Copeland, A., Clum, A., Becraft, E. D., Malmstrom, R. R., Birren, B., Podar, M., Bork, P., Weinstock, G. M., Garrity, G. M., Dodsworth, J. A., Yooseph, S., Sutton, G., Glöckner, F. O., Gilbert, J. A., Nelson, W. C., Hallam, S. J., Jungbluth, S. P., Ettema, T. J. G., Tighe, S., Konstantinidis, K. T., Liu, W.-T., Baker, B. J., Rattei, T., Eisen, J. A., Hedlund, B., McMahon, K. D., Fierer, N., Knight, R., Finn, R., Cochrane, G., Karsch-Mizrachi, I., Tyson, G. W., Rinke, C., Kyrpides, N. C., Schriml, L., Garrity, G. M., Hugenholtz, P., Sutton, G., Yilmaz, P., Meyer, F., Glöckner, F. O., Gilbert, J. A., Knight, R., Finn, R., Cochrane, G., Karsch-Mizrachi, I., Lapidus, A., Meyer, F., Yilmaz, P., Parks, D. H., Murat Eren, A., Schriml, L., Banfield, J. F., Hugenholtz, P., Woyke, T. & The Genome Standards, C. 2017. Minimum information about a single amplified genome (MISAG) and a metagenome-assembled genome (MIMAG) of bacteria and archaea. *Nature Biotechnology*, 35, 725-731.
- Brachman, P. S. 2003. Infectious diseases—past, present, and future. *International Journal of Epidemiology*, 32, 684-686.
- Braybrook, J. & Dean, L. 2012. LGC: clinical about clinical measurement. *Bioanalysis*, 4, 125-31.
- Brinkworth, A. J., Hammer, C. H., Olano, L. R., Kobayashi, S. D., Chen, L., Kreiswirth, B. N. & DeLeo, F. R. 2015. Identification of Outer Membrane and Exoproteins of Carbapenem-Resistant Multilocus Sequence Type 258 *Klebsiella pneumoniae*. *PloS one*, 10, e0123219-e0123219.
- Bronkhorst, A. J., Ungerer, V. & Holdenrieder, S. 2019. The emerging role of cell-free DNA as a molecular marker for cancer management. *Biomolecular detection and quantification*, 17, 100087-100087.
- Brotons, P., Bassat, Q., Lanaspá, M., Henares, D., Perez-Arguello, A., Madrid, L., Balcells, R., Acacio, S., Andres-Franch, M., Marcos, M. A., Valero-Rello, A. & Muñoz-Almagro, C. 2017. Nasopharyngeal bacterial load as a marker for rapid and easy diagnosis of invasive pneumococcal disease in children from Mozambique. *PLOS ONE*, 12, e0184762.
- Brown, D., Canton, R., Dubreuil, L., Gatermann, S., Giske, C., MacGowan, A., Martinez-Martinez, L., Mouton, J., Skov, R., Steinbakk, M., Walton, C., Heuer, O., Struelens, M. J., Diaz Hogberg, L. & Kahlmeter, G. 2015. Widespread implementation of EUCAST breakpoints for antibacterial susceptibility testing in Europe. *Euro Surveill*, 20.
- Brukner, I., Longtin, Y., Oughton, M., Forgetta, V. & Dascal, A. 2015. Assay for estimating total bacterial load: relative qPCR normalisation of bacterial load with associated clinical implications. *Diagn Microbiol Infect Dis*, 83, 1-6.
- Brumfield, K. D., Huq, A., Colwell, R. R., Olds, J. L. & Leddy, M. B. 2020. Microbial resolution of whole genome shotgun and 16S amplicon metagenomic sequencing using publicly available NEON data. *PLOS ONE*, 15, e0228899.

- Bruner, K. M., Hosmane, N. N. & Siliciano, R. F. 2015. Towards an HIV-1 cure: measuring the latent reservoir. *Trends Microbiol*, 23, 192-203.
- Bruner, K. M., Murray, A. J., Pollack, R. A., Soliman, M. G., Laskey, S. B., Capoferri, A. A., Lai, J., Strain, M. C., Lada, S. M., Hoh, R., Ho, Y. C., Richman, D. D., Deeks, S. G., Siliciano, J. D. & Siliciano, R. F. 2016. Defective proviruses rapidly accumulate during acute HIV-1 infection. *Nat Med*.
- Bulletin-6407 Droplet Digital™ PCR Applications Guide. Bulletin 6407 Rev A US/EG 13-0579 ed.: Bio-Rad.
- Bunk, D. M. 2007. Reference materials and reference measurement procedures: an overview from a national metrology institute. *The Clinical biochemist. Reviews*, 28, 131-137.
- Burd, E. M. 2010. Validation of laboratory-developed molecular assays for infectious diseases. *Clinical microbiology reviews*, 23, 550-576.
- Busby, E., Whale, A. S., Ferns, R. B., Grant, P. R., Morley, G., Campbell, J., Foy, C. A., Nastouli, E., Huggett, J. F. & Garson, J. A. 2017. Instability of 8E5 calibration standard revealed by digital PCR risks inaccurate quantification of HIV DNA in clinical samples by qPCR. *Scientific Reports*, 7, 1209.
- Bushnell, B. 2014. *BBMap: A Fast, Accurate, Splice-Aware Aligner* [Online]. United States. Available: <https://www.osti.gov/servlets/purl/1241166> [Accessed 10th August 2020].
- Bustin, S., Dhillon, H. S., Kirvell, S., Greenwood, C., Parker, M., Shipley, G. L. & Nolan, T. 2015. Variability of the Reverse Transcription Step: Practical Implications. *Clinical Chemistry*, 61, 202-212.
- Bustin, S. A., Benes, V., Garson, J., Hellemans, J., Huggett, J., Kubista, M., Mueller, R., Nolan, T., Pfaffl, M. W., Shipley, G., Wittwer, C. T., Schjerling, P., Day, P. J., Abreu, M., Aguado, B., Beaulieu, J. F., Beckers, A., Bogaert, S., Browne, J. A., Carrasco-Ramiro, F., Ceelen, L., Ciborowski, K., Cornillie, P., Coulon, S., Cuypers, A., De Brouwer, S., De Ceuninck, L., De Craene, J., De Naeyer, H., De Spiegelare, W., Deckers, K., Dheedene, A., Durinck, K., Ferreira-Teixeira, M., Fieuw, A., Gallup, J. M., Gonzalo-Flores, S., Goossens, K., Heindryckx, F., Herring, E., Hoenicka, H., Icardi, L., Jaggi, R., Javad, F., Karampelias, M., Kibenge, F., Kibenge, M., Kumps, C., Lambertz, I., Lammens, T., Markey, A., Messiaen, P., Mets, E., Morais, S., Mudarra-Rubio, A., Nakiwala, J., Nelis, H., Olsvik, P. A., Perez-Novo, C., Plusquin, M., Remans, T., Rihani, A., Rodrigues-Santos, P., Rondou, P., Sanders, R., Schmidt-Bleek, K., Skovgaard, K., Smeets, K., Tabera, L., Toegel, S., Van Acker, T., Van den Broeck, W., Van der Meulen, J., Van Gele, M., Van Peer, G., Van Poucke, M., Van Roy, N., Vergult, S., Wauman, J., Tshuikina-Wiklander, M., Willems, E., Zaccara, S., Zeka, F. & Vandesompele, J. 2013. The need for transparency and good practices in the qPCR literature. *Nat Methods*, 10, 1063-7.
- Bustin, S. A., Benes, V., Garson, J. A., Hellemans, J., Huggett, J., Kubista, M., Mueller, R., Nolan, T., Pfaffl, M. W., Shipley, G. L., Vandesompele, J. & Wittwer, C. T. 2009. The MIQE guidelines: minimum information for publication of quantitative real-time PCR experiments. *Clin Chem*, 55, 611-22.
- Bustin, S. A. & Nolan, T. 2004. Pitfalls of Quantitative Real-Time Reverse-Transcription Polymerase Chain Reaction. *Journal of Biomolecular Techniques : JBT*, 15, 155-166.

- Bustin, S. A. & Nolan, T. 2020. RT-qPCR Testing of SARS-CoV-2: A Primer. *Int J Mol Sci*, 21.
- Butler, S., Hansen, M. & Bushman, F. 2001. A Quantitative Assay for HIV DNA Integration In Vivo. *Nature Medicine*, 7, 631-634.
- Caliendo, A. M., Gilbert, D. N., Ginocchio, C. C., Hanson, K. E., May, L., Quinn, T. C., Tenover, F. C., Alland, D., Blaschke, A. J., Bonomo, R. A., Carroll, K. C., Ferraro, M. J., Hirschhorn, L. R., Joseph, W. P., Karchmer, T., MacIntyre, A. T., Reller, L. B., Jackson, A. F. & Infectious Diseases Society of, A. 2013. Better tests, better care: improved diagnostics for infectious diseases. *Clinical infectious diseases : an official publication of the Infectious Diseases Society of America*, 57 Suppl 3, S139-S170.
- Cankar, K., Štebih, D., Dreo, T., Žel, J. & Gruden, K. 2006. Critical points of DNA quantification by real-time PCR – effects of DNA extraction method and sample matrix on quantification of genetically modified organisms. *BMC Biotechnology*, 6, 37.
- Carbonnelle, E., Grohs, P., Jacquier, H., Day, N., Tenza, S., Dewailly, A., Vissouarn, O., Rottman, M., Herrmann, J. L., Podglajen, I. & Raskine, L. 2012. Robustness of two MALDI-TOF mass spectrometry systems for bacterial identification. *J Microbiol Methods*, 89, 133-6.
- Carneiro, J., Resende, A. & Pereira, F. 2017. The HIV oligonucleotide database (HIVoligoDB). *Database : the journal of biological databases and curation*, bax005.
- Casabianca, A., Gori, C., Orlandi, C., Forbici, F., Federico Perno, C. & Magnani, M. 2007. Fast and sensitive quantitative detection of HIV DNA in whole blood leucocytes by SYBR green I real-time PCR assay. *Mol Cell Probes*, 21, 368-78.
- Cedillo v. HHS 2007. Respondent's Exhibit QQ: Declaration of Nicholas Chadwick, PhD. No. 98-916V ed.
- Chávez, V. 2019. Chapter 24 - Sources of pre-analytical, analytical and post-analytical errors in the microbiology laboratory. In: Dasgupta, A. & Sepulveda, J. L. (eds.) *Accurate Results in the Clinical Laboratory (Second Edition)*. Elsevier.
- Chen, J.-W., Lau, Y. Y., Krishnan, T., Chan, K.-G. & Chang, C.-Y. 2018. Recent Advances in Molecular Diagnosis of Pseudomonasaeruginosa Infection by State-of-the-Art Genotyping Techniques. *Frontiers in Microbiology*, 9.
- Chevaliez, S., Dauvillier, C., Dubernet, F., Poveda, J.-D., Laperche, S., Hézode, C. & Pawlotsky, J.-M. 2017a. The New Aptima HBV Quant Real-Time TMA Assay Accurately Quantifies Hepatitis B Virus DNA from Genotypes A to F. *Journal of Clinical Microbiology*, 55, 1211-1219.
- Chevaliez, S., Dubernet, F., Dauvillier, C., Hézode, C. & Pawlotsky, J.-M. 2017b. The New Aptima HCV Quant Dx Real-time TMA Assay Accurately Quantifies Hepatitis C Virus Genotype 1-6 RNA. *Journal of Clinical Virology*, 91, 5-11.
- Chi, S. Y., Kim, T. O., Park, C. W., Yu, J. Y., Lee, B., Lee, H. S., Kim, Y. I., Lim, S. C. & Kwon, Y. S. 2012. Bacterial pathogens of ventilator associated pneumonia in a tertiary referral hospital. *Tuberculosis and respiratory diseases*, 73, 32-37.
- Cho, Y. T., Su, H., Wu, W. J., Wu, D. C., Hou, M. F., Kuo, C. H. & Shiea, J. 2015. Biomarker Characterization by MALDI-TOF/MS. *Adv Clin Chem*, 69, 209-54.

- Christner, M., Trusch, M., Rohde, H., Kwiatkowski, M., Schlüter, H., Wolters, M., Aepfelbacher, M. & Hentschke, M. 2014. Rapid MALDI-TOF Mass Spectrometry Strain Typing during a Large Outbreak of Shiga-Toxigenic *Escherichia coli*. *PLOS ONE*, 9, e101924.
- Chun, T.-W., Stuyver, L., Mizell, S. B., Ehler, L. A., Mican, J. A. M., Baseler, M., Lloyd, A. L., Nowak, M. A. & Fauci, A. S. 1997a. Presence of an inducible HIV-1 latent reservoir during highly active antiretroviral therapy. *Proceedings of the National Academy of Sciences*, 94, 13193-13197.
- Chun, T. W., Carruth, L., Finzi, D., Shen, X., DiGiuseppe, J. A., Taylor, H., Hermankova, M., Chadwick, K., Margolick, J., Quinn, T. C., Kuo, Y. H., Brookmeyer, R., Zeiger, M. A., Barditch-Crovo, P. & Siliciano, R. F. 1997b. Quantification of latent tissue reservoirs and total body viral load in HIV-1 infection. *Nature*, 387, 183-8.
- Chung, H. J., Hur, M., Yoon, S., Hwang, K., Lim, H. S., Kim, H., Moon, H. W. & Yun, Y. M. 2020. Performance Evaluation of the QXDx BCR-ABL %IS Droplet Digital PCR Assay. *Annals of laboratory medicine*, 40, 72-75.
- Clark, K., Karsch-Mizrachi, I., Lipman, D. J., Ostell, J. & Sayers, E. W. 2016. GenBank. *Nucleic acids research*, 44, D67-D72.
- Clementi, M., Menzo, S., Bagnarelli, P., Manzin, A., Valenza, A. & Varaldo, P. E. 1993. Quantitative PCR and RT-PCR in virology. *PCR Methods Appl*, 2, 191-6.
- Clouse, K. A., Powell, D., Washington, I., Poli, G., Strebel, K., Farrar, W., Barstad, P., Kovacs, J., Fauci, A. S. & Folks, T. M. 1989. Monokine regulation of human immunodeficiency virus-1 expression in a chronically infected human T cell clone. *J Immunol*, 142, 431-8.
- Cnops, L., van Griensven, J., Honko, A. N., Bausch, D. G., Sprecher, A., Hill, C. E., Colebunders, R., Johnson, J. C., Griffiths, A., Palacios, G. F., Kraft, C. S., Kobinger, G., Hewlett, A., Norwood, D. A., Sabeti, P., Jahrling, P. B., Formenty, P., Kuhn, J. H. & Ariën, K. K. 2016. Essentials of filoviral load quantification. *The Lancet Infectious Diseases*, 16, e134-e138.
- Coggon, D., Rose, G. & Barker, D. 2020. Measurement error and bias. *Epidemiology for the uninitiated*. fourth edition ed. BMJ.
- Coia, J. E., Duckworth, G. J., Edwards, D. I., Farrington, M., Fry, C., Humphreys, H., Mallaghan, C. & Tucker, D. R. 2006. Guidelines for the control and prevention of meticillin-resistant *Staphylococcus aureus* (MRSA) in healthcare facilities. *Journal of Hospital Infection*, 63, S1-S44.
- Corbisier, P., Pinheiro, L., Mazoua, S., Kortekaas, A.-M., Chung, P. Y. J., Gerganova, T., Roebben, G., Emons, H. & Emslie, K. 2015. DNA copy number concentration measured by digital and droplet digital quantitative PCR using certified reference materials. *Analytical and Bioanalytical Chemistry*, 407, 1831-1840.
- Corman, V. M., Landt, O., Kaiser, M., Molenkamp, R., Meijer, A., Chu, D. K., Bleicker, T., Brunink, S., Schneider, J., Schmidt, M. L., Mulders, D. G., Haagmans, B. L., van der Veer, B., van den Brink, S., Wijsman, L., Goderski, G., Romette, J. L., Ellis, J., Zambon, M., Peiris, M., Goossens, H., Reusken, C., Koopmans, M. P. & Drosten, C. 2020. Detection of 2019 novel coronavirus (2019-nCoV) by real-time RT-PCR. *Euro Surveill*, 25.
- Corpet, F. 1988. Multiple sequence alignment with hierarchical clustering. *Nucleic Acids Res*, 16, 10881-90.

- Coxon, C. H., Longstaff, C. & Burns, C. 2019. Applying the science of measurement to biology: Why bother? *PLOS Biology*, 17, e3000338.
- Craigie, R. & Bushman, F. D. 2012. HIV DNA integration. *Cold Spring Harb Perspect Med*, 2, a006890.
- Croucher, N. J., Page, A. J., Connor, T. R., Delaney, A. J., Keane, J. A., Bentley, S. D., Parkhill, J. & Harris, S. R. 2015. Rapid phylogenetic analysis of large samples of recombinant bacterial whole genome sequences using Gubbins. *Nucleic Acids Res*, 43, e15.
- Croxatto, A., Prod'hom, G. & Greub, G. 2012. Applications of MALDI-TOF mass spectrometry in clinical diagnostic microbiology. *FEMS Microbiology Reviews*, 36, 380-407.
- D'Amato, R. F., Wallman, A. A., Hochstein, L. H., Colaninno, P. M., Scardamaglia, M., Ardila, E., Ghouri, M., Kim, K., Patel, R. C. & Miller, A. 1995. Rapid diagnosis of pulmonary tuberculosis by using Roche AMPLICOR *Mycobacterium tuberculosis* PCR test. *Journal of clinical microbiology*, 33, 1832-1834.
- Daar, E. S., Moudgil, T., Meyer, R. D. & Ho, D. D. 1991. Transient High Levels of Viremia in Patients with Primary Human Immunodeficiency Virus Type 1 Infection. *New England Journal of Medicine*, 324, 961-964.
- Darton, T., Guiver, M., Naylor, S., Jack, D. L., Kaczmarek, E. B., Borrow, R. & Read, R. C. 2009. Severity of meningococcal disease associated with genomic bacterial load. *Clin Infect Dis*, 48, 587-94.
- David, M. Z. & Daum, R. S. 2017. Treatment of *Staphylococcus aureus* Infections. *Curr Top Microbiol Immunol*, 409, 325-383.
- De Bièvre, P. 2010. Making measurement results metrologically traceable to SI units requires more than just expressing them in SI units. *Accreditation and Quality Assurance*, 15, 267-268.
- De Bruyne, K., Slabbinck, B., Waegeman, W., Vauterin, P., De Baets, B. & Vandamme, P. 2011. Bacterial species identification from MALDI-TOF mass spectra through data analysis and machine learning. *Syst Appl Microbiol*, 34, 20-9.
- De Mey, M., Lequeux, G. J., Maertens, J., De Muynck, C. I., Soetaert, W. K. & Vandamme, E. J. 2008. Comparison of protein quantification and extraction methods suitable for *E. coli* cultures. *Biologicals*, 36, 198-202.
- Deichmann, M., Bentz, M. & Haasa, R. 1997. Ultra-sensitive FISH is a useful tool for studying chronic HIV-1 infection. *Journal of Virological Methods*, 65, 19-25.
- Dekker, J. P. 2018. Metagenomics for Clinical Infectious Disease Diagnostics Steps Closer to Reality. *Journal of Clinical Microbiology*, 56, e00850-18.
- Demeke, T. & Jenkins, G. R. 2010. Influence of DNA extraction methods, PCR inhibitors and quantification methods on real-time PCR assay of biotechnology-derived traits. *Analytical and Bioanalytical Chemistry*, 396, 1977-1990.
- Deprez, L., Corbisier, P., Kortekaas, A. M., Mazoua, S., Beaz Hidalgo, R., Trapmann, S. & Emons, H. 2016. Validation of a digital PCR method for quantification of DNA copy number concentrations by using a certified reference material. *Biomol Detect Quantif*, 9, 29-39.

- Desire, N., Dehee, A., Schneider, V., Jacomet, C., Goujon, C., Girard, P. M., Rozenbaum, W. & Nicolas, J. C. 2001. Quantification of human immunodeficiency virus type 1 proviral load by a TaqMan real-time PCR assay. *J Clin Microbiol*, 39, 1303-10.
- Devonshire, A., Whale, A., Gutteridge, A., Jones, G., Cowen, S., Foy, C. & Huggett, J. 2014a. Towards Standardisation of Cell-Free DNA Measurement in Plasma: Controls for Extraction Efficiency, Fragment Size Bias and Quantification (Electronic Supplementary Material). *Analytical and Bioanalytical Chemistry*.
- Devonshire, A. S., Honeyborne, I., Gutteridge, A., Whale, A. S., Nixon, G., Wilson, P., Jones, G., McHugh, T. D., Foy, C. A. & Huggett, J. F. 2015. Highly reproducible absolute quantification of *Mycobacterium tuberculosis* complex by digital PCR. *Anal Chem*, 87, 3706-13.
- Devonshire, A. S., O'Sullivan, D. M., Honeyborne, I., Jones, G., Karczmarczyk, M., Pavsic, J., Gutteridge, A., Milavec, M., Mendoza, P., Schimmel, H., Van Heuverswyn, F., Gorton, R., Cirillo, D. M., Borroni, E., Harris, K., Barnard, M., Heydenrych, A., Ndusilo, N., Wallis, C. L., Pillay, K., Barry, T., Reddington, K., Richter, E., Mozioglu, E., Akyurek, S., Yalcinkaya, B., Akgoz, M., Zel, J., Foy, C. A., McHugh, T. D. & Huggett, J. F. 2016a. The use of digital PCR to improve the application of quantitative molecular diagnostic methods for tuberculosis. *BMC Infect Dis*, 16, 366.
- Devonshire, A. S., Sanders, R., Whale, A. S., Nixon, G. J., Cowen, S., Ellison, S. L., Parkes, H., Pine, P. S., Salit, M., McDaniel, J., Munro, S., Lund, S., Matsukura, S., Sekiguchi, Y., Kawaharasaki, M., Granjeiro, J. M., Falagan-Lotsch, P., Saraiva, A. M., Couto, P., Yang, I., Kwon, H., Park, S. R., Demsar, T., Zel, J., Blejec, A., Milavec, M., Dong, L., Zhang, L., Sui, Z., Wang, J., Viroonudomphol, D., Prawettongsopon, C., Partis, L., Baoutina, A., Emslie, K., Takatsu, A., Akyurek, S., Akgoz, M., Vonsky, M., Konopelko, L. A., Cundapi, E. M., Urquiza, M. P., Huggett, J. F. & Foy, C. A. 2016b. An international comparability study on quantification of mRNA gene expression ratios: CCQM-P103.1. *Biomol Detect Quantif*, 8, 15-28.
- Devonshire, A. S., Whale, A. S., Gutteridge, A., Jones, G., Cowen, S., Foy, C. A. & Huggett, J. F. 2014b. Towards standardisation of cell-free DNA measurement in plasma: controls for extraction efficiency, fragment size bias and quantification. *Anal Bioanal Chem*, 406, 6499-512.
- Diancourt, L., Passet, V., Nemec, A., Dijkshoorn, L. & Brisse, S. 2010. The Population Structure of *Acinetobacter baumannii*: Expanding Multiresistant Clones from an Ancestral Susceptible Genetic Pool. *PLOS ONE*, 5, e10034.
- Dijkshoorn, L., Ursing, B. M. & Ursing, J. B. 2000. Strain, clone and species: comments on three basic concepts of bacteriology. *J Med Microbiol*, 49, 397-401.
- Dobnik, D., Demšar, T., Huber, I., Gerdes, L., Broeders, S., Roosens, N., Debode, F., Berben, G. & Žel, J. 2018. Inter-laboratory analysis of selected genetically modified plant reference materials with digital PCR. *Analytical and Bioanalytical Chemistry*, 410, 211-221.
- Domenico, P., Marx, J. L., Schoch, P. E. & Cunha, B. A. 1992. Rapid plasmid DNA isolation from mucoid gram-negative bacteria. *Journal of clinical microbiology*, 30, 2859-2863.

- Dong, J., Olano, J. P., McBride, J. W. & Walker, D. H. 2008. Emerging pathogens: challenges and successes of molecular diagnostics. *The Journal of molecular diagnostics : JMD*, 10, 185-197.
- Dong, L., Wang, S., Fu, B. & Wang, J. 2018. Evaluation of droplet digital PCR and next generation sequencing for characterizing DNA reference material for KRAS mutation detection. *Scientific Reports*, 8, 9650.
- Dong, L., Wang, X., Wang, S., Du, M., Niu, C., Yang, J., Li, L., Zhang, G., Fu, B., Gao, Y. & Wang, J. 2020a. Interlaboratory assessment of droplet digital PCR for quantification of BRAF V600E mutation using a novel DNA reference material. *Talanta*, 207, 120293.
- Dong, L., Zhou, J., Niu, C., Wang, Q., Pan, Y., Sheng, S., Wang, X., Zhang, Y., Yang, J., Liu, M., Zhao, Y., Zhang, X., Zhu, T., Peng, T., Xie, J., Gao, Y., Wang, D., Zhao, Y., Dai, X. & Fang, X. 2020b. Highly accurate and sensitive diagnostic detection of SARS-CoV-2 by digital PCR. *Pre-print*.
- Dongngam, C., Chareonsirisuthigul, T. & Limsuwanachot, N. 2015. Development of highly sensitive detection for BCR-ABL transcripts in chronic myeloid leukemia by droplet digital PCR. *Genomics and Genetics*, 8, 150-159.
- Dryden, M., Andradevic, A. T., Bassetti, M., Bouza, E., Chastre, J., Baguneid, M., Esposito, S., Giamarellou, H., Gyssens, I., Nathwani, D., Unal, S., Voss, A. & Wilcox, M. 2015. Managing skin and soft-tissue infection and nosocomial pneumonia caused by MRSA: a 2014 follow-up survey. *Int J Antimicrob Agents*, 45 Suppl 1, S1-14.
- Du, X., Zhu, Y., Song, Y., Li, T., Luo, T., Sun, G., Yang, C., Cao, C., Lu, Y. & Li, M. 2013. Molecular Analysis of Staphylococcus epidermidis Strains Isolated from Community and Hospital Environments in China. *PLOS ONE*, 8, e62742.
- Duncan, M. W., Nedelkov, D., Walsh, R. & Hattan, S. J. 2016. Applications of MALDI Mass Spectrometry in Clinical Chemistry. *Clinical Chemistry*, 62, 134-143.
- Dwivedi, S., Purohit, P., Misra, R., Pareek, P., Goel, A., Khattri, S., Pant, K. K., Misra, S. & Sharma, P. 2017. Diseases and Molecular Diagnostics: A Step Closer to Precision Medicine. *Indian Journal of Clinical Biochemistry*, 32, 374-398.
- Egli, A., Tschudin-Sutter, S., Oberle, M., Goldenberger, D., Frei, R. & Widmer, A. F. 2015. Matrix-assisted laser desorption/ionization time of flight mass-spectrometry (MALDI-TOF MS) based typing of extended-spectrum beta-lactamase producing *E. coli* - a novel tool for real-time outbreak investigation. *PLoS One*, 10, e0120624.
- Eriksson, S., Graf, E. H., Dahl, V., Strain, M. C., Yukl, S. A., Lysenko, E. S., Bosch, R. J., Lai, J., Chioma, S., Emad, F., Abdel-Mohsen, M., Hoh, R., Hecht, F., Hunt, P., Somsouk, M., Wong, J., Johnston, R., Siliciano, R. F., Richman, D. D., O'Doherty, U., Palmer, S., Deeks, S. G. & Siliciano, J. D. 2013. Comparative analysis of measures of viral reservoirs in HIV-1 eradication studies. *PLoS Pathog*, 9, e1003174.
- EURAMET 2015. HLT08 INFECT-MET: Final Publishable report. *Metrology for monitoring infectious diseases, antimicrobial resistance, and harmful micro-organisms*.
- EURAMET 2019. 15HLT07 AntiMicroResist: Final Publishable Report. *Novel materials and methods for the detection, traceable monitoring and evaluation of antimicrobial resistance*.

- Falak, S., Macdonald, R., Busby, E., O'sullivan, D., Milavec, M., Plauth, A., Kammel, M., Zeichhardt, H., Grunert, H., Huggett, J. & Kummrow, A. In preparation. An Assessment of the Reproducibility of Reverse Transcription Digital PCR Quantification of HIV-1 Viral RNA Genome.
- Felton, L. A. 2013. *Remington - Essentials of Pharmaceutics*, Pharmaceutical Press.
- Fenollar, F. & Raoult, D. 2004. Molecular genetic methods for the diagnosis of fastidious microorganisms. *Apmis*, 112, 785-807.
- Fernandez-Carballo, B. L., Broger, T., Wyss, R., Banaei, N. & Denkinger, C. M. 2019. Toward the Development of a Circulating Free DNA-Based In Vitro Diagnostic Test for Infectious Diseases: a Review of Evidence for Tuberculosis. *J Clin Microbiol*, 57.
- Ferreira, L., Sánchez-Juanes, F., Muñoz-Bellido, J. L. & González-Buitrago, J. M. 2011. Rapid method for direct identification of bacteria in urine and blood culture samples by matrix-assisted laser desorption ionization time-of-flight mass spectrometry: intact cell vs. extraction method. *Clinical Microbiology and Infection*, 17, 1007-1012.
- Field, D., Garrity, G., Gray, T., Morrison, N., Selengut, J., Sterk, P., Tatusova, T., Thomson, N., Allen, M. J., Angiuoli, S. V., Ashburner, M., Axelrod, N., Baldauf, S., Ballard, S., Boore, J., Cochrane, G., Cole, J., Dawyndt, P., De Vos, P., DePamphilis, C., Edwards, R., Faruque, N., Feldman, R., Gilbert, J., Gilna, P., Glöckner, F. O., Goldstein, P., Guralnick, R., Haft, D., Hancock, D., Hermjakob, H., Hertz-Fowler, C., Hugenholtz, P., Joint, I., Kagan, L., Kane, M., Kennedy, J., Kowalchuk, G., Kottmann, R., Kolker, E., Kravitz, S., Kyrpides, N., Leebens-Mack, J., Lewis, S. E., Li, K., Lister, A. L., Lord, P., Maltsev, N., Markowitz, V., Martiny, J., Methe, B., Mizrachi, I., Moxon, R., Nelson, K., Parkhill, J., Proctor, L., White, O., Sansone, S.-A., Spiers, A., Stevens, R., Swift, P., Taylor, C., Tateno, Y., Tett, A., Turner, S., Ussery, D., Vaughan, B., Ward, N., Whetzl, T., San Gil, I., Wilson, G. & Wipat, A. 2008. The minimum information about a genome sequence (MIGS) specification. *Nature biotechnology*, 26, 541-547.
- Field, N., Cohen, T., Struelens, M. J., Palm, D., Cookson, B., Glynn, J. R., Gallo, V., Ramsay, M., Sonnenberg, P., Maccannell, D., Charlett, A., Egger, M., Green, J., Vineis, P. & Abubakar, I. 2014. Strengthening the Reporting of Molecular Epidemiology for Infectious Diseases (STROME-ID): an extension of the STROBE statement. *Lancet Infect Dis*, 14, 341-52.
- Fishovitz, J., Hermoso, J. A., Chang, M. & Mobashery, S. 2014. Penicillin-binding protein 2a of methicillin-resistant *Staphylococcus aureus*. *IUBMB life*, 66, 572-577.
- Fitzpatrick, M. A., Ozer, E. A. & Hauser, A. R. 2016. Utility of Whole-Genome Sequencing in Characterizing Acinetobacter Epidemiology and Analyzing Hospital Outbreaks. *J Clin Microbiol*, 54, 593-612.
- Flores-Treviño, S., Garza-González, E., Mendoza-Olazarán, S., Morfín-Otero, R., Camacho-Ortiz, A., Rodríguez-Noriega, E., Martínez-Meléndez, A. & Bocanegra-Ibarias, P. 2019. Screening of biomarkers of drug resistance or virulence in ESCAPE pathogens by MALDI-TOF mass spectrometry. *Scientific Reports*, 9, 18945.
- Folks, T., Powell, D., Lightfoote, M., Koenig, S., Fauci, A., Benn, S., Rabson, A., Daugherty, D., Gendelman, H., Hoggan, M., Venkatesan, S. & Martin, M. 1986. Biological and Biochemical Characterization of a Cloned Leu-3- Cell Surviving Infection with the

- Acquired Immune Deficiency Syndrome Retrovirus. *The Journal of Experimental Medicine*, 164, 280-290.
- Folks, T. M., Clouse, K. A., Justement, J., Rabson, A., Duh, E., Kehrl, J. H. & Fauci, A. S. 1989. Tumor necrosis factor alpha induces expression of human immunodeficiency virus in a chronically infected T-cell clone. *Proc Natl Acad Sci U S A*, 86, 2365-8.
- Folks, T. M., Justement, J., Kinter, A., Dinarello, C. A. & Fauci, A. S. 1987. Cytokine-induced expression of HIV-1 in a chronically infected promonocyte cell line. *Science*, 238, 800-2.
- Foster, T. 1996. Staphylococcus. In: Baron, S. (ed.) *Medical Microbiology*. 4th edition ed. Galveston (TX): University of Texas Medical Branch at Galveston.
- Fryer, J. F., Baylis, S. A., Gottlieb, A. L., Ferguson, M., Vincini, G. A., Bevan, V. M., Carman, W. F. & Minor, P. D. 2008. Development of working reference materials for clinical virology. *J Clin Virol*, 43, 367-71.
- Fuentes-Arderiu, X. 2002. Uncertainty of Measurement in Clinical Microbiology. *EJIFCC*, 13, 129-131.
- Gall, A., Morris, C., Kellam, P. & Berry, N. 2014. Complete Genome Sequence of the WHO International Standard for HIV-1 RNA Determined by Deep Sequencing. *Genome Announcements*, 2, e01254-13.
- Gálvez, C., Urrea, V., Dalmau, J., Jimenez, M., Clotet, B., Monceaux, V., Huot, N., Leal, L., González-Soler, V., González-Cao, M., Müller-Trutwin, M., Sáez-Cirión, A., García, F., Blanco, J., Martínez-Picado, J. & Salgado, M. 2020. Extremely low viral reservoir in treated chronically HIV-1-infected individuals. *EBioMedicine*, 57, 102830.
- Gantzer, M. L. & Miller, W. G. 2012. Harmonisation of Measurement Procedures: how do we get it done? *The Clinical biochemist. Reviews*, 33, 95-100.
- Garrison, E. & Marth, G. 2012. Haplotype-based variant detection from short-read sequencing. *arXiv*, 1207.
- Gart, J. J. *The Poisson Distribution: The Theory and Application of Some Conditional Tests*. 1975 Dordrecht. Springer Netherlands, 125-140.
- Gasteiger, E., Hoogland, C., Gattiker, A., Duvaud, S. e., Wilkins, M. R., Appel, R. D. & Bairoch, A. 2005. Protein Identification and Analysis Tools on the ExPASy Server. In: Walker, J. M. (ed.) *The Proteomics Protocols Handbook*. Totowa, NJ: Humana Press.
- Geraghty, R. J., Capes-Davis, A., Davis, J. M., Downward, J., Freshney, R. I., Knezevic, I., Lovell-Badge, R., Masters, J. R., Meredith, J., Stacey, G. N., Thraves, P., Vias, M. & Cancer Research, U. K. 2014. Guidelines for the use of cell lines in biomedical research. *Br J Cancer*, 111, 1021-46.
- Gerard, G. F., Fox, D. K., Nathan, M. & D'Alessio, J. M. 1997. Reverse Transcriptase. *Molecular Biotechnology*, 8, 61-77.
- Gerard, G. F., Potter, R. J., Smith, M. D., Rosenthal, K., Dhariwal, G., Lee, J. & Chatterjee, D. K. 2002. The role of template-primer in protection of reverse transcriptase from thermal inactivation. *Nucleic acids research*, 30, 3118-3129.
- Ghebremedhin, M., Heitkamp, R., Yesupriya, S., Clay, B. & Crane, N. J. 2017. Accurate and Rapid Differentiation of *Acinetobacter baumannii* Strains by Raman Spectroscopy: a Comparative Study. *J Clin Microbiol*, 55, 2480-2490.

- Ghosh, M. K., Kuhn, L., West, J., Semrau, K., Decker, D., Thea, D. M. & Aldrovandi, G. M. 2003. Quantitation of human immunodeficiency virus type 1 in breast milk. *J Clin Microbiol*, 41, 2465-70.
- Gibellini, D. 2004. Quantitative detection of human immunodeficiency virus type 1 (HIV-1) proviral DNA in peripheral blood mononuclear cells by SYBR green real-time PCR technique. *Journal of Clinical Virology*, 29, 282-289.
- Gill, C., van de Wijgert, J. H. H. M., Blow, F. & Darby, A. C. 2016. Evaluation of Lysis Methods for the Extraction of Bacterial DNA for Analysis of the Vaginal Microbiota. *PLoS one*, 11, e0163148-e0163148.
- Ginocchio, C. 2016. Respiratory infections. In: Leonard, D. G. B. (ed.) *Molecular Pathology in Clinical Practice*. Springer International Publishing.
- Ginocchio, C. C. 2001. HIV-1 Viral Load Testing: Methods and Clinical Applications. *Laboratory Medicine*, 32, 142-152.
- Ginocchio, C. C. 2004. Life beyond PCR: alternative target amplification technologies for the diagnosis of infectious diseases, part I. *Clinical microbiology newsletter*, 26, 121-128.
- Ginocchio, C. C., Kemper, M., Stellrecht, K. A. & Witt, D. J. 2003. Multicenter evaluation of the performance characteristics of the NucliSens HIV-1 QT assay used for quantitation of human immunodeficiency virus type 1 RNA. *J Clin Microbiol*, 41, 164-73.
- Gorchynski, J. & Rose, J. K. 2008. Complications of MRSA Treatment: Linezolid-induced Myelosuppression Presenting with Pancytopenia. *The western journal of emergency medicine*, 9, 177-178.
- Gorton, R. L., Seaton, S., Ramnarain, P., McHugh, T. D. & Kibbler, C. C. 2014. Evaluation of a short, on-plate formic acid extraction method for matrix-assisted laser desorption ionization-time of flight mass spectrometry-based identification of clinically relevant yeast isolates. *Journal of clinical microbiology*, 52, 1253-1255.
- Graffunder, E. M. & Venezia, R. A. 2002. Risk factors associated with nosocomial methicillin-resistant *Staphylococcus aureus* (MRSA) infection including previous use of antimicrobials. *Journal of Antimicrobial Chemotherapy*, 49, 999-1005.
- Greathouse, K. L., Sinha, R. & Vogtmann, E. 2019. DNA extraction for human microbiome studies: the issue of standardization. *Genome Biology*, 20, 212.
- Gu, W., Miller, S. & Chiu, C. Y. 2019. Clinical Metagenomic Next-Generation Sequencing for Pathogen Detection. *Annual review of pathology*, 14, 319-338.
- Gullett, J. C. & Nolte, F. S. 2015. Quantitative nucleic acid amplification methods for viral infections. *Clin Chem*, 61, 72-8.
- Gupta, R. K., Abdul-Jawad, S., McCoy, L. E., Mok, H. P., Peppas, D., Salgado, M., Martinez-Picado, J., Nijhuis, M., Wensing, A. M. J., Lee, H., Grant, P., Nastouli, E., Lambert, J., Pace, M., Salasc, F., Monit, C., Innes, A. J., Muir, L., Waters, L., Frater, J., Lever, A. M. L., Edwards, S. G., Gabriel, I. H. & Olavarria, E. 2019. HIV-1 remission following CCR5Δ32/Δ32 haematopoietic stem-cell transplantation. *Nature*, 568, 244-248.
- Gustafsson, O. J. R., Winderbaum, L. J., Condina, M. R., Boughton, B. A., Hamilton, B. R., Undheim, E. A. B., Becker, M. & Hoffmann, P. 2018. Balancing sufficiency and impact in reporting standards for mass spectrometry imaging experiments. *GigaScience*, 7.

- Gwinn, M., MacCannell, D. R. & Khabbaz, R. F. 2017. Integrating Advanced Molecular Technologies into Public Health. *Journal of Clinical Microbiology*, 55, 703-714.
- Hallerberg, A. E. 1973. The metric system: past, present; future? *The Arithmetic Teacher*, 20, 247-255.
- Hamidian, M., Nigro, S. J. & Hall, R. M. 2017. Problems with the Oxford Multilocus Sequence Typing Scheme for *Acinetobacter baumannii*: Do Sequence Type 92 (ST92) and ST109 Exist? *J Clin Microbiol*, 55, 2287-2289.
- Haque, M., Sartelli, M., McKimm, J. & Abu Bakar, M. 2018. Health care-associated infections - an overview. *Infection and drug resistance*, 11, 2321-2333.
- Hart, P. J., Wey, E., McHugh, T. D., Balakrishnan, I. & Belgacem, O. 2015. A method for the detection of antibiotic resistance markers in clinical strains of *Escherichia coli* using MALDI mass spectrometry. *J Microbiol Methods*, 111, 1-8.
- Hartman, P., Beckman, K., Silverstein, K., Yohe, S., Schomaker, M., Henzler, C., Onsongo, G., Lam, H. C., Munro, S., Daniel, J., Billstein, B., Deshpande, A., Hauge, A., Mroz, P., Lee, W., Holle, J., Wiens, K., Karnuth, K., Kemmer, T., Leary, M., Michel, S., Pohlman, L., Thayanithy, V., Nelson, A., Bower, M. & Thyagarajan, B. 2019. Next generation sequencing for clinical diagnostics: Five year experience of an academic laboratory. *Molecular Genetics and Metabolism Reports*, 19, 100464.
- Hassoun, A., Linden, P. K. & Friedman, B. 2017. Incidence, prevalence, and management of MRSA bacteremia across patient populations—a review of recent developments in MRSA management and treatment. *Critical Care*, 21, 211.
- Hatano, H., Delwart, E. L., Norris, P. J., Lee, T.-H., Dunn-Williams, J., Hunt, P. W., Hoh, R., Stramer, S. L., Linnen, J. M., McCune, J. M., Martin, J. N., Busch, M. P. & Deeks, S. G. 2009. Evidence for Persistent Low-Level Viremia in Individuals Who Control Human Immunodeficiency Virus in the Absence of Antiretroviral Therapy. *Journal of Virology*, 83, 329-335.
- Hayden, R. T., Gu, Z., Ingersoll, J., Abdul-Ali, D., Shi, L., Pounds, S. & Caliendo, A. M. 2013. Comparison of droplet digital PCR to real-time PCR for quantitative detection of cytomegalovirus. *J Clin Microbiol*, 51, 540-6.
- Haynes, R. J., Kline, M. C., Toman, B., Scott, C., Wallace, P., Butler, J. M. & Holden, M. J. 2013. Standard Reference Material 2366 for Measurement of Human Cytomegalovirus DNA. *The Journal of Molecular Diagnostics*, 15, 177-185.
- He, H.-J., Das, B., Cleveland Megan, H., Chen, L., Camalier Corinne, E., Liu, L.-C., Norman Kara, L., Fellowes Andrew, P., McEvoy Christopher, R., Lund Steve, P., Almeida, J., Steffen Carolyn, R., Karlovich, C., Williams, P. M. & Cole Kenneth, D. 2019. Development and interlaboratory evaluation of a NIST Reference Material RM 8366 for EGFR and MET gene copy number measurements. *Clinical Chemistry and Laboratory Medicine (CCLM)*.
- Henegariu, O., Heerema, N. A., Dlouhy, S. R., Vance, G. H. & Vogt, P. H. 1997. Multiplex PCR: critical parameters and step-by-step protocol. *Biotechniques*, 23, 504-11.
- Henrich, T. J., Deeks, S. G. & Pillai, S. K. 2017. Measuring the Size of the Latent Human Immunodeficiency Virus Reservoir: The Present and Future of Evaluating Eradication Strategies. *J Infect Dis*, 215, S134-s141.

- Henrich, T. J., Gallien, S., Li, J. Z., Pereyra, F. & Kuritzkes, D. R. 2012. Low-level detection and quantitation of cellular HIV-1 DNA and 2-LTR circles using droplet digital PCR. *J Virol Methods*, 186, 68-72.
- Hill-Cawthorne, G. A., Hudson, L. O., El Ghany, M. F. A., Piepenburg, O., Nair, M., Dodgson, A., Forrest, M. S., Clark, T. G. & Pain, A. 2014. Recombinations in staphylococcal cassette chromosome mec elements compromise the molecular detection of methicillin resistance in *Staphylococcus aureus*. *PLoS one*, 9, e101419-e101419.
- Hindson, B. J., Ness, K. D., Masquelier, D. A., Belgrader, P., Heredia, N. J., Makarewicz, A. J., Bright, I. J., Lucero, M. Y., Hiddessen, A. L., Legler, T. C., Kitano, T. K., Hodel, M. R., Petersen, J. F., Wyatt, P. W., Steenblock, E. R., Shah, P. H., Bousse, L. J., Troup, C. B., Mellen, J. C., Wittmann, D. K., Erndt, N. G., Cauley, T. H., Koehler, R. T., So, A. P., Dube, S., Rose, K. A., Montesclaros, L., Wang, S., Stumbo, D. P., Hodges, S. P., Romine, S., Milanovich, F. P., White, H. E., Regan, J. F., Karlin-Neumann, G. A., Hindson, C. M., Saxonov, S. & Colston, B. W. 2011. High-throughput droplet digital PCR system for absolute quantitation of DNA copy number. *Analytical chemistry*, 83, 8604-8610.
- Ho, D. D., Moudgil, T. & Alam, M. 1989. Quantitation of Human Immunodeficiency Virus Type 1 in the Blood of Infected Persons. *New England Journal of Medicine*, 321, 1621-1625.
- Hofmann, W. P., Dries, V., Herrmann, E., Gartner, B., Zeuzem, S. & Sarrazin, C. 2005. Comparison of transcription mediated amplification (TMA) and reverse transcription polymerase chain reaction (RT-PCR) for detection of hepatitis C virus RNA in liver tissue. *J Clin Virol*, 32, 289-93.
- Holzkecht, B. J., Dargis, R., Pedersen, M., Pinholt, M. & Christensen, J. J. 2018. Typing of vancomycin-resistant enterococci with MALDI-TOF mass spectrometry in a nosocomial outbreak setting. *Clinical Microbiology and Infection*.
- Honeyborne, I., McHugh, T. D., Phillips, P. P., Bannoo, S., Bateson, A., Carroll, N., Perrin, F. M., Ronacher, K., Wright, L., van Helden, P. D., Walzl, G. & Gillespie, S. H. 2011. Molecular bacterial load assay, a culture-free biomarker for rapid and accurate quantification of sputum *Mycobacterium tuberculosis* bacillary load during treatment. *J Clin Microbiol*, 49, 3905-11.
- Honeyborne, I., Mtafya, B., Phillips, P., Hoelscher, M., Ntinginya, E., Kohlenberg, A., Rachow, A., Rojas-Ponce, G., McHugh, T., Heinrich, N. o. b. o. t. P. A. C. f. t. & (PanACEA), E. o. A.-t. A. 2014. The Molecular Bacterial Load Assay Replaces Solid Culture for Measuring Early Bactericidal Response to Antituberculosis Treatment. *Journal of Clinical Microbiology*, 52, 3064–3067.
- Hortin, G. L. 2006. The MALDI-TOF Mass Spectrometric View of the Plasma Proteome and Peptidome. *Clinical Chemistry*, 52, 1223-1237.
- Hu, W.-S. & Hughes, S. H. 2012. HIV-1 Reverse Transcription. *Cold Spring Harbor Perspectives in Medicine*, 2, a006882.
- Huggett, J., Harris, K., McHugh, T. D., Moran-Gilad, J. & Zumla, A. 2020a. Diagnostic tests for covid-19—improving accuracy and global harmonisation. Available from: <https://blogs.bmj.com/bmj/2020/05/06/diagnostic-tests-for-covid-19-improving-accuracy-and-global-harmonisation/> [Accessed 6th May 2020].

- Huggett, J. F., Benes, V., Bustin, S. A., Garson, J. A., Harris, K., Kammel, M., Kubista, M., McHugh, T. D., Moran-Gilad, J., Nolan, T., Pfaffl, M. W., Salit, M., Shipley, G., Vallone, P. M., Vandesompele, J., Wittwer, C. & Zeichhardt, H. 2020b. Cautionary note on contamination of reagents used for molecular detection of SARS-CoV-2. *Clinical Chemistry*.
- Huggett, J. F., Cowen, S. & Foy, C. A. 2015. Considerations for digital PCR as an accurate molecular diagnostic tool. *Clin Chem*, 61, 79-88.
- Huggett, J. F., Foy, C. A., Benes, V., Emslie, K., Garson, J. A., Haynes, R., Hellemans, J., Kubista, M., Mueller, R. D., Nolan, T., Pfaffl, M. W., Shipley, G. L., Vandesompele, J., Wittwer, C. T. & Bustin, S. A. 2013. The digital MIQE guidelines: Minimum Information for Publication of Quantitative Digital PCR Experiments. *Clin Chem*, 59, 892-902.
- Huggett, J. F., Garson, J. A. & Whale, A. S. 2016. Digital PCR and Its Potential Application to Microbiology. *Molecular Microbiology: Diagnostic Principles and Practice, 3rd Edition*.
- Huggett, J. F. & Whale, A. 2013. Digital PCR as a novel technology and its potential implications for molecular diagnostics. *Clin Chem*, 59, 1691-3.
- Hughes, P., Marshall, D., Reid, Y., Parkes, H. & Gelber, C. 2007. The costs of using unauthenticated, over-passaged cell lines: how much more data do we need? *Biotechniques*, 43, 575, 577-8, 581-2 passim.
- Huletsky, A., Giroux, R., Rossbach, V., Gagnon, M., Vaillancourt, M., Bernier, M., Gagnon, F., Truchon, K., Bastien, M., Picard, F. J., van Belkum, A., Ouellette, M., Roy, P. H. & Bergeron, M. G. 2004. New Real-Time PCR Assay for Rapid Detection of Methicillin-Resistant *Staphylococcus aureus* Directly from Specimens Containing a Mixture of Staphylococci. *Journal of Clinical Microbiology*, 42, 1875-1884.
- Hutcheon, J. A., Chiolerio, A. & Hanley, J. A. 2010. Random measurement error and regression dilution bias. *BMJ*, 340, c2289.
- Íñigo, M., Coello, A., Fernández-Rivas, G., Rivaya, B., Hidalgo, J., Quesada, M. D. & Ausina, V. 2016. Direct Identification of Urinary Tract Pathogens from Urine Samples, Combining Urine Screening Methods and Matrix-Assisted Laser Desorption Ionization–Time of Flight Mass Spectrometry. *Journal of Clinical Microbiology*, 54, 988-993.
- INSTAND 2020. INSTAND EQA scheme (340) Virus Genome Detection Coronaviruses incl. SARS-CoV-2 - June/July 2020. In: Zeichhardt, H. & Kammel, M. (eds.).
- Ito, T., Kuwahara-Arai, K., Katayama, Y., Uehara, Y., Han, X., Kondo, Y. & Hiramatsu, K. 2014. Staphylococcal Cassette Chromosome mec (SCCmec) Analysis of MRSA. In: Ji, Y. (ed.) *Methicillin-Resistant Staphylococcus Aureus (MRSA) Protocols*. Totowa, NJ: Humana Press.
- Iyengar, V. 2007. Metrology in physics, chemistry, and biology: differing perceptions. *Biol Trace Elem Res*, 116, 1-4.
- Jaafoura, S., de Goer de Herve, M. G., Hernandez-Vargas, E. A., Hendel-Chavez, H., Abdoh, M., Mateo, M. C., Krzysiek, R., Merad, M., Seng, R., Tardieu, M., Delfraissy, J. F., Goujard, C. & Taoufik, Y. 2014. Progressive contraction of the latent HIV reservoir around a core of less-differentiated CD4(+) memory T Cells. *Nat Commun*, 5, 5407.

- Jabbour, R. E. & Snyder, A. P. 2014. 14 - Mass spectrometry-based proteomics techniques for biological identification. *In: Schaudies, R. P. (ed.) Biological Identification*. Woodhead Publishing.
- Jamaluddin, T. Z. M. T., Kuwahara-Arai, K., Hisata, K., Terasawa, M., Cui, L., Baba, T., Sotozono, C., Kinoshita, S., Ito, T. & Hiramatsu, K. 2008. Extreme Genetic Diversity of Methicillin-Resistant *Staphylococcus epidermidis* Strains Disseminated among Healthy Japanese Children. *Journal of Clinical Microbiology*, 46, 3778-3783.
- Jeong, S., Hong, J. S., Kim, J. O., Kim, K. H., Lee, W., Bae, I. K., Lee, K. & Jeong, S. H. 2016. Identification of *Acinetobacter* Species Using Matrix-Assisted Laser Desorption Ionization-Time of Flight Mass Spectrometry. *Annals of laboratory medicine*, 36, 325-334.
- Jing, R., Wang, H., Ju, S. & Cui, M. 2018. Reference materials for molecular diagnostics: Current achievements and future strategies. *Clinical biochemistry*, 56, 11-17.
- Johnson, J. K., Robinson, G. L., Zhao, L., Harris, A. D., Stine, O. C. & Thom, K. A. 2016. Comparison of molecular typing methods for the analyses of *Acinetobacter baumannii* from ICU patients. *Diagnostic microbiology and infectious disease*, 86, 345-350.
- Joint Committee for Guides in Metrology 2012. International vocabulary of metrology – Basic and general concepts and associated terms (VIM). 3rd ed.
- Jolley, K. A., Bray, J. E. & Maiden, M. C. J. 2018. Open-access bacterial population genomics: BIGSdb software, the PubMLST.org website and their applications. *Wellcome Open Res*, 3, 124.
- Jones, A. R., Twedt, D., Swaim, W. & Gottfried, E. 1996. Diurnal change of blood count analytes in normal subjects. *Am J Clin Pathol*, 106, 723-7.
- Jones, G. M., Busby, E., Garson, J. A., Grant, P. R., Nastouli, E., Devonshire, A. S. & Whale, A. S. 2016. Digital PCR dynamic range is approaching that of real-time quantitative PCR. *Biomolecular Detection and Quantification*, 10 31–33.
- Jones, G. R. D. 2017. The role of EQA in harmonization in laboratory medicine - a global effort. *Biochimica medica*, 27, 23-29.
- Jones, M., Williams, J., Gartner, K., Phillips, R., Hurst, J. & Frater, J. 2014. Low copy target detection by Droplet Digital PCR through application of a novel open access bioinformatic pipeline, 'definetherain'. *J Virol Methods*, 202, 46-53.
- Jordan, A., Bisgrove, D. & Verdin, E. 2003. HIV reproducibly establishes a latent infection after acute infection of T cells in vitro. *The EMBO journal*, 22, 1868-1877.
- Kabamba-Mukadi, B., Henrivaux, P., Ruelle, J., Delferriere, N., Bodeus, M. & Goubau, P. 2005. Human immunodeficiency virus type 1 (HIV-1) proviral DNA load in purified CD4+ cells by LightCycler real-time PCR. *BMC Infect Dis*, 5, 15.
- Kalmeijer, M. D., van Nieuwland-Bollen, E., Bogaers-Hofman, D. & de Baere, G. A. 2000. Nasal carriage of *Staphylococcus aureus* is a major risk factor for surgical-site infections in orthopedic surgery. *Infect Control Hosp Epidemiol*, 21, 319-23.
- Kang, L., Li, N., Li, P., Zhou, Y., Gao, S., Gao, H., Xin, W. & Wang, J. 2017. MALDI-TOF mass spectrometry provides high accuracy in identification of *Salmonella* at species level but is limited to type or subtype *Salmonella* serovars. *European Journal of Mass Spectrometry*, 23, 70-82.

- Karlsson, E. K., Kwiatkowski, D. P. & Sabeti, P. C. 2014. Natural selection and infectious disease in human populations. *Nature reviews. Genetics*, 15, 379-393.
- Katto, S. 2017. *Development of SI-traceable and High Accurate Method for Quantitative Analysis of DNA*. Doctor of Philosophy in Biotechnology, University of Tsukuba.
- Kelley, K., Cosman, A., Belgrader, P., Chapman, B. & Sullivan, D. C. 2013. Detection of Methicillin-Resistant *Staphylococcus aureus* by a Duplex Droplet Digital PCR Assay. *Journal of Clinical Microbiology*, 51, 2033-2039.
- Kellogg, D. E., Sninsky, J. J. & Kwok, S. 1990. Quantitation of HIV-1 proviral DNA relative to cellular DNA by the polymerase chain reaction. *Anal Biochem*, 189, 202-8.
- Kelly-Cirino, C. D., Nkengasong, J., Kettler, H., Tongio, I., Gay-Andrieu, F., Escadafal, C., Piot, P., Peeling, R. W., Gadde, R. & Boehme, C. 2019. Importance of diagnostics in epidemic and pandemic preparedness. *BMJ Global Health*, 4, e001179.
- Kiedrowski, M. R., Crosby, H. A., Hernandez, F. J., Malone, C. L., McNamara, J. O., 2nd & Horswill, A. R. 2014. *Staphylococcus aureus nuc2* is a functional, surface-attached extracellular nuclease. *PloS one*, 9, e95574-e95574.
- Kielbinski, L. J., Hagedorn, P. H., Lindow, M. & Vinther, J. 2017. RNase H sequence preferences influence antisense oligonucleotide efficiency. *Nucleic acids research*, 45, 12932-12944.
- Kim, J.-U., Cha, C.-H., An, H.-K., Lee, H.-J. & Kim, M.-N. 2013. Multiplex Real-Time PCR Assay for Detection of Methicillin-Resistant *Staphylococcus aureus* (MRSA) Strains Suitable in Regions of High MRSA Endemicity. *Journal of Clinical Microbiology*, 51, 1008-1013.
- Kim, Y.-M., Poline, J.-B. & Dumas, G. 2018. Experimenting with reproducibility: a case study of robustness in bioinformatics. *GigaScience*, 7, giy077.
- Kiselinova, M., De Spiegelaere, W., Buzon, M. J., Malatinkova, E., Lichterfeld, M. & Vandekerckhove, L. 2016. Integrated and Total HIV-1 DNA Predict Ex Vivo Viral Outgrowth. *PLoS Pathog*, 12, e1005472.
- Kiselinova, M., Pasternak, A. O., De Spiegelaere, W., Vogelaers, D., Berkhout, B. & Vandekerckhove, L. 2014. Comparison of Droplet Digital PCR and Seminested Real-Time PCR for Quantification of Cell-Associated HIV-1 RNA. *PLOS ONE*, 9, e85999.
- Klingström, T., Bongcam-Rudloff, E. & Pettersson, O. V. 2018. A comprehensive model of DNA fragmentation for the preservation of High Molecular Weight DNA. *bioRxiv*, 254276.
- Koepfli, C., Nguiragool, W., Hofmann, N. E., Robinson, L. J., Ome-Kaius, M., Sattabongkot, J., Felger, I. & Mueller, I. 2016. Sensitive and accurate quantification of human malaria parasites using droplet digital PCR (ddPCR). *Sci Rep*, 6, 39183.
- Koetsier, G. & Cantor, E. 2019. *A Practical Guide to Analyzing Nucleic Acid Concentration and Purity with Microvolume Spectrophotometers*.
- Koh, C. M. 2013. Chapter Two - Storage of Bacteria and Yeast. In: Lorsch, J. (ed.) *Methods in Enzymology*. Academic Press.
- Kondo, M., Sudo, K., Tanaka, R., Sano, T., Sagara, H., Iwamuro, S., Takebe, Y., Imai, M. & Kato, S. 2009. Quantitation of HIV-1 group M proviral DNA using TaqMan MGB real-time PCR. *J Virol Methods*, 157.
- Koreen, L., Ramaswamy, S. V., Graviss, E. A., Naidich, S., Musser, J. M. & Kreiswirth, B. N. 2004. spa Typing Method for Discriminating among *Staphylococcus aureus* Isolates:

- Implications for Use of a Single Marker To Detect Genetic Micro- and Macrovariation. *Journal of Clinical Microbiology*, 42, 792-799.
- Kothari, A., Morgan, M. & Haake, D. A. 2014. Emerging Technologies for Rapid Identification of Bloodstream Pathogens. *Clinical Infectious Diseases*, 59, 272-278.
- Kralik, P., Beran, V. & Pavlik, I. 2012. Enumeration of *Mycobacterium avium* subsp. paratuberculosis by quantitative real-time PCR, culture on solid media and optical densitometry. *BMC research notes*, 5, 114-114.
- Kralik, P. & Ricchi, M. 2017. A Basic Guide to Real Time PCR in Microbial Diagnostics: Definitions, Parameters, and Everything. *Frontiers in microbiology*, 8, 108-108.
- Kulkarni, N., Alessandrì, L., Panero, R., Arigoni, M., Olivero, M., Ferrero, G., Cordero, F., Beccuti, M. & Calogero, R. A. 2018. Reproducible bioinformatics project: a community for reproducible bioinformatics analysis pipelines. *BMC Bioinformatics*, 19, 349.
- Kulski, J. 2016. Next-Generation Sequencing — An Overview of the History, Tools, and “Omic” Applications. In: Kulski, J. (ed.) *Next Generation Sequencing - Advances, Applications and Challenges*.
- Kuypers, J. & Jerome, K. R. 2017. Applications of Digital PCR for Clinical Microbiology. *J Clin Microbiol*, 55, 1621-1628.
- Larrouy-Maumus, G., Clements, A., Filloux, A., McCarthy, R. R. & Mostowy, S. 2016. Direct detection of lipid A on intact Gram-negative bacteria by MALDI-TOF mass spectrometry. *Journal of microbiological methods*, 120, 68-71.
- Lasch, P., Fleige, C., Stämmler, M., Layer, F., Nübel, U., Witte, W. & Werner, G. 2014. Insufficient discriminatory power of MALDI-TOF mass spectrometry for typing of *Enterococcus faecium* and *Staphylococcus aureus* isolates. *Journal of Microbiological Methods*, 100, 58-69.
- Lee, M. K., Park, K. Y., Jin, T., Kim, J. H. & Seo, S. J. 2017. Rapid Detection of *Staphylococcus aureus* and Methicillin-Resistant *S. aureus* in Atopic Dermatitis by Using the BD Max StaphSR Assay. *Annals of laboratory medicine*, 37, 320-322.
- Lefterova, M. I., Suarez, C. J., Banaei, N. & Pinsky, B. A. 2015. Next-Generation Sequencing for Infectious Disease Diagnosis and Management: A Report of the Association for Molecular Pathology. *The Journal of Molecular Diagnostics*, 17, 623-634.
- Levesque-Sergerie, J.-P., Duquette, M., Thibault, C., Delbecchi, L. & Bissonnette, N. 2007. Detection limits of several commercial reverse transcriptase enzymes: impact on the low- and high-abundance transcript levels assessed by quantitative RT-PCR. *BMC molecular biology*, 8, 93-93.
- Lewis, J. S., Fakile, O., Foss, E., Legarza, G., Leskys, A., Lowe, K. & Powning, D. 1993. Direct DNA probe assay for *Neisseria gonorrhoeae* in pharyngeal and rectal specimens. *Journal of clinical microbiology*, 31, 2783-2785.
- Li, H.-T., Lin, B.-C., Huang, Z.-F., Yang, C.-Z. & Huang, W.-M. 2019. Clinical value of droplet digital PCR in rapid diagnosis of invasive fungal infection in neonates. *Zhongguo dang dai er ke za zhi = Chinese journal of contemporary pediatrics*, 21, 45-51.
- Li, P., Zhao, Z., Wang, Y., Xing, H., Parker, D. M., Yang, Z., Baum, E., Li, W., Sattabongkot, J., Sirichaisinthop, J., Li, S., Yan, G., Cui, L. & Fan, Q. 2014. Nested PCR detection of

- malaria directly using blood filter paper samples from epidemiological surveys. *Malaria Journal*, 13, 175.
- Lim, K., Park, M., Lee, M. H., Woo, H. J. & Kim, J.-B. 2016. Development and Assessment of New RT-qPCR Assay for Detection of HIV-1 Subtypes. *Biomedical Science Letters*, 22, 83-97.
- Lin, C.-H., Chen, Y.-C. & Pan, T.-M. 2011. Quantification bias caused by plasmid DNA conformation in quantitative real-time PCR assay. *PloS one*, 6, e29101-e29101.
- Lindgren, A., Karami, N., Karlsson, R., Ahren, C., Welker, M., Moore, E. R. B. & Stadler, L. S. 2018. Development of a rapid MALDI-TOF MS based epidemiological screening method using MRSA as a model organism. *Eur J Clin Microbiol Infect Dis*, 37, 57-68.
- Lindqvist, R. P., Karlsson, K.-J. & Mattsson, L. 2016. A Theoretical and Practical Approach to Geometrical Part Assurance. *Procedia CIRP*, 43, 351-355.
- Liu, T., Zhang, Y. & Wan, Q. 2018. Methicillin-resistant *Staphylococcus aureus* bacteremia among liver transplant recipients: epidemiology and associated risk factors for morbidity and mortality. *Infection and drug resistance*, 11, 647-658.
- Lodish, H., Berk, A., Zipursky, S. & al, e. 2000. Growth of Microorganisms in Culture. *Molecular Cell Biology*. 4th edition ed. New York: W. H. Freeman.
- Lorenzo-Redondo, R., Fryer, H. R., Bedford, T., Kim, E.-Y., Archer, J., Kosakovsky Pond, S. L., Chung, Y.-S., Penugonda, S., Chipman, J. G., Fletcher, C. V., Schacker, T. W., Malim, M. H., Rambaut, A., Haase, A. T., McLean, A. R. & Wolinsky, S. M. 2016. Persistent HIV-1 replication maintains the tissue reservoir during therapy. *Nature*, 530, 51-56.
- Losada-Urzáiz, F., González-Gaya, C. & Sebastián-Pérez, M. Á. 2015. Metrological Regulations for Quality Control Equipment Calibration in Pharmaceutical Industry. *Procedia Engineering*, 132, 811-815.
- Luo, J., Li, J., Yang, H., Yu, J. & Wei, H. 2017. Accurate Detection of Methicillin-Resistant *Staphylococcus aureus* in Mixtures by Use of Single-Bacterium Duplex Droplet Digital PCR. *J Clin Microbiol*, 55, 2946-2955.
- Madej, R. M., Davis, J., Holden, M. J., Kwang, S., Labourier, E. & Schneider, G. J. 2010. International Standards and Reference Materials for Quantitative Molecular Infectious Disease Testing. *The Journal of Molecular Diagnostics : JMD*, 12, 133-143.
- Madhav, N., Oppenheim, B., Gallivan, M., Mulembakani, P., Rubin, E. & Wolfe, N. 2017. Pandemics: Risks, Impacts, and Mitigation. In: Jamison DT, G. H., Horton S, et al. (ed.) *Disease Control Priorities: Improving Health and Reducing Poverty*. 3rd edition ed. Washington (DC): The International Bank for Reconstruction and Development / The World Bank.
- Madic, J., Zocovic, A., Senlis, V., Fradet, E., Andre, B., Muller, S., Dangla, R. & Droniou, M. E. 2016. Three-color crystal digital PCR. *Biomolecular detection and quantification*, 10, 34-46.
- Malnati, M. S., Scarlatti, G., Gatto, F., Salvatori, F., Cassina, G., Rutigliano, T., Volpi, R. & Lusso, P. 2008. A universal real-time PCR assay for the quantification of group-M HIV-1 proviral load. *Nat Protoc*, 3, 1240-8.

- Manak, M. M., Hack, H. R., Nair, S. V., Worlock, A., Malia, J. A., Peel, S. A. & Jagodzinski, L. L. 2016. Evaluation of Hologic Aptima HIV-1 Quant Dx Assay on the Panther System on HIV Subtypes. *Journal of Clinical Microbiology*, 54, 2575-2581.
- Margolis, D. M., Garcia, J. V., Hazuda, D. J. & Haynes, B. F. 2016. Latency reversal and viral clearance to cure HIV-1. *Science*, 353, aaf6517.
- Markus, H., Contente-Cuomo, T., Farooq, M., Liang, W. S., Borad, M. J., Sivakumar, S., Gollins, S., Tran, N. L., Dhruv, H. D., Berens, M. E., Bryce, A., Sekulic, A., Ribas, A., Trent, J. M., LoRusso, P. M. & Murtaza, M. 2018. Evaluation of pre-analytical factors affecting plasma DNA analysis. *Scientific Reports*, 8, 7375.
- Marx, V. 2017. Microbiology: the return of culture. *Nature Methods*, 14, 37-40.
- Masters, J. R., Thomson, J. A., Daly-Burns, B., Reid, Y. A., Dirks, W. G., Packer, P., Toji, L. H., Ohno, T., Tanabe, H., Arlett, C. F., Kelland, L. R., Harrison, M., Virmani, A., Ward, T. H., Ayres, K. L. & Debenham, P. G. 2001. Short tandem repeat profiling provides an international reference standard for human cell lines. *Proc Natl Acad Sci U S A*, 98, 8012-7.
- Mattiuazzo, G., Ashall, J., Doris, K. S., MacLellan-Gibson, K., Nicolson, C., Wilkinson, D. E., Harvey, R., Almond, N., Anderson, R., Efsthathiou, S., Minor, P. D. & Page, M. 2015. Development of Lentivirus-Based Reference Materials for Ebola Virus Nucleic Acid Amplification Technology-Based Assays. *PLOS ONE*, 10, e0142751.
- Mattiuazzo, G., Bentley, E., Hassall, M., Ashall, J., Wilkinson, D., Rigsby, P., Hockley, J. & Page, M. 2019. Production and application of reference materials for high containment RNA viruses. *International Journal of Infectious Diseases*, 79, 128-129.
- Mazzola, L. & Pérez-Casas, C. 2015. HIV/AIDS Diagnostics Technology Landscape. 5th edition ed.: UNITAID.
- McAdow, M., Missiakas, D. M. & Schneewind, O. 2012. *Staphylococcus aureus* secretes coagulase and von Willebrand factor binding protein to modify the coagulation cascade and establish host infections. *Journal of innate immunity*, 4, 141-148.
- McFall, S. M., Wagner, R. L., Jangam, S. R., Yamada, D. H., Hardie, D. & Kelso, D. M. 2015. A simple and rapid DNA extraction method from whole blood for highly sensitive detection and quantitation of HIV-1 proviral DNA by real-time PCR. *J Virol Methods*, 214, 37-42.
- McFarland, J. 1907. The Nephelometer: An Instrument for Estimating the Number of Bacteria in Suspensions Used for Calculating the Opsonic Index and For Vaccines. *JAMA*, XLIX, 1176-1178.
- McOrist, A. L., Jackson, M. & Bird, A. R. 2002. A comparison of five methods for extraction of bacterial DNA from human faecal samples. *Journal of Microbiological Methods*, 50, 131-139.
- Mediavilla-Gradolph, M. C., De Toro-Peinado, I., Bermúdez-Ruiz, M. P., García-Martínez, M. d. I. Á., Ortega-Torres, M., Montiel Quezel-Guerraz, N. & Palop-Borrás, B. 2015. Use of MALDI-TOF MS for Identification of Nontuberculous *Mycobacterium* Species Isolated from Clinical Specimens. *BioMed research international*, 2015, 854078-854078.
- Mehta, A. & Silva, L. P. 2015. MALDI-TOF MS profiling approach: how much can we get from it? *Frontiers in Plant Science*, 6.

- Mehta, S., Hadley, S., Hutzler, L., Slover, J., Phillips, M. & Bosco, J. A. 2013. Impact of Preoperative MRSA Screening and Decolonization on Hospital-acquired MRSA Burden. *Clinical Orthopaedics and Related Research*®, 471, 2367-2371.
- Mellmann, A., Bimet, F., Bizet, C., Borovskaya, A. D., Drake, R. R., Eigner, U., Fahr, A. M., He, Y., Ilina, E. N., Kostrzewa, M., Maier, T., Mancinelli, L., Moussaoui, W., Prévost, G., Putignani, L., Seachord, C. L., Tang, Y. W. & Harmsen, D. 2009. High Interlaboratory Reproducibility of Matrix-Assisted Laser Desorption Ionization-Time of Flight Mass Spectrometry-Based Species Identification of Nonfermenting Bacteria. *Journal of Clinical Microbiology*, 47, 3732-3734.
- Mellors, J. W., Munoz, A., Giorgi, J. V., Margolick, J. B., Tassoni, C. J., Gupta, P., Kingsley, L. A., Todd, J. A., Saah, A. J. & Detels, R. 1997. Plasma viral load and CD4+ lymphocytes as prognostic markers of HIV-1 infection. *Ann Intern Med*, 126.
- Mencacci, A., Monari, C., Leli, C., Merlini, L., De Carolis, E., Vella, A., Cacioni, M., Buzi, S., Nardelli, E., Bistoni, F., Sanguinetti, M. & Vecchiarelli, A. 2013. Typing of nosocomial outbreaks of *Acinetobacter baumannii* by use of matrix-assisted laser desorption ionization-time of flight mass spectrometry. *J Clin Microbiol*, 51, 603-6.
- Méric, G., Mageiros, L., Pensar, J., Laabei, M., Yahara, K., Pascoe, B., Kittivan, N., Tadee, P., Post, V., Lambie, S., Bowden, R., Bray, J. E., Morgenstern, M., Jolley, K. A., Maiden, M. C. J., Feil, E. J., Didelot, X., Miragaia, M., de Lencastre, H., Moriarty, T. F., Rohde, H., Massey, R., Mack, D., Corander, J. & Sheppard, S. K. 2018. Disease-associated genotypes of the commensal skin bacterium *Staphylococcus epidermidis*. *Nature Communications*, 9, 5034.
- Mermel, L. A., Cartony, J. M., Covington, P., Maxey, G. & Morse, D. 2011. Methicillin-Resistant *Staphylococcus aureus* Colonization at Different Body Sites: a Prospective, Quantitative Analysis. *Journal of Clinical Microbiology*, 49, 1119-1121.
- Messacar, K., Parker, S. K., Todd, J. K. & Dominguez, S. R. 2017. Implementation of Rapid Molecular Infectious Disease Diagnostics: the Role of Diagnostic and Antimicrobial Stewardship. *Journal of Clinical Microbiology*, 55, 715-723.
- Mexas, A. M., Graf, E. H., Pace, M. J., Yu, J. J., Papasavvas, E., Azzoni, L., Busch, M. P., Di Mascio, M., Foulkes, A. S., Migueles, S. A., Montaner, L. J. & O'Doherty, U. 2012. Concurrent measures of total and integrated HIV DNA monitor reservoirs and ongoing replication in eradication trials. *AIDS (London, England)*, 26, 2295-2306.
- Meyer, V. R. 2007. Measurement uncertainty. *Journal of Chromatography A*, 1158, 15-24.
- Miao, Q., Ma, Y., Wang, Q., Pan, J., Zhang, Y., Jin, W., Yao, Y., Su, Y., Huang, Y., Wang, M., Li, B., Li, H., Zhou, C., Li, C., Ye, M., Xu, X., Li, Y. & Hu, B. 2018. Microbiological Diagnostic Performance of Metagenomic Next-generation Sequencing When Applied to Clinical Practice. *Clinical Infectious Diseases*, 67, S231-S240.
- Milbury, C. A., Zhong, Q., Lin, J., Williams, M., Olson, J., Link, D. R. & Hutchison, B. 2014. Determining lower limits of detection of digital PCR assays for cancer-related gene mutations. *Biomolecular Detection and Quantification*, 1, 8-22.
- Miles, A. A., Misra, S. S. & Irwin, J. O. 1938. The estimation of the bactericidal power of the blood. *J Hyg (Lond)*, 38, 732-49.

- Miotke, L., Lau, B. T., Rumma, R. T. & Ji, H. P. 2014. Correction to High Sensitivity Detection and Quantitation of DNA Copy Number and Single Nucleotide Variants with Single Color Droplet Digital PCR. *Analytical Chemistry*, 86, 4635-4635.
- Miranda, J. A. & Steward, G. F. 2017. Variables influencing the efficiency and interpretation of reverse transcription quantitative PCR (RT-qPCR): An empirical study using Bacteriophage MS2. *Journal of Virological Methods*, 241, 1-10.
- Mitchell, M., Mali, S., King, C. C. & Bark, S. J. 2015. Enhancing MALDI Time-Of-Flight Mass Spectrometer Performance through Spectrum Averaging. *PLOS ONE*, 10, e0120932.
- Moreau, H. 1953. The genesis of the metric system and the work of the International Bureau of Weights and Measures. *Journal of Chemical Education*, 30, 3.
- Morley, A. A. 2014. Digital PCR: A brief history. *Biomolecular Detection and Quantification*, 1, 1-2.
- Morris, C., Govind, S., Fryer, J. & Almond, N. 2019. SoGAT—25 years of improving the measurement of nucleic acids in infectious disease diagnostics (a review). *Metrologia*, 56, 044007.
- Morris, C. & NIBSC. 2019. *RE: The Medicines and Healthcare Products Regulatory Agency*.
- Mortier, V., Demecheleer, E., Staelens, D., Schauvliege, M., Dauwe, K., Dinakis, S., Hebberecht, L., Vancoillie, L. & Verhofstede, C. 2018. Quantification of total HIV-1 DNA in buffy coat cells, feasibility and potential added value for clinical follow-up of HIV-1 infected patients on ART. *Journal of Clinical Virology*, 106, 58-63.
- Moseley, S. L., Huq, I., Alim, A. R., So, M., Samadpour-Motalebi, M. & Falkow, S. 1980. Detection of enterotoxigenic *Escherichia coli* by DNA colony hybridization. *J Infect Dis*, 142, 892-8.
- Mullis, K. B. & Faloona, F. A. 1987. [21] Specific synthesis of DNA in vitro via a polymerase-catalyzed chain reaction. *Methods in Enzymology*. Academic Press.
- Musial, C. E., Tice, L. S., Stockman, L. & Roberts, G. D. 1988. Identification of mycobacteria from culture by using the Gen-Probe Rapid Diagnostic System for *Mycobacterium avium* complex and *Mycobacterium tuberculosis* complex. *J Clin Microbiol*, 26, 2120-3.
- Nair, S. V., Kim, H. C., Fortunko, J., Foote, T., Peling, T., Tran, C., Nugent, C. T., Joo, S., Kang, Y., Wilkins, B., Lednovich, K. & Worlock, A. 2016. Aptima HIV-1 Quant Dx—A fully automated assay for both diagnosis and quantification of HIV-1. *Journal of Clinical Virology*, 77, 46-54.
- Najar-Peerayeh, S., Jazayeri Moghadas, A. & Behmanesh, M. 2014. Antibiotic Susceptibility and mecA Frequency in *Staphylococcus epidermidis*, Isolated From Intensive Care Unit Patients. *Jundishapur journal of microbiology*, 7, e11188-e11188.
- Narayanan, S. 2000. The preanalytic phase. An important component of laboratory medicine. *American journal of clinical pathology*, 113, 429-452.
- Nelson, M. U. & Gallagher, P. G. 2012. Methicillin-resistant *Staphylococcus aureus* in the neonatal intensive care unit. *Seminars in perinatology*, 36, 424-430.
- NHS. 2017. MRSA [Online]. Available: <https://www.nhs.uk/conditions/mrsa/> [Accessed 12th December 2019].
- Nihonyanagi, S., Kanoh, Y., Okada, K., Uozumi, T., Kazuyama, Y., Yamaguchi, T., Nakazaki, N., Sakurai, K., Hirata, Y., Munekata, S., Ohtani, S., Takemoto, T., Bandoh, Y. & Akahoshi,

- T. 2012. Clinical usefulness of multiplex PCR lateral flow in MRSA detection: a novel, rapid genetic testing method. *Inflammation*, 35, 927-934.
- Nixon, G., Garson, J. A., Grant, P., Nastouli, E., Foy, C. A. & Huggett, J. F. 2014a. Comparative study of sensitivity, linearity, and resistance to inhibition of digital and nondigital polymerase chain reaction and loop mediated isothermal amplification assays for quantification of human cytomegalovirus. *Anal Chem*, 86, 4387-94.
- Nixon, G. J., Svenstrup, H. F., Donald, C. E., Carder, C., Stephenson, J. M., Morris-Jones, S., Huggett, J. F. & Foy, C. A. 2014b. A novel approach for evaluating the performance of real time quantitative loop-mediated isothermal amplification-based methods. *Biomolecular Detection and Quantification*, 2, 4-10.
- Nolan, T., Huggett, J. & Sanchez, E. 2013. Good practice guide for the application of quantitative PCR (qPCR). *LGC*.
- Normand, A.-C., Cassagne, C., Gautier, M., Becker, P., Ranque, S., Hendrickx, M. & Piarroux, R. 2017. Decision criteria for MALDI-TOF MS-based identification of filamentous fungi using commercial and in-house reference databases. *BMC microbiology*, 17, 25-25.
- O'Doherty, U., Swiggard, W. J., Jeyakumar, D., McGain, D. & Malim, M. H. 2002. A sensitive, quantitative assay for human immunodeficiency virus type 1 integration. *J Virol*, 76, 10942-50.
- O'Neill, J. 2014. Review on Antimicrobial Resistance Antimicrobial Resistance: Tackling a crisis for the health and wealth of nations. London: Review on Antimicrobial Resistance.
- O'Rourke, M. B., Djordjevic, S. P. & Padula, M. P. 2016. The quest for improved reproducibility in MALDI mass spectrometry. *Mass Spectrometry Reviews*, n/a-n/a.
- O'Sullivan, D. M., Laver, T., Temisak, S., Redshaw, N., Harris, K. A., Foy, C. A., Studholme, D. J. & Huggett, J. F. 2014. Assessing the accuracy of quantitative molecular microbial profiling. *Int J Mol Sci*, 15, 21476-91.
- O'Connell, G. C., Chantler, P. D. & Barr, T. L. 2017. High Interspecimen Variability in Nucleic Acid Extraction Efficiency Necessitates the Use of Spike-In Control for Accurate qPCR-based Measurement of Plasma Cell-Free DNA Levels. *Laboratory Medicine*, 48, 332-338.
- Oberle, M., Wohlwend, N., Jonas, D., Maurer, F. P., Jost, G., Tschudin-Sutter, S., Vranckx, K. & Egli, A. 2016. The Technical and Biological Reproducibility of Matrix-Assisted Laser Desorption Ionization-Time of Flight Mass Spectrometry (MALDI-TOF MS) Based Typing: Employment of Bioinformatics in a Multicenter Study. *PLoS One*, 11, e0164260.
- Ochodo, E. A., Kakourou, A., Mallett, S. & Deeks, J. J. 2018. Point-of-care viral load tests to detect high HIV viral load levels in HIV-positive people on antiretroviral therapy. *Cochrane Database of Systematic Reviews*.
- Oehlschläger, F., Schwille, P. & Eigen, M. 1996. Detection of HIV-1 RNA by nucleic acid sequence-based amplification combined with fluorescence correlation spectroscopy. *Proceedings of the National Academy of Sciences*, 93, 12811-12816.
- Okello, J. B. A., Rodriguez, L., Poinar, D., Bos, K., Okwi, A. L., Bimenya, G. S., Sewankambo, N. K., Henry, K. R., Kuch, M. & Poinar, H. N. 2010. Quantitative assessment of the sensitivity of various commercial reverse transcriptases based on armored HIV RNA. *PLoS one*, 5, e13931-e13931.

- Olson, N. D., Jackson, S. A. & Lin, N. J. 2015. Report from the Standards for Pathogen Identification via Next-Generation Sequencing (SPIN) Workshop. *Standards in Genomic Sciences*, 10, 119.
- Olson, N. D. & Morrow, J. B. 2012. DNA extract characterization process for microbial detection methods development and validation. *BMC Research Notes*, 5, 668.
- Ondov, B. D., Treangen, T. J., Melsted, P., Mallonee, A. B., Bergman, N. H., Koren, S. & Phillippy, A. M. 2016. Mash: fast genome and metagenome distance estimation using MinHash. *Genome Biol*, 17, 132.
- Opota, O., Prod'hom, G. & Greub, G. 2017. Applications of MALDI-TOF Mass Spectrometry in Clinical Diagnostic Microbiology. *MALDI-TOF and Tandem MS for Clinical Microbiology*.
- Ostrowski, M., Benko, E., Yue, F. Y., Kim, C. J., Huibner, S., Lee, T., Singer, J., Pankovich, J., Laeyendecker, O., Kaul, R., Kandel, G. & Kovacs, C. 2015. Intensifying Antiretroviral Therapy With Raltegravir and Maraviroc During Early Human Immunodeficiency Virus (HIV) Infection Does Not Accelerate HIV Reservoir Reduction. *Open forum infectious diseases*, 2, ofv138-ofv138.
- Padley, D. J., Heath, A. B., Sutherland, C., Chiodini, P. L. & Baylis, S. A. 2008. Establishment of the 1st World Health Organization International Standard for *Plasmodium falciparum* DNA for nucleic acid amplification technique (NAT)-based assays. *Malar J*, 7, 139.
- Pagano, M., Martins, A. F. & Barth, A. L. 2016. Mobile genetic elements related to carbapenem resistance in *Acinetobacter baumannii*. *Brazilian journal of microbiology*, 47, 785-792.
- Palarea-Albaladejo, J., McLean, K., Wright, F. & Smith, D. G. E. 2018. MALDIrppa: quality control and robust analysis for mass spectrometry data. *Bioinformatics (Oxford, England)*, 34, 522-523.
- Pallen, M. J. 2014. Diagnostic metagenomics: potential applications to bacterial, viral and parasitic infections. *Parasitology*, 141, 1856-62.
- Papp-Wallace, K. M., Endimiani, A., Taracila, M. A. & Bonomo, R. A. 2011. Carbapenems: Past, Present, and Future. *Antimicrobial Agents and Chemotherapy*, 55, 4943-4960.
- Parchen, R. G. & de Valk, C. G. 2019. The Ongoing Revolution of MALDI-TOF Mass Spectrometry for Molecular Diagnostics. In: van Pelt-Verkuil, E., van Leeuwen, W. B. & te Witt, R. (eds.) *Molecular Diagnostics: Part 1: Technical Backgrounds and Quality Aspects*. Singapore: Springer Singapore.
- Park, S., Choi, J. & Jeong, J. 2012. Development of Metrology for Modern Biology. *Modern Metrology Concerns*.
- Pasternak, A. O., Lukashov, V. V. & Berkhout, B. 2013. Cell-associated HIV RNA: a dynamic biomarker of viral persistence. *Retrovirology*, 10, 41.
- Patel, A., Harris, K. A. & Fitzgerald, F. 2017. What is broad-range 16S rDNA PCR? *Archives of disease in childhood - Education & practice edition*, 102, 261-264.
- Patton, S., Normanno, N., Blackhall, F., Murray, S., Kerr, K. M., Dietel, M., Filipits, M., Benlloch, S., Popat, S., Stahel, R. & Thunnissen, E. 2014. Assessing standardization of molecular testing for non-small-cell lung cancer: results of a worldwide external quality assessment (EQA) scheme for EGFR mutation testing. *British Journal of Cancer*, 111, 413-420.

- Pavsic, J., Devonshire, A., Blejec, A., Foy, C. A., Van Heuverswyn, F., Jones, G. M., Schimmel, H., Zel, J., Huggett, J. F., Redshaw, N., Karczmarczyk, M., Mozioglu, E., Akyurek, S., Akgoz, M. & Milavec, M. 2017. Inter-laboratory assessment of different digital PCR platforms for quantification of human cytomegalovirus DNA. *Anal Bioanal Chem*.
- Pavsic, J., Devonshire, A. S., Parkes, H., Schimmel, H., Foy, C. A., Karczmarczyk, M., Gutierrez-Aguirre, I., Honeyborne, I., Huggett, J. F., McHugh, T. D., Milavec, M., Zeichhardt, H. & Zel, J. 2015. Standardization of Nucleic Acid Tests for Clinical Measurements of Bacteria and Viruses. *J Clin Microbiol*, 53, 2008-14.
- Pavšič, J., Žel, J. & Milavec, M. 2016. Digital PCR for direct quantification of viruses without DNA extraction. *Analytical and Bioanalytical Chemistry*, 408, 67-75.
- Perez, V. L., Rowe, T., Justement, J. S., Butera, S. T., June, C. H. & Folks, T. M. 1991. An HIV-1-infected T cell clone defective in IL-2 production and Ca²⁺ mobilization after CD3 stimulation. *J Immunol*, 147, 3145-8.
- Persson, S., Karlsson, M., Borsch-Reniers, H., Ellström, P., Eriksson, R. & Simonsson, M. 2019. Missing the Match Might Not Cost You the Game: Primer-Template Mismatches Studied in Different Hepatitis A Virus Variants. *Food and environmental virology*, 11, 297-308.
- Petruso, K. M. 1981. Early Weights and Weighing in Egypt and the Indus Valley. *M Bulletin (Museum of Fine Arts, Boston)*, 79, 44-51.
- Pfyffer, G. E. & Wittwer, F. 2012. Incubation time of mycobacterial cultures: how long is long enough to issue a final negative report to the clinician? *Journal of clinical microbiology*, 50, 4188-4189.
- Pierpont, M. 2016. *Multiplex Real Time PCR and Melt Curve Assay Development for the Simultaneous Detection and Identification of Streptococcus pneumoniae and Staphylococcus aureus*. Master of science, Northern Michigan University.
- Pinheiro-de-Oliveira, T. F., Fonseca-Júnior, A. A., Camargos, M. F., Laguardia-Nascimento, M., Giannattasio-Ferraz, S., Cottorello, A. C. P., de Oliveira, A. M., Góes-Neto, A. & Barbosa-Stancioli, E. F. 2019. Reverse transcriptase droplet digital PCR to identify the emerging vesicular virus Senecavirus A in biological samples. *Transboundary and Emerging Diseases*, 0.
- Plint, A. C., Moher, D., Morrison, A., Schulz, K., Altman, D. G., Hill, C. & Gaboury, I. 2006. Does the CONSORT checklist improve the quality of reports of randomised controlled trials? A systematic review. *Med J Aust*, 185, 263-7.
- Polage, C. R., Gyorke, C. E., Kennedy, M. A., Leslie, J. L., Chin, D. L., Wang, S., Nguyen, H. H., Huang, B., Tang, Y.-W., Lee, L. W., Kim, K., Taylor, S., Romano, P. S., Panacek, E. A., Goodell, P. B., Solnick, J. V. & Cohen, S. H. 2015. Overdiagnosis of *Clostridium difficile* Infection in the Molecular Test Era. *JAMA Internal Medicine*, 175, 1792-1801.
- Pomari, E., Piubelli, C., Perandin, F. & Bisoffi, Z. 2019. Digital PCR: a new technology for diagnosis of parasitic infections. *Clinical Microbiology and Infection*, 25, 1510-1516.
- Poole, K. 2012. Bacterial stress responses as determinants of antimicrobial resistance. *Journal of Antimicrobial Chemotherapy*, 67, 2069-2089.
- Pourcel, C., Minandri, F., Hauck, Y., D'Arezzo, S., Imperi, F., Vergnaud, G. & Visca, P. 2011. Identification of variable-number tandem-repeat (VNTR) sequences in *Acinetobacter*

- baumannii* and interlaboratory validation of an optimized multiple-locus VNTR analysis typing scheme. *J Clin Microbiol*, 49, 539-48.
- Powell, E. A. & Babady, N. E. 2018. Digital PCR in the Clinical Microbiology Laboratory: Another Tool on the Molecular Horizon. *Clinical Microbiology Newsletter*, 40, 27-32.
- Prescott G, Hockley J, Atkinson E, Rigsby P, Morris C & al., e. 2017. International collaborative study to establish the 4th WHO international standard for HIV-1 NAT assays. WHO/BS/2017.2314.
- Public Health England. 2019. *MRSA bacteraemia: monthly data by location of onset* [Online]. Available: <https://www.gov.uk/government/statistics/mrsa-bacteraemia-monthly-data-by-location-of-onset> [Accessed 12th December 2019].
- Quan, P.-L., Sauzade, M. & Brouzes, E. 2018. dPCR: A Technology Review. *Sensors (Basel, Switzerland)*, 18, 1271.
- Quillent, C., Dumey, N., Dauguet, C. & Clavel, F. 1993. Reversion of a Polymerase-Defective Integrated HIV-1 Genome. *AIDS Research and Human Retroviruses*, 9, 1031-1037.
- Rafei, R., Kempf, M., Eveillard, M., Dabboussi, F., Hamze, M. & Joly-Guillou, M. L. 2014. Current molecular methods in epidemiological typing of *Acinetobacter baumannii*. *Future Microbiol*, 9, 1179-94.
- Ramplung, T., Page, M. & Horby, P. 2019. International Biological Reference Preparations for Epidemic Infectious Diseases. *Emerging Infectious Disease journal*, 25, 205.
- Ranjbar, R., Karami, A., Farshad, S., Giammanco, G. M. & Mammina, C. 2014. Typing methods used in the molecular epidemiology of microbial pathogens: a how-to guide. *New Microbiol*, 37, 1-15.
- Rasmussen, A. L. 2015. Probing the Viromic Frontiers. *mBio*, 6, e01767-15.
- Redd, A. D., Quinn, T. C. & Tobian, A. A. R. 2013. Frequency and implications of HIV superinfection. *The Lancet. Infectious diseases*, 13, 622-628.
- Relova, D., Rios, L., Acevedo, A. M., Coronado, L., Perera, C. L. & Pérez, L. J. 2018. Impact of RNA Degradation on Viral Diagnosis: An Understated but Essential Step for the Successful Establishment of a Diagnosis Network. *Veterinary sciences*, 5, 19.
- Richard, J. J. 2014. The effect of heat conduction on the realization of the primary standard for sound pressure. *Metrologia*, 51, 423.
- Richman, D., Margolis, D., Delaney, M., Greene, W., Hazuda, D. & Pomerantz, R. 2009. The Challenge of Finding a Cure for HIV Infection. *Science*, 323, 1304-1307.
- Rim, J. H., Lee, Y., Hong, S. K., Park, Y., Kim, M., Souza, R., Park, E. S., Yong, D. & Lee, K. 2015. Insufficient Discriminatory Power of Matrix-Assisted Laser Desorption Ionization Time-of-Flight Mass Spectrometry Dendrograms to Determine the Clonality of Multi-Drug-Resistant *Acinetobacter baumannii* Isolates from an Intensive Care Unit. *BioMed Research International*, 2015, 8.
- Rittié, L. & Perbal, B. 2008. Enzymes used in molecular biology: a useful guide. *Journal of cell communication and signaling*, 2, 25-45.
- Roberts, C. H., Last, A., Molina-Gonzalez, S., Cassama, E., Butcher, R., Nabicassa, M., McCarthy, E., Burr, S. E., Mabey, D. C., Bailey, R. L. & Holland, M. J. 2013. Development

- and evaluation of a next-generation digital PCR diagnostic assay for ocular *Chlamydia trachomatis* infections. *J Clin Microbiol*, 51, 2195-203.
- Robertson, B. D. & Meyer, T. F. 1992. Genetic variation in pathogenic bacteria. *Trends in Genetics*, 8, 422-427.
- Röder, B., Frühwirth, K., Vogl, C., Wagner, M. & Rossmann, P. 2010. Impact of Long-Term Storage on Stability of Standard DNA for Nucleic Acid-Based Methods. *Journal of Clinical Microbiology*, 48, 4260-4262.
- Roth, S. 1974. Tissue Culture. Methods and Applications. Paul F. Kruse, Jr. , M. K. Patterson, Jr. *The Quarterly Review of Biology*, 49, 150-151.
- Rouzioux, C. & Avettand-Fenoël, V. 2018. Total HIV DNA: a global marker of HIV persistence. *Retrovirology*, 15, 30.
- Rutsaert, S., Bosman, K., Trypsteen, W., Nijhuis, M. & Vandekerckhove, L. 2018a. Digital PCR as a tool to measure HIV persistence. *Retrovirology*, 15, 16.
- Rutsaert, S., De Spiegelaere, W., Van Hecke, C., De Scheerder, M.-A., Kiselinova, M., Vervisch, K., Trypsteen, W. & Vandekerckhove, L. 2018b. In-depth validation of total HIV-1 DNA assays for quantification of various HIV-1 subtypes. *Scientific Reports*, 8, 17274.
- Rychlik, M., Zappa, G., Añorga, L., Belc, N., Castanheira, I., Donard, O. F. X., Kouřimská, L., Ogrinc, N., Ocké, M. C., Presser, K. & Zoani, C. 2018. Ensuring Food Integrity by Metrology and FAIR Data Principles. *Frontiers in chemistry*, 6, 49-49.
- Saha, B. K., Tian, B. & Bucy, R. P. 2001. Quantitation of HIV-1 by real-time PCR with a unique fluorogenic probe. *Journal of Virological Methods*, 93, 33-42.
- Şahin, F., Kıyan, M., Karasartova, D., Çalgin, M. K., Akhter, S. & Türegün Atasoy, B. 2016. A new method for the disruption of cell walls of gram-positive bacteria and mycobacteria on the point of nucleic acid extraction: sand method. *Mikrobiyoloji bulteni*, 50, 34-43.
- Sakarikou, C., Ciotti, M., Dolfa, C., Angeletti, S. & Favalli, C. 2017. Rapid detection of carbapenemase-producing *Klebsiella pneumoniae* strains derived from blood cultures by Matrix-Assisted Laser Desorption Ionization-Time of Flight Mass Spectrometry (MALDI-TOF MS). *BMC Microbiol*, 17, 54.
- Salipante, S. J. & Jerome, K. R. 2019. Digital PCR-An Emerging Technology with Broad Applications in Microbiology. *Clin Chem*.
- Salipante, S. J., SenGupta, D. J., Cummings, L. A., Land, T. A., Hoogstraat, D. R. & Cookson, B. T. 2015. Application of whole-genome sequencing for bacterial strain typing in molecular epidemiology. *J Clin Microbiol*, 53, 1072-9.
- Sanders, R., Huggett, J. F., Bushell, C. A., Cowen, S., Scott, D. J. & Foy, C. A. 2011. Evaluation of digital PCR for absolute DNA quantification. *Anal Chem*, 83, 6474-84.
- Sanders, R., Mason, D., Foy, C. & Huggett, J. 2013. Evaluation of Digital PCR for Absolute RNA Quantification. *PLOS ONE*, 8 e75296.
- Sanders, R., Mason, D. J., Foy, C. A. & Huggett, J. F. 2014. Considerations for accurate gene expression measurement by reverse transcription quantitative PCR when analysing clinical samples. *Anal Bioanal Chem*, 406, 6471-83.
- Sauget, M., Valot, B., Bertrand, X. & Hocquet, D. 2017. Can MALDI-TOF Mass Spectrometry Reasonably Type Bacteria? *Trends Microbiol*, 25, 447-455.

- Sax, P. E., Boswell, S. L., White-Guthro, M. & Hirsch, M. S. 1995. Potential Clinical Implications of Interlaboratory Variability in CD4+ T-Lymphocyte Counts of Patients Infected with Human Immunodeficiency Virus. *Clinical Infectious Diseases*, 21, 1121-1125.
- Schumaker, S., Borrer, C. M. & Sandrin, T. R. 2012. Automating data acquisition affects mass spectrum quality and reproducibility during bacterial profiling using an intact cell sample preparation method with matrix-assisted laser desorption/ionization time-of-flight mass spectrometry. *Rapid Communications in Mass Spectrometry*, 26, 243-253.
- Schwaber, J., Andersen, S. & Nielsen, L. 2019. Shedding light: The importance of reverse transcription efficiency standards in data interpretation. *Biomolecular Detection and Quantification*, 17, 100077.
- Sedlackova, T., Repiska, G., Celec, P., Szemes, T. & Minarik, G. 2013. Fragmentation of DNA affects the accuracy of the DNA quantitation by the commonly used methods. *Biological procedures online*, 15, 5-5.
- Sedlak, R. H., Cook, L., Huang, M. L., Magaret, A., Zerr, D. M., Boeckh, M. & Jerome, K. R. 2014. Identification of chromosomally integrated human herpesvirus 6 by droplet digital PCR. *Clin Chem*, 60, 765-72.
- Sedlak, R. H. & Jerome, K. R. 2013. Viral diagnostics in the era of digital polymerase chain reaction. *Diagn Microbiol Infect Dis*, 75, 1-4.
- Sedlak, R. H., Nguyen, T., Palileo, I., Jerome, K. R. & Kuypers, J. 2017. Superiority of Digital Reverse Transcription-PCR (RT-PCR) over Real-Time RT-PCR for Quantitation of Highly Divergent Human Rhinoviruses. *J Clin Microbiol*, 55, 442-449.
- Senechal, B. & James, V. L. A. 2012. Ten years of external quality assessment of human immunodeficiency virus type 1 RNA quantification. *Journal of clinical microbiology*, 50, 3614-3619.
- Shah, H. & Gharbia, S. 2017. *MALDI-TOF and Tandem MS for Clinical Microbiology*, Wiley.
- Shanmugakani, R. K., Srinivasan, B., Glesby, M. J., Westblade, L. F., Cárdenas, W. B., Raj, T., Erickson, D. & Mehta, S. 2020. Current state of the art in rapid diagnostics for antimicrobial resistance. *Lab on a Chip*, 20, 2607-2625.
- Sharma-Kuinkel, B. K., Rude, T. H. & Fowler, V. G., Jr. 2016. Pulse Field Gel Electrophoresis. *Methods Mol Biol*, 1373, 117-30.
- Shaw, A. G., Vento, T. J., Mende, K., Kreft, R. E., Ehrlich, G. D., Wenke, J. C., Spirk, T., Landrum, M. L., Zera, W., Cheatle, K. A., Guymon, C., Calvano, T. P., Rini, E. A., Tully, C. C., Beckius, M. L. & Murray, C. K. 2013. Detection of methicillin-resistant and methicillin-susceptible *Staphylococcus aureus* colonization of healthy military personnel by traditional culture, PCR, and mass spectrometry. *Scand J Infect Dis*, 45, 752-9.
- Shaw, L. P., Doyle, R. M., Kavaliunaite, E., Spencer, H., Balloux, F., Dixon, G. & Harris, K. A. 2019. Children with cystic fibrosis are infected with multiple subpopulations of *Mycobacterium abscessus* with different antimicrobial resistance profiles. *Clin Infect Dis*.
- Sheridan, G. E., Masters, C. I., Shallcross, J. A. & MacKey, B. M. 1998. Detection of mRNA by reverse transcription-PCR as an indicator of viability in *Escherichia coli* cells. *Applied and environmental microbiology*, 64, 1313-1318.

- Shiramizu, B., Gartner, S., Williams, A., Shikuma, C., Ratto-Kim, S., Watters, M., Aguon, J. & Valcour, V. 2005. Circulating proviral HIV DNA and HIV-associated dementia. *AIDS*, 19, 45-52.
- Šimundić, A.-M. 2009. Measures of Diagnostic Accuracy: Basic Definitions. *EJIFCC*, 19, 203-211.
- Sindt, N. M., Robison, F., Brick, M. A., Schwartz, H. F., Heuberger, A. L. & Prenni, J. E. 2018. MALDI-TOF-MS with PLS Modeling Enables Strain Typing of the Bacterial Plant Pathogen *Xanthomonas axonopodis*. *Journal of The American Society for Mass Spectrometry*, 29, 413-421.
- Singhal, N., Kumar, M., Kanaujia, P. K. & Viridi, J. S. 2015. MALDI-TOF mass spectrometry: an emerging technology for microbial identification and diagnosis. *Frontiers in Microbiology*, 6, 791.
- Singleton, P. 2000. Nucleic Acid Amplification II: NASBA, TMA, SDA. *DNA Methods in Clinical Microbiology*. Dordrecht: Springer Netherlands.
- Sivaganesan, M., Varma, M., Siefiring, S. & Haugland, R. 2018. Quantification of plasmid DNA standards for U.S. EPA fecal indicator bacteria qPCR methods by droplet digital PCR analysis. *Journal of microbiological methods*, 152, 135-142.
- Smidt, N., Rutjes, A. W. S., van der Windt, D. A. W. M., Ostelo, R. W. J. G., Bossuyt, P. M., Reitsma, J. B., Bouter, L. M. & de Vet, H. C. W. 2006. The quality of diagnostic accuracy studies since the STARD statement. *Has it improved?*, 67, 792-797.
- Sonza, S., Mutimer, H. P., Oelrichs, R., Jardine, D., Harvey, K., Dunne, A., Purcell, D. F., Birch, C. & Crowe, S. M. 2001. Monocytes harbour replication-competent, non-latent HIV-1 in patients on highly active antiretroviral therapy. *Aids*, 15, 17-22.
- Sousa, C., Botelho, J., Grosso, F., Silva, L., Lopes, J. & Peixe, L. 2015. Unsuitability of MALDI-TOF MS to discriminate *Acinetobacter baumannii* clones under routine experimental conditions. *Frontiers in Microbiology*, 6.
- Speers, D. J. 2006. Clinical applications of molecular biology for infectious diseases. *The Clinical biochemist. Reviews*, 27, 39-51.
- Spinali, S., van Belkum, A., Goering, R. V., Girard, V., Welker, M., Van Nuenen, M., Pincus, D. H., Arsac, M. & Durand, G. 2015. Microbial typing by matrix-assisted laser desorption ionization-time of flight mass spectrometry: do we need guidance for data interpretation? *J Clin Microbiol*, 53, 760-5.
- Spivak, A. M. & Planelles, V. 2018. Novel Latency Reversal Agents for HIV-1 Cure. *Annual review of medicine*, 69, 421-436.
- Squara, P., Imhoff, M. & Cecconi, M. 2015. Metrology in medicine: from measurements to decision, with specific reference to anesthesia and intensive care. *Anesthesia and analgesia*, 120, 66-75.
- Sreejith, K. R., Ooi, C. H., Jin, J., Dao, D. V. & Nguyen, N.-T. 2018. Digital polymerase chain reaction technology – recent advances and future perspectives. *Lab on a Chip*, 18, 3717-3732.
- Stamatakis, A. 2014. RAxML version 8: a tool for phylogenetic analysis and post-analysis of large phylogenies. *Bioinformatics*, 30, 1312-3.

- Steensels, D., Deplano, A., Denis, O., Simon, A. & Verroken, A. 2017. MALDI-TOF MS typing of a nosocomial methicillin-resistant *Staphylococcus aureus* outbreak in a neonatal intensive care unit. *Acta Clin Belg*, 72, 219-225.
- Steinmetzer, K., Seidel, T., Stallmach, A. & Ermantraut, E. 2010. HIV load testing with small samples of whole blood. *J Clin Microbiol*, 48, 2786-92.
- Stephan, R., Cernela, N., Ziegler, D., Pfluger, V., Tonolla, M., Ravasi, D., Fredriksson-Ahomaa, M. & Hachler, H. 2011. Rapid species specific identification and subtyping of *Yersinia enterocolitica* by MALDI-TOF mass spectrometry. *J Microbiol Methods*, 87, 150-3.
- Stock, M., Davis, R., de Mirandés, E. & Milton, M. J. T. 2019. The revision of the SI—the result of three decades of progress in metrology. *Metrologia*, 56, 022001.
- Stone, M. H. 2014. The Cubit: A History and Measurement Commentary. *Journal of Anthropology*, 2014, 489757.
- Strain, M. C., Lada, S. M., Luong, T., Rought, S. E., Gianella, S., Terry, V. H., Spina, C. A., Woelk, C. H. & Richman, D. D. 2013. Highly precise measurement of HIV DNA by droplet digital PCR. *PLoS One*, 8, e55943.
- Strain, M. C. & Richman, D. D. 2013. New assays for monitoring residual HIV burden in effectively treated individuals. *Current opinion in HIV and AIDS*, 8, 106-110.
- Stuart, D., James, B., Patrick, A., Kilian, M., Richard, G., Andrea, M. & Lars, N. 2016. Air–vacuum transfer; establishing traceability to the new kilogram. *Metrologia*, 53, A95.
- Sunshine, S., Kirchner, R., Amr, S. S., Mansur, L., Shakhbatyan, R., Kim, M., Bosque, A., Siliciano, R. F., Planelles, V., Hofmann, O., Ho Sui, S. & Li, J. Z. 2016. HIV Integration Site Analysis of Cellular Models of HIV Latency with a Probe-Enriched Next-Generation Sequencing Assay. *J Virol*, 90, 4511-9.
- Surdo, M., Bertoli, A., Colucci, G., Sarmati, L., Andreoni, M., Perno, C. F., Ceccherini-Silberstein, F. & Ciotti, M. 2016. Total HIV-1 DNA detection and quantification in peripheral blood by COBAS(R)AmpliPrep/COBAS(R) TaqMan(R) HIV-1 Test, v2.0. *Clin Chem Lab Med*, 54, e57-9.
- Taberlet, P., Griffin, S., Goossens, B., Questiau, S., Manceau, V., Escaravage, N., Waits, L. P. & Bouvet, J. 1996. Reliable Genotyping of Samples with Very Low DNA Quantities Using PCR. *Nucleic Acids Research*, 24, 3189-3194.
- Tan, S. C. & Yip, B. C. 2013. Erratum to “DNA, RNA, and Protein Extraction: The Past and the Present”. *BioMed Research International*, 2013, 628968.
- Tang, Y. W., Procop, G. W. & Persing, D. H. 1997. Molecular diagnostics of infectious diseases. *Clinical chemistry*, 43, 2021-2038.
- Taylor, C. F., Paton, N. W., Lilley, K. S., Binz, P.-A., Julian, R. K., Jones, A. R., Zhu, W., Apweiler, R., Aebersold, R., Deutsch, E. W., Dunn, M. J., Heck, A. J. R., Leitner, A., Macht, M., Mann, M., Martens, L., Neubert, T. A., Patterson, S. D., Ping, P., Seymour, S. L., Souda, P., Tsugita, A., Vandekerckhove, J., Vondriska, T. M., Whitelegge, J. P., Wilkins, M. R., Xenarios, I., Yates, J. R. & Hermjakob, H. 2007. The minimum information about a proteomics experiment (MIAPE). *Nature Biotechnology*, 25, 887-893.

- Taylor, S. C., Laperriere, G. & Germain, H. 2017. Droplet Digital PCR versus qPCR for gene expression analysis with low abundant targets: from variable nonsense to publication quality data. *Scientific Reports*, 7, 2409.
- Taylor, S. C., Nadeau, K., Abbasi, M., Lachance, C., Nguyen, M. & Fenrich, J. 2019. The Ultimate qPCR Experiment: Producing Publication Quality, Reproducible Data the First Time. *Trends in Biotechnology*, 37, 761-774.
- Teague, E. C. 1989. The National Institute of Standards and Technology molecular measuring machine project: Metrology and precision engineering design. *Journal of Vacuum Science & Technology B: Microelectronics Processing and Phenomena*, 7, 1898-1902.
- Telwatte, S., Morón-López, S., Aran, D., Kim, P., Hsieh, C., Joshi, S., Montano, M., Greene, W. C., Butte, A. J., Wong, J. K. & Yukl, S. A. 2019. Heterogeneity in HIV and cellular transcription profiles in cell line models of latent and productive infection: implications for HIV latency. *Retrovirology*, 16, 32.
- Temin, H. M. & Mizutani, S. 1970. RNA-dependent DNA polymerase in virions of Rous sarcoma virus. *Nature*, 226, 1211-3.
- Terrault, N. A., Pawlotsky, J. M., McHutchison, J., Anderson, F., Kraiden, M., Gordon, S., Zitron, I., Perrillo, R., Gish, R., Holodniy, M. & Friesenhahn, M. 2005. Clinical utility of viral load measurements in individuals with chronic hepatitis C infection on antiviral therapy. *J Viral Hepat*, 12, 465-72.
- The BREATHER Trial Group 2016. Weekends-off efavirenz-based antiretroviral therapy in HIV-infected children, adolescents, and young adults (BREATHER): a randomised, open-label, non-inferiority, phase 2/3 trial. *The Lancet HIV*, 3, e421-e430.
- The dMIQE Group & Huggett, J. F. 2020. The Digital MIQE Guidelines Update: Minimum Information for Publication of Quantitative Digital PCR Experiments for 2020. *Clinical Chemistry*, 66, 1012-1029.
- Thomas, J., Ruggiero, A., Procopio, F. A., Pantaleo, G., Paxton, W. A. & Pollakis, G. 2019. Comparative analysis and generation of a robust HIV-1 DNA quantification assay. *Journal of Virological Methods*, 263, 24-31.
- Thomas, J. B., Duewer, D. L., Mugenya, I. O., Phinney, K. W., Sander, L. C., Sharpless, K. E., Sniegowski, L. T., Tai, S. S., Welch, M. J. & Yen, J. H. 2012. Preparation and value assignment of standard reference material 968e fat-soluble vitamins, carotenoids, and cholesterol in human serum. *Analytical and Bioanalytical Chemistry*, 402, 749-762.
- Toh-Boyo, G. M., Wulff, S. S. & Basile, F. 2012. Comparison of sample preparation methods and evaluation of intra- and intersample reproducibility in bacteria MALDI-MS profiling. *Analytical chemistry*, 84, 9971-9980.
- Tomaschek, F., Higgins, P. G., Stefanik, D., Wisplinghoff, H. & Seifert, H. 2016. Head-to-Head Comparison of Two Multi-Locus Sequence Typing (MLST) Schemes for Characterization of *Acinetobacter baumannii* Outbreak and Sporadic Isolates. *PloS one*, 11, e0153014-e0153014.
- Trypsteen, W., Kiselina, M., Vandekerckhove, L. & De Spiegelaere, W. 2016. Diagnostic utility of droplet digital PCR for HIV reservoir quantification. *Journal of Virus Eradication*, 2, 1-8.

- Turano, A. & Pirali, F. 1988. Quantification Methods in Microbiology. *In*: Balows, A., Hausler, W. J., Ohashi, M., Turano, A. & Lennete, E. H. (eds.) *Laboratory Diagnosis of Infectious Diseases: Principles and Practice*. New York, NY: Springer New York.
- Turton, J. F., Matos, J., Kaufmann, M. E. & Pitt, T. L. 2009. Variable number tandem repeat loci providing discrimination within widespread genotypes of *Acinetobacter baumannii*. *Eur J Clin Microbiol Infect Dis*, 28, 499-507.
- Ueda, O., Tanaka, S., Nagasawa, Z., Hanaki, H., Shobuike, T. & Miyamoto, H. 2015. Development of a novel matrix-assisted laser desorption/ionization time-of-flight mass spectrum (MALDI-TOF-MS)-based typing method to identify methicillin-resistant *Staphylococcus aureus* clones. *Journal of Hospital Infection*, 90, 147-155.
- UNAIDS. 2019. *Global HIV & AIDS statistics — 2019 fact sheet* [Online]. Available: <https://www.unaids.org/en/resources/fact-sheet> [Accessed 14th August 2020].
- van Belkum, A., Welker, M., Pincus, D., Charrier, J. P. & Girard, V. 2017. Matrix-Assisted Laser Desorption Ionization Time-of-Flight Mass Spectrometry in Clinical Microbiology: What Are the Current Issues? *Ann Lab Med*, 37, 475-483.
- Van den Bruel, A., Cleemput, I., Aertgeerts, B., Ramaekers, D. & Buntinx, F. 2007. The evaluation of diagnostic tests: evidence on technical and diagnostic accuracy, impact on patient outcome and cost-effectiveness is needed. *J Clin Epidemiol*, 60, 1116-22.
- Verdecia, J., Hernandez, J., Izzo, C., Sottile, E. & Isache, C. 2019. Methicillin-resistant *Staphylococcus aureus* (MRSA) sepsis complicated by warm autoimmune haemolytic anaemia secondary to antimicrobial therapy. *BMJ Case Reports*, 12, e229114.
- Verhofstede, C., Franssen, K., Marissens, D., Verhelst, R., van der Groen, G., Lauwers, S., Zissis, G. & Plum, J. 1996. Isolation of HIV-1 RNA from plasma: evaluation of eight different extraction methods. *Journal of virological methods*, 60, 155-159.
- Vermehren, J., Maasoumy, B., Maan, R., Cloherty, G., Berkowski, C., Feld, J. J., Cornberg, M., Pawlotsky, J.-M., Zeuzem, S., Manns, M. P., Sarrazin, C. & Wedemeyer, H. 2016. Applicability of Hepatitis C Virus RNA Viral Load Thresholds for 8-Week Treatments in Patients With Chronic Hepatitis C Virus Genotype 1 Infection. *Clinical Infectious Diseases*, 62, 1228-1234.
- Veselkov, K., Sleeman, J., Claude, E., Vissers, J. P. C., Galea, D., Mroz, A., Laponogov, I., Towers, M., Tonge, R., Mirnezami, R., Takats, Z., Nicholson, J. K. & Langridge, J. I. 2018. BASIS: High-performance bioinformatics platform for processing of large-scale mass spectrometry imaging data in chemically augmented histology. *Scientific Reports*, 8, 4053.
- Vogt, S., Löffler, K., Dinkelacker, A. G., Bader, B., Autenrieth, I. B., Peter, S. & Liese, J. 2019. Fourier-Transform Infrared (FTIR) Spectroscopy for Typing of Clinical *Enterobacter cloacae* Complex Isolates. *Frontiers in Microbiology*, 10.
- Vranckx, K., De Bruyne, K. & Pot, B. 2017. Analysis of MALDI-TOF MS Spectra using the BioNumerics Software. *MALDI-TOF and Tandem MS for Clinical Microbiology*. John Wiley & Sons, Ltd.
- Wakefield, A. J., Murch, S. H., Anthony, A., Linnell, J., Casson, D. M., Malik, M., Berelowitz, M., Dhillon, A. P., Thomson, M. A., Harvey, P., Valentine, A., Davies, S. E. & Walker-Smith,

- J. A. 1998. RETRACTED: Ileal-lymphoid-nodular hyperplasia, non-specific colitis, and pervasive developmental disorder in children. *The Lancet*, 351, 637-641.
- Wang, C.-C., Lai, Y.-H., Ou, Y.-M., Chang, H.-T. & Wang, Y.-S. 2016. Critical factors determining the quantification capability of matrix-assisted laser desorption/ionization- time-of-flight mass spectrometry. *Philosophical transactions. Series A, Mathematical, physical, and engineering sciences*, 374, 20150371.
- Wang, H.-Y., Lien, F., Liu, T.-P., Chen, C.-H., Chen, C.-J. & Lu, J.-J. 2018. Application of a MALDI-TOF analysis platform (ClinProTools) for rapid and preliminary report of MRSA sequence types in Taiwan. *PeerJ*, 6, e5784-e5784.
- Watzinger, F., Suda, M., Preuner, S., Baumgartinger, R., Ebner, K., Baskova, L., Niesters, H. G. M., Lawitschka, A. & Lion, T. 2004. Real-time quantitative PCR assays for detection and monitoring of pathogenic human viruses in immunosuppressed pediatric patients. *Journal of clinical microbiology*, 42, 5189-5198.
- Weerakoon, K. G., Gordon, C. A., Williams, G. M., Cai, P., Gobert, G. N., Olveda, R. M., Ross, A. G., Olveda, D. U. & McManus, D. P. 2017. Droplet Digital PCR Diagnosis of Human Schistosomiasis: Parasite Cell-Free DNA Detection in Diverse Clinical Samples. *J Infect Dis*, 216, 1611-1622.
- Welte, T. & Pletz, M. W. 2010. Antimicrobial treatment of nosocomial methicillin-resistant *Staphylococcus aureus* (MRSA) pneumonia: current and future options. *International Journal of Antimicrobial Agents*, 36, 391-400.
- Whale, A. S., Bushell, C. A., Grant, P. R., Cowen, S., Gutierrez-Aguirre, I., O'Sullivan, D. M., Zel, J., Milavec, M., Foy, C. A., Nastouli, E., Garson, J. A. & Huggett, J. F. 2016a. Detection of Rare Drug Resistance Mutations by Digital PCR in a Human Influenza A Virus Model System and Clinical Samples. *J Clin Microbiol*, 54, 392-400.
- Whale, A. S., Cowen, S., Foy, C. A. & Huggett, J. F. 2013. Methods for applying accurate digital PCR analysis on low copy DNA samples. *PLoS One*, 8, e58177.
- Whale, A. S., Devonshire, A. S., Karlin-Neumann, G., Regan, J., Javier, L., Cowen, S., Fernandez-Gonzalez, A., Jones, G. M., Redshaw, N., Beck, J., Berger, A. W., Combaret, V., Dahl Kjersgaard, N., Davis, L., Fina, F., Forshew, T., Fredslund Andersen, R., Galbiati, S., Gonzalez Hernandez, A., Haynes, C. A., Janku, F., Lacave, R., Lee, J., Mistry, V., Pender, A., Pradines, A., Proudhon, C., Saal, L. H., Stieglitz, E., Ulrich, B., Foy, C. A., Parkes, H., Tzonev, S. & Huggett, J. F. 2017. International Interlaboratory Digital PCR Study Demonstrating High Reproducibility for the Measurement of a Rare Sequence Variant. *Anal Chem*, 89, 1724-1733.
- Whale, A. S., Huggett, J. F. & Tzonev, S. 2016b. Fundamentals of multiplexing with digital PCR. *Biomolecular Detection and Quantification*.
- Whale, A. S., Jones, G. M., Pavšič, J., Dreo, T., Redshaw, N., Akyurek, S., Akgoz, M., Divieto, C., PaolaSassi, M., He, H.-J., Cole, K. D., Bae, Y.-K., Park, S.-R., Deprez, L., Corbisier, P., Garrigou, S., Taly, V., Larios, R., Cowen, S., O'Sullivan, D. M., Bushell, C. A., Goenaga-Infante, H., Foy, C. A., Woolford, A. J., Parkes, H., Huggett, J. F. & Devonshire, A. S. 2018. Assessment of Digital PCR as a Primary Reference Measurement Procedure to Support Advances in Precision Medicine. *Clinical Chemistry*.

- White, A. 1963. Increased Infection Rates in Heavy Nasal Carriers of Coagulase-Positive *Staphylococci*. *Antimicrob Agents Chemother (Bethesda)*, 161, 667-70.
- White, H., Deprez, L., Corbisier, P., Hall, V., Lin, F., Mazoua, S., Trapmann, S., Aggerholm, A., Andrikovics, H., Akiki, S., Barbany, G., Boeckx, N., Bench, A., Catherwood, M., Cayuela, J. M., Chudleigh, S., Clench, T., Colomer, D., Daraio, F., Dulucq, S., Farrugia, J., Fletcher, L., Foroni, L., Ganderton, R., Gerrard, G., Gineikienė, E., Hayette, S., El Housni, H., Izzo, B., Jansson, M., Johnels, P., Jurcek, T., Kairisto, V., Kizilers, A., Kim, D. W., Lange, T., Lion, T., Polakova, K. M., Martinelli, G., McCarron, S., Merle, P. A., Milner, B., Mitterbauer-Hohendanner, G., Nagar, M., Nickless, G., Nomdedéu, J., Nymoen, D. A., Leibundgut, E. O., Ozbek, U., Pajič, T., Pfeifer, H., Preudhomme, C., Raudsepp, K., Romeo, G., Sacha, T., Talmaci, R., Touloumenidou, T., Van der Velden, V. H. J., Waits, P., Wang, L., Wilkinson, E., Wilson, G., Wren, D., Zadro, R., Ziermann, J., Zoi, K., Müller, M. C., Hochhaus, A., Schimmel, H., Cross, N. C. P. & Emons, H. 2015. A certified plasmid reference material for the standardisation of BCR–ABL1 mRNA quantification by real-time quantitative PCR. *Leukemia*, 29, 369-376.
- Widerström, M. 2016. Significance of *Staphylococcus epidermidis* in Health Care-Associated Infections, from Contaminant to Clinically Relevant Pathogen: This Is a Wake-Up Call! *Journal of clinical microbiology*, 54, 1679-1681.
- Wieser, A., Schneider, L., Jung, J. & Schubert, S. 2012. MALDI-TOF MS in microbiological diagnostics-identification of microorganisms and beyond (mini review). *Appl Microbiol Biotechnol*, 93, 965-74.
- Wilburn, K. M., Mwandumba, H. C., Jambo, K. C., Boliar, S., Solouki, S., Russell, D. G. & Gludish, D. W. 2016. Heterogeneous loss of HIV transcription and proviral DNA from 8E5/LAV lymphoblastic leukemia cells revealed by RNA FISH:FLOW analyses. *Retrovirology*, 13, 55.
- Williams, J. P., Hurst, J., Stohr, W., Robinson, N., Brown, H., Fisher, M., Kinloch, S., Cooper, D., Schechter, M., Tambussi, G., Fidler, S., Carrington, M., Babiker, A., Weber, J., Koelsch, K. K., Kelleher, A. D., Phillips, R. E., Frater, J. & Investigators, S. P. 2014. HIV-1 DNA predicts disease progression and post-treatment virological control. *Elife*, 3, e03821.
- Williams, T. L., Andrzejewski, D., Lay, J. O. & Musser, S. M. 2003. Experimental factors affecting the quality and reproducibility of MALDI TOF mass spectra obtained from whole bacteria cells. *Journal of the American Society for Mass Spectrometry*, 14, 342-351.
- Wise, S. A. 2018. What is novel about certified reference materials? *Analytical and Bioanalytical Chemistry*, 410, 2045-2049.
- Woloshin, S., Patel, N. & Kesselheim, A. S. 2020. False Negative Tests for SARS-CoV-2 Infection — Challenges and Implications. *New England Journal of Medicine*, 383, e38.
- Wolters, M., Rohde, H., Maier, T., Belmar-Campos, C., Franke, G., Scherpe, S., Aepfelbacher, M. & Christner, M. 2011. MALDI-TOF MS fingerprinting allows for discrimination of major methicillin-resistant *Staphylococcus aureus* lineages. *Int J Med Microbiol*, 301, 64-8.
- World Health Organisation. 2018. *R&D Blueprint 2018: List of priority diseases* [Online]. Available: <https://www.who.int/blueprint/priority-diseases/en/> [Accessed 09th July 2020].

- World Health Organisation. 2020a. *Public reports of WHO prequalified IVDs* [Online]. Available: https://www.who.int/diagnostics_laboratory/evaluations/pq-list/hiv-vrl/public_report/en/ [Accessed 15th July 2020].
- World Health Organisation. 2020b. *WHO Coronavirus Disease (COVID-19) Dashboard* [Online]. Available: <https://covid19.who.int/> [Accessed 31st May 2020].
- World Health Organization 2006. Recommendations for the preparation, characterization and establishment of international and other biological reference standards (revised 2004). *WHO Technical Report Series*.
- World Health Organization 2017a. Global priority list of antibiotic-resistant bacteria to guide research, discovery, and development of new antibiotics.
- World Health Organization 2017b. *WHO Expert Committee on Biological Standardization, sixty-seventh report*, World Health Organization.
- Xiao, X., Zhang, J., Quanyi Zhang, Q., Wang, L., Tan, Y., Guo, Z., Yang, R., Jingfu Qiu, J. & Zhou, D. 2011. Two methods for extraction of high-purity genomic DNA from mucoid Gram-negative bacteria *African Journal of Microbiology Research*, 5, 4013-4018.
- Xu, J., Zhao, S., Teng, T., Abdalla, A. E., Zhu, W., Xie, L., Wang, Y. & Guo, X. 2020. Systematic Comparison of Two Animal-to-Human Transmitted Human Coronaviruses: SARS-CoV-2 and SARS-CoV. *Viruses*, 12.
- Yam, W. C., Siu, G. K. H., Ho, P. L., Ng, T. K., Que, T. L., Yip, K. T., Fok, C. P. K., Chen, J. H. K., Cheng, V. C. C. & Yuen, K. Y. 2013. Evaluation of the LightCycler methicillin-resistant *Staphylococcus aureus* (MRSA) advanced test for detection of MRSA nasal colonization. *Journal of clinical microbiology*, 51, 2869-2874.
- Yang, S. & Rothman, R. E. 2004. PCR-based diagnostics for infectious diseases: uses, limitations, and future applications in acute-care settings. *Lancet Infect Dis*, 4, 337-48.
- Yu, F., Yan, L., Wang, N., Yang, S., Wang, L., Tang, Y., Gao, G., Wang, S., Ma, C., Xie, R., Wang, F., Tan, C., Zhu, L., Guo, Y. & Zhang, F. 2020. Quantitative Detection and Viral Load Analysis of SARS-CoV-2 in Infected Patients. *Clinical Infectious Diseases*.
- Zemanick, E. T., Wagner, B. D., Sagel, S. D., Stevens, M. J., Accurso, F. J. & Harris, J. K. 2010. Reliability of quantitative real-time PCR for bacterial detection in cystic fibrosis airway specimens. *PLoS One*, 5, e15101.
- Zhang, L., Borrer, C. M. & Sandrin, T. R. 2014. A Designed Experiments Approach to Optimization of Automated Data Acquisition during Characterization of Bacteria with MALDI-TOF Mass Spectrometry. *PLOS ONE*, 9, e92720.
- Zhang, Z., Kang, S.-M., Li, Y. U. N. & Morrow, C. D. 1998. Genetic analysis of the U5-PBS of a novel HIV-1 reveals multiple interactions between the tRNA and RNA genome required for initiation of reverse transcription. *RNA*, 4, 394-406.
- Zhou, M., Yang, Q., Kudinha, T., Sun, L., Zhang, R., Liu, C., Yu, S., Xiao, M., Kong, F., Zhao, Y. & Xu, Y.-C. 2017. An Improved In-house MALDI-TOF MS Protocol for Direct Cost-Effective Identification of Pathogens from Blood Cultures. *Frontiers in Microbiology*, 8.
- Zhvansky, E. S., Pekov, S. I., Sorokin, A. A., Shurkhay, V. A., Eliferov, V. A., Potapov, A. A., Nikolaev, E. N. & Popov, I. A. 2019. Metrics for evaluating the stability and reproducibility of mass spectra. *Scientific Reports*, 9, 914.

- Ziegler, I., Cajander, S., Rasmussen, G., Ennefors, T., Mölling, P. & Strålin, K. 2019a. High nucleic acid load in whole blood is associated with sepsis, mortality and immune dysregulation in *Staphylococcus aureus* bacteraemia. *Infect Dis (Lond)*, 51, 216-226.
- Ziegler, I., Lindström, S., Källgren, M., Strålin, K. & Mölling, P. 2019b. 16S rDNA droplet digital PCR for monitoring bacterial DNAemia in bloodstream infections. *PLOS ONE*, 14, e0224656.
- Zippelius, A., Lutterbüse, R., Riethmüller, G. & Pantel, K. 2000. Analytical Variables of Reverse Transcription-Polymerase Chain Reaction-based Detection of Disseminated Prostate Cancer Cells. *Clinical Cancer Research*, 6, 2741-2750.
- Zucha, D., Androvic, P., Kubista, M. & Valihrač, L. 2019. Performance Comparison of Reverse Transcriptases for Single-Cell Studies. *Clinical chemistry, clinchem*.2019.307835.

10. Appendices

10.1. Appendix 1

Glossary of definitions for metrology

Further definitions can be found in the International Vocabulary of Metrology (Joint Committee for Guides in Metrology, 2012).

Term	Definition
Measurement accuracy	Represents a measurement with minimal error (both random and systematic) that is close to the true value.
Measurement error	Reflects random error; sometimes referred to as 'noise'. Individual values within a set of measurements may vary but the overall mean of those measurements will not be affected.
Measurement bias	Reflects systematic error, where a particular result for a measurement may be favoured over another. This may alter the mean value of a set of measurements.
Reproducibility	Reflects the variation in a measurement of a single quantity (i.e. between experiments, analysts, laboratories, or any given condition).
Measurement precision	The closeness of agreement of replicate measurements (biological or technical) on the same object.
Measurement uncertainty	Characterisation of the dispersion of values surrounding a measurement.
Calibration	Establishes a relationship between nominal input value and instrument response based on the measurement of a calibrator.
Calibrator	A measurement standard used for calibration.
Orthogonal method	A method for analysis of a molecule, chemical or physical property that is based on different fundamental properties from the primary method
Pseudonymisation	Masking the identity of a sample's origin by using a unique pseudonym, such a code containing numbers of letters.

10.2. Appendix 2

Synthetic HXB2 HIV-1 molecule design

DNA sequence of synthetic molecule for human immunodeficiency virus type1 (HIV-1). Key to sequences - 1: *BspHI* restriction site 2: T7 RNA polymerase promoter sequence 3: *NotI* restriction site 4: DNA sequence for HIV-1 (HXB2) HIV1/HTLV-III/LAV reference genome (NCBI accession number K03455.1), positions 1 to 5,619. 5: *XmaI* restriction site 6: T3 RNA polymerase promoter sequence in reverse complement orientation.

```
TCATGA1TAATACGACTCACTATAG2GCGGCCGC3TGGAAGGGCTAATTCCTCCCAACGAAGACAAGAT
ATCCTTGATCTGTGGATCTACCACACACAAGGCTACTTCCCTGATTAGCAGAATAACACACCAGGGCC
AGGGATCAGATATCCACTGACCTTTGGATGGTGTCTACAAGCTAGTACCAGTTGAGCCAGAGAAGTTAG
AAGAAGCCAACAAAGGAGAGAACACCAGCTTGTACACCCCTGTGAGCCTGCATGGAATGGATGACCCG
GAGAGAGAAGTGTTAGAGTGGAGGTTTGACAGCCGCCTAGCATTTTCATCACATGGCCCCGAGAGCTGCA
TCCGGAGTACTTCAAGAACTGCTGACATCGAGCTTGCTACAAGGGACTTTCCGCTGGGGACTTTCCAG
GGAGGCGTGGCCTGGGCGGGACTGGGGAGTGGCGAGCCCTCAGATCCTGCATATAAGCAGCTGCTTTT
TGCCTGTACTGGGTCTCTCTGGTTAGACCAGATCTGAGCCTGGGAGCTCTCTGGCTAACTAGGGAACC
CACTGCTTAAGCCTCAATAAAGCTTGCCCTTGAGTGCTTCAAGTAGTGTGTGCCCGTCTGTTGTGTGAC
TCTGGTAACTAGAGATCCCTCAGACCCTTTTAGTCAGTGTGGAAAAATCTCTAGCAGTGGCGCCCGAAC
AGGGACCTGAAAGCGAAAGGGAAACCAGAGGAGCTCTCTCGACGCAGGACTCGGCTTGCTGAAGCGCG
CACGGCAAGAGGCGAGGGGCGGCGACTGGTGAGTACGCCAAAAATTTTACTAGCGGAGGCTAGAAGG
AGAGAGATGGGTGCGAGAGCGTCAGTATTAAGCGGGGAGAATTAGATCGATGGGAAAAAATTCGGTT
AAGGCCAGGGGAAAGAAAAATATAAATTA AAAACATATAGTATGGGCAAGCAGGGAGCTAGAACGAT
TCGCAGTTAATCCTGGCCTGTTAGAAACATCAGAAGGCTGTAGACAAATACTGGGACAGCTACAACCA
TCCCTTCAGACAGGATCAGAAGAACTTAGATCATTATATAATACAGTAGCAACCCTCTATTGTGTGCA
TCAAAGGATAGAGATAAAAGACACCAAGGAAGCTTTAGACAAGATAGAGGAAGAGCAAAACAAAAGTA
AGAAAAAGCACAGCAAGCAGCAGCTGACACAGGACACAGCAATCAGGTCAGCCAAAATTTACCCCTATA
GTGCAGAACATCCAGGGGCAATGGTACATCAGGCCATATCACCTAGAACTTTAAATGCATGGGTAAA
AGTAGTAGAAGAGAAGGCTTTCAGCCAGAAGTGATACCCATGTTTTTCAGCATTATCAGAAGGAGCCA
CCCCACAAGATTTAAACACCATGCTAAACACAGTGGGGGACATCAAGCAGCCATGCAAATGTTAAAA
GAGACCATCAATGAGGAAGCTGCAGAATGGGATAGAGTGCATCCAGTGCATGCAGGGCCTATTGCACC
AGGCCAGATGAGAGAACCAAGGGGAAGTGACATAGCAGGAACTACTAGTACCCTTCAGGAACAAATAG
```

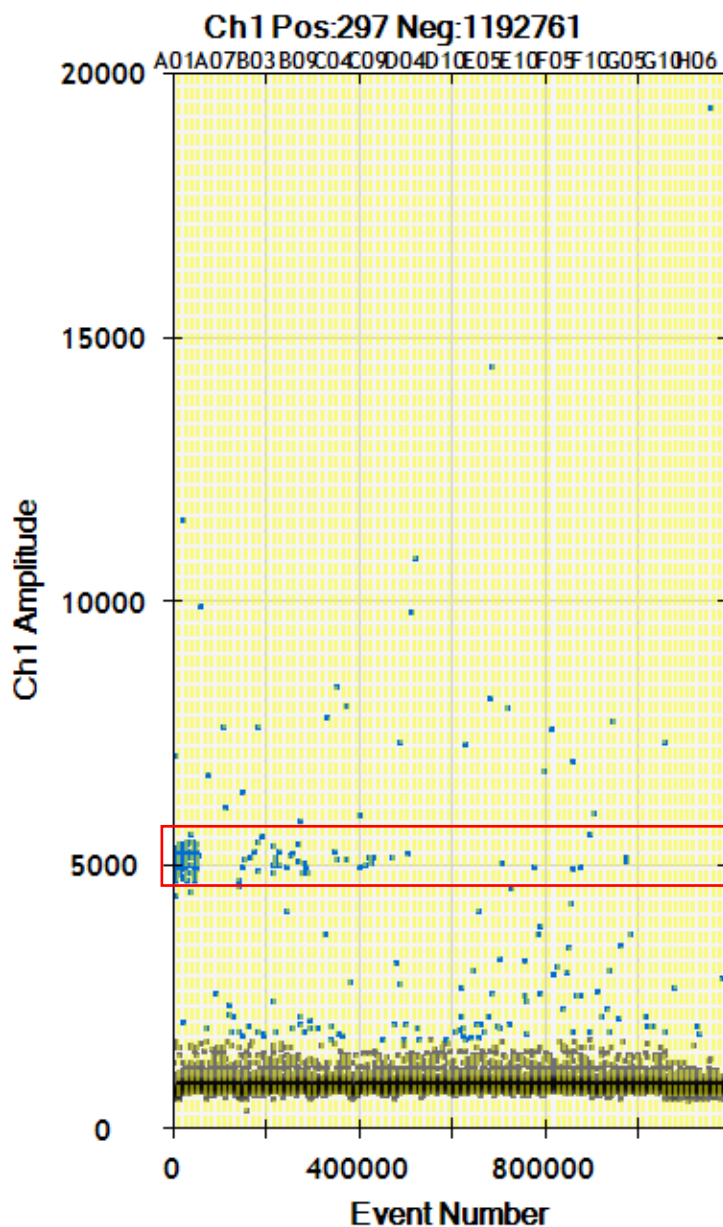
GATGGATGACAAATAATCCACCTATCCCAGTAGGAGAAATTTATAAAAGATGGATAATCCTGGGATTA
AATAAAATAGTAAGAATGTATAGCCCTACCAGCATTCTGGACATAAGACAAGGACCAAAGGAACCCTT
TAGAGACTATGTAGACCGGTTCTATAAACTCTAAGAGCCGAGCAAGCTTACAGGAGGTAAAAAATT
GGATGACAGAAACCTTGTGGTCCAAAATGCGAACCCAGATTGTAAGACTATTTTAAAAGCATTGGGA
CCAGCGGCTACACTAGAAGAAATGATGACAGCATGTCAGGGAGTAGGAGGACCCGGCCATAAGGCAAG
AGTTTTGGCTGAAGCAATGAGCCAAGTAACAAATTCAGCTACCATAATGATGCAGAGAGGCAATTTTA
GGAACCAAAGAAAGATTGTTAAGTGTTCATTTGTGGCAAAGAAGGGCACACAGCCAGAAATTGCAGG
GCCCCTAGGAAAAAGGGCTGTTGAAATGTGGAAAGGAAGGACACCAAATGAAAGATTGTACTGAGAG
ACAGGCTAATTTTTTAGGGAAGATCTGGCCTTCCACAGGGAAGGCCAGGGAATTTTCTTCAGAGCA
GACCAGAGCCAACAGCCCCACCAGAAGAGAGCTTCAGGTCTGGGGTAGAGACAACAACCTCCCCCTCAG
AAGCAGGAGCCGATAGACAAGGAAGTGTATCCTTTAACTTCCCTCAGGTCACTCTTTGGCAACGACCC
CTCGTCACAATAAAGATAGGGGGGCAACTAAAGGAAGCTCTATTAGATACAGGAGCAGATGATACAGT
ATTAGAAGAAATGAGTTTGCCAGGAAGATGGAAACCAAAAATGATAGGGGGAATTGGAGGTTTTATCA
AAGTAAGACAGTATGATCAGATACTCATAGAAATCTGTGGACATAAAGCTATAGGTACAGTATTAGTA
GGACCTACACCTGTCAACATAATTGGAAGAAATCTGTTGACTCAGATTGGTTGCACCTTAAATTTTCC
CATTAGCCCTATTGAGACTGTACCAGTAAAATTAAGCCAGGAATGGATGGCCAAAAGTTAAACAAT
GGCCATTGACAGAAGAAAAATAAAAGCATTAGTAGAAATTTGTACAGAGATGGAAAAGGAAGGGAAA
ATTTCAAAAATTGGGCCTGAAAATCCATACAATACTCCAGTATTTGCCATAAAGAAAAAAGACAGTAC
TAAATGGAGAAAATTAGTAGATTTTCAGAGAACTTAATAAGAGAACTCAAGACTTCTGGGAAGTTCAAT
TAGGAATACCACATCCCGCAGGGTTAAAAAAGAAAAAATCAGTAACAGTACTGGATGTGGGTGATGCA
TATTTTTCAGTTCCCTTAGATGAAGACTTCAGGAAGTATACTGCATTTACCATACCTAGTATAAACAA
TGAGACACCAGGATTAGATATCAGTACAATGTGCTTCCACAGGGATGGAAAGGATCACCAGCAATAT
TCCAAAAGTAGCATGACAAAAATCTTAGAGCCTTTTAGAAAACAAAATCCAGACATAGTTATCTATCAA
TACATGGATGATTTGTATGTAGGATCTGACTTAGAAATAGGGCAGCATAGAACAAAAATAGAGGAGCT
GAGACAACATCTGTTGAGGTGGGGACTTACCACACCAGACAAAAAACATCAGAAAGAACCTCCATTCC
TTTGGATGGGTTATGAACTCCATCCTGATAAATGGACAGTACAGCCTATAGTGCTGCCAGAAAAAGAC
AGCTGGACTGTCAATGACATACAGAAGTTAGTGGGGAAATTGAATTGGGCAAGTCAGATTTACCCAGG
GATTAAAGTAAGGCAATTATGTAACTCCTTAGAGGAACCAAAGCACTAACAGAAGTAATACCACTAA
CAGAAGAAGCAGAGCTAGAACTGGCAGAAAACAGAGAGATTCTAAAAGAACCAGTACATGGAGTGTAT
TATGACCCATCAAAGACTTAATAGCAGAAATACAGAAGCAGGGGCAAGGCCAATGGACATATCAAAT
TTATCAAGAGCCATTTAAAAATCTGAAAACAGGAAAATATGCAAGAATGAGGGGTGCCCACACTAATG

ATGTAAAACAATTAACAGAGGCAGTGCAAAAAATAACCACAGAAAGCATAGTAATATGGGGAAAAGACT
CCTAAATTTAAACTGCCCATACAAAAGGAAACATGGGAAACATGGTGGACAGAGTATTGGCAAGCCAC
CTGGATTCTGAGTGGGAGTTTGTTAATACCCCTCCCTTAGTGAAATTATGGTACCAGTTAGAGAAAAG
AACCCATAGTAGGAGCAGAAACCTTCTATGTAGATGGGGCAGCTAACAGGGAGACTAAATTAGGAAAA
GCAGGATATGTTACTAATAGAGGAAGACAAAAAGTTGTCACCCTAACTGACACAACAAATCAGAAGAC
TGAGTTACAAGCAATTTATCTAGCTTTGCAGGATTCGGGATTAGAAGTAAACATAGTAACAGACTCAC
AATATGCATTAGGAATCATTCAAGCACAACCAGATCAAAGTGAATCAGAGTTAGTCAATCAAATAATA
GAGCAGTTAATAAAAAAGGAAAAGGTCTATCTGGCATGGGTACCAGCACACAAAGGAATTGGAGGAAA
TGAACAAGTAGATAAAATTAGTCAGTGCTGGAATCAGGAAAGTACTATTTTTTAGATGGAATAGATAAGG
CCCAAGATGAACATGAGAAATATCACAGTAATTGGAGAGCAATGGCTAGTGATTTTAACTGCCACCT
GTAGTAGCAAAAGAAATAGTAGCCAGCTGTGATAAATGTCAGCTAAAAGGAGAAGCCATGCATGGACA
AGTAGACTGTAGTCCAGGAATATGGCAACTAGATTGTACACATTTAGAAGGAAAAGTTATCCTGGTAG
CAGTTCATGTAGCCAGTGGATATATAGAAGCAGAAGTTATTCCAGCAGAAACAGGGCAGGAAACAGCA
TATTTTCTTTTAAAATTAGCAGGAAGATGGCCAGTAAAAACAATACATACTGACAATGGCAGCAATTT
CACCGGTGCTACGGTTAGGGCCGCCTGTTGGTGGGCGGAATCAAGCAGGAATTTGGAATTCCTTACA
ATCCCCAAAGTCAAGGAGTAGTAGAATCTATGAATAAAGAATTAAGAAAAATTATAGGACAGGTAAGA
GATCAGGCTGAACATCTTAAGACAGCAGTACAAATGGCAGTATTCATCCACAATTTTAAAAGAAAAGG
GGGGATTGGGGGTACAGTGCAGGGGAAAGAATAGTAGACATAATAGCAACAGACATACAACTAAAG
AATTACAAAAACAAATTACAAAAATTCAAATTTTCGGGTTTATTACAGGGACAGCAGAAATCCACTT
TGAAAGGACCAGCAAAGCTCCTCTGAAAGGTGAAGGGCAGTAGTAATACAAGATAATAGTGACAT
AAAAGTAGTGCCAAGAAGAAAAGCAAAGATCATTAGGGATTATGGAAAACAGATGGCAGGTGATGATT
GTGTGGCAAGTAGACAGGATGAGGATTAGAACATGGAAAAGTTTAGTAAAACACCATATGTATGTTTC
AGGGAAAGCTAGGGGATGGTTTTATAGACATCACTATGAAAGCCCTCATCCAAGATAAGTTCAGAAG
TACACATCCCCTAGGGGATGCTAGATTGGTAATAACAACATATTGGGGTCTGCATACAGGAGAAAAGA
GACTGGCATTGTTGGTTCAGGGAGTCTCCATAGAATGGAGGAAAAAGAGATATAGCACACAAGTAGACCC
TGAAGTAGCAGACCAACTAATTCATCTGTATTACTTTGACTGTTTTTCAGACTCTGCTATAAGAAAAGG
CCTTATTAGGACACATAGTTAGCCCTAGGTGTGAATATCAAGCAGGACATAACAAGGTAGGATCTCTA
CAATACTTGGCACTAGCAGCATTAAATAACACCAAAAAAGATAAAGCCACCTTTGCCTAGTGTTACGAA
ACTGACAGAGGATAGATGGAACAAGCCCCAGAAGACCAAGGGCCACAGAGGGAGCCACACAATGAATG
GACACTAG⁴CCCGGG⁵CTTTAGTGAGGGTTAATT⁶

10.3. Appendix 3

Spurious positives observed for RT-dPCR

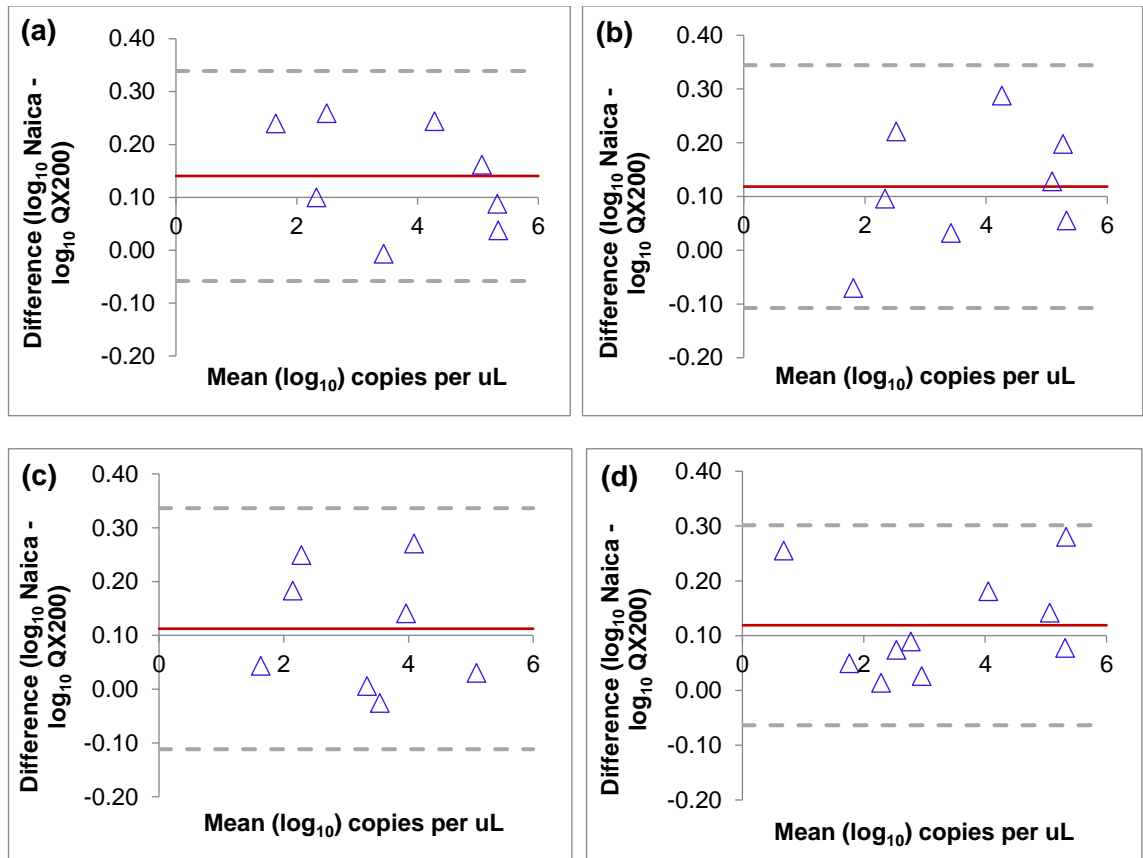
HIV-1 *pol* assay (Strain *et al.*, 2013) using the Bio-Rad one-step RT-ddPCR Advanced kit. Blue dots represent FAM-positive partitions, grey dots represent no amplification. The expected Ch1 (FAM) amplitude (peak resolution) is indicated by the red box.



10.4. Appendix 4

Bland-Altman plots to compare Naica and QX200 clinical sample results.

Log₁₀-transformed copy number concentrations are plotted for each assay (a) *mecA* duplexed with *femA* (b) *mecA* duplexed with *coA* (c) *femA* and (d) *coA*. The solid red line represents the mean difference, dashed lines represent ± 1.96 SD.



10.5. Appendix 5

Clinical isolates included MALDI-TOF MS analysis along with randomly assigned study identifiers

Unique study identifier	Species identity	Experiment
MBT16-003	<i>A. baumannii</i>	Peak intensity/data analysis method/typing
MBT16-005	<i>A. baumannii</i>	Peak intensity/data analysis method/typing
MBT16-008	<i>A. baumannii</i>	Peak intensity/data analysis method/typing
MBT16-011	<i>A. baumannii</i>	Peak intensity/data analysis method/typing
MBT16-014	<i>S. aureus</i>	MALDI typing
MBT16-015	<i>A. baumannii</i>	Peak intensity/data analysis method/typing
MBT16-016	<i>A. baumannii</i>	Peak intensity/data analysis method/typing
MBT16-017	<i>S. aureus</i>	MALDI typing
MBT16-018	<i>A. baumannii</i>	Peak intensity/data analysis method/typing
MBT16-025	<i>A. baumannii</i>	Peak intensity/data analysis method/typing
MBT16-029	<i>A. baumannii</i>	Peak intensity/data analysis method/typing
MBT16-030	<i>A. baumannii</i>	Peak intensity/data analysis method/typing
MBT16-031	<i>A. baumannii</i>	Peak intensity/data analysis method/typing
MBT16-033	<i>A. baumannii</i>	Peak intensity/data analysis method/typing
MBT16-034	<i>S. aureus</i>	MALDI typing
MBT16-035	<i>A. baumannii</i>	Peak intensity/data analysis method/typing
MBT16-039	<i>A. baumannii</i>	Peak intensity/data analysis method/typing
MBT16-040	<i>A. baumannii</i>	Peak intensity/data analysis method/typing
MBT16-042	<i>A. baumannii</i>	Peak intensity/data analysis method/typing
MBT16-046	<i>S. aureus</i>	MALDI typing
MBT16-057	<i>S. aureus</i>	MALDI typing
MBT16-059	<i>A. baumannii</i>	Peak intensity/data analysis method/typing
MBT16-060	<i>A. baumannii</i>	Peak intensity/data analysis method/typing
MBT16-062	<i>A. baumannii</i>	Peak intensity/data analysis method/typing
MBT16-067	<i>S. aureus</i>	MALDI typing
MBT16-068	<i>S. aureus</i>	MALDI typing
MBT16-069	<i>S. aureus</i>	MALDI typing

10.6. Appendix 6

Reference laboratory typing results

Pulsed-field gel electrophoresis (PFGE) and variable nucleotide tandem repeat (VNTR) profiles of the 18 *A. baumannii* isolates from the Royal Free London NHS Foundation Trust.

Study ID	Year isolated	PFGE result	VNTR profile
MBT16-003	2014	OXA-23 clone 1	10,20,12, 6
MBT16-005	2015	OXA-23 clone 1	9,20,10, 6
MBT16-008	2014	OXA-23 clone 1	9,20,11, 6
MBT16-011	2015	OXA-23 clone 1	9,20,10, 6
MBT16-015	2015	OXA-23 clone 1	-,20,12, 6
MBT16-016	2014	OXA-23 clone 1	10,20,12, 6
MBT16-018	2014	OXA-23 clone 1	10,20,12, 6
MBT16-025	2015	OXA-23 clone 1	10,20,12, 7
MBT16-029	2015	OXA-23 clone 1	10,20,12, 6
MBT16-030	2015	OXA-23 clone 1	10,20,12, 6
MBT16-031	2015	OXA-23 clone 1	10,20,13, 6
MBT16-033	2014	OXA-23 clone 1	10,20,12, 6
MBT16-039	2015	OXA-23 clone 1	9,20,10, 6
MBT16-040	2015	OXA-23 clone 1	10,20,12, 6
MBT16-042	2014	OXA-23 clone 1	10,20,12, 6
MBT16-059	2014	OXA-23 clone 1	10,20,12, 6
MBT16-060	2015	OXA-23 clone 1	10,20,12, 6
MBT16-062	2015	-	-

10.7. Appendix 7

MALDI-TOF MS peaks recorded at different culture stages

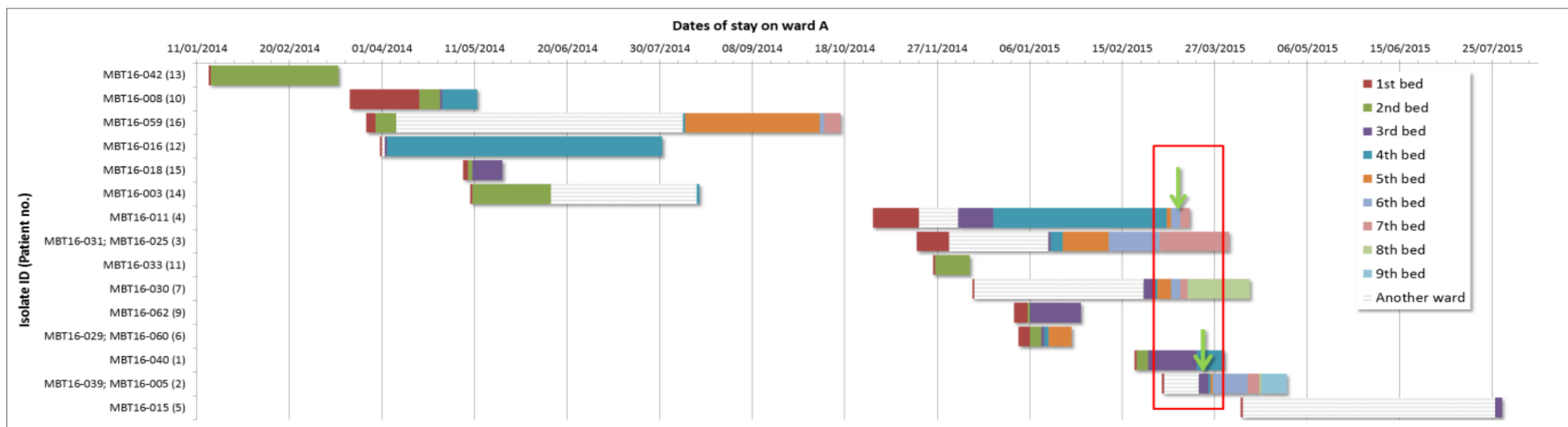
MALDI-TOF MS peaks recorded in FlexAnalysis (version 3.4) for a clinical isolate of *K. pneumoniae* at different culture stages. Conditions i, ii and iii refer to those described in Chapter 6, Section 6.2.6.1.

Peak class (m/z) per condition		
i	ii	iii
2179.7	2179.4	2689.4
2689.3	2264.2	2855.8
2855.7	2688.9	3048.1
3076.1	2855.4	3076.3
3144.3	3075.3	3144.3
3580.0	3143.7	3711.2
3623.0	3579.4	3853.6
3662.1	3622.2	4156.4
3853.6	3661.5	4366.2
4156.5	3852.8	4740.8
4366.1	4155.2	4772.6
4498.7	4341.1	5013.9
4740.6	4365.2	5070.1
4772.7	4739.4	5143.2
4927.5	4771.6	5281.8
5145.2	4926.1	5383.2
5383.3	5144.2	6098.4
6154.9	5382.1	6155.2
6292.2	6153.4	6292.4
6386.9	6290.7	7162.0
7162.2	7160.2	7247.2
7248.1	7245.5	7432.0
7432.8	7430.3	7708.5
7710.0	7706.5	8314.9
8317.2	8312.7	8377.5
8377.4	8374.5	9485.8
9486.7	9481.6	9547.4
9549.8	9545.0	9858.3
9859.5	9851.4	
n=29	n=29	n=22

10.8. Appendix 8

Timeline of patient migration within ward A and other hospital wards.

The red box highlights the time point in which Patients 2 & 4 crossed on ward A; green arrows indicate approximate date of first MDR *A. baumannii* isolation. Patient ID is given along with isolate number.



10.9. Appendix 9

dPCR MIQE (dMIQE2020) table

dMIQE2020 checklist for authors, reviewers, and editors. Authors should fill detail whether information is provided. Where 'yes' is selected use comment box to detail location of information or to include the information. Where 'no' is selected use comment box to outline rationale for omission. Sections 4 and 5 may not apply depending on experiment.

ITEM TO CHECK	PROVIDED	COMMENT
	Y/N	
1. SPECIMEN		
Detailed description of specimen type and numbers	Y	Chapter 4, 5
Sampling procedure (including time to storage)	N	Residual samples received as pre-extracted nucleic acid after primary analysis had been performed by initial laboratory
Sample aliquotation, storage conditions and duration	N	Residual samples received as pre-extracted nucleic acid after primary analysis had been performed by initial laboratory
2. NUCLEIC ACID EXTRACTION		
Description of extraction method including amount of sample processed	Y	Chapter 3, 4, 5
Volume of solvent used to elute/resuspend extract	Y	Chapter 3, 4, 5
Number of extraction replicates	Y	Chapter 3, 4, 5
Extraction blanks included?	Y	

3. NUCLEIC ACID ASSESSMENT AND STORAGE		
Method to evaluate quality of nucleic acids	Y	Qubit 2.0 fluorometer, NanoDrop 2000, Agilent Bioanalyzer 2100
Method to evaluate quantity of nucleic acids (including molecular weight and calculations when using mass)	Y	Section 2.1.4
Storage conditions: temperature, concentration, duration, buffer, aliquots	Y	Chapter 3, 4, 5
Clear description of dilution steps used to prepare working DNA solution	Y	Chapter 3, 4, 5
4. NUCLEIC ACID MODIFICATION		
Template modification (digestion, sonication, pre-amplification, bisulphite etc.)	n/a	
Details of repurification following modification if performed	n/a	
5. REVERSE TRANSCRIPTION		
cDNA priming method and concentration	Y	Chapter 3
One or two step protocol (include reaction details for two step)	Y	Chapter 3
Amount of RNA added per reaction	Y	Chapter 3
Detailed reaction components and conditions	Y	Chapter 3
Estimated copies measured with and without addition of RT*	Y	Chapter 3, Appendix 3
Manufacturer of reagents used with catalogue and lot numbers	Y	Chapter 3
Storage of cDNA: temperature, concentration, duration, buffer and aliquots	Y	Chapter 3
6. dPCR OLIGONUCLEOTIDES DESIGN AND TARGET INFORMATION		
Sequence accession number or official gene symbol	Y	Chapter 3, 4, 5
Method (software) used for design and <i>in silico</i> verification	Y	Chapter 3, 4, 5
Location of amplicon	Y	Chapter 5, also in relevant source publications
Amplicon length	Y	Chapter 5, also in relevant source publications
Primer and probe sequences (or amplicon context sequence)**	Y	Chapter 3, 4, 5
Location and identity of any modifications	Y	Chapter 3, 4, 5

Manufacturer of oligonucleotides	Y	Section 2.1.3
7. dPCR PROTOCOL		
Manufacturer of dPCR instrument and instrument model	Y	Chapter 3, 4, 5
Buffer/kit manufacturer with catalogue and lot number	Y	Chapter 3, 4, 5
Primer and probe concentration	Y	Section 2.1.5
Pre-reaction volume and composition (incl. amount of template and if restriction enzyme added)	Y	Section 2.1.5
Template treatment (initial heating or chemical denaturation)	Y	Chapter 3
Polymerase identity and concentration, Mg ⁺⁺ and dNTP concentrations***	Y	Included in manufacturer's specifications
Complete thermocycling parameters	Y	Section 2.1.5, Chapter 3, 4, 5
8. ASSAY VALIDATION		
Details of optimisation performed	N	Details can be provided as supplementary methods
Analytical specificity (vs. related sequences) and limit of blank (LOB)	Y	Chapter 5, also in relevant source publications
Analytical sensitivity/LoD and how this was evaluated	Y	Chapter 3, 5, (Busby <i>et al.</i> , 2017)
Testing for inhibitors (from biological matrix/extraction)	Y	Chapter 3, 5; linear dilution series analysed
9. DATA ANALYSIS		
Description of dPCR experimental design	Y	Chapter 3, 4, 5
Comprehensive details negative and positive of controls (whether applied for QC or for estimation of error)	Y	Chapter 3, 4, 5
Partition classification method (thresholding)	Y	Chapter 3, 4, 5
Examples of positive and negative experimental results (including fluorescence plots in supplemental material)	Y	Chapter 3, 5, (Busby <i>et al.</i> , 2017)
Description of technical replication	Y	Chapter 3, 4, 5
Repeatability (intra-experiment variation)	Y	Chapter 3, 4, 5

Reproducibility (inter-experiment/user/lab etc. variation)	Y	Chapter 3, 5
Number of partitions measured (average and standard deviation)	Y	Chapter 4, 5
Partition volume	Y	Chapter 3, 4, 5
Copies per partition (λ or equivalent) (average and standard deviation)	Y	Chapter 3, 4, 5
dPCR analysis program (source, version)	Y	Chapter 3, 4, 5; Section 2.1.5
Description of normalisation method	Y	Chapter 4
Statistical methods used for analysis	Y	Chapter 3, 4, 5
Data transparency	N	Can be provided as supplementary data

* Assessing the absence of DNA using a no RT assay (or where RT has been inactivated) is essential when first extracting RNA. Once the sample has been validated as DNA-free, inclusion of a no-RT control is desirable, but no longer essential.

** Disclosure of the primer and probe sequence is highly desirable and strongly encouraged. However, since not all commercial pre-designed assay vendors provide this information when it is not available assay context sequences must be submitted (Bustin et al. Primer sequence disclosure: A clarification of the miqe guidelines. Clin Chem 2011;57:919-21.)

*** Details of reaction components is highly desirable, however not always possible for commercial disclosure reasons. Inclusion of catalogue number is essential where component reagent details are not available.

10.10. Appendix 10

MIAPE-MS checklist

Supplementary Guidelines. The MIAPE-MS Reporting guidelines for mass spectrometry (MIAPE-MS version 2.24).	
<p>1. General features</p> <p>a) Global descriptors</p> <ul style="list-style-type: none"> – Date stamp (as YYYY-MM-DD) – Responsible person (or institutional role if more appropriate); provide name, affiliation, and stable contact information – Instrument manufacturer and model – Customisations (summary) <p>b) Control and analysis software</p> <ul style="list-style-type: none"> – Software name and version – Switching criteria (tandem only) – Isolation width (global, or by MS level) – Location of 'parameters' file 	<p>Chapter 6; Section 6.2.5</p> <p>Institute</p> <p>Instrument manufacturer and model</p> <p>Control and analysis software: name and version</p>

2. Ion sources

As each spectrum is acquired using only one ionisation source, select the one that applies

a) Electrospray Ionisation (ESI)

- Supply type (static, or fed)
- Interface manufacturer, model, and catalog number (where available)
- Sprayer type, coating, manufacturer, model, and catalogue number (where available)
- Relevant voltages where appropriate (tip, cone, acceleration)
- Other parameters if discriminant for the experiment (such as nebulising gas and pressure)

b) MALDI

- Plate composition (or type)
- Matrix composition (if applicable)
- Deposition technique
- Relevant voltages where appropriate (Grid, acceleration)
- PSD (or LID/ISD) summary, if performed
- Operation with or without delayed extraction
- Laser type (e.g. nitrogen) and wavelength (nm),
- Other laser related parameters, if discriminating for the experiment (such as pulse energy (J), attenuation, focus diameter (m), pulse duration (ns at FWHM), frequency (Hz) and average shots fired per spectrum)

Chapter 2; Section 2.2.4

Chapter 6; Section 6.2.5

Matrix composition

Deposition technique

Additional information:

Ion source voltages: 20.0 kV, 18.1 kV

Laser frequency: 60.0 Hz

Typical shot count: 40

3. Post-source component

As a MS experiment performed on one instrument cannot be acquired using all existing analysers and detectors, select the elements that apply

a) Ion optics, 'simple' quadrupoles, hexapoles

– No parameters to be captured

b) Time-of-flight drift tube (TOF)

– Reflectron status (on, off, none)

c) Ion trap

– Final MS stage achieved

d) Collision cell

– Gas type and pressure (bar)

– Collision energy

e) FT-ICR

– As for 'Ion trap' (3c) and 'Collision cell' (3d) combined, no further parameters required

f) Detectors

– Detector type

– Detector sensitivity

4. Spectrum and peak list generation and annotation

For this section; if software other than that listed in 1b (Control and analysis software) is used to perform a task, the producer, name, and version of that software must be supplied in each case

a) Spectrum description

- Location of source ('raw') file including file name and type
- Identifying information for the target area (MALDI-like methods only)
- MS level for this spectrum
- Ion mode for this spectrum
- Precursor m/z and charge, with the full mass spectrum containing that peak (for MS level 2 and higher)

b) Peak list generation

- Parameters triggering the generation of peak lists from raw data, including filtering for exclusion of peak lists from raw spectra, where appropriate
- Acquisition number (from the 'raw' file) of all acquisitions combined in the peak list, the total number combined and whether summed or averaged
- Smoothing; whether applied, parameters
- Background threshold, or algorithm used
- Signal-to-noise estimation and method
- Percentage peak height for centroiding; or algorithm used, if appropriate

Chapter 6; Section 6.2.5 & Section 6.2.8

Ion mode: positive

- Whether charge states were calculated, spectra were deconvoluted and peaks were deisotoped (with methods described as appropriate)
 - Relative times for all acquisitions combined in the peak list (electrospray only)
 - Base peak m/z , where appropriate
 - Metastable peaks removed, if applicable
 - m/z and intensity values
- c) Quantitation for selected ions (in addition to 4a) and 4b)
- Only applicable if a quantitation experiment has been performed
- Experimental protocol, canonical reference where available with deviations
 - Number of combined samples and MS runs analysed
 - Quantitation approach (e.g. integration)
 - Normalisation technique
 - Location of quantitation data, with file name and type (where appropriate)

10.11. Appendix 11

List of peer-reviewed publications and manuscripts in draft

- 10.11.1. Jones, G. M., Busby, E., Garson, J. A., Grant, P. R., Nastouli, E., Devonshire, A. S. & Whale, A. S. 2016. Digital PCR Dynamic Range is Approaching that of Real-Time Quantitative PCR. *Biomolecular Detection and Quantification*, 10, 31–33.
- 10.11.2. Busby, E., Whale, A. S., Ferns, R. B., Grant, P. R., Morley, G., Campbell, J., Foy, C. A., Nastouli, E., Huggett, J. F. & Garson, J. A. 2017. Instability of 8E5 Calibration Standard Revealed by Digital PCR Risks Inaccurate Quantification of HIV DNA in Clinical Samples by qPCR. *Scientific Reports*, 7, 1209.
- 10.11.3. Falak, S., Macdonald, R., Busby, E., O'Sullivan, D., Milavec, M., Plauth, A., Kammel, M., Zeichhardt, H., Grunert, H., Huggett, J. & Kummrow, A. An Assessment of the Reproducibility of Reverse Transcription Digital PCR Quantification of HIV-1 Viral RNA Genome.
- 10.11.4. Busby, E., Doyle, R., Solanki, P., Leboreiro Babe, C., Pang, V., Méndez-Cervantes, G., Harris, K., O'Sullivan, D., Huggett, J., McHugh, T. & Wey, E. Evaluation of MALDI-TOF MS and other emerging methods for molecular typing of *Acinetobacter baumannii*.



Research Paper

Digital PCR dynamic range is approaching that of real-time quantitative PCR



Gerwyn M. Jones^{a,1}, Eloise Busby^{a,1}, Jeremy A. Garson^b, Paul R. Grant^c, Eleni Nastouli^c, Alison S. Devonshire^a, Alexandra S. Whale^{a,*}

^a Molecular and Cell Biology Team, LGC, Teddington, United Kingdom

^b Department of Infection, Division of Infection and Immunity, University College London, London, UK

^c Virology Laboratory, Clinical Microbiology and Virology, University College London Hospital NHS Foundation Trust, London, United Kingdom

ARTICLE INFO

Article history:

Received 9 September 2016

Received in revised form 19 October 2016

Accepted 24 October 2016

Available online 2 November 2016

ABSTRACT

Digital PCR (dPCR) has been reported to be more precise and sensitive than real-time quantitative PCR (qPCR) in a variety of models and applications. However, in the majority of commercially available dPCR platforms, the dynamic range is dependent on the number of partitions analysed and so is typically limited to four orders of magnitude; reduced compared with the typical seven orders achievable by qPCR. Using two different biological models (HIV DNA analysis and *KRAS* genotyping), we have demonstrated that the RainDrop Digital PCR System (RainDance Technologies) is capable of performing accurate and precise quantification over six orders of magnitude thereby approaching that achievable by qPCR.

© 2016 The Author(s). Published by Elsevier GmbH. This is an open access article under the CC BY-NC-ND license (<http://creativecommons.org/licenses/by-nc-nd/4.0/>).

Digital PCR (dPCR) is a sensitive, precise and robust method that could enable quantification of a range of novel biomarker measurements [1]. However, the method is not without its disadvantages that include cost, technical complexity and a reduced dynamic range when compared with real-time quantitative PCR (qPCR).

For dPCR, quantification is typically performed by determining the proportion of positive partitions in the reaction and applying a Poisson correction to account for the fact that at higher DNA concentrations, a positive partition will be more likely to contain more than one molecule [2]. Alternatively, if the DNA concentration is low enough to ensure single molecule occupancy of each positive partition, the Poisson correction is not necessary and the number of positive partitions alone enables quantification.

With both approaches, the dynamic range is determined by the total number of partitions in the reaction. When considering dynamic range, the RainDrop Digital PCR System (RainDance Technologies) could theoretically compete with qPCR as it can generate up to ten million partitions per reaction, giving a potential upper limit in excess of 100 million molecules per reaction if Poisson correction is applied. However, current the recommendations from RainDance are to use low partition occupancy (<10% positive parti-

tions) which makes Poisson correction unnecessary but lessens the dynamic range.

dPCR accuracy is dependent on a number of physical factors such as the partition volume and, when applying a Poisson correction, the partition volume variation should either be small or factored into the calculation [3,4]. We hypothesised that the low occupancy recommendation for the RainDance platform could be due to the challenge of maintaining precise volume of the very small ~5 pL partitions at higher DNA concentrations, as increased volume variation would result in an underestimation of the DNA copy number concentration [3].

To investigate this hypothesis, we performed a series of dynamic range experiments using two target molecules based on HIV DNA analysis and *KRAS* genotyping (Fig. S1). Both target molecules were dsDNA fragments: a 300 bp fragment containing a region of the *LTR-gag* junction from the HIV HXB2 reference genome (NCBI Accession K03455.1, bases 451 to 750) and a 186 bp fragment containing the *KRAS* G12D point mutation (NCBI Accession NG.007524.1, bases 10458 to 10671) (Fig. S1). The target fragments were initially quantified using the Qubit 2.0 fluorimeter with the High Sensitivity DNA assay (ThermoFisher Scientific) and converted to copy number concentration using a standard method [5].

For each target fragment, a seven-point 10-fold calibration curve was volumetrically prepared from ~50 million to ~50 copies per 50 µL PCR reaction (approximate λ range of 5 to 0.000005) before storing each dilution as single use 50 µL aliquots at -20 °C (Table 1). To mimic the interfering sequences that are present in samples

* Corresponding author.

E-mail address: alexandra.whale@gcggroup.com (A.S. Whale).

¹ These authors contributed equally to this work.

Table 1
Template Dilutions Workflow.

Nominal copies/reaction	[Plasmid] (c/ μ L)	Plasmid vol (μ L)	Diluent vol (μ L)	Total vol (μ L)
N/A	1.00E+08			200.00
N/A	1.00E+07	20.0	180.0	200.0
50000000	2.50E+06	100.0	300.0	400.0
5000000	2.50E+05	40.0	360.0	400.0
500000	2.50E+04	40.0	360.0	400.0
50000	2.50E+03	40.0	360.0	400.0
5000	2.50E+02	40.0	360.0	400.0
500	2.50E+01	40.0	360.0	400.0
50	2.50E+00	40.0	360.0	400.0
0	0.00E+00	0.0	400.0	400.0

Each dilution was prepared volumetrically from a master stock of 1×10^8 copies/ μ L. The dilutions were stored in single use 50 μ L aliquots at 20 °C for the duration of the study (1 month). For each dPCR and qPCR experiment, 20 μ L was added to the 50 μ L reaction.

Table 2
Experimental set up.

Platform	qPCR	dPCR
Mastermix	TaqMan Genotyping mastermix (ThermoFisherScientific)	TaqMan Genotyping mastermix (ThermoFisherScientific)
Other reagents	N/A	RainDrop Stabilizer (2 μ L per 50 μ L rxn)
<i>KRAS</i> G12D/WT duplex assay [9]	900 nM <i>KRAS</i> Forward: 5'-AGGCCTGCTGAAAATGACTGAATAT-3' 900 nM <i>KRAS</i> Reverse: 5'-GCTGTATCGTCAAGGCACTCTT-3' 250 nM <i>KRAS</i> WT Probe: 5'-[VIC]TTGGAGCTGGTGGCGT[NFQ/MGB]-3' 250 nM <i>KRAS</i> G12D Probe: 5'-[FAM]TGGAGCTGATGGCGT[NFQ/MGB]-3'	
HIV <i>LTR-gag</i> /PDH duplex assay	900 nM <i>LTR-gag</i> Forward: 5'-GCCTCAATAAAGCTTGCCTTGA-3' 900 nM <i>LTR-gag</i> Reverse: 5'-GGCGCCACTGCTAGAGATTTT-3' 200 nM <i>LTR-gag</i> Probe: 5'-[FAM]TGTGACTCTGGTAACTAGAGATCCCTCAGAC[BHQ1]-3' 900 nM PDH Forward: 5'-TGAAAGTTATACAAAATTGAGGTCCTGTT-3' 900 nM PDH Revers: 5'-TCCACAGCCCTCGACTAACC-3' 200 nM PDH Probe: 5'-[VIC]CCCCAGATACACTTAAGGGA[MGB]-3'	
Oligonucleotide purification method	HPLC	
Sample volume	20 μ L	22.5 μ L
Total reaction volume prepared	50 μ L	55 μ L
Consumable	96-well plate	RainDrop source chip
Reaction volume loaded	50 μ L	50 μ L
Partition volume	N/A	5 pL
Partition number	N/A	Up to 10 million
Instrumentation	ABI 7900HT (ThermoFisherScientific)	Droplets generated: RainDrop Source Instrument (RainDance). Thermal cycling: DNA Engine Tetrad (Bio-rad). Droplets read: RainDrop Sense instrument (Instrument Control Software v2.1.3.11157) (RainDance)
<i>KRAS</i> Cycling Parameters	95 °C for 15 min, followed by 45 cycles of 94 °C for 60 s and 64 °C for 60 s	95 °C for 10 min, followed by 45 cycles of 95 °C for 15 s and 64 °C for 60 s, then 98 °C for 10 min, 12 °C for 15 min, and 4 °C hold
HIV/PDH Cycling Parameters	95 °C for 15 min, followed by 45 cycles of 94 °C for 60 s and 60 °C for 60 s	95 °C for 10 min, followed by 45 cycles of 95 °C for 15 s and 60 °C for 60 s, then 98 °C for 10 min, 12 °C for 10 min, and 4 °C hold
Analysis software	SDS v2.4 (ThermoFisherScientific)	RainDrop Analyst II software (1.0.0.520)
Analysis parameters	Auto baseline setting, thresholds set manually and applied to all samples within an experiment	Droplets classified independently using polygonal gates, which were then universally applied across all samples within an experiment

used for HIV analysis and *KRAS* genotyping, a constant background of fragmented human gDNA (Cambio; 0.25 ng/ μ L final concentration), prepared in TE buffer, was added to the dilution series. The fragmentation state was chosen to enable droplet formation (high concentration, high molecular weight gDNA interferes with droplet formation and must be fragmented prior to droplet generation) as

well as mimicking the template sizes commonly found in cell free DNA [6]. The dilution series was analysed simultaneously by qPCR (ABI 7900HT) and dPCR (RainDance RainDrop) with single replicates for each dilution and the whole experiment was repeated on five days (Tables 2 & S1, Figs. S2, S3 & S4).

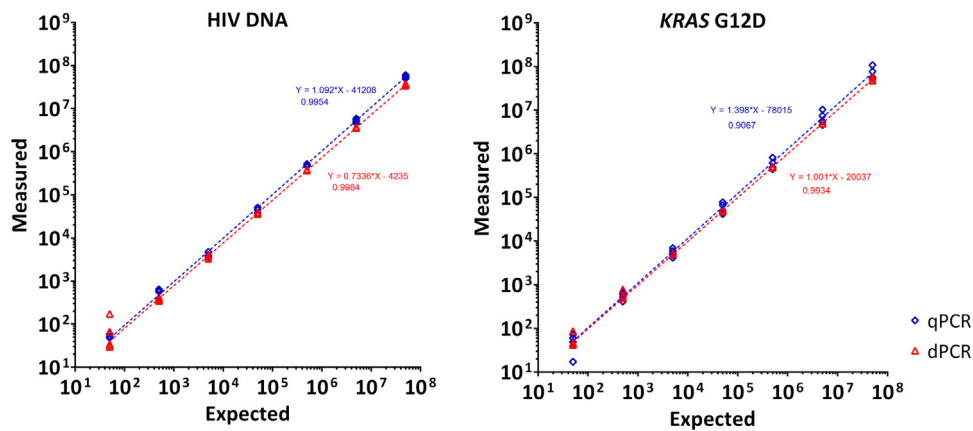


Fig. 1. Dynamic range experiments using qPCR and dPCR to measure HIV DNA and the KRAS G12D single nucleotide variant. Each plot compares measured versus expected copies per 50 μL reaction mix of a 10-fold standard curve performed by qPCR and dPCR. Each standard curve dilution was measured with a single reaction and repeated on five different days.

Quantification by qPCR was performed and the slope and intercept of the calibration curve was calculated from the dilution series. The copy number concentration for each dilution point was re-calculated from the slope; a good linear dynamic range was observed over six orders of magnitude for both target fragments (Fig. 1 and Table S2). Quantification by dPCR was performed by applying the Poisson correction to the proportion of positive partitions in each reaction. Comparable linear dynamic ranges were observed between both targets and platform (Fig. 1) demonstrating firstly, that the partition volume precision is high in the RainDrop Digital PCR System and secondly, that the Poisson correction is suitable for this instrument with high occupancy partitions.

In previous applications of dPCR, dilution has been necessary to quantify higher copy number samples [7]. Crucially this requires a prior knowledge of the concentration range necessitating some initial analysis of the sample. We have demonstrated here that dPCR is capable of directly quantifying DNA over a six log linear dynamic range thereby approaching the seven logs typically achievable by qPCR. A further benefit is that dPCR is an absolute method as the DNA molecules are being directly counted.

A method that can precisely quantify specific nucleic acid molecules over a large dynamic range has numerous applications, which is one of the main reasons that qPCR is widely used in research and clinical laboratories. While qPCR can be precise, its accuracy is dependent on a calibrator. Quantification of the initial calibrator, its commutability, and the fact that the uncertainty of the calibration is seldom considered, limits the accuracy and reproducibility of qPCR. As dPCR directly counts the number of DNA molecules in a sample it does not need the same level of calibration as qPCR and so is more reproducible [8]. Current dPCR experiments are more complex to perform than qPCR, but the digital readout is much simpler to analyse.

With further development to reduce the technical complexity, dPCR could become the method of choice for research and clinical use. Furthermore the digital readout would also make the method suitable for automation both in routine testing laboratories and ultimately point of care. The data presented here demonstrates that a commercially available dPCR platform can perform quantification over a broad dynamic range approaching that achievable by qPCR in a single reaction.

Acknowledgments

We acknowledge Adam Corner of RainDance Technologies, Inc. for advice and access to the RainDrop instrument. The work described in this paper was funded in part by the UK govern-

ment Department for Business, Energy & Industrial Strategy (BEIS) and the European Metrology Research Programme (EMRP) joint research project (SIB54) Bio-SITrace (<http://biositrace.lgcgroup.com>) which is jointly funded by the EMRP participating countries within EURAMET and the European Union.

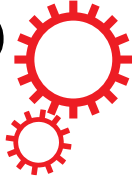
Appendix A. Supplementary data

Supplementary data associated with this article can be found, in the online version, at <http://dx.doi.org/10.1016/j.bdq.2016.10.001>.

References

- [1] E. Day, P.H. Dear, F. McCaughan, Digital PCR strategies in the development and analysis of molecular biomarkers for personalized medicine, *Methods* (2012).
- [2] J.F. Huggett, C.A. Foy, V. Benes, K. Emslie, J.A. Garson, R. Haynes, J. Hellemans, M. Kubista, R.D. Mueller, T. Nolan, et al., The Digital MIQE Guidelines: Minimum Information for Publication of Quantitative Digital PCR Experiments, *Clin. Chem.* 59 (2013) 892–902.
- [3] J.F. Huggett, S. Cowen, C.A. Foy, Considerations for digital PCR as an accurate molecular diagnostic tool, *Clin. Chem.* 61 (2015) 79–88.
- [4] B.K. Jacobs, E. Goetghebuer, L. Clement, Impact of variance components on reliability of absolute quantification using digital PCR, *BMC Bioinf.* 15 (2014) 283.
- [5] S. Dhanasekaran, T.M. Doherty, J. Kenneth, Comparison of different standards for real-time PCR-based absolute quantification, *J. Immunol. Methods* 354 (2010) 34–39.
- [6] A.S. Devonshire, A.S. Whale, A. Gutteridge, G. Jones, S. Cowen, C.A. Foy, J.F. Huggett, Towards standardisation of cell-free DNA measurement in plasma: controls for extraction efficiency, fragment size bias and quantification, *Anal. Bioanal. Chem.* 406 (2014) 6499–6512.
- [7] P. Corbisier, L. Pinheiro, S. Mazoua, A.M. Kortekaas, P.Y. Chung, T. Gerganova, G. Roebben, H. Emons, K. Emslie, DNA copy number concentration measured by digital and droplet digital quantitative PCR using certified reference materials, *Anal. Bioanal. Chem.* 407 (2015) 1831–1840.
- [8] A.S. Devonshire, I. Honeyborne, A. Gutteridge, A.S. Whale, G. Nixon, P. Wilson, G. Jones, T.D. McHugh, C.A. Foy, J.F. Huggett, Highly reproducible absolute quantification of *Mycobacterium tuberculosis* complex by digital PCR, *Anal. Chem.* (2015).
- [9] V. Taly, D. Pekin, L. Benhaim, S.K. Kotsopoulos, D. Le Corre, X. Li, I. Atochin, D.R. Link, A.D. Griffiths, K. Pallier, Multiplex picodroplet digital PCR to detect KRAS mutations in circulating DNA from the plasma of colorectal cancer patients, *Clin. Chem.* 59 (2013) 1722–1731.

SCIENTIFIC REPORTS



OPEN

Instability of 8E5 calibration standard revealed by digital PCR risks inaccurate quantification of HIV DNA in clinical samples by qPCR

Eloise Busby¹, Alexandra S. Whale¹, R. Bridget Ferns², Paul R. Grant³, Gary Morley¹, Jonathan Campbell¹, Carole A. Foy¹, Eleni Nastouli^{3,4}, Jim F. Huggett^{1,5} & Jeremy A. Garson^{2,6}

Establishing a cure for HIV is hindered by the persistence of latently infected cells which constitute the viral reservoir. Real-time qPCR, used for quantification of this reservoir by measuring HIV DNA, requires external calibration; a common choice of calibrator is the 8E5 cell line, which is assumed to be stable and to contain one HIV provirus per cell. In contrast, digital PCR requires no external calibration and potentially provides 'absolute' quantification. We compared the performance of qPCR and dPCR in quantifying HIV DNA in 18 patient samples. HIV DNA was detected in 18 by qPCR and in 15 by dPCR, the difference being due to the smaller sample volume analysed by dPCR. There was good quantitative correlation ($R^2 = 0.86$) between the techniques but on average dPCR values were only 60% of qPCR values. Surprisingly, investigation revealed that this discrepancy was due to loss of HIV DNA from the 8E5 cell calibrant. 8E5 extracts from two other sources were also shown to have significantly less than one HIV DNA copy per cell and progressive loss of HIV from 8E5 cells during culture was demonstrated. We therefore suggest that the copy number of HIV in 8E5 extracts be established by dPCR prior to use as calibrator.

HIV continues to be a major issue for global health, with approximately 36.7 million people living with HIV at the end of 2014 and about 2 million individuals becoming infected each year (WHO 2015). Despite the advent of effective combination antiretroviral therapy (cART), establishing a cure is hindered by the persistence of latently infected host cells, even in the absence of detectable plasma viraemia^{1,2}. These cells, usually CD4+ resting T cells, constitute the viral reservoir³ and have the potential to release progeny virions, therefore being responsible for viral rebound after discontinuation of therapy^{4,5}. With the advent of novel strategies for HIV cure that include latency reversing agents^{6,7} accurate and robust methods are required for measurement and monitoring of the latent reservoir⁸.

A routine method for quantification of HIV RNA viral load, real-time quantitative PCR (qPCR), is also increasingly being used for measuring HIV DNA associated with the viral reservoir⁹. qPCR requires calibration and for this to be reproducible it is essential that the calibrator must be stable when shared between laboratories. A popular choice of calibrator for quantifying HIV DNA by qPCR is 8E5 (ATCC® CRL-8993)¹⁰⁻¹⁷, a lymphoblastic leukaemia cell line which has been reported by several studies to contain one integrated HIV genome per cell^{12, 18, 19}.

¹Molecular and Cell Biology Team, LGC, Teddington, UK. ²Department of Infection, Division of Infection and Immunity, University College London, London, UK. ³Department of Clinical Virology, University College London Hospital NHS Foundation Trust, and the UCL/UCLH NIHR Biomedical Research Centre, London, UK. ⁴Department of Population Policy and Practice, UCL GOS Institute of Child Health, London, UK. ⁵School of Biosciences & Medicine, Faculty of Health & Medical Science, University of Surrey, Guildford, GU2 7XH, UK. ⁶National Transfusion Microbiology Laboratories, NHS Blood and Transplant, Colindale, London, UK. Jim F. Huggett and Jeremy A. Garson contributed equally to this work. Correspondence and requests for materials should be addressed to J.F.H. (email: jim.huggett@lgcgroup.com) or J.A.G. (email: j.garson@ucl.ac.uk)

Digital PCR (dPCR) is a more recently developed method that offers absolute quantification²⁰. It has been used to value assign a variety of qPCR calibrators, including those for BCR-ABL²¹ and *Mycobacterium tuberculosis*²². dPCR has also been used in the direct quantification of HIV DNA from patients in a number of studies^{23–27} and unlike qPCR has the advantage of not requiring an external calibration standard. However, false positives and issues surrounding threshold determination have been reported to limit the usefulness of dPCR when employed for the most sensitive measurements of HIV DNA²⁸. In this study we investigated the application of dPCR instruments in the context of HIV DNA measurement, both for comparison with qPCR analysis of patient samples and as a method for value assigning 8E5 calibration standards from three different sources.

Methods

Patient samples and 8E5 cell calibration standards. Anonymised peripheral blood mononuclear cell samples (PBMC) were obtained from HIV-positive individuals receiving antiretroviral therapy as part of a recently published clinical trial²⁹ comparing Short Cycle Therapy (SCT) with continuous antiretroviral therapy. The study had received appropriate ethical committee approval.

Aliquots of DNA extracted from the 8E5 cell line¹⁹ were obtained from three separate institutions and designated Standard 1, Standard 2 and Standard 3. Standard 1 had been used for clinical research on HIV DNA levels; Standard 2 had been used in research as a source of HIV RNA; Standard 3 was a freshly obtained 8E5 cell culture from the American Type Culture Collection (ATCC® CRL-8993™) distributed by LGC, Teddington, UK. The passage numbers of the 8E5 cells from which Standard 1 and Standard 2 were obtained were unknown.

Culture of 8E5 cells (Standard 3). Briefly, one vial of 8E5 cells (ATCC® CRL-8993™) was taken from liquid nitrogen and thawed at 37 °C for 1–2 minutes. 500 µL of cells was removed from the vial for culture and the remaining 300 µL (approximately 2.4×10^6 cells) retained for DNA extraction as passage 0 (P0). The full culture methodology is described in Supplementary Information. Following the single initial flask (designated passage 1), successive passages were maintained in triplicate (three separate flasks for passages 2, 3 and 4). During each passage cells were taken, pelleted and stored at –80 °C prior to DNA extraction.

DNA extraction. 120 µL of each PBMC sample was lysed in 120 µL ATL buffer and the nucleic acid extracted on the QIA Symphony platform (Qiagen) using the DSP Virus/Pathogen Mini Kit (Qiagen) according to manufacturer's protocols. Extracts were eluted in 60 µL and stored at –20 °C prior to analysis. DNA was extracted from the 8E5 Standard 3 cell pellets from each culture passage using the QIAamp DNA Blood Mini Kit (Qiagen). Supplemental to the manufacturer's protocol, extracts were treated with 4 µL of RNase A (Qiagen) prior to the addition of lysis buffer. Final elution volume was 200 µL in buffer AE.

PCR assay design and primer sequences. Sequence information for the primers and probes used in the study is given in Table S1 of Supplementary Information. All PCR assays were performed in duplex format (i.e. two PCRs in the same reaction tube) consisting of one human reference gene assay (either pyruvate dehydrogenase, PDH or RNase P) and one assay specific for HIV-1. The HIV LTR-*gag* assay was designed to span a highly conserved region of the LTR-*gag* junction to allow amplification of a single Long Terminal Repeat.

qPCR analysis of clinical samples. qPCR analysis of 18 PBMC sample extracts was performed using an Applied Biosystems® 7500 Real-Time PCR System. Experiments were implemented in accordance with the MIQE guidelines³⁰ (Table S2, Supplementary Information). To prepare a qPCR calibration curve consisting of ~50,000 to ~5 HIV DNA copies per reaction (assuming 1 HIV DNA copy per 8E5 cell), DNA extracted from the 8E5 cell line Standard 1, (DNA concentration initially established by Qubit fluorometric quantitation; ThermoFisher Scientific Inc.), was serially diluted using a tenfold dilution series in 5 µg/mL carrier RNA (Qiagen) dissolved in nuclease-free water. Twenty µL of each clinical sample extract (~1.2 µg DNA, equivalent to approximately 200,000 cells) was added to a total reaction volume of 50 µL. Full details of the PDH/HIV LTR-*gag* duplex qPCR assay protocol, cycling parameters and primer/probe sequences are given in Supplementary Information.

Digital PCR basic protocol. Duplex format dPCR experiments were implemented in accordance with the dMIQE guidelines (Supplementary Information)³¹. Two dPCR instruments were employed during the study; the RainDrop® Digital PCR System (RainDance Technologies) was used to measure the clinical samples and 8E5 extracts, and the QX200™ Droplet Digital™ PCR System (BioRad) was used to measure the 8E5 extracts only. Positive and negative partitions were selected for the RainDrop® and QX200™ manually using ellipse and quadrant gating, respectively, as recommended by the manufacturer using the instruments' software. Full experimental protocols for both dPCR instruments and details of primers and probes used in the duplex assays are given in Supplementary Information. No template controls (NTCs) were included in all experiments.

Digital PCR analysis of clinical samples. 5 µL (equivalent to approximately 50,000 cells) of the same 18 clinical sample extracts that had previously been analysed by qPCR were analysed using the RainDrop® dPCR platform as described above. The samples were amplified using the PDH/HIV LTR-*gag* duplex assay and NTCs of nuclease-free water were included as controls. The extracts were coded and the operator had no prior knowledge of the qPCR results on the same samples.

Digital PCR characterisation of 8E5 cells. The 8E5 DNA extracts from Standards 1, 2 and 3 were assessed using the RainDrop® platform with duplex primer sets to PDH/HIV LTR-*gag*, PDH/HIV *pol* and RNase P/HIV LTR-*gag* (Table S1). For the Standard 3 cells all four culture passage extracts and the initial passage zero (P0) extract were analysed using both RainDrop® and QX200™ instruments with the PDH/HIV LTR-*gag* duplex assay.

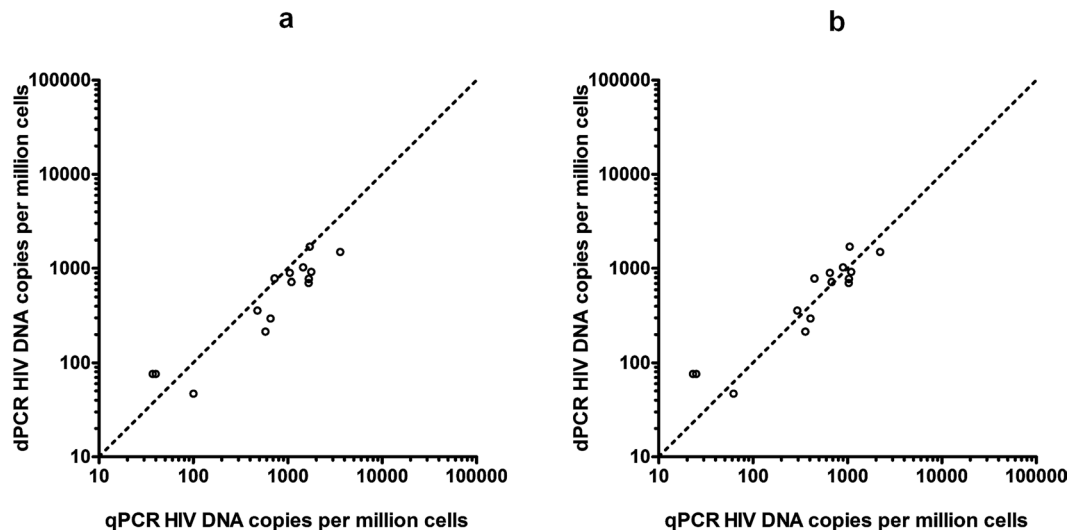


Figure 1. Comparison between dPCR and qPCR results from 18 PBMC samples from HIV-positive patients, expressed as HIV DNA copies per million cells. The three samples in which HIV DNA was not detected by dPCR are not plotted. (a) qPCR quantities calculated assuming one HIV DNA copy per 8E5 cell. (b) qPCR quantities calculated assuming 0.6 HIV DNA copy per 8E5 cell as determined experimentally by dPCR NB. The dashed line represents equivalence.

Effect of different 8E5 calibrator sources on qPCR analysis of clinical samples. Analysis of an additional seven HIV-positive clinical sample PBMC extracts was performed using qPCR as above. This experiment utilised the three different 8E5 cell Standards 1, 2 and 3 (passage 2) simultaneously as calibrators in the same run. HIV DNA copies were calculated per million cells using either the published quantity of 1 HIV DNA copy per 8E5 cell^{12, 18, 19} for all three different 8E5 sources or alternatively, the quantity determined empirically for the respective 8E5 extracts by dPCR during the present study.

Data Analysis. Data from dPCR and qPCR experiments were subject to threshold and baseline setting in the relevant instrument software, and were exported as .csv files to be analysed in Microsoft Excel 2010. For dPCR experiments the average number of copies per droplet (λ) was calculated as described previously³². dPCR and qPCR analyses of the clinical samples were compared by using a paired t-test on the log transformed HIV DNA copies per million cells. Agreement between methods was investigated using a Bland-Altman analysis and data evaluated for linearity using linear regression.

Results

Analysis of clinical samples by qPCR and dPCR. 18 PBMC DNA samples from HIV-positive patients were analysed by dPCR and qPCR using the PDH/HIV LTR-*gag* duplex assays. HIV DNA was detected in all 18 samples by qPCR but in only 15 samples by dPCR. The three dPCR negative samples were near the lower limit of detection by qPCR (Supplementary Information, Table S3) and were probably undetected by dPCR due to the lower volume of template used (RainDrop[®] dPCR used ~5 μ L whereas the qPCR used 20 μ L, an approximately 4 fold greater volume of template). When the HIV DNA copies per million cells were calculated the dPCR and qPCR results correlated well ($R^2 = 0.86$), however the dPCR results were on average only ~60% of the qPCR results, a statistically significant difference ($p = 0.02$) (Fig. 1a). Linear regression on the data generated from Bland-Altman analysis found no evidence of a trend in the observed bias which was independent of HIV DNA concentration (Figure S3). No false positive dPCR results were observed in the NTCs (Supplementary Information, Table S4).

Discrepancy between qPCR and dPCR due to loss of HIV DNA from 8E5 cells. In order to determine whether the ~60% discrepancy between dPCR and qPCR results might have been due to erroneous calibration of the qPCR, we investigated the calibrator (8E5 Standard 1) that had been used to calibrate the qPCR assay. Surprisingly, RainDrop[®] dPCR analysis of 8E5 Standard 1 with the PDH/HIV LTR-*gag* duplex assay revealed a ratio of PDH copies to HIV copies of approximately 3.2:1, whereas according to the literature^{12, 18, 19} the expected PDH:HIV ratio should have been exactly 2:1. This surprising finding was confirmed by repeating the dPCR analysis of 8E5 Standard 1 with a different dPCR instrument (QX200[™]) and with a different region of the HIV genome (*pol*) as PCR target. To exclude the possibility that the unexpected PDH:HIV ratio in 8E5 Standard 1 might have been caused by an increase in the PDH reference gene copy number we repeated the assays using a different human reference gene (RNase P) located on a different chromosome. In all cases the results confirmed that the PDH:HIV ratio in 8E5 Standard 1 was approximately 3.2:1 which is equivalent to approximately 0.6 HIV DNA copies per 8E5 cell. These findings are summarised in Fig. 2a. When the qPCR results on the 18 clinical samples were corrected to take into account the actual HIV DNA content of the 8E5 Standard 1 used as calibrator, the ~60% discrepancy between qPCR and dPCR findings became statistically insignificant ($p = 0.41$) (Fig. 1b).

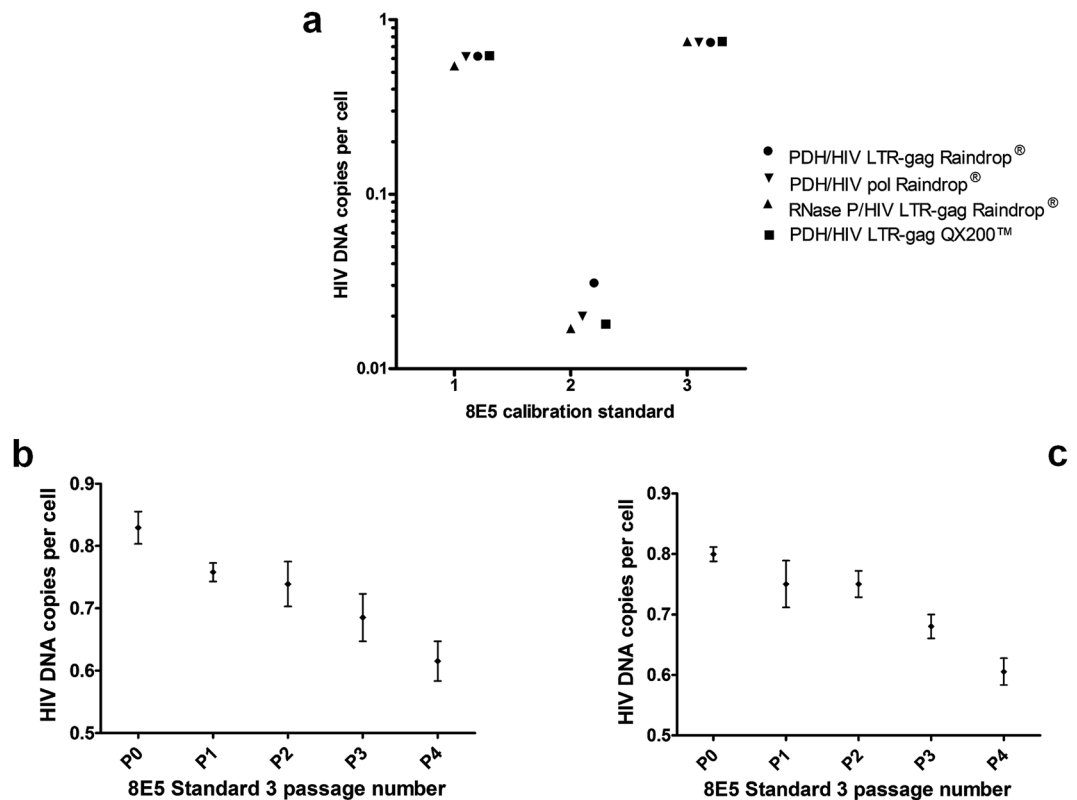


Figure 2. HIV DNA copies per cell calculated for different 8E5 sources. **(a)** Comparison of 8E5 Standards 1, 2 and 3 analysed by dPCR. **(b)** Effect of culture passage on HIV DNA content per cell for 8E5 Standard 3 measured using the RainDrop® dPCR platform **(c)** Effect of culture passage on HIV DNA content per cell for 8E5 Standard 3 measured using the QX200™ dPCR platform. Mean values with standard deviations are plotted.

To establish whether this loss of HIV DNA from the 8E5 calibrator was unique to the particular source of 8E5 that had been used, we obtained additional aliquots of 8E5 (designated Standard 2 and Standard 3 for the purposes of this study) from two independent institutions. 8E5 DNA extracts from Standard 2 and Standard 3 were analysed with both RainDrop® and QX200™ dPCR instruments by duplex assays using both regions of the HIV genome as target and both human reference genes. Remarkably, the magnitude of the loss of HIV DNA from 8E5 Standard 2 proved to be even greater (~0.02 HIV DNA copies per cell) than for Standard 1. In contrast, the loss of HIV DNA from 8E5 Standard 3 (~0.8 HIV DNA copies per cell) was less marked. The results of this dPCR characterisation of 8E5 Standards 2 and 3 are shown in Fig. 2a.

For the ATCC stock (8E5 Standard 3) five separate culture passages were analysed starting from baseline (P0) to passage 4. One DNA extract representing each culture flask per passage was analysed on RainDrop® and QX200™ dPCR platforms using the PDH/HIV LTR-gag duplex assay. The HIV DNA copies were observed to decrease relative to PDH copies with successive passages, equating to a fall in HIV DNA copy number from ~0.8 to ~0.6 copies per cell (Fig. 2b and c). Short Tandem Repeat (STR) analysis was performed by the supplier prior to culture, with the unique DNA profile being concordant with the cell line specification, suggesting proliferation of an additional non related clonal population was unlikely to be the source of this HIV DNA copy number change. No false positive results were observed for either instrument during these comparisons (Table S4).

Different sources of 8E5 calibrator may generate significant inaccuracies in HIV DNA quantification of clinical samples.

To assess the effect of using different sources of 8E5 calibration material on the qPCR quantification of HIV DNA in clinical samples, three separate standard curves were constructed from 8E5 Standards 1, 2 and 3 in the same experimental run. Seven additional patient PBMC samples were tested in duplicate by qPCR using the PDH/HIV LTR-gag duplex assay and the means (expressed in HIV DNA copies per million cells) calculated for each sample (Fig. 3). When the previously reported one HIV DNA copy per 8E5 cell was assumed for all three Standards, the values calculated using 8E5 Standard 2 as calibrator were approximately 45 times higher than those calculated using the 8E5 Standards 1 and 3 which agreed with each other (Fig. 3a). When the dPCR derived values of HIV DNA copies per 8E5 cell were applied to the respective 8E5 Standard 1, 2 and 3 extracts the results with all three sources of 8E5 calibrator became concordant (Fig. 3b).

Discussion

Detection of total cellular HIV DNA, comprising integrated proviral DNA and unintegrated forms such as LTR circles, offers a means of monitoring the latent viral reservoir in the absence of circulating HIV RNA⁵. However, it should be noted that HIV DNA assays are unable to differentiate between replication competent and incompetent

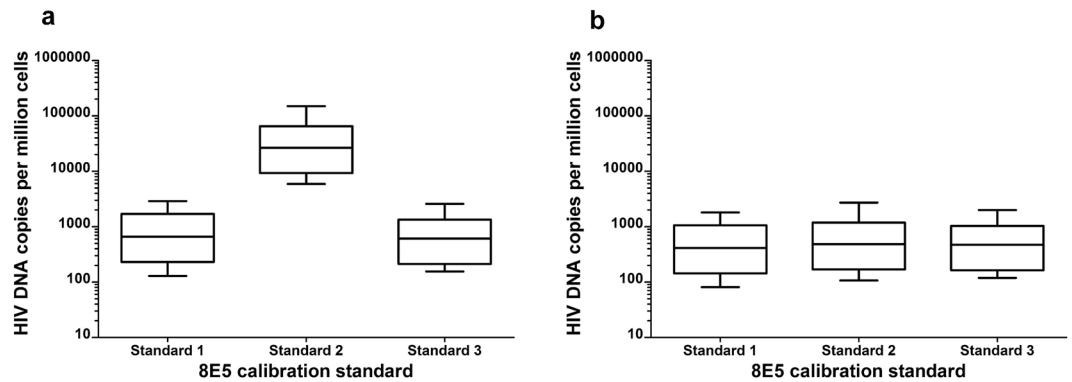


Figure 3. Median HIV DNA copies per million cells (boxplots with interquartile and range) of seven clinical samples assayed in duplicate by qPCR using 8E5 Standards 1, 2 and 3 for calibration. **(a)** Calculated assuming one HIV DNA copy per 8E5 cell for all three Standards. **(b)** Calculated using the actual number of HIV DNA copies per 8E5 cell as determined by dPCR for each of the three Standards.

HIV genomes and therefore do not actually measure the *functional* viral reservoir, which is most directly assessed by viral outgrowth assays²⁴. Notwithstanding these reservations, HIV DNA assays have been widely used as an alternative to viral outgrowth assays because the latter are disadvantaged by being relatively expensive, labour intensive, technically demanding and requiring large amounts of blood. There is data supporting the use of HIV DNA assays and reports indicating a correlation between HIV DNA levels and clinically important parameters such as disease progression, post-treatment virological control and time to viral rebound on stopping cART⁵. qPCR is a widely used method for measuring total cellular HIV DNA⁹ as it is a versatile technique that is already well established for HIV RNA viral load measurement. It is comparatively inexpensive and readily scalable both in terms of reaction volume and throughput.

More recently, digital PCR has also been applied for HIV DNA measurement with some success but concerns have been raised regarding its sensitivity²⁸. In this study we aimed to compare qPCR with dPCR for measuring total cellular HIV DNA in clinical samples and attempted to explain why discrepancies between the techniques may have occurred. We found that the results were broadly comparable, but that dPCR had reduced sensitivity related to the lower sample volume protocol employed. We did not observe the false positive dPCR results reported by others²⁸ with either RainDrop[®] or QX200[™] platforms (Table S4) and so did not have the challenge associated with setting thresholds to omit false positives. This demonstrates that dPCR could be effective as an alternative to qPCR for measurement of HIV DNA in patient samples if adequate sample volumes are used and strict contamination control measures maintained.

While dPCR may offer a powerful alternative ‘absolute’ method to qPCR for research use, the fact that the latter technique is so well established means it is likely to remain the method of choice for most clinical analyses of HIV DNA in the short term at least. However, this study has demonstrated that dPCR has an important role in improving qPCR accuracy and reproducibility by characterising and value assigning the calibration materials used for qPCR quantitation; we identified that qPCR overestimated the amount of HIV DNA per million cells due to unexpected instability of the 8E5 cell calibrator. The 8E5 cell line has been repeatedly reported and assumed to contain one HIV DNA proviral genome per cell^{12, 18, 19} but our findings suggest that this assumption is unsafe and that different batches of 8E5 may contain different amounts of HIV DNA per cell (varying in this study from ~0.02 to ~0.8 copies per cell).

To determine the HIV DNA copy number in the master stock and investigate the effect of culture on HIV DNA copies, a fresh culture was obtained from ATCC and serially passaged four times. This experiment demonstrated that HIV DNA copies were being lost in culture with serial passage (Fig. 2b and c). Coincidentally, during the preparation of the present manuscript, a study by Wilburn and colleagues was published, also raising concerns over the use of 8E5 for calibrating HIV DNA assays³³. Wilburn’s study, based on fluorescent *in situ* hybridisation (FISH) and flow cytometry also concluded that, contrary to expectation, deletion of the HIV proviral genome could occur during culture of 8E5 cells and that different batches of 8E5 cells could contain dramatically varying numbers of cells lacking viral genomes. The mechanism of HIV DNA loss is unclear but it may be relevant that the provirus in 8E5 cells is inserted at 13q14-q21 which contains common fragile sites¹⁸ and could therefore render 8E5 susceptible to proviral loss through genomic instability.

Although qPCR is applied routinely in clinical virology, for the method to be reproducible it is widely recognised that reference materials are needed³⁴ from which calibration standards can be derived. Reference materials do not currently exist for HIV DNA measurement, however the 8E5 cell line, with a reported single HIV DNA copy per cell, has been widely used as a calibrator over many years^{10–17}. We demonstrate here that using the 8E5 cell line and assuming one HIV DNA copy per cell could lead to inaccuracies which could in turn result in misleading quantitative estimates of the HIV reservoir. Although 8E5 is commonly employed for calibration of HIV DNA qPCR assays, alternative calibrators such as the U1 cell line and HIV plasmids have been used in some studies^{23, 27}. Bias of the type described here with 8E5 calibration has not to our knowledge been reported in studies that have utilised these alternatives, however the dPCR approach that we describe can also be used to determine the HIV content of different calibrators.

While we have identified this potential problem and demonstrated the significant bias that may ensue (Fig. 3a) we have also demonstrated how dPCR can be used to rectify any bias and harmonise the quantitative findings from 8E5 sources containing different quantities of HIV DNA (Fig. 3b). It would seem prudent to recommend that laboratories embarking on new quantitative studies into HIV DNA using qPCR obtain a fresh stock of 8E5 or other chosen calibrator and establish its actual HIV DNA content empirically using dPCR. Previous studies that may have used 8E5 with potentially varying HIV DNA quantities can apply the dPCR methods described here to determine the HIV DNA content of the batch used and, if necessary, recalculate their findings based on the new value assignment.

References

- Churchill, M. J., Deeks, S. G., Margolis, D. M., Siliciano, R. F. & Swanstrom, R. HIV reservoirs: what, where and how to target them. *Nature reviews. Microbiology* **14**, 55–60, doi:10.1038/nrmicro.2015.5 (2016).
- Richman, D. *et al.* The Challenge of Finding a Cure for HIV Infection. *Science* **323**, 1304–1307, doi:10.1126/science.1165706 (2009).
- Siliciano, J. M. & Siliciano, R. F. The Remarkable Stability of the Latent Reservoir for HIV-1 in Resting Memory CD4+ T Cells. *The Journal of infectious diseases* **212**, 1345–1347, doi:10.1093/infdis/jiv219 (2015).
- Bruner, K. M. *et al.* Defective proviruses rapidly accumulate during acute HIV-1 infection. *Nature medicine*, doi:10.1038/nm.4156 (2016).
- Williams, J. P. *et al.* HIV-1 DNA predicts disease progression and post-treatment virological control. *eLife* **3**, e03821, doi:10.7554/eLife.03821 (2014).
- Barton, K. M. *et al.* Selective HDAC inhibition for the disruption of latent HIV-1 infection. *PLoS one* **9**, e102684, doi:10.1371/journal.pone.0102684 (2014).
- Margolis, D. M., Garcia, J. V., Hazuda, D. J. & Haynes, B. F. Latency reversal and viral clearance to cure HIV-1. *Science* **353**, aaf6517, doi:10.1126/science.aaf6517 (2016).
- Bruner, K. M., Hosmane, N. N. & Siliciano, R. F. Towards an HIV-1 cure: measuring the latent reservoir. *Trends in microbiology* **23**, 192–203, doi:10.1016/j.tim.2015.01.013 (2015).
- Sedlak, R. H. & Jerome, K. R. Viral diagnostics in the era of digital polymerase chain reaction. *Diagnostic microbiology and infectious disease* **75**, 1–4, doi:10.1016/j.diagmicrobio.2012.10.009 (2013).
- Avettand-Fenoel, V. *et al.* LTR real-time PCR for HIV-1 DNA quantitation in blood cells for early diagnosis in infants born to seropositive mothers treated in HAART area (ANRS CO 01). *Journal of medical virology* **81**, 217–223, doi:10.1002/jmv.21390 (2009).
- Beck, I. A. *et al.* Simple, sensitive, and specific detection of human immunodeficiency virus type 1 subtype B DNA in dried blood samples for diagnosis in infants in the field. *Journal of clinical microbiology* **39**, 29–33, doi:10.1128/JCM.39.1.29-33.2001 (2001).
- Desire, N. *et al.* Quantification of human immunodeficiency virus type 1 proviral load by a TaqMan real-time PCR assay. *Journal of clinical microbiology* **39**, 1303–1310, doi:10.1128/JCM.39.4.1303-1310.2001 (2001).
- Ghosh, M. K. *et al.* Quantitation of human immunodeficiency virus type 1 in breast milk. *Journal of clinical microbiology* **41**, 2465–2470, doi:10.1128/JCM.41.6.2465-2470.2003 (2003).
- Jaafoura, S. *et al.* Progressive contraction of the latent HIV reservoir around a core of less-differentiated CD4(+) memory T Cells. *Nature communications* **5**, 5407, doi:10.1038/ncomms6407 (2014).
- Kabamba-Mukadi, B. *et al.* Human immunodeficiency virus type 1 (HIV-1) proviral DNA load in purified CD4+ cells by LightCycler real-time PCR. *BMC infectious diseases* **5**, 15, doi:10.1186/1471-2334-5-15 (2005).
- McFall, S. M. *et al.* A simple and rapid DNA extraction method from whole blood for highly sensitive detection and quantification of HIV-1 proviral DNA by real-time PCR. *J Virol Methods* **214**, 37–42, doi:10.1016/j.jviromet.2015.01.005 (2015).
- Shiramizu, B. *et al.* Circulating proviral HIV DNA and HIV-associated dementia. *Aids* **19**, 45–52, doi:10.1097/00002030-200501030-00005 (2005).
- Deichmann, M., Bentz, M. & Haasa, R. Ultra-sensitive FISH is a useful tool for studying chronic HIV-1 infection. *Journal of Virological Methods* **65**, 19–25, doi:10.1016/S0166-0934(96)02164-7 (1997).
- Folks, T. *et al.* Biological and Biochemical Characterization of a Cloned Leu-3- Cell Surviving Infection with the Acquired Immune Deficiency Syndrome Retrovirus. *The Journal of Experimental Medicine* **164**, 280–290, doi:10.1084/jem.164.1.280 (1986).
- Day, E., Dear, P. H. & McCaughan, F. Digital PCR strategies in the development and analysis of molecular biomarkers for personalized medicine. *Methods* **59**, 101–107, doi:10.1016/j.ymeth.2012.08.001 (2013).
- Cross, N. C., White, H. E., Muller, M. C., Saglio, G. & Hochhaus, A. Standardized definitions of molecular response in chronic myeloid leukemia. *Leukemia* **26**, 2172–2175, doi:10.1038/leu.2012.104 (2012).
- Devonshire, A. S. *et al.* The use of digital PCR to improve the application of quantitative molecular diagnostic methods for tuberculosis. *BMC infectious diseases* **16**, 366, doi:10.1186/s12879-016-1696-7 (2016).
- Bosman, K. J. *et al.* Comparison of digital PCR platforms and semi-nested qPCR as a tool to determine the size of the HIV reservoir. *Scientific reports* **5**, 13811, doi:10.1038/srep13811 (2015).
- Eriksson, S. *et al.* Comparative analysis of measures of viral reservoirs in HIV-1 eradication studies. *PLoS pathogens* **9**, e1003174, doi:10.1371/journal.ppat.1003174 (2013).
- Henrich, T. J., Gallien, S., Li, J. Z., Pereyra, F. & Kuritzkes, D. R. Low-level detection and quantitation of cellular HIV-1 DNA and 2-LTR circles using droplet digital PCR. *J Virol Methods* **186**, 68–72, doi:10.1016/j.jviromet.2012.08.019 (2012).
- Jones, M. *et al.* Low copy target detection by Droplet Digital PCR through application of a novel open access bioinformatic pipeline, 'definetherain'. *J Virol Methods* **202**, 46–53, doi:10.1016/j.jviromet.2014.02.020 (2014).
- Strain, M. C. *et al.* Highly precise measurement of HIV DNA by droplet digital PCR. *PLoS One* **8**, e55943, doi:10.1371/journal.pone.0055943 (2013).
- Trypsteen, W., Kiselinova, M., Vandekerckhove, L. & De Spiegelaere, W. Diagnostic utility of droplet digital PCR for HIV reservoir quantification. *Journal of Virus Eradication* **2**, 1–8 (2016).
- BREATHHER (PENTA 16) Trial Group. Weekends-off efavirenz-based antiretroviral therapy in HIV-infected children, adolescents, and young adults (BREATHHER): a randomised, open-label, non-inferiority, phase 2/3 trial. *The lancet. HIV* **3**, e421–430, doi:10.1016/S2352-3018(16)30054-6 (2016).
- Bustin, S. A. *et al.* The MIQE guidelines: minimum information for publication of quantitative real-time PCR experiments. *Clinical chemistry* **55**, 611–622, doi:10.1373/clinchem.2008.112797 (2009).
- Huggett, J. F. *et al.* The digital MIQE guidelines: Minimum Information for Publication of Quantitative Digital PCR Experiments. *Clinical chemistry* **59**, 892–902, doi:10.1373/clinchem.2013.206375 (2013).
- Whale, A. S. *et al.* Detection of Rare Drug Resistance Mutations by Digital PCR in a Human Influenza A Virus Model System and Clinical Samples. *Journal of clinical microbiology* **54**, 392–400, doi:10.1128/JCM.02611-15 (2016).
- Wilburn, K. M. *et al.* Heterogeneous loss of HIV transcription and proviral DNA from 8E5/LAV lymphoblastic leukemia cells revealed by RNA FISH:FLOW analyses. *Retrovirology* **13**, 55, doi:10.1186/s12977-016-0289-2 (2016).
- Fryer, J. F. *et al.* Development of working reference materials for clinical virology. *J Clin Virol* **43**, 367–371, doi:10.1016/j.jcv.2008.08.011 (2008).

Acknowledgements

The work described in this paper was funded by the UK government Department for Business, Energy & Industrial Strategy (BEIS). RBF received funding from the NIHR Biomedical Research Centre and the UCLH/UCL BRC funded NIHR Health Informatics Collaborative Study. We also acknowledge the contributions of Karina Butler, Dianne Gibb, Deenan Pillay (PENTA BREATHER Clinical Trial), Sarah Watters (UCL), Simon Carne and David Bibby (Virus Reference Department, Public Health England, London, UK). Finally, we are grateful to Simon Cowen (LGC) for his assistance with the statistical analysis.

Author Contributions

J.A.G. and J.F.H. jointly designed the study and interpreted the data. E.B., A.S.W., R.B.F. and G.M. performed laboratory assays and interpreted data. P.G. contributed to assay design and development, and E.N., J.J.C. and C.A.F. contributed to design of the study and sample procurement. E.B., J.F.H. and J.A.G. prepared the manuscript. All authors reviewed the manuscript.

Additional Information

Supplementary information accompanies this paper at doi:[10.1038/s41598-017-01221-5](https://doi.org/10.1038/s41598-017-01221-5)

Competing Interests: The authors declare that they have no competing interests.

Publisher's note: Springer Nature remains neutral with regard to jurisdictional claims in published maps and institutional affiliations.



Open Access This article is licensed under a Creative Commons Attribution 4.0 International License, which permits use, sharing, adaptation, distribution and reproduction in any medium or format, as long as you give appropriate credit to the original author(s) and the source, provide a link to the Creative Commons license, and indicate if changes were made. The images or other third party material in this article are included in the article's Creative Commons license, unless indicated otherwise in a credit line to the material. If material is not included in the article's Creative Commons license and your intended use is not permitted by statutory regulation or exceeds the permitted use, you will need to obtain permission directly from the copyright holder. To view a copy of this license, visit <http://creativecommons.org/licenses/by/4.0/>.

© The Author(s) 2017

An Assessment of the Reproducibility of Reverse Transcription Digital PCR Quantification of HIV-1 Viral RNA Genome.

Samreen Falak^{*1}, Rainer Macdonald¹, Eloise J Busby², Denise M O’Sullivan², Mojca Milavec⁴, Annabell Plauth¹, Martin Kammel^{5,6}, Heinz Zeichhardt^{5,6}, Hans-Peter Grunert⁷, Jim F. Huggett^{*2,3}, Andreas Kummrow^{*1}.

1. Physikalisch Technische Bundesanstalt, Abbestr. 2-12, D-10587 Berlin, Germany

2. National Measurement Laboratory, LGC, Queens Road, Teddington, Middlesex, TW11 0LY, United Kingdom

3. School of Biosciences & Medicine, Faculty of Health & Medical Science, University of Surrey, Guildford, GU2 7XH, United Kingdom

4. Department of Biotechnology and Systems Biology, National Institute of Biology, Ljubljana, Slovenia

5. INSTAND, Gesellschaft zur Foerderung der Qualitaetssicherung in medizinischen Laboratorien e.V., Ueberstr.20, D-40223 Dusseldorf, Germany

6. IQVD GmbH, Institut fuer Qualitaetssicherung in der Virusdiagnostik, Potsdamer Chaussee 80, D-14129 Berlin, Germany

7. GBD Gesellschaft fuer Biotechnologische Diagnostik mbH, Berlin, Potsdamer Chaussee 80, D-14129 Berlin Germany

* Shared first authors

ABSTRACT: Viral load monitoring in human immunodeficiency virus type 1 (HIV-1) infection is often performed using reverse transcription quantitative PCR (RT-qPCR) to observe response to treatment and identify the development of resistance. Traceability is achieved using a calibration hierarchy traceable to the International Unit (IU). IU values are determined using consensus agreement derived from estimations by different laboratories. Such a consensus approach is necessary due to the fact that there are currently no reference measurement procedures available that can independently assign a reference value to viral reference materials for molecular *in vitro* diagnostic tests. Digital PCR (dPCR) is a technique that has the potential to be used for this purpose. In this paper, we investigate the ability of dPCR to quantify HIV-1 genomic RNA without calibration. Criteria investigated included the performance of HIV-1 RNA extraction steps, choice of reverse transcription approach and selection of target gene with assays performed in both single and duplex format. We developed a protocol which was subsequently applied by two independent laboratories as part of an external quality assurance (EQA) scheme for HIV-1 genome detection. Our findings suggest that RT-dPCR could be used as reference measurement procedure to aid the value assignment of HIV-1 reference materials for routine calibration of HIV-1 viral load testing.

Antiretroviral therapy (ART) has rendered infection by HIV, which initially had high mortality, a manageable chronic condition. Approximately 37.9 million people are currently living with HIV, and globally 62% of adults and 54% of children living with HIV receive lifelong antiretroviral therapy [1]. Effective ART can enable sustained suppression of viral load in the plasma (to below 50 copies/mL) [2, 3]. To ensure ART is being effective, the patient’s viral load is monitored by measuring the quantity of the RNA genome in response to treatment [4,5]. Reverse transcription quantitative PCR (RT-qPCR) is the routine method for measuring HIV RNA [6] which relies on calibration for quantitative measurement [7,8]. For these measurements to be reproducible the calibration must be traceable to support standardization.

Traceability of HIV-1 load measurements is supported by the World Health Organization (WHO) via the development and distribution of reference materials (RMs), called WHO International standards [9, 10]. The WHO RMs have enabled global comparisons of the viral load of HIV-1, and other viruses like hepatitis B and C viruses, to be made with traceability to the

international unit (IU), the value of which is assigned by consensus. These reference materials enable harmonization of the associated quantitative measurements, allow performance assessment during the development and routine application of tests, and comparison of the diagnostic services offered at national and international levels [11].

Although the WHO International standards for HIV-1 are assigned to IU, diagnostic reporting is frequently still based on copies/mL taking into account a conversion factor [9]. This is due to the introduction and application of quantitative PCR systems for HIV-1 viral load testing before the development of the first WHO International standard for HIV-1. While international standards have revolutionized global viral measurement, where traceability relies on a reference material challenges occur when it runs out and requires replacement. In clinical chemistry this challenge is often resolved by using units that are traceable to either a reference measurement procedure or, preferably, the International Standard System of Units [11,12]. Reference measurement procedures provide an accurate characterization of reference material to a high metrological order. To

date, it is not clear whether such an approach could assist in improving the harmonization of global viral load measurements as suitable reference measurement procedures have not existed.

Digital PCR (dPCR) is a method that can be performed as an SI traceable reference measurement procedure when measuring DNA in buffered solution [13] and can perform with high reproducibility when incorporating extraction protocol to measure DNA from whole bacteria [14] and viruses [15]. When combined with reverse transcription (RT), dPCR also has the potential to provide accurate and robust quantification of HIV RNA in plasma samples in the clinically relevant low concentration range [16]. Previous dPCR studies reported to date have quantified HIV-1 DNA as well as cell associated and synthetic RNA [7]. In several studies, dPCR has been used in the measurement of HIV DNA from patients and was found to be more robust to mismatches between primers and probes and target sequence of HIV [17-22].

Despite these promising studies, the measurement of RNA by RT-dPCR has not been investigated to the same extent as for DNA. Such assessments are required if the method is to support reference material production as a reference measurement procedure for HIV-1, hepatitis C or coronavirus. In this study, we developed a procedure incorporating extraction and RT-dPCR to reproducibly quantify HIV-1 RNA from whole virus samples and evaluated it on EQA samples and the WHO 4th HIV-1 international standard.

EXPERIMENTAL SECTION

The "Minimum Information for Publication of dPCR experiments" (dMIQE) checklist [23] is given in Supporting Information (Table S1).

Sample collection. HIV-1 positive samples (group M, subtype F) derived from External Quality Assessment (EQA) schemes performed by INSTAND e.V. (<https://www.instand-ev.de>). The sample sets corresponded to panels of the INSTAND EQA schemes No. 360 and No. 382, distributed in June 2017, March 2018 and March 2019 (<https://www.instand-ev.de>). The samples were prepared by the manufacturer spiking HIV stock material (heat inactivated) into human plasma at different dilution levels. Viral loads are available as consensus value from the EQA schemes. In addition, the WHO 4th HIV-1 international standard of HIV-1 subtype B virus was included in the study (WHO-IS NIBSC code: 16/194, NIBSC Hertfordshire UK). The nominal concentration for the WHO standard is $5.10 \log_{10}$ IU/mL [9].

HIV-1 RNA extraction methods. Three different RNA extraction kits were assessed for HIV-1 RNA extraction from plasma samples: i) QIAamp viral RNA mini kit (Qiagen #52904), ii) High Pure Viral RNA kit (Roche Applied Science #1185882001) and iii) NucleoSpin RNA virus (Macherey-Nagel #740956.50). All kits used silica gel membrane columns for extractions and centrifugation. Six replicate extractions were performed on three different days, for each of the three methods. For evaluation of these RNA extraction methods, the EQA sample 360126 (term March 2018) was used. For each extraction, 200 μ L of reconstituted plasma sample was processed following the manufacturer instructions for the respective kit. A

negative control for the extraction method was included consisting of 200 μ L deionized water instead of plasma sample. DNase digestion was performed on-column using RNase-Free DNase Set (50), (Qiagen #79254) according to manufacturer instructions. The RNA was eluted applying 60 μ L elution buffer. Following extraction, the RNA concentration was measured using a NanoDrop 2000 spectrophotometer (Thermo Fisher Scientific), and either used immediately or stored for up to seven days at -20 °C until subsequent use.

HIV-1 primers and probes. Previously published primers and probe sequences targeting the HIV-1 *gag* (targeting the p24 sequence of *gag*) and *pol* (targeting the exon/intron boundary of *pol* and *vif* genes) were chosen [24, 25]. Sequence of primers and probes and reaction parameters are listed in Table S2. The assays were selected to target specific sequences from various HIV-1 groups M, N, O with major subtypes. The duplex assays annealing temperature optimization is shown in Supporting Information Figure S1.

RT-dPCR methods. For two-step RT-dPCR, RNA was reverse transcribed to cDNA using the SuperScript IV First-Strand Synthesis System (Invitrogen #18091050) details shown in Supporting Information (Table S3 A, B and C).

One-step RT-dPCR reaction details are listed in Supporting Information Table S3D.

All dPCR (singleplex, duplex) reaction mixtures were prepared for EQA samples and controls (no-template control containing nuclease-free water instead of RNA, and an RT-negative control). Droplets were generated in DG8 cartridges using QX200 Droplet Digital System manual droplet generator (Bio-Rad, QX200). The generated water-in-oil emulsions were transferred to a 96-well PCR plate and amplified in a cycler (Bio-Rad, C1000). The thermal cycling conditions for two-step dPCR are shown in Supporting Information (Table S3 C). After PCR cycling, the plates were transferred to a QX200 Droplet Digital System droplet reader (Bio-Rad). Thermal cycling conditions for one-step RT-dPCR were exactly the same as for two step dPCR (Table S3 C) except addition of the reverse transcription step (60 min at 50 °C) prior to amplification.

WHO 4th HIV-1 international standard. The WHO 4th HIV-1 standard material based on subtype B virus (WHO-IS NIBSC code: 16/194, NIBSC Hertfordshire UK) was evaluated by duplex assay for *gag* and *pol* by one-step RT-dPCR assay format. The lyophilized plasma sample of WHO 4th HIV-1 standard was reconstituted in 1 mL of ddH₂O and left at RT for 20 min prior to the RNA extraction followed by duplex one-step RT-dPCR.

Intermediate precision. Repeatability (inter- and intra-assay variation) of HIV-1 dPCR assays was assessed measuring the WHO 4th HIV-1 international standard material. Five extracts were prepared on different days and RT-dPCR was performed with a duplex assay of *gag* and *pol* primers and probes. Coefficient of variation (CV) of the concentration was calculated based on a total of 31 replicates. The influence of extraction was assessed by comparing the averaged concentration of extracts that had at least four replicates.

Limit of detection and quantification. For a duplex RT-dPCR assay characterization, eleven dilution series of extracted

RNA were produced from the reference WHO 4th HIV-1 International Standard material using nuclease free water. Eleven dilution steps 2×, 4×, 8×, 16×, 32×, 64×, 128×, 256×, 512×, 1024×, 2048× and a negative template control (NTC) consisting of nuclease free water were tested. Sixteen replicates of each dilution were measured by dPCR in four separate runs in consecutive days, containing four technical replicates except for dilutions series 2×, 1024× and 2048× which were measured once, and each contained four technical replicates. The verified values from RT-dPCR were used to calculate the assigned copy number of the targets for the dilution series is shown in Supporting Information Table S5.

EQA participation. In EQA scheme March 2019, 118 laboratories have participated in the Virus Genome Detection HIV-1 (RNA) Program 1 (360) and 40 laboratories in the Virus Genome Detection-HIV-1 (RNA) additional Training Program 2 (382). Each program covers samples with four different dilution levels. The target value for each EQA sample is determined as consensus value from all quantitative results for the respective sample (based on the robust average according to algorithm A/DIN ISO 13528/Annex C).

Data acquisition and analysis. The dPCR data acquisition and processing was performed using the QuantaSoft™ Analysis Pro version 1.0.596 and 1.7.4 (Bio-Rad) using absolute quantification. Software counts the number of valid droplets and records the associated fluorescence signals of positive droplets (amplified products) and negative droplets without the amplification product as described previously [26]. The threshold was applied automatically by the software or set manually (if required) for both channels FAM and HEX. The data generated by the QX200 droplet reader were excluded from subsequent analysis if the number of accepted droplets were below 10000 per well. Exported data were further analyzed using Microsoft Excel spreadsheets. Coefficient of variation (CV) was calculated as relative standard deviation and expressed as percentage value. Grubbs outlier test was performed using Origin 2019 software. Respective examples for positive and negative samples are shown in Supporting Information (Figure S2 and S3).

RESULTS AND DISCUSSION

Singleplex and duplex RT-dPCR. To characterize and compare the performance of a singleplex and a duplex assay, the absolute concentration of HIV-1 RNA was determined for an EQA plasma sample (360126), and the reference WHO 4th HIV-1 international standard. RNA was extracted using QIAamp viral RNA mini kit. For both assays, copy number ratios of duplex to singleplex assays are presented in Table 1.

Table 1. Performance of singleplex and duplex assays

Sample	Target	Mean concentration (cp/μL)		Ratio
		Singleplex	Duplex	
EQA plasma sample (360126)	<i>gag</i>	13.5	12.5	0.93
	<i>pol</i>	10.8	10.1	0.94
	<i>gag</i>	32.2	30.9	0.96

WHO 4 th HIV-1 Standard	<i>pol</i>	28.9	27.2	0.94
------------------------------------	------------	------	------	------

Typical CV values for the results shown in table 1 were 10 % to 12 %. The ratio between duplex to singleplex shows that the concentration measured by the duplex assay is on average lower by 5 % compared to the singleplex approach (Table 1) which is less than the observed CV. This shows that the duplex assay does not compromise quantification when compared to the singleplex approach and the former was chosen for the remainder of the study. Duplex formats provide an additional level of confidence and are commonly used for a wide range of molecular testing applications [14, 27-28].

RNA extraction methods for RNA quantification of HIV-1 using one-step duplex RT-dPCR. When different extraction procedures were compared, we observed that the choice of RNA extraction kit resulted in a clear difference in the measured viral concentrations (Figure 1). A large difference in the viral RNA concentration was observed between High Pure Viral RNA kit and the other two kits. The QIAamp Viral RNA mini kit and NucleoSpin RNA Virus yielded comparable concentration for both assays and days. This demonstrated that selection of the extraction method is critical as it can influence copy number concentration estimates following downstream molecular analyses as it has been observed in mycobacterium tuberculosis [14].

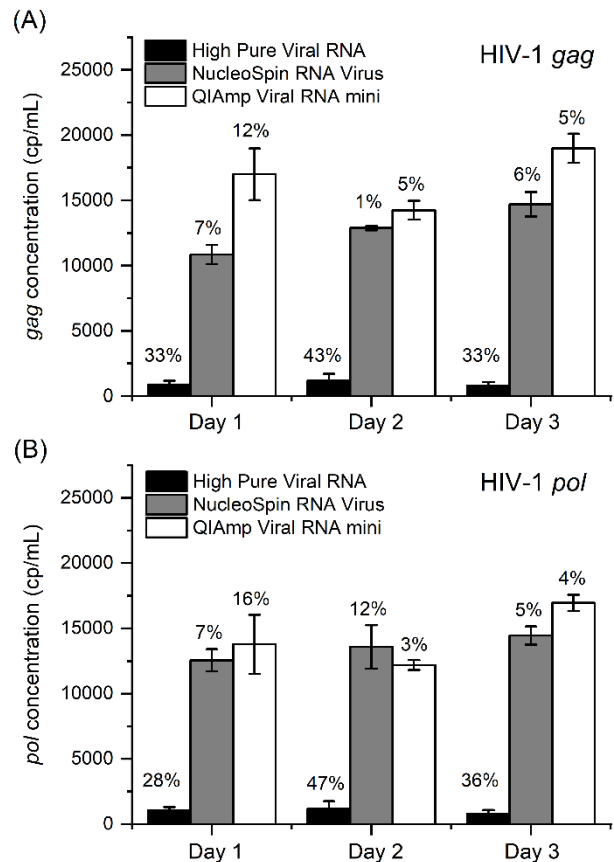


Figure 1. Evaluation of extraction methods with commercial kits. Absolute RNA concentrations were shown in cp/mL for (A) *gag* and (B) *pol* genes separately. Error bars depict standard deviations with the numbers above bars outlining coefficient of variation. ($n = 6$).

Overall, extraction analysis showed that the QIAamp viral RNA mini kit consistently yielded the highest signal for the plasma-based samples, and consequently was chosen for the subsequent HIV-1 RNA measurements performed in this study. It is known that the extraction can contribute towards a major source of bias in dPCR [14]. The matrix complexity could be due to the confound mixture of genomic background and or RNA secondary structure. Therefore, different RNA extraction kits used in this study contributed to some order of discordance in RNA extraction and differences have been observed in the copy number concentration obtained from different extraction kits.

Reverse transcription RT-dPCR assay for HIV. A comparison of the one-step RT-ddPCR Supermix for probes with the SuperScript IV reverse transcriptase was performed (Figure 2). All four dilution levels of EQA 2018 samples and the WHO 4th HIV-1 standard were included in the analysis. The concentrations measured when using the one-step RT-dPCR Supermix were consistently higher, despite matched input concentrations of RNA. Our results demonstrate that the Supermix for one-step RT-ddPCR provided greater efficiency (Figure 2).

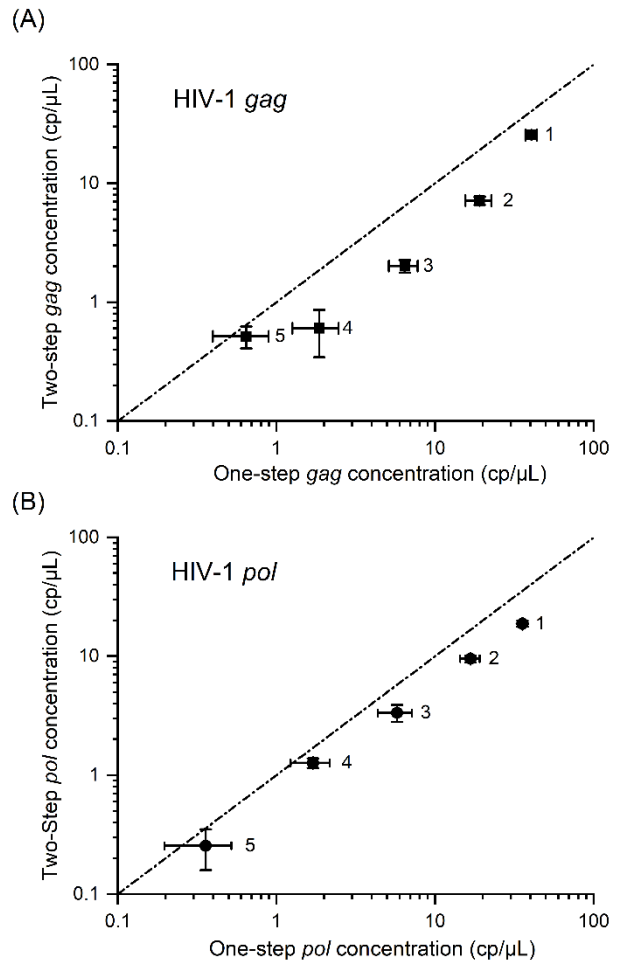


Figure 2. Assessment of one-step dPCR on X-axis and two-step dPCR on Y-axis. A) representing *gag* and B) *pol* targets (1: WHO 4th HIV-1 international standard; 2: INSTAND EQA (March 2018) sample 360126; 3: 360128; 4: 360125; 5: 360127).

In one-step format, both the RNA conversion and gene specific PCR amplification occur in a single tube. In contrast, two-step needed two separate reactions for RNA conversion and amplification. In addition, gene-specific primers in one-step have revealed an efficient cDNA synthesis compared to using random hexamers and oligo dT primers in two-step particularly for samples like HIV-1 with low copy number concentrations. This observation has previously been reported for one- and two-step RT-qPCR [32].

This observation is in line with recent findings of Myerski et al. [29]. The studies of Rački et al. [30] and Sedlack et al. [31] reported that one-step RT-dPCR had higher precision, repeatability and reduced susceptibility to inhibition in low waterborne RNA virus samples in line with observations found here for HIV plasma samples. In addition, one-step reaction is time efficient and minimizes the risk of contamination. Based on this, one-step format was chosen for the remaining experiments in this study

Intermediate precision of RT-dPCR. The intermediate precision of the selected RT-dPCR measurement procedure was

assessed by repeated experiments including repeated extractions conducted on separate days within the same laboratory

The intermediate precision of the duplex assay was analyzed using the WHO 4th HIV-1 standard material at a nominal concentration of 125900 IU/mL. The intermediate precision was examined by measuring 31 replicates in five days. Grubbs outlier testing did not indicate outliers at a significance value of 0.05 when applied to all replicates or when applied to average values characterizing individual extracts. The intermediate precision expressed as % CV was 8.8 % for *gag* and 12.3 % for *pol* as shown in Table 2 (for details see Table S4).

Table 2. Intermediate precision of duplex one-step RT-dPCR assay.

Inter-assay variability (cp/μL)						CV %
Gene	#1	#2	#3	#4	#5	
<i>gag</i>	36.5	37.0	32.6	40.5	33.4	8.8
<i>pol</i>	33.0	28.6	29.3	36.3	27.0	12.3

The variation of results reflected by the intermediate precision is negligible when compared to the variation allowed in EQA for virologic laboratories discussed below. The intermediate precision found here is clearly lower than the interlaboratory variation of 0.43 on a log10 scale reported by Prescott et al. for the same material [9].

Limit of detection and limit of quantification. The limit of detection (LOD) and limit of quantification (LOQ) are important for measurement of RNA concentration. These parameters can be influenced by various steps involved in detection of viral RNA including preanalytics ending in extraction, reverse transcription and the final detection by dPCR. The specific contribution of dPCR to LOD and LOQ is discussed here by analyzing the underlying counting procedure. The LOD is defined as the HIV RNA concentration, for which the probability of falsely claiming the absence of HIV RNA is 5 % [34]. In digital dPCR, the statistical distribution in repeat measurements is not Gaussian at low sample concentration but discrete (Figure S4). Therefore, it is not possible to derive the LOD from the standard deviation of repeat measurements. In the absence of a blank value (BV) the theoretical LOD for dPCR can be calculated from counting statistics assuming Poisson distribution (see Supporting Information). The LOD concentration for RNA in the sample material is

$$c_{LOD} = \frac{-\ln 0.05}{N_{tot} V_d D}, \tag{1}$$

where N_{tot} is the number of accepted droplets and V_d is the droplet size. In Equation (1) the LOD is corrected by the dilution factor D that results from concentration changes introduced by extraction and addition of reagents ($D = 1.29$ in the present measurements). For $N_{tot} = 13000$ and $V_d = 0.85$ nL this gives $c_{LOD} = 210$ cp/mL in the reaction. The limit of detection can be improved by averaging replicate measurements, which effectively increases N_{tot} . The blank value determined by measurement of negative template controls was determined to be in the range of 16 cp/mL for the plasma sample (sample number should be added).

The limit of quantification (LOQ) is defined here as the minimum concentration for which the relative standard deviation (RSD) is smaller than a predefined value R , e.g. $R = 0.2$. The ultimate limit for LOQ is given by counting statistics and can be calculated (Supporting Information) from

$$c_{LOQ} = \frac{1}{R^2 N_{tot} V_d D}. \tag{2}$$

For $R = 0.2$, $N_{tot} = 13000$ and $V_d = 0.85$ nL Eq. (2) gives $c_{LOQ} = 1750$ cp/mL. The averaged results shown in Figure 3A demonstrate that the LOQ can also be improved by averaging replicate measurements.

The average quantity of HIV-1 target concentration measured by duplex RT-dPCR was approximately 32000 cp/mL in the plasma sample (sample number should be added). The LOQ was calculated and compared on a serial dilution of WHO 4th HIV-1 international standard the highest concentration being a 1:2 dilution (Figure 3).

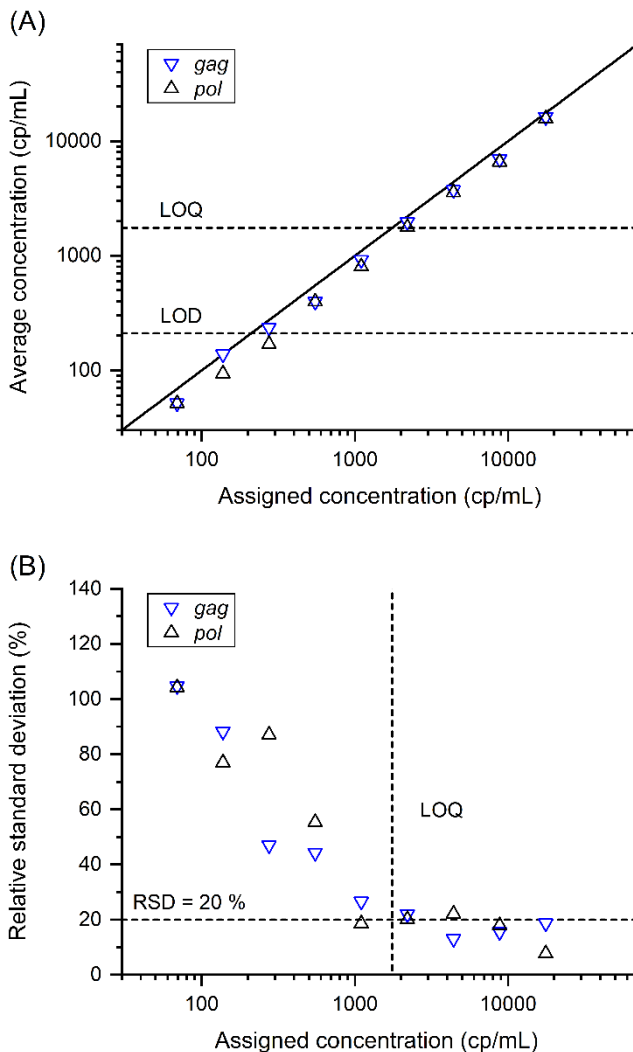


Figure 3. A dilution series using the WHO 4th HIV-1 standard measured by the duplex one-step RT-dPCR in the plasma for *gag* and *pol* genes: A) observed average concentration (symbols)

closely follow expected concentration in plasma calculated from dilution factor (solid line); B) plot of the relative standard deviation of replicate measurements to determine limit of quantification.

Our data demonstrate that the observed concentration determined by averaging all replicate measurements followed the expected concentration down to about 100 cp/mL for the assay used here (Figure 3A). In Figure 3B, the vertical dashed line indicates the theoretical LOQ determined assuming a threshold level of $R = 20\%$. Counting statistics was assumed in derivation of above formulas. The observed relative standard deviation does not exceed the threshold level of 20% significantly above the calculated LOQ expected from Eq. (2), (Table S5). This demonstrates that quantification is limited by counting statistics.

Averaging over replicate measurements reduces the uncertainty contribution from counting statistics by effectively increasing the number of droplets contributing to the result. It can be inferred from Eq. (2) that the LOQ would be improved in proportion to the number of replicate measurements used for averaging, provided that counting statistics would be the only limiting factor. Figure 3A demonstrates that this is indeed possible here. However, it should be noted that the efficiency of other procedures involved in the complete detection process should be factored in to describe LOD and LOQ for viral detection by dPCR in the same way as for qPCR, e.g. reverse transcription or extraction efficiency.

Measurement of WHO 4th HIV-1 international standard by duplex one-step RT-dPCR. The concentration of the WHO 4th HIV-1 standard material was measured using the digital PCR method described here. The average concentration measured by RT-dPCR was for *gag* 35300 cp/mL \pm 700 cp/mL and for *pol* 31100 cp/mL \pm 900 cp/mL. The numerical concentration determined by dPCR in cp/mL was lower by a factor of 3.57 for *gag* and 4.05 for *pol* when compared to the specified concentration given as IU/mL. However, this factor can be used to convert concentration measured by dPCR into IU/mL.

Concentrations determined by commercial assays are reported in cp/mL. The conversion factor of those concentrations values into IU/mL values is routinely determined as part of the WHO prequalification of in vitro diagnostic products. Typical conversion factors for a number of manufacturers are listed in Table 3. The conversion factors for commercial assays are smaller than the value determined here for the dPCR assay. Thus, the HIV concentration reported by using a commercial assay will be correspondingly larger, e.g. by a factor of 2.1 for assays from Abbott, Roche and Cepheid.

Table 3. Typical conversion factor to IU.

manufacturer	conversion factor	Ref.
Abbott	1.74 IU/cp	[35]
Roche	1.67 IU/cp	[36]
Cepheid	1.73 IU/cp	[37]
Hologic	2.86 IU/cp	[38]
Siemens	1.00 IU/cp *	

* assays calibrated by 1st HIV international standard

Interlaboratory comparison. In 2019, PTB and NML participated in EQA schemes organized by the German EQA provider INSTAND e.V. for HIV-1 virus genome detection. Both participants were blind to the content of the respective samples and used the protocol developed by the study. Results are shown as symbols in Figure 4A. RT-dPCR results demonstrate good reproducibility between laboratories (target *gag*). The acceptance range in these EQA schemes is ± 0.6 on a log 10 concentration scale in respect of the target value [39]. In this EQA scheme, the centre of the acceptance range is calculated as the robust average of the concentrations of all participating laboratories (107 clinical laboratories used RT qPCR, two used RT-dPCR). The EQA scheme covers a wide concentration range of 42 cp/mL to 37000 cp/mL as required for medical diagnosis [40]. Direct comparison of concentration determined in cp/mL resulted in both dPCR results being below the mean value, however, all were within the acceptance range with the exception of one result (Figure 4a).

Participants of the EQA scheme have to report their results in cp/mL, and not relative to the accepted WHO international standard [9,39]. Digital PCR measured the concentration in cp/mL without calibration while qPCR used by other participants obtained results based on difference calibration material. Thus, the qPCR results implicitly include a conversion factor such as listed in Table 3. Figure 4B shows the effect of inclusion of the conversion factor 3.57 determined above. When dPCR values were also converted in this way (Figure 4b) all results were still within the acceptance range and with data generally closer to the mean value.

Overall, results obtained by two metrological laboratories using RT-dPCR with and without applying conversion factors to determine IU were in good agreement and fit well to the results obtained by conventional qPCR and met the requirements of the EQA scheme.

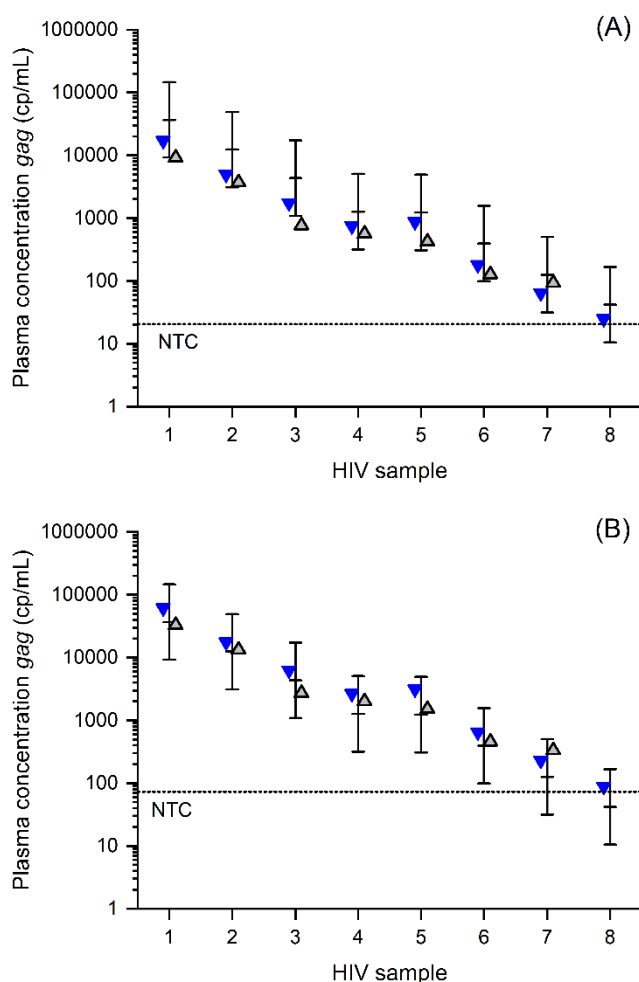


Figure 4. Results of the EQA schemes performed in March 2019 by INSTAND: A) represents the HIV-1 EQA scheme results directly obtained by digital PCR; B) HIV-1 EQA scheme results invoking a calibration with WHO 4th HIV-1 standard. Bars show the acceptance range based on the consensus value from all quantitative results for the respective sample for the Virus Genome Detection HIV-1 (RNA) Program 1 (360) and the Virus Genome Detection-HIV-1 (RNA) additional Training Program 2 (382) (INSTAND) of the EQA scheme. The acceptance range is ± 0.6 on a log₁₀ concentration scale [27]. Symbols represent the results submitted by the two laboratories using duplex RT-dPCR assay demonstrating reproducibility between metrological laboratories.

CONCLUSION

This paper demonstrates that RT dPCR has the potential to be a reference measurement procedure for HIV-1 RNA measurement. Sources of bias affecting HIV-1 RT-dPCR measurements were identified including comparison of different methods for HIV RNA extraction from whole virus, comparison of different RT enzymes performed one- or two-step formats. Intermediate precision (performed in between and within days)

and reproducibility (performed between two laboratories participating in clinical EQA scheme) was determined. These data demonstrate applicability and reproducibility of the developed RT-dPCR assay for HIV-1 RNA quantification in a complex genomic background.

To the best of our knowledge, this study is the first study to apply RT-dPCR for absolute quantification of viral HIV-1 RNA in terms of copies /mL as well as IU applied to plasma-based EQA samples and the WHO HIV-1 4th standard. Our results demonstrated the applicability of simultaneous use of *gag* and *pol* primers for detecting HIV-1 RNA in a duplex RT-dPCR assay. Our findings support that RT-dPCR offers good linearity, repeatability (within laboratory) in measurement of HIV viral load. The experiments did not require specific modifications on technical instrumentation so that measurements should also be feasible for a range of other laboratories. Good reproducibility (in between laboratories) can be expected from the results reported here.

This approach was demonstrated here to achieve sufficient sensitivity required for medical diagnosis as demonstrated by successful participation in the INSTAND EQA schemes 2019. Digital PCR is a promising method for implementation of a reference measurement procedure to quantify viral RNA and as a method for value assignment of reference materials and calibrators.

ASSOCIATED CONTENT

Supporting Information

Additional information as noted in the text is available in Supporting Information. The Supporting Information is available free of charge on the ACS Publications website.

HIV_Final_Suppl_.docx

AUTHOR INFORMATION

Corresponding Author

* Samreen Falak, Samreen.Falak@ptb.de, Jim F. Huggett, jim.huggett@lgcgroup.com, and Andreas Kummrow, andreas.kummrow@ptb.de

Author Contributions

The manuscript was written through contributions of all authors. All authors have given approval to the final version of the manuscript.

ACKNOWLEDGMENT

This project has received funding from the EMPIR programme co-financed by the Participating States and from the European Union's Horizon 2020 research and innovation programme.

REFERENCES

- (1) WHO HIV/AIDS Key facts. Available at <https://www.who.int/news-room/fact-sheets/detail/hiv-aids>. Accessed 05/7/2020.
- (2) Sitnik, R., Pinho, J.R.R. Quantitation of HIV-1 RNA viral load using nucleic acid sequence based amplification methodology and

comparison with other surrogate markers for disease progression. *Mem. Inst. Oswaldo Cruz* **1998**, *93*, 411-415.

(3) Mellors, J.W., Rinaldo, C.R., Gupta, P., White, R.M., Todd, J.A., Kingsley, L.A. Prognosis in HIV-1 infection predicted by the quantity of virus in plasma. *Science* **1996**, *272*, 1167-1170.

(4) Dybul, M., Fauci, A.S., Barlett, J.G., Kaplan, J.E., Pau, A.K. Guidelines for Using Antiretroviral Agents among HIV-Infected Adults and Adolescents. *Ann. Intern. Med.* **2002**, *137*, 381-433.

(5) Panel on Antiretroviral Guidelines for Adults and Adolescents. *Guidelines for the Use of Antiretroviral Agents in Adults and adolescents with HIV*. Department of Health and Human Services. Available at <http://www.aidsinfo.nih.gov/ContentFiles/AdultandAdolescentGL.pdf>. Accessed 1/10/2020.

(6) Désiré, N., Dehée, A., Schneider, V., Jacomet, C., Goujon, C., Girard, P.M., Rozenbaum, W., Nicolas, J.C. Quantification of human immunodeficiency virus type 1 proviral load by a TaqMan real-time PCR assay. *J. Clin. Microbiol.* **2001**, *39*, 1303-1310.

(7) Trypsteen, W., Kiselina, M., Vandekerckhove, L., De Spiegelaere, W. Diagnostic utility of droplet digital PCR for HIV reservoir quantification. *J. Virus Erad.* **2016**, *2*, 162-169.

(8) Busby, E., Whale, A.S., Ferns, R.B., Grant, P.R., Morley, G., Campbell, J., Foy, C.A., Nastouli, E., Huggett, J.F., Garson, J.A. Instability of 8E5 calibration standard revealed by digital PCR risks inaccurate quantification of HIV DNA in clinical samples by qPCR. *Sci. Rep.* **2017**, *7*, 1209.

(9) Prescott, G., Hockley, J., Atkinson, E., Rigsby, P., Morris, C., et al. (2017). International collaborative study to establish the 4th WHO international standard for HIV-1 NAT assays. WHO/BS/2017.2314.

(10) Morris, C., Govind, S., Fryer, J., Almond, N. SoGAT—25 years of improving the measurement of nucleic acids in infectious disease diagnostics (a review). *Metrologia* **2019**, *56*, 044007.

(11) ISO 17511:2003. In vitro diagnostic medical devices—measurement of quantities in biological samples—metrological traceability of values assigned to calibrators and control materials. Geneva, Switzerland: ISO; 2003

(12) Inglis, B., Ullrich, J., Milton, M.J.T. (eds). *The International System of Units*, 9th ed.; BIPM: Sèvres, 2019.

(13) Whale, A.S., Jones, G.M., Pavšič, J., Dreo, T., Redshaw, N., Akyürek, S., Agöz, M., Divieto, C., Sassi, M.P., He, H.J., Cole, K.D., Bae, Y.K., Park, S.R., Deprez, L., Corbisier, P., Garrigou, S., Taly, V., Larios, R., Cowen, S., O'Sullivan, D.M., Bushell, C.A., Goenaga-Infante, H., Foy, C.A., Woolford, A.J., Parkes, H., Huggett, J.F., Devonshire, A.S. Assessment of digital PCR as a primary reference measurement procedure to support advances in precision medicine. *Clin. Chem.* **2018**, *64*, 1296-1307.

(14) Devonshire, A.S., Honeyborne, I., Gutteridge, A., Whale, A.S., Nixon, G., Wilson, P., Jones, G., McHugh, T.D., Foy, C.A., Huggett, J.F. Highly reproducible absolute quantification of Mycobacterium tuberculosis complex by digital PCR. *Anal. Chem.* **2015**, *87*, 3706-3713.

(15) Pavšič, J., Devonshire, A., Blejcek, A., Foy, C.A., Van Heuverswyn, F., Schimmel, H., Žel, J., Huggett, J.F., Redshaw, N., Karczmarczyk, M., Mozioglu, E., Akyürek, S., Agöz, M., Milavec, M. Inter-laboratory assessment of different digital PCR platforms for quantification of human cytomegalovirus DNA. *Anal. Bioanal. Chem.* **2017**, *409*, 2601-2614.

(16) Sedlak, R.H., Jerome, K.R. Viral diagnostics in the era of digital polymerase chain reaction. *Diagn. Microbiol. Infect. Dis.* **2013**, *75*, 1-4.

(17) Sanders, R., Mason, D.J., Foy, C.A., Huggett, J.F. Evaluation of digital PCR for absolute RNA quantification. *PLoS One* **2013**, *8*, e75296.

(18) Bustin SA, Benes V, Garson JA, Helleman J, Huggett J, et al. The MIQE guidelines: minimum information for publication of quantitative real-time PCR experiments. *Clin Chem* **2009** *55*: 611–622 (19) Eriksson, S., Graf, E.H., Dahl, V., Strain, M.C., Yukl, S.A., Lysenko,

E.S., Bosch, R.J., Lai, J., Chioma, S., Emad, F., Abdel-Mohsen, M., Hoh, R., Hecht, F., Hunt, P., Somsouk, M., Wong, J., Johnston, R., Siliciano, R.F., Richman, D.D., O'Doherty, U., Palmer, S., Deeks, S.G., Siliciano, J.D. Comparative analysis of measures of viral reservoirs in HIV-1 eradication studies. *PLoS Pathog.* **2013**, *9*, e1003174.

(20) Henrich, T.J., Gallien, S., Li, J.Z., Pereyra, F., Kuritzkes, D.R. Low-level detection and quantitation of cellular HIV-1 DNA and 2-LTR circles using droplet digital PCR. *J. Virol. Methods* **2012**, *186*, 68-72.

(21) Jones, M., Williams, J., Gärtner, K., Phillips, R., Hurst, J., Frater, J. Low copy target detection by Droplet Digital PCR through application of a novel open access bioinformatic pipeline, 'definetherain'. *J. Virol. Methods* **2014**, *202*, 46-53.

(22) Strain, M.C., Lada, S.M., Luong, T., Rought, S.E., Gianella, S., Terry, V.H., Spina, C.A., Woelk, C.H., Richman, D.D. Highly precise measurement of HIV DNA by droplet digital PCR. *PLoS One* **2013**, *8*, e55943.

(23) Huggett, J.F., Foy, C.A., Benes, V., Emslie, K., Garson, J.A., Haynes, R., Helleman, J., Kubista, M., Mueller, R.D., Nolan, T., Pfaffl, M.W., Shipley, G.L., Vandesompele, J., Wittwer, C.T., Bustin, S.A. The digital MIQE guidelines: Minimum Information for Publication of Quantitative Digital PCR Experiments. *Clin. Chem.* **2013**, *59*, 892-902.

(24) Kondo, M., Sudo, K., Tanaka, R., Sano, T., Sagara, H., Iwamuro, S., Takebe, Y., Imai, M., Kato, S. Quantitation of HIV-1 group M proviral DNA using TaqMan MGB real-time PCR. *J. Virol. Methods* **2009**, *157*, 141-146.

(25) Lim, K., Park, M., Lee, M.H., Woo, H.J., Kim, J.B. Development and assessment of new RT-qPCR assay for detection of HIV-1 subtypes. *Biomed. Sci. Letters* **2016**, *22*, 83-97.

(26) Whale, A.S., Bushell, C.A., Grant, P.R., Cowen, S., Gutierrez-Aguirre, I., O'Sullivan, D.M., Žel, J., Milavec, M., Foy, C.A., Nastouli, E., Garson, J.A., Huggett, J.F. Detection of Rare Drug Resistance Mutations by Digital PCR in a Human Influenza A Virus Model System and Clinical Samples. *J. Clin. Microbiol.* **2016**, *54*, 392-400.

(27) Whale, A.S., Huggett, J.F., Tzonev, S. Fundamentals of multiplexing with digital PCR. *Biomol. Detect. Quantif.* **2016**, *10*, 15-23.

(28) Elenitoba-Johnson, K.S., Bohling, S.D., Wittwer, C.T., King, T.C. Multiplex PCR by multicolor fluorimetry and fluorescence melting curve analysis. *Nat. Med.* **2001**, *7*, 249-253.

(29) Myerski, A., Siegel, A., Engstrom, J., McGowan, I., Brand, R.M. The Use of Droplet Digital PCR to Quantify HIV-1 Replication in the Colorectal Explant Model. *AIDS Res. Hum. Retrovir.* **2019**, *35*, 326-334.

(30) Rački, N., Morisset, D., Gutierrez Aguirre, I., Ravnikar, M. One step RT droplet digital PCR: a breakthrough in the quantification of waterborne RNA viruses. *Anal. Bioanal. Chem.* **2014**, *406*, 661-667.

(31) Sedlak, R.H., Nguyen, T., Palileo, I., Jerome, K.R., Kuypers, J. Superiority of Digital Reverse Transcription PCR (RT PCR) over Real Time RT PCR for Quantitation of Highly Divergent Human Rhinoviruses. *J. Clin. Microbiol.* **2017**, *55*, 442-449.

(32) Wacker, M.J., Godard, M.P. Analysis of one step and two step real time RT PCR using SuperScript III. *J. Biomol. Tech.* **2005**, *16*, 266-271.

(33) Curry, J., McHale, C., Smith, M.T. Low efficiency of the Moloney murine leukemia virus reverse transcriptase during reverse transcription of rare t(8;21) fusion gene transcripts. *Biotechniques* **2002**, *32*, 768-775.

(34) ISO/IEC Guide 99:2007, International vocabulary of metrology -- Basic and general concepts and associated terms (VIM)

(35) Abbott RealTime HIV-1 (Manual), WHO Prequalification of Diagnostics Programme, PQDx 0146-027-00 vs 4.0 (2019). Available at https://www.who.int/diagnostics_laboratory/evaluations/pq-list/hiv-vrl/191217_amended_pqpr_0146_027_00_v4.pdf. Accessed 4/14/2020.

(36) COBAS AmpliPrep/COBAS TaqMan HIV-1 Test (TaqMan 96), WHO Prequalification of Diagnostics Programme, PQDx 0147-046-00 vs 3.0 (2019). Available at https://www.who.int/diagnostics_laboratory/evaluations/pq-list/hiv-vrl/191111_amended_final_pqpr_0147_046_00.pdf. Accessed 4/14/2020.

(37) Xpert® HIV-1 Viral Load with GeneXpert® Dx, GeneXpert® Infinity-48, GeneXpert® Infinity-48s and GeneXpert® Infinity-80, WHO Prequalification of Diagnostics Programme, PQDx 0192-070-00, PQDx 0193-070-00, PQDx 0194-070-00, PQDx 0195-070-00, vs. 2.0 (2017). Available at https://www.who.int/diagnostics_laboratory/evaluations/pq-list/hiv-vrl/170720_final_pq_report_pqdx_0192_0193_0194_0195_070-00.pdf. Accessed 4/14/2020.

(38) Aptima™ HIV-1 Quant Dx Assay, WHO Prequalification of Diagnostics Programme, PQDx 0236-078-00 vs. 5.0 (2018). Available at https://www.who.int/diagnostics_laboratory/evaluations/pq-list/180207_final_pqpr_0236_078_00_v5_IFU_v4.pdf. Accessed 4/14/2020.

(39) Revision of the “Guideline of the German Medical Association on Quality Assurance in Medical Laboratory Examinations – Rili-BAEK”. *J. Lab. Med.* **2015**, *39*, 26-69.

(40) Finzi, D., Siliciano, R.F. Viral dynamics in HIV-1 infection. *Cell* **1998**, *93*, 665-671.

Evaluation of MALDI-TOF MS and other emerging methods for molecular typing of *Acinetobacter baumannii*

Eloise J Busby¹, Ronan M Doyle², Priya Solanki^{*3}, Clara Leboreiro Babe^{*3}, Vicky Pang⁴, Gema Méndez-Cervantes⁵, Kathryn A Harris², Denise M O'Sullivan¹, Jim F Huggett^{1,6}, Timothy D McHugh³, Emmanuel Q Wey^{**3,4}

* These authors contributed equally to this work

** Corresponding author Emmanuel.vey@nhs.net

¹ LGC, Queens Road, Teddington, Middlesex, UK

² Department of Microbiology, Virology and Infection Control, Great Ormond Street Hospital for Children NHS Foundation Trust, London, UK

³ Centre for Clinical Microbiology, Royal Free Campus, Division of Infection and Immunity, Faculty of Medical Sciences, University College London, UK

⁴ Royal Free Hospital NHS Foundation Trust, London, UK

⁵ Clover Bioanalytical Software, SL. Granada, Spain

⁶ School of Biosciences & Medicine, Faculty of Health & Medical Science, University of Surrey, Guildford, UK

Abstract

Colonisation and subsequent infections with *Acinetobacter baumannii* are a concern for vulnerable patient groups within the hospital setting, with outbreaks involving multi drug-resistant strains being described as a particular threat to patient outcome. Reliable molecular typing methods can help to trace transmission routes and manage outbreaks. In addition to current reference methods, Matrix Assisted Laser Desorption/Ionisation-Time of Flight Mass Spectrometry (MALDI-TOF MS) may hold a role for making initial in-house judgements on strain relatedness however limited studies on method reproducibility exist for this application. We applied MALDI typing to 18 *A. baumannii* isolates associated with a nosocomial outbreak and evaluated different methods for data analysis. An evaluation applying high replication was implemented to evaluate peak reproducibility for MALDI typing. In addition, we analysed the isolates using whole genome sequencing (WGS) and Fourier-transform infrared spectroscopy (FTIR) as orthogonal methods to further explore the applicability of emerging techniques for bacterial strain typing. Despite all isolates being classified as the same strain by reference methods, a related group of isolates was consistently observed for all methods that clustered away from the main group. This finding, combined with epidemiological data from the outbreak, indicates that we have identified a separate transmission event unrelated to the main outbreak. Our study suggests that there could be a role for these emerging methods in supporting microbiological diagnoses in hospitals to more quickly confirm or rule out transmission events, however limitations exist surrounding sample size and method reproducibility; particularly for MALDI-TOF MS. Further studies are necessary to characterise these techniques before they can be integrated into routine services.

Introduction

Carbapenem resistant organisms (CRO) including *Acinetobacter baumannii* are a significant threat to patients within Intensive Care Units (ICU), on oncology wards and those that are immunocompromised. *A. baumannii* possesses the ability to form biofilms and colonize the respiratory tract (Howard et al., 2012), and it poses a significant transmission risk within the hospital setting. *A. baumannii* is responsible for an increasing number of difficult-to-treat respiratory, soft tissue and bloodstream infections. Risk factors for acquisition of *A. baumannii* colonization and subsequent bacteraemia, particularly with multi drug resistant organisms, include length of hospital stay, ICU admission and having an intravenous catheter or Ventriculoperitoneal (VP) shunt (Baran et al., 2008, Blanco et al., 2017). Minimisation of nosocomial transmission of *A. baumannii* amongst vulnerable patient cohorts is critical. Reliable and robust methods for molecular strain typing of nosocomial *A. baumannii* isolates can assist with determining transmission routes and tracing outbreaks (ECDC, 2016).

Matrix Assisted Laser Desorption/Ionisation-Time of Flight Mass Spectrometry (MALDI-TOF MS) has been widely reported as a method for identifying bacterial species, and as a promising technique for strain typing bacteria (Rafei et al., 2014, Mehta and Silva, 2015, Johnson et al., 2016). MALDI-TOF MS has been successfully implemented to resolve nosocomial and foodborne outbreak-associated bacterial strains (Christner et al., 2014, Barbuddhe et al., 2008, Stephan et al., 2011, Egli et al., 2015, Steensels et al., 2017), including for *A. baumannii* (Mencacci et al., 2013). However, there is limited evidence supporting the robustness of MALDI-TOF in this context, and conflicting evidence exists suggesting that MALDI-TOF MS is unreliable and unsuitable for strain typing *A. baumannii* (Ghebremedhin et al., 2017, Sousa et al., 2015, Rim et al., 2015). Numerous experimental factors are known to affect the consistency of MALDI-TOF MS performance (Williams et al., 2003); including upstream sample preparation, data acquisition and analysis. However, development of in-house capability for strain typing using modified MALDI-TOF MS protocols could improve diagnostic outputs and outbreak surveillance; an attractive option as many clinical microbiology services already possess the necessary instrumentation.

Pulsed-field gel electrophoresis (PFGE), Multiple locus variable number of tandem repeat analysis (MLVA) and multi locus sequence typing (MLST) are methods favoured by many bacterial reference laboratories for molecular typing of *A. baumannii* (Pourcel et al., 2011). However, these methods can be labour-intensive and costly with lengthy lead times for hospitals to receive results. In addition, two MLST schemes exist for typing *A. baumannii*; denoted 'Oxford' (Bartual et al., 2005) and 'Pasteur' (Diancourt et al., 2010). Whilst both schemes are valuable tools they have only three out of seven housekeeping gene targets in common (Tomaschek et al., 2016), making typing of *A. baumannii* in this way difficult to standardise and harmonise. Whole genome sequencing (WGS) is also gaining traction as a new reference method for bacterial strain typing (Fitzpatrick et al., 2016) although application for this purpose tends to be on a case-by-case basis (Lewis et al., 2010, Izwan et al., 2015, Fang et al., 2016, Alouane et al., 2017, Li et al., 2017), and the feasibility of adopting the technique into routine practice is still to be fully evaluated (Willems et al., 2016, Venditti et al., 2018). WGS could provide a broader analysis, offering information on drug resistance and a full spectrum of genes, therefore facilitating better resolution between strains of *A. baumannii*. Similarly to the reference methods, WGS is not presently available in the typical routine diagnostic laboratory. Another emerging technique, Fourier-transform infrared spectroscopy (FTIR), shows potential for strain typing of bacteria in the clinical laboratory setting (Quintelas et al., 2018). A study by (Dinkelacker et al., 2018) highlighted a potential role for FTIR to recognize clonal relationships between isolates of *Klebsiella pneumoniae* owing to high discriminatory power offered by the technique.

We hypothesise that MALDI-TOF MS, along with these emerging molecular methods, may hold a supporting role for in-house identification of outbreaks of *A. baumannii* in a nosocomial setting.

Our study explored the technical robustness and reproducibility of MALDI-TOF MS for bacterial typing. An approach to assess the reproducibility of different stages of the experimental protocol was followed to introduce metrics for peak discrimination. We compared outputs from different MALDI-TOF MS data analysis methods with WGS and FTIR to ascertain whether these methods offered equivalent resolution for typing compared with the reference methods. The work was performed on a cohort of *A. baumannii* isolates obtained from patients following stays of varying lengths on a surgery ward over a two year period.

Materials and Methods

Drug resistant clinical isolates

Isolates of multi drug resistant (MDR) *Acinetobacter baumannii* (n=18) associated with an outbreak at the Royal Free London NHS Foundation Trust were collected from 15 patients between 2014 and 2015. The outbreak was associated with a single surgery ward (ward A) however patients had migrated between 15 wards over the two year period (wards B-L), including an intensive/critical care unit (ICU/CCU) and an outpatient department (OPD). Length of stay on ward A varied between 1 and 184 days. The isolates were confirmed as *A. baumannii* species using the MALDI-TOF Microflex (Bruker UK) following the manufacturers protocol. Antimicrobial susceptibility testing (AST) was implemented according to EUCAST breakpoint guidelines (Brown et al., 2015). AST was performed using a BD Phoenix™ platform (Becton Dickinson) and minimum inhibitory concentrations (MICs) were established using ETEST® AST reagent strips (bioMérieux). Isolates were assigned a unique study identifier to remove patient information (e.g. MBT16-001) and stored on Cryobank™ beads (ThermoFisher Scientific Inc.) in glycerol at -80 °C.

Reference laboratory strain typing of isolates

Organisms were sent on nutrient agar slopes for reference laboratory characterisation by pulsed-field gel electrophoresis (PFGE) and variable number tandem repeat (VNTR) profiling at four loci (1, 10, 845,3468) (Turton et al., 2009, Pourcel et al., 2011). All 18 isolates were classified as belonging to European clone II lineage OXA-23 clone 1. PFGE data and VNTR profiles are included in Table S1. Isolate MBT16-062 was not sent to the reference laboratory but was included in this study for prospective analysis. The authors were blind to the reference laboratory typing results prior to commencing experimental work.

MALDI-TOF MS strain typing protocol

Isolates were recovered from -80°C onto pre-poured Colombia blood agar containing 5% horse blood (ThermoFisher Scientific) and incubated aerobically at 37 °C for 24 hours. Strain typing was performed using a MALDI-TOF Microflex (Bruker UK) according to the Bruker MALDI Biotyper protocol and described previously (Holzknecht et al., 2018). Measurements were obtained using flexControl software (version 3.4). Triplicate spots of formic acid extracted protein solution were overlaid with 1 µL fresh α -Cyano-4-hydroxycinnamic acid (HCCA) matrix (Bruker UK), allowed to air dry, and measured in triplicate over three separate days to obtain 27 spectra per isolate. Spectra were recorded in positive linear mode within the range of 2 and 20 kDa. External calibration of each MALDI typing experiment was through measurement of Bacterial Test Standard (BTS) solution (Bruker UK).

Whole genome sequencing

DNA was extracted from all isolates as previously described (Shaw et al., 2019). Total DNA concentration was estimated using a Qubit fluorometer (ThermoFisher). 50 ng of DNA was prepared using NEBNext Ultra II FS DNA Library Prep Kit for Illumina (New England Biolabs) and post-PCR clean-up was carried out using Ampure XP beads (Beckman). Library size was validated using the Agilent 2200 TapeStation with Agilent D1000 ScreenTape System (Willoughby, Australia) and 75bp paired-end reads were sequenced on a NextSeq 550 system (Illumina).

Fourier-transform infrared spectroscopy (FTIR)

The 34 *A. baumannii* isolates were recovered from cryo-storage onto pre-poured Tryptic Soy Agar (VWR) and incubated aerobically at 37°C for 24 hours. A second passage from a single colony of each isolate was performed and, after 24-hours, an overloaded 1 µL loop of confluent growth collected. The cells were added to a 1.5 mL suspension vial containing inert metal cylinders (Bruker IR Biotyper Kit) and 50 µL 70% (v/v) ethanol and vortexed to obtain a homogenous suspension. 50µL of HiPerSov Chromanorm® water (VWR) was added and each vial vortexed for 1 min. Quintuple 15 µL spots of each isolate were pipetted onto a 96-spot microtiter plate. Duplicate 12 µL spots of Bruker Infrared Test Standards 1 and 2 (IRTS1 and IRTS2) were included during each run. The standards were prepared according to the manufacturer's instructions. The microtiter plate was dried above a 37°C hotplate for 30 minutes and strain typing was performed using an IR Biotyper and the IR Biotyper Software (Bruker UK).

Data analysis

Bruker FlexAnalysis method

Following acquisition each of the 27 spectra were analysed as described in the MALDI Biotyper protocol using the MBT_standard.FAMSMMethod in FlexAnalysis (version 3.4). Peaks were detected using a centroid algorithm within a 2.0 m/z width range. Baseline subtraction and curve smoothing were performed using TopHat and SavitzkyGolay algorithms, respectively. Replicate spectra were visually inspected and any peaks below 500 arbitrary units (a.u.), or deviating outside of a mass tolerance of $\sim\pm 0.025\%$ of the estimated m/z value, were excluded. Mass peak lists for all isolates were recorded in Excel (Microsoft) and peaks potentially representing unique biomarkers for individual strains were recorded (Table 1). Peaks that satisfied the following criteria were considered as strain specific biomarkers: (i) above 500 a.u. for at least two out of three technical replicate spectra (ii) at least 5.0 m/z (Da) difference from peaks of a similar size (iii) present for at least one but not all of the 18 isolates.

Bioinformatic analysis of MALDI-TOF MS spectra

Processed spectra files (referred to as mzXml files) were exported from FlexAnalysis for each isolate for analysis in BioNumerics software (Applied Maths, version 7.6). Peak matching was performed in BioNumerics based on m/z data with a constant tolerance of 0.5, linear tolerance of 300 parts per million (ppm) and a detection rate of 50 new peak classes per spectra. Similarity matrices were generated based on the Pearson correlation coefficient and isolates clustered using the unweighted pair group method with arithmetic mean (UPGMA). The cophenetic correlation between isolates was calculated and expressed as a percentage on the dendrogram. For each isolate, peak classes with intensity values were exported into MS Excel for further analysis.

Confirmatory bioinformatic analysis of spectra was performed using Clover MS data analysis software (Clover BioSoft). Spectra were summarised for each isolate and a peak matrix generated. Summarised spectra were clustered by UPGMA.

Calculating variability in peak height as a metric for reproducibility of MALDI spectra

Using the numerical data exported into MS Excel from BioNumerics, two peak classes that were common to all 18 *A. baumannii* isolates and one that could represent a strain-specific biomarker were identified. Peak height (intensity) values were normalised to the total intensity for each spectra, and a mean value with relative standard deviation calculated. This was performed for triplicate technical replicates, triplicate 'spots' of co-crystallised matrix and protein extract, and triplicate days of experiments. A mean of the relative standard deviation (rsd) at each of these three time points was calculated for each isolate and plotted.

Whole genome phylogenetic analysis

Fastq files containing paired end sequences for each isolate were screened against all complete *A. baumannii* reference genomes found on NCBI Refseq database using Mash (Ondov et al., 2016) to identify the closest matching reference sequence. The best matching genome was *A. baumannii* strain BAL062 (Accession: NZ_LT594095) and all samples were mapped to this reference using BBmap (Bushnell, 2014). Single nucleotide variants (SNVs) were called against the reference using FreeBayes (Garrison and Marth, 2012) and variants were only taken forward if (i) read depth >5, (ii) mapping quality >30, (iii) base quality >20, (iv) alternate read frequency >80%, (v) if there were >2 reads on both strands and (vi) >2 reads with variant present at both the 5' and 3' ends of the fragments. Variant positions were also masked if not present at >5 read depth in 90% of samples. Possible recombination sites were identified and masked using Gubbins (Croucher et al., 2015) and a maximum likelihood phylogenetic tree was inferred from the aligned variant sites using RAxML under the GTRCAT model (Stamatakis, 2014).

Results

MALDI-TOF MS strain typing of *A. baumannii*

The Bruker MALDI Biotyper protocol was applied to the 18 OXA-23 clone 1 *A. baumannii* isolates. Although a single practical approach was followed, data were analysed using two methods; Bruker FlexAnalysis to analyse spectra, and subsequently using two separate bioinformatics software programmes for analysis of exported peak data. To evaluate MALDI-TOF MS as a robust typing method, 27 spectra were included for each isolate across a total of three days. The Bruker FlexAnalysis method involved visual identification of peaks that could represent strain-specific biomarkers. Four peaks that satisfied the inclusion criteria for strain typing were identified (Table S2a), and the isolates were grouped into a total of 8 classes representing different 'MALDI Biotypes' (Table S2b). Two of the isolates (MBT16-015 [G] and MBT16-030 [H]) were unique Biotypes, as their MALDI profiles did not match with any of the other isolates.

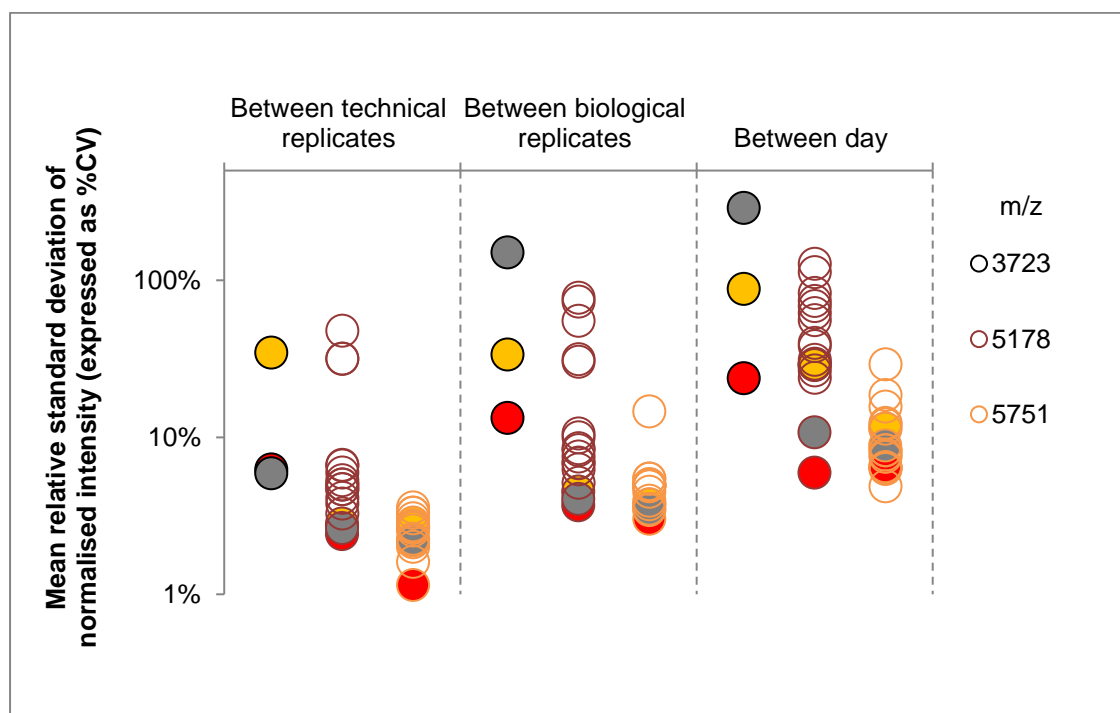
Following baseline subtraction and curve smoothing in FlexAnalysis, the pre-processed MALDI spectra were imported into BioNumerics 7.6. Spectra were summarised for each isolate and clustered using the unweighted pair group method with arithmetic mean (UPGMA). Two main clusters were identified using this method; designated Group I and Group II (Figure S1). Of note, the isolates that clustered into Group II using the bioinformatics analysis method also fell within the same MALDI Biotype 'group B' designated in Table S2b (isolates MBT16-005, MBT16-011 &

MBT16-039). This finding was confirmed when the same spectra were clustered using additional data analysis software (Figure S2).

Peak intensity as a metric for discrimination of peak classes using MALDI-TOF MS typing

The Group II/MALDI Biotype B isolates clustered together using both the Bruker FlexAnalysis and bioinformatic methods and could represent a diverse group of organisms. MALDI-TOF MS is often criticised for being limited in terms of reproducibility for its application to strain typing. We examined peak height (intensity) for these isolates to ascertain whether better reproducibility of spectra enables better MALDI strain typing resolution. For peaks that were shared among the *A. baumannii* isolates (m/z 5178 and 5751 determined using BioNumerics), the Group II isolates exhibited the lowest relative standard deviation (rsd) compared to the other isolates (< 0.30 rsd, 30% CV). This finding could suggest that better reproducibility between spectra permitted discrimination of these isolates from the rest of the cohort due to higher resolution of MALDI-TOF MS for typing. However, when this approach was applied to a peak at m/z 3723, identified by BioNumerics as unique to these three isolates, the mean rsd was up to 10-fold higher indicating a decrease in reproducibility between peak height values. Regardless of peak class there was an overall trend of increasing variability in peak height at progressive stages of the experiment protocol, with technical replicates exhibiting the lowest variability and between-day replicates exhibiting the highest (Figure 1).

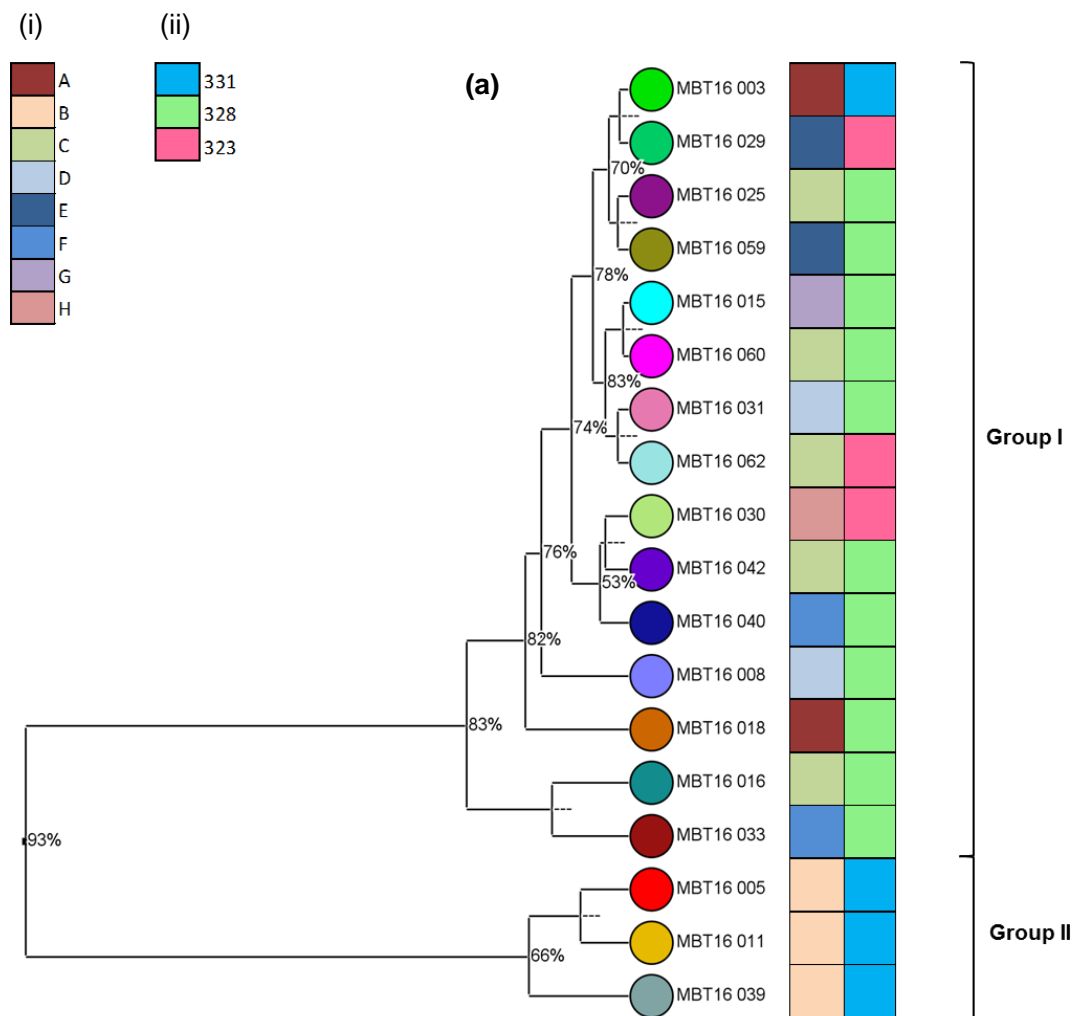
Figure 1: Variability in peak height at different stages of the MALDI-TOF MS typing protocol. The 'Group II/MALDI Biotype B' isolates are represented by the following coloured spots: Red – MBT16-005, Yellow – MBT16-011, Grey – MBT16-039. Unfilled spots represent the other 15 isolates. m/z 5178 and 5751 represent peak classes common to all isolates; m/z 3723 represents a peak only observed for the Group II/MALDI Biotype B isolates following analysis in BioNumerics.

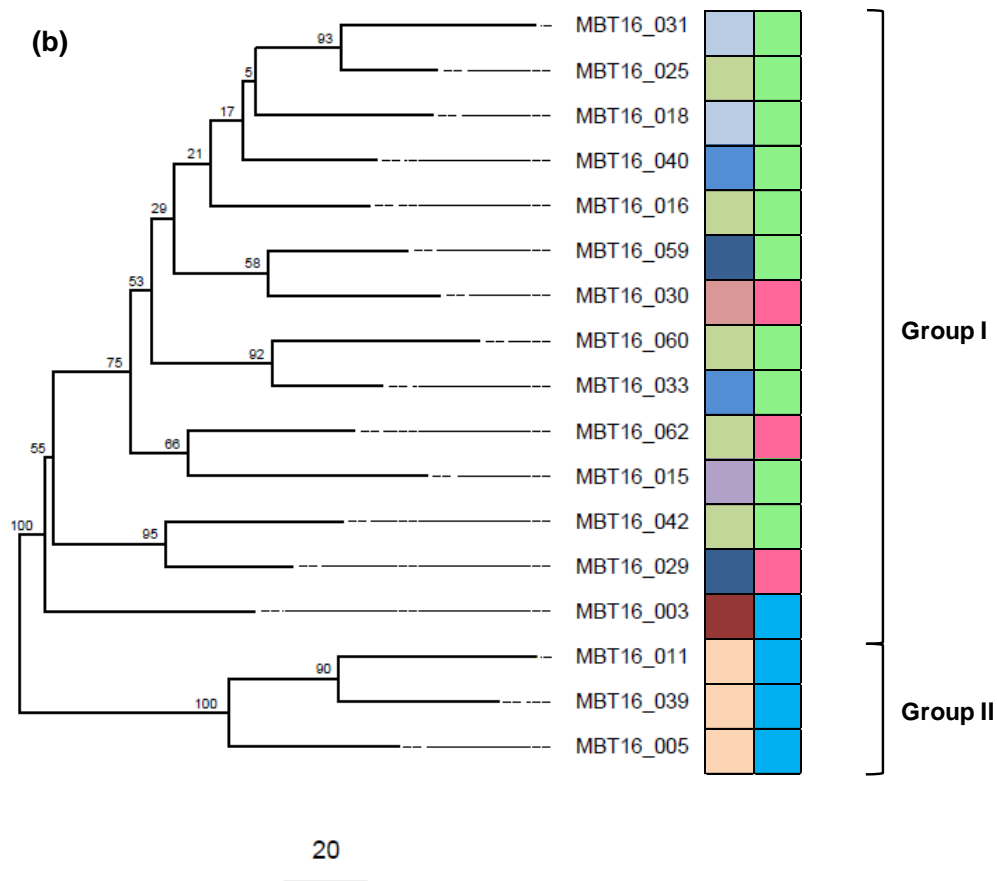


Comparison of methods for strain typing *A. baumannii*

The 8 MALDI Biotypes (Table S2b) and 2 bioinformatic MALDI groups (Figures S1 and S2) were compared with WGS and FTIR typing (Figure 2). There was limited correlation between The MALDI Biotypes and the other methods, with the exception of the group B isolates (MBT16-005, MBT16-011 & MBT16-039) which consistently clustered together as a distinct group for all four methods. The bioinformatic MALDI analysis and WGS clustered the isolates into two main nodes, whereas FTIR identified three clusters (331, 328 & 323). The FlexAnalysis method appears to overinflate the isolate diversity compared to the other methods, with 8 groups being identified based on visual inspection of spectra. There was limited correlation in the order in which the 'Group I' isolates were clustered in relation to each other by MALDI bioinformatics (BioNumerics) and WGS, with the exception of isolates MBT16-003 & MBT16-029 and MBT16-018 & MBT16-040. However, these same relationships were not observed when MALDI spectra were clustered using an orthogonal bioinformatics approach (Figure S2).

Figure 2: (a) UPGMA hierarchal clustering of MALDI-TOF MS spectra compared with MALDI Biotype (i) and IR Biotype cluster (ii). (b) WGS SNV analysis compared with MALDI Biotype (i) and FTIR cluster (ii).





Discussion

*Can MALDI-TOF MS strain type *A. baumannii*? Data analysis method and peak matrix algorithm play a key role*

Our study initially aimed to determine whether MALDI-TOF MS had sufficient reproducibility and resolution to identify biomarker peaks that could be used to strain type clinical isolates of *A. baumannii*. A single experimental approach was followed using a cohort of closely related isolates with a number of shared peaks (Table S1), and spectra were analysed using different methods. Analysis was performed on a small number of peak classes; 4 out of approximately 9 observable peaks per spectra which was similar to that observed by (Sousa et al., 2015) and (Jeong et al., 2016). The Bruker FlexAnalysis method, which involved visual inspection of peak classes, yielded 8 MALDI Biotype groups for the isolates that were assigned based on the presence or absence of particular peak classes (Table S2). This approach has been described previously for strain typing with varying levels of success (Oberle et al., 2016, Holzkecht et al., 2018). Overall there was poor correlation with the other methods, with the exception of three isolates which formed a distinct cluster for all methods tested in this study (Figure 2). The FlexAnalysis method was based on non-normalised spectral data which may result in subjective classification of peaks owing to variable baseline signals between spectra.

Bioinformatic analyses and machine learning may be of benefit when handling MALDI strain typing data (Spinali et al., 2015, Oberle et al., 2016). In our hands, the MALDI analysis approach

using BioNumerics offered more objectivity because the software is able to access peak data for the entire spectrum rather than the 4 classification peaks for the FlexAnalysis method and apply peak height normalisation algorithms. This may enable a more robust approach to typing, and as a result potentially offer better resolution. The bioinformatics analysis workflow was repeated for the MALDI spectra using additional software (Clover MS data analysis software), which demonstrated good agreement with the BioNumerics method in terms of isolate clusters (Figure S2). Several peaks identified using the MALDI bioinformatics workflows can be attributed to published ribosomal proteins for *A. baumannii* (Table S3). This suggests that the peak finding algorithms of these methods are fit-for-purpose for finding reference peak masses, and could be applied to identify additional strain-specific peaks and those attributed to drug resistance. Further work to explore the capability of additional commercial software for data analysis could be of benefit for future studies on spectral typing methods.

Following bioinformatic analysis of spectra, we evaluated how different stages of the experimental protocol could influence typing of *A. baumannii* by impacting upon peak identification. Studies suggest that the quality and reproducibility of MALDI-TOF MS fingerprints can be influenced by sample preparation steps, matrix choice and instrumental performance, among other factors (De Bruyne et al., 2011). This could influence the ionisation of a protein and therefore whether it is included in subsequent strain typing analysis. Our chosen metric, peak height (intensity) has been correlated with ionisation efficiency (Duncan et al., 2016). Figure 1 shows that peak height became increasingly variable between co-crystallisation and day-to-day. The height of peaks common to all *A. baumannii* isolates (e.g. 5751 m/z) appeared to be more reproducible across the experiments for these three isolates, whereas a peak chosen to represent a potential strain-specific biomarker (3073 m/z) exhibited higher variability with some individual spectra failing to be called by the software. This suggests that variability introduced during sample preparation could directly influence discrimination of isolates by particular peak classes. Studies have advocated that standardising MALDI-TOF MS workflows could permit better typing resolution (Singhal et al., 2015, Spinali et al., 2015, Oberle et al., 2016). Future work incorporating a cohort of diverse strains could provide an opportunity to further evaluate the reproducibility of MALDI typing for a larger number of peak classes.

Potential identification of a nosocomial transmission event using four independent methods

We compared the MALDI-TOF MS FlexAnalysis and bioinformatics *A. baumannii* strain typing results with WGS and FTIR (Figure 2). WGS, which is increasingly used for bacterial strain typing (Schurch et al., 2018, Salipante et al., 2015), and MALDI bioinformatics approaches clustered the isolates into two groups, with the 'Group I' isolates appearing to be closely related in line with reference laboratory interpretation (Figure S3a). Any observed differences, such as MALDI peak classes assigned by bioinformatics software or SNP differences by WGS, may represent the typical diversity between isolates of the same strain. Further comparisons with a broader cohort of isolates from this hospital would further help to contextualise the relatedness between these isolates. The outbreak in question in this study was identified as being associated with a single surgery ward (ward A), multiple beds of which were inhabited by the patients during this time period (Figure S3b). However, patients had also spent time on numerous other wards of varying specialties within the hospital including intensive care units. There were overlaps in time in which patients stayed on ward A, presenting possible opportunities for transmission to occur. This snapshot of the typical high level of patient migration within a hospital highlights the requirement for timely and adequate cross infection control strategies, and how accurate typing methods can help to quickly confirm or rule out a potential outbreak.

Of the 18 isolates tested in this study, three isolates were classified as being separate from the main group by all of the methods (respectively denoted as Group II/cluster 331/MALDI Biotype B

by MALDI bioinformatics & WGS/FTIR/MALDI FlexAnalysis method). These isolates were also identified as belonging to European clone II lineage OXA-23 clone 1 following reference typing. However, according to the methods applied in our study diversity could exist between groups I & II indicating that they are not identical and possibly not from the same transmission route. It is worth noting that for these three isolates, MBT16-005 and MBT16-039 were obtained from the same patient (Patient ID: 2). MBT16-011 was obtained from another individual (Patient ID: 4) who stayed on ward A in the same male 4-bedded bay during this time period. MDR *A. baumannii* was identified first in patient 4, followed by patient 2 thirteen days later. It is possible that we have identified an incidental transmission event between these two patients within ward A that is separate from the main outbreak cluster. This finding, identified by in-house methods independently to reference laboratory typing, could have implications for future infection control strategies where isolated transmission events can be disassociated from larger outbreaks.

Our study introduced the use of FTIR for strain typing *A. baumannii*, which classified the isolates into three clusters. Similarly to MALDI and WGS, FTIR grouped the three 'Group II' isolates into cluster 331 along with an isolate not grouped by the other methods (MBT16-003). 16 reference isolates of *A. baumannii* collected from clinical samples obtained from the Royal Free London NHS Foundation Trust during 2014 and 2015 were included in the FTIR analysis. Figure S4 indicates that these reference isolates cluster disparately from the 18 outbreak isolates which cluster within close proximity to one another. This result further supports the reference laboratory interpretation that the isolates are closely related, if not the same strain. Our results show promise for FTIR as a typing method; however given the relative infancy of the technique further studies should be conducted before the method can be considered for routine clinical use.

Integration of emerging molecular strain typing methods into routine clinical diagnostics

We have evaluated three emerging techniques and multiple data analysis workflows for bacterial strain typing from the point of view of clinical diagnostic laboratories, who may wish to acquire in-house capabilities for analysis of possible transmission events. The potential identification of a distinct clonal group using independent methods in our study might suggest that a combination of molecular tests, along with bioinformatic analyses, could help to more reliably assign *A. baumannii* strain types. This could be applied where transmission events are suspected prior to sending isolates for reference laboratory typing. Further work utilising a larger number of diverse organisms is required to more scrupulously evaluate the applicability of the methods to typing, in particular MALDI-TOF MS and FTIR. Whilst there may be a promising role for these emerging techniques in-house, further reviews such as that conducted by (van Belkum et al., 2007) on selecting methods for strain typing bacteria could help to guide laboratories in choosing suitable methods.

Conclusions

Using MALDI-TOF MS with different data analysis approaches and orthogonal methods for molecular strain typing of *A. baumannii* (WGS and FTIR), we have detected a transmission event between two patients that appears to be distinct from a cohort of isolates associated with a nosocomial outbreak. This finding is supported by epidemiological data and patient migration information within the hospital indicating opportunities for transmission. However, we have empirically demonstrated that the MALDI-TOF MS experimental protocol introduces variability at different stages, which may impact upon resolution of the technique when assigning a particular peak class biomarker status. This work demonstrates how new and emerging methods might be incorporated to provide faster epidemiological data during outbreak scenarios, however further work on a larger cohort of more diverse organisms is required to select which method is most appropriate for incorporation into routine practice. In-house applicability of these methods as initial epidemiological screening tools prior to reference laboratory typing could help to reduce the time taken to make clinical decisions whilst awaiting reference laboratory results, providing an economic overall benefit to patient care.

Acknowledgements

This work was funded by the EuraMet EMPIR programme under the AntiMicroResist project. Acknowledgement is given to Indran Balakrishnan and Gemma Vanstone for sourcing patient isolates and to Giuseppina Maniscalco for assistance with collecting and culturing the organisms. Acknowledgement is given to the Infection control Nurses at the Royal Free London NHS Foundation Trust for their assistance with gathering epidemiological and patient data. The authors are grateful to Jane Turton (PHE) for critical review of manuscript.

References

- ALOUANE, T., UWINGABIYE, J., LEMNOUER, A., LAHLOU, L., LAAMARTI, M., KARTTI, S., BENHRIF, O., EL MISBAHI, H., FRIKH, M., BENLAHLOU, Y., BSSAIBIS, F., EL ABBASSI, S., KABBAGE, S., MALEB, A., ELOUENNASS, M. & IBRAHIMI, A. 2017. First Whole-Genome Sequences of Two Multidrug-Resistant *Acinetobacter baumannii* Strains Isolated from a Moroccan Hospital Floor. *Genome announcements*, 5, e00298-17.
- BARAN, G., ERBAY, A., BODUR, H., ÖNGÜRÜ, P., AKINCI, E., BALABAN, N. & ÇEVİK, M. A. 2008. Risk factors for nosocomial imipenem-resistant *Acinetobacter baumannii* infections. *International Journal of Infectious Diseases*, 12, 16-21.
- BARBUDDHE, S. B., MAIER, T., SCHWARZ, G., KOSTRZEWA, M., HOF, H., DOMANN, E., CHAKRABORTY, T. & HAIN, T. 2008. Rapid identification and typing of listeria species by matrix-assisted laser desorption ionization-time of flight mass spectrometry. *Appl Environ Microbiol*, 74, 5402-7.
- BARTUAL, S. G., SEIFERT, H., HIPPLER, C., LUZON, M. A., WISPLINGHOFF, H. & RODRIGUEZ-VALERA, F. 2005. Development of a multilocus sequence typing scheme for characterization of clinical isolates of *Acinetobacter baumannii*. *J Clin Microbiol*, 43, 4382-90.
- BLANCO, N., HARRIS, A. D., ROCK, C., JOHNSON, J. K., PINELES, L., BONOMO, R. A., SRINIVASAN, A., PETTIGREW, M. M., THOM, K. A. & THE, C. D. C. E. P. 2017. Risk Factors and Outcomes Associated with Multidrug-Resistant *Acinetobacter baumannii* upon Intensive Care Unit Admission. *Antimicrobial agents and chemotherapy*, 62, e01631-17.
- BROWN, D., CANTON, R., DUBREUIL, L., GATERMANN, S., GISKE, C., MACGOWAN, A., MARTINEZ-MARTINEZ, L., MOUTON, J., SKOV, R., STEINBAKK, M., WALTON, C., HEUER, O., STRUELENS,

- M. J., DIAZ HOGBERG, L. & KAHLMETER, G. 2015. Widespread implementation of EUCAST breakpoints for antibacterial susceptibility testing in Europe. *Euro Surveill*, 20.
- BUSHNELL, B. 2014. *BBMap: A Fast, Accurate, Splice-Aware Aligner* [Online]. United States. Available: <https://www.osti.gov/servlets/purl/1241166> [Accessed 10th August 2020].
- CHRISTNER, M., TRUSCH, M., ROHDE, H., KWIATKOWSKI, M., SCHLÜTER, H., WOLTERS, M., AEPFELBACHER, M. & HENTSCHKE, M. 2014. Rapid MALDI-TOF Mass Spectrometry Strain Typing during a Large Outbreak of Shiga-Toxigenic Escherichia coli. *PLOS ONE*, 9, e101924.
- CROUCHER, N. J., PAGE, A. J., CONNOR, T. R., DELANEY, A. J., KEANE, J. A., BENTLEY, S. D., PARKHILL, J. & HARRIS, S. R. 2015. Rapid phylogenetic analysis of large samples of recombinant bacterial whole genome sequences using Gubbins. *Nucleic Acids Res*, 43, e15.
- DE BRUYNE, K., SLABBINCK, B., WAEGEMAN, W., VAUTERIN, P., DE BAETS, B. & VANDAMME, P. 2011. Bacterial species identification from MALDI-TOF mass spectra through data analysis and machine learning. *Syst Appl Microbiol*, 34, 20-9.
- DIANCOURT, L., PASSET, V., NEMEC, A., DIJKSHOORN, L. & BRISSE, S. 2010. The Population Structure of *Acinetobacter baumannii*: Expanding Multiresistant Clones from an Ancestral Susceptible Genetic Pool. *PLOS ONE*, 5, e10034.
- DINKELACKER, A. G., VOGT, S., OBERHETTINGER, P., MAUDER, N., RAU, J., KOSTRZEWA, M., ROSSEN, J. W. A., AUTENRIETH, I. B., PETER, S. & LIESE, J. 2018. Typing and Species Identification of Clinical Klebsiella Isolates by Fourier Transform Infrared Spectroscopy and Matrix-Assisted Laser Desorption Ionization–Time of Flight Mass Spectrometry. *Journal of Clinical Microbiology*, 56, e00843-18.
- DUNCAN, M. W., NEDELKOV, D., WALSH, R. & HATTAN, S. J. 2016. Applications of MALDI Mass Spectrometry in Clinical Chemistry. *Clinical Chemistry*, 62, 134-143.
- ECDC, E. C. F. D. P. A. C. 2016. Carbapenem-resistant *Acinetobacter baumannii* in healthcare settings. Stockholm.
- EGLI, A., TSCHUDIN-SUTTER, S., OBERLE, M., GOLDENBERGER, D., FREI, R. & WIDMER, A. F. 2015. Matrix-assisted laser desorption/ionization time of flight mass-spectrometry (MALDI-TOF MS) based typing of extended-spectrum beta-lactamase producing *E. coli* - a novel tool for real-time outbreak investigation. *PLoS One*, 10, e0120624.
- FANG, Y., QUAN, J., HUA, X., FENG, Y., LI, X., WANG, J., RUAN, Z., SHANG, S. & YU, Y. 2016. Complete genome sequence of *Acinetobacter baumannii* XH386 (ST208), a multi-drug resistant bacteria isolated from pediatric hospital in China. *Genomics Data*, 7, 269-274.
- FITZPATRICK, M. A., OZER, E. A. & HAUSER, A. R. 2016. Utility of Whole-Genome Sequencing in Characterizing *Acinetobacter* Epidemiology and Analyzing Hospital Outbreaks. *J Clin Microbiol*, 54, 593-612.
- GARRISON, E. & MARTH, G. 2012. Haplotype-based variant detection from short-read sequencing. *arXiv*, 1207.
- GHEBREMEDHIN, M., HEITKAMP, R., YESUPRIYA, S., CLAY, B. & CRANE, N. J. 2017. Accurate and Rapid Differentiation of *Acinetobacter baumannii* Strains by Raman Spectroscopy: a Comparative Study. *J Clin Microbiol*, 55, 2480-2490.
- HOLZKNECHT, B. J., DARGIS, R., PEDERSEN, M., PINHOLT, M. & CHRISTENSEN, J. J. 2018. Typing of vancomycin-resistant enterococci with MALDI-TOF mass spectrometry in a nosocomial outbreak setting. *Clinical Microbiology and Infection*.
- HOWARD, A., O'DONOGHUE, M., FEENEY, A. & SLEATOR, R. D. 2012. *Acinetobacter baumannii*: an emerging opportunistic pathogen. *Virulence*, 3, 243-250.
- IZWAN, I., TEH, L. K. & SALLEH, M. Z. 2015. The genome sequence of *Acinetobacter baumannii* isolated from a septicemic patient in a local hospital in Malaysia. *Genomics Data*, 6, 128-129.
- JEONG, S., HONG, J. S., KIM, J. O., KIM, K. H., LEE, W., BAE, I. K., LEE, K. & JEONG, S. H. 2016. Identification of *Acinetobacter* Species Using Matrix-Assisted Laser Desorption Ionization–Time of Flight Mass Spectrometry. *Annals of laboratory medicine*, 36, 325-334.

- JOHNSON, J. K., ROBINSON, G. L., ZHAO, L., HARRIS, A. D., STINE, O. C. & THOM, K. A. 2016. Comparison of molecular typing methods for the analyses of *Acinetobacter baumannii* from ICU patients. *Diagnostic microbiology and infectious disease*, 86, 345-350.
- LEWIS, T., LOMAN, N. J., BINGLE, L., JUMAA, P., WEINSTOCK, G. M., MORTIBOY, D. & PALLEN, M. J. 2010. High-throughput whole-genome sequencing to dissect the epidemiology of *Acinetobacter baumannii* isolates from a hospital outbreak. *Journal of Hospital Infection*, 75, 37-41.
- LI, P., HUANG, Y., YU, L., LIU, Y., NIU, W., ZOU, D., LIU, H., ZHENG, J., YIN, X., YUAN, J., YUAN, X. & BAI, C. 2017. Isolation and Whole-genome Sequence Analysis of the Imipenem Heteroresistant *Acinetobacter baumannii* Clinical Isolate HRAB-85. *International Journal of Infectious Diseases*, 62, 94-101.
- MEHTA, A. & SILVA, L. P. 2015. MALDI-TOF MS profiling approach: how much can we get from it? *Frontiers in Plant Science*, 6.
- MENCACCI, A., MONARI, C., LELI, C., MERLINI, L., DE CAROLIS, E., VELLA, A., CACIONI, M., BUZI, S., NARDELLI, E., BISTONI, F., SANGUINETTI, M. & VECCHIARELLI, A. 2013. Typing of nosocomial outbreaks of *Acinetobacter baumannii* by use of matrix-assisted laser desorption ionization-time of flight mass spectrometry. *J Clin Microbiol*, 51, 603-6.
- OBERLE, M., WOHLWEND, N., JONAS, D., MAURER, F. P., JOST, G., TSCHUDIN-SUTTER, S., VRANCKX, K. & EGLI, A. 2016. The Technical and Biological Reproducibility of Matrix-Assisted Laser Desorption Ionization-Time of Flight Mass Spectrometry (MALDI-TOF MS) Based Typing: Employment of Bioinformatics in a Multicenter Study. *PLoS One*, 11, e0164260.
- ONDOV, B. D., TREANGEN, T. J., MELSTED, P., MALLONEE, A. B., BERGMAN, N. H., KOREN, S. & PHILLIPPY, A. M. 2016. Mash: fast genome and metagenome distance estimation using MinHash. *Genome Biol*, 17, 132.
- POURCEL, C., MINANDRI, F., HAUCK, Y., D'AREZZO, S., IMPERI, F., VERGNAUD, G. & VISCA, P. 2011. Identification of variable-number tandem-repeat (VNTR) sequences in *Acinetobacter baumannii* and interlaboratory validation of an optimized multiple-locus VNTR analysis typing scheme. *J Clin Microbiol*, 49, 539-48.
- QUINTELAS, C., FERREIRA, E. C., LOPES, J. A. & SOUSA, C. 2018. An Overview of the Evolution of Infrared Spectroscopy Applied to Bacterial Typing. *Biotechnology Journal*, 13, 1700449.
- RAFEI, R., KEMPF, M., EVEILLARD, M., DABBOUSSI, F., HAMZE, M. & JOLY-GUILLOU, M. L. 2014. Current molecular methods in epidemiological typing of *Acinetobacter baumannii*. *Future Microbiol*, 9, 1179-94.
- RIM, J. H., LEE, Y., HONG, S. K., PARK, Y., KIM, M., SOUZA, R., PARK, E. S., YONG, D. & LEE, K. 2015. Insufficient Discriminatory Power of Matrix-Assisted Laser Desorption Ionization Time-of-Flight Mass Spectrometry Dendrograms to Determine the Clonality of Multi-Drug-Resistant *Acinetobacter baumannii* Isolates from an Intensive Care Unit. *BioMed Research International*, 2015, 8.
- SALIPANTE, S. J., SENGUPTA, D. J., CUMMINGS, L. A., LAND, T. A., HOOGESTRAAT, D. R. & COOKSON, B. T. 2015. Application of whole-genome sequencing for bacterial strain typing in molecular epidemiology. *J Clin Microbiol*, 53, 1072-9.
- SCHURCH, A. C., ARREDONDO-ALONSO, S., WILLEMS, R. J. L. & GOERING, R. V. 2018. Whole genome sequencing options for bacterial strain typing and epidemiologic analysis based on single nucleotide polymorphism versus gene-by-gene-based approaches. *Clin Microbiol Infect*, 24, 350-354.
- SHAW, L. P., DOYLE, R. M., KAVALIUNAITE, E., SPENCER, H., BALLOUX, F., DIXON, G. & HARRIS, K. A. 2019. Children with cystic fibrosis are infected with multiple subpopulations of *Mycobacterium abscessus* with different antimicrobial resistance profiles. *Clin Infect Dis*.
- SINGHAL, N., KUMAR, M., KANAUIA, P. K. & VIRDI, J. S. 2015. MALDI-TOF mass spectrometry: an emerging technology for microbial identification and diagnosis. *Frontiers in Microbiology*, 6, 791.

- SOUSA, C., BOTELHO, J., GROSSO, F., SILVA, L., LOPES, J. & PEIXE, L. 2015. Unsuitability of MALDI-TOF MS to discriminate *Acinetobacter baumannii* clones under routine experimental conditions. *Frontiers in Microbiology*, 6.
- SPINALI, S., VAN BELKUM, A., GOERING, R. V., GIRARD, V., WELKER, M., VAN NUENEN, M., PINCUS, D. H., ARSAC, M. & DURAND, G. 2015. Microbial typing by matrix-assisted laser desorption ionization-time of flight mass spectrometry: do we need guidance for data interpretation? *J Clin Microbiol*, 53, 760-5.
- STAMATAKIS, A. 2014. RAxML version 8: a tool for phylogenetic analysis and post-analysis of large phylogenies. *Bioinformatics*, 30, 1312-3.
- STEENSELS, D., DEPLANO, A., DENIS, O., SIMON, A. & VERROKEN, A. 2017. MALDI-TOF MS typing of a nosocomial methicillin-resistant *Staphylococcus aureus* outbreak in a neonatal intensive care unit. *Acta Clin Belg*, 72, 219-225.
- STEPHAN, R., CERNELA, N., ZIEGLER, D., PFLUGER, V., TONOLLA, M., RAVASI, D., FREDRIKSSON-AHOMAA, M. & HACHLER, H. 2011. Rapid species specific identification and subtyping of *Yersinia enterocolitica* by MALDI-TOF mass spectrometry. *J Microbiol Methods*, 87, 150-3.
- TOMASCHEK, F., HIGGINS, P. G., STEFANIK, D., WISPLINGHOFF, H. & SEIFERT, H. 2016. Head-to-Head Comparison of Two Multi-Locus Sequence Typing (MLST) Schemes for Characterization of *Acinetobacter baumannii* Outbreak and Sporadic Isolates. *PLoS one*, 11, e0153014-e0153014.
- TURTON, J. F., MATOS, J., KAUFMANN, M. E. & PITT, T. L. 2009. Variable number tandem repeat loci providing discrimination within widespread genotypes of *Acinetobacter baumannii*. *Eur J Clin Microbiol Infect Dis*, 28, 499-507.
- VAN BELKUM, A., TASSIOS, P. T., DIJKSHOORN, L., HAEGGMAN, S., COOKSON, B., FRY, N. K., FUSSING, V., GREEN, J., FEIL, E., GERNER-SMIDT, P., BRISSE, S. & STRUELENS, M. 2007. Guidelines for the validation and application of typing methods for use in bacterial epidemiology. *Clin Microbiol Infect*, 13 Suppl 3, 1-46.
- VENDITTI, C., VULCANO, A., D'AREZZO, S., GRUBER, C. E. M., SELLERI, M., ANTONINI, M., LANINI, S., MARANI, A., PURO, V., NISII, C. & DI CARO, A. 2018. Epidemiological investigation of an *Acinetobacter baumannii* outbreak using Core Genome Multilocus Sequence Typing. *bioRxiv*.
- WILLEMS, S., KAMPMEIER, S., BLETZ, S., KOSSOW, A., KÖCK, R., KIPP, F. & MELLMANN, A. 2016. Whole-Genome Sequencing Elucidates Epidemiology of Nosocomial Clusters of *Acinetobacter baumannii*. *Journal of Clinical Microbiology*, 54, 2391-2394.
- WILLIAMS, T. L., ANDRZEJEWSKI, D., LAY, J. O. & MUSSER, S. M. 2003. Experimental factors affecting the quality and reproducibility of MALDI TOF mass spectra obtained from whole bacteria cells. *Journal of the American Society for Mass Spectrometry*, 14, 342-351.